Secondary Frost Heave in Freezing Soils

by
Christopher Noon

A thesis submitted for the degree of
Doctor of Philosophy
at the University of Oxford

Corpus Christi College
Oxford

Hilary Term 1996



Figure 1: View from the balcony of Rosie O'Grady's, Oxford. In chapter 7, the parameter $\mathcal{N}$ determines the stability of the secondary frost heave process.

Secondary Frost Heave in Freezing Soils

Christopher Noon
Corpus Christi College, Oxford
D. Phil. Thesis, Hilary Term 1996

Abstract

Frost heave describes the phenomenon whereby soil freezing causes upwards surface motion due to the action of capillary suction imbibing water from the unfrozen region below. The expansion of water on freezing is a small part of the overall surface heave and it is the flow of water towards the freezing front which is largely responsible for the uplift.

In this thesis, we analyse a model of frost heave due to Miller (1972, 1978) which is referred to as *secondary frost heave*. Secondary frost heave is characterised by the existence of a *partially frozen zone*, underlying the frozen soil, in which ice and water coexist in the pore space. In the first part of the thesis we follow earlier work of Fowler, Krantz and Noon where we show that the Miller model for incompressible soils can be dramatically simplified. The second part of the thesis then uses this simplification procedure to develop simplified models for saline and compressible soils. In the latter case, the development of the theory leads to the consideration of non-equilibrium soil consolidation theory and the formation of segregated *massive* ice within permafrost. The final part of the thesis extends the simplified Miller model to the analysis of differential frost heave and the formation of patterned ground (e.g. earth hummocks and stone circles). We show that an instability mechanism exists which provides a plausible theory for the formation of these types of patterned ground.

Acknowledgements

The production of this thesis owes a great deal to many people. In particular, my supervisor Dr. Andrew Fowler, who has provided enthusiasm, insight and regular trips to Rosie O'Grady's and my family for their continual encouragement. In addition, I gratefully acknowledge Dr. S. O'Brien and Dr. W.B. Krantz for discussion and Felix Ng, for providing a 'crash course' in the wonders of Unix, Xfig and Matlab.

I would also like to thank my colleagues Pete Cowling, Stuart Doole, Chris Aldridge, Louise Terrill, Simon Acomb, Paul Emms, Taryn Malcolm, Michael Vynnycky and Iain Simpson for discussion and providing help and encouragement.

Finally I gratefully acknowledge the financial support provided by an S.E.R.C earmarked studentship and my employer, Hewitt Associates.

Contents

1 Introduction **1**

1.1 Historical Perspective 1

1.2 Extensions 6

2 Secondary Frost Heave Models **9**

2.1 Introduction 9

2.2 The Miller Model 10

2.2.1 Conservation of Mass 11

2.2.2 Conservation of Energy 12

2.2.3 Osmosis and the Clapeyron equation 13

2.2.4 Solute Transport Equation 14

2.2.5 Similitude and the Capillary Relation 15

2.2.6 The Liquid and Ice Fluxes 17

2.2.7 Mechanics of the Soil Matrix 19

2.2.8 Initiation of an Ice Lens 22

2.2.9 Frozen and Unfrozen Regions 23

2.2.10 Boundary Conditions 24

2.3 Other Models 28

2.3.1 The Hydrodynamic Model 28

2.3.2 Other Models 30

3 Continuous Approximation **32**

3.1 Introduction 32

3.2 Non-dimensionalisation 33

3.2.1 Model Summary 33

3.2.2 Non-dimensionalisation 36

3.2.3 Parameter Values 41
3.3 Continuous Approximation 44
3.3.1 Lens Spacing 44
3.3.2 Continuous Approximation 50
3.3.3 Continuous Model 51
3.3.4 Field Boundary Conditions 54
3.4 Temperature Solution 54
3.5 Reduced Equations 55

4 Incompressible, Solute Free Soils in One Dimension 58
4.1 Introduction 58
4.2 Thin Fringe Approximation 59
4.3 Variation in Heave Rate 65
4.3.1 Lens Initiation Constraint 66
4.3.2 The Heave Parameter, α_{fk} 72
4.4 Linear System 74
4.5 Approximate Analytic Solution 75
4.5.1 Small Time Analysis 75
4.5.2 Long Time Analysis 76
4.6 Lens Spacing and Lens Thickness 76
4.7 Numerical Solution 78
4.7.1 Heave and Frozen Front Depth 79
4.7.2 Lens Spacing and Thickness 80

5 Saline Soils 83
5.1 Introduction 83
5.2 Solution to the Fringe Equations 84
5.3 Physical Implications 89
5.4 Approximate Analytic Solution 90
5.4.1 Small Time Analysis 90
5.4.2 Long Time Solution 91
5.5 Numerical Solution 92
5.5.1 The Numerical Procedure 92

5.5.2 The Numerical Solution 93
5.6 Discussion 94

6 Massive Ice Formation **98**
6.1 Introduction 98
6.2 The Fringe Equations 101
6.3 The Rheology of the Unfrozen Region 103
6.3.1 The Governing Equations 104
6.3.2 The Constitutive Relations 104
6.3.3 Model for Groundwater Flow 107
6.4 Non-dimensionalisation and Simplification 109
6.5 Purely Elastic Strains 111
6.6 Elastic/Plastic Strains 112
6.7 Thin Region Approximation 112
6.8 Analysis of Time Scales 118
6.9 Discussion and Numerical Solution. 121
6.9.1 Numerical Solution 121
6.9.2 The Final Ice Lens 126

7 Differential Frost Heave **133**
7.1 Introduction 133
7.2 The Frost Heave Equations 136
7.3 The Frozen Soil Equations 138
7.4 Linearised Problem 141
7.5 Linear Stability Analysis 145
7.6 Analysis of the Dispersion Relation 151
7.7 Change in Effective Stress 153
7.8 The Effect of Surface Snow Covering 162
7.8.1 Neutral Stability 167

8 Conclusion **171**
8.1 Discussion of Results 171
8.2 Further Work 176

A **177**

B **178**

Chapter 1

Introduction

1.1 Historical Perspective

In areas that experience prolonged periods of sub-zero temperatures it is noticed that if 'propitious' freezing conditions prevail, the ground surface may rise. This phenomenon is commonly referred to as *frost heave* and is not, as may be first thought, solely due to the expansion of water when it changes phase to ice. In fact, although this volume change is about 9%, in general it has little or no effect on the amount the surface heaves. The extent of heave depends primarily on pore size and consequently the distribution of particle sizes in the soil. Generally it is found that soils composed of coarse silt and gravel do not heave at all whereas finer soils can produce considerable heave. Within these finer soils it is found that soils in the fine silt to coarse clay range can produce spectacular heave, providing the overburden is not too great, while even finer soils produce only small amounts of surface heave but are capable of overcoming substantial loads.

Frost heave is responsible for numerous environmental problems including damage to roads, pavements and the foundations of buildings. Other less obvious problems are caused by the weakening of ground when a frozen soil, especially one which has heaved, thaws. This occurs because frost heave and freezing of soil in general, induces a moisture flow up towards the freezing front thereby increasing its frozen water content and dramatically decreasing the frozen soil's permeability due to a decrease in water fraction and the presence of ice lenses. Thawing occurs naturally from the soil surface downwards and hence the thawed soil can become saturated causing it to suffer a complete loss of strength.

Differential frost heave refers to the situation whereby the heave has some form of spatial dependence (as is most common in the field situation) which arises through variations in temperature, soil type or applied load. One particularly interesting occurrence of differential frost heave is in the formation of *patterned ground*, which is the term generally given to large regular geometric formations of earth, stones or vegetation that form on the surface of the ground. Typical examples of these phenomena include pingos, palsas, earth hummocks and stone circles.

Frost heave has been the subject of research since the early part of this century. Early experiments were conducted using closed systems[1] and these seemed to confirm the theory of the time that heave was a result of the increase in volume which occurs when water changes phase to ice. However, this theory was unable to explain such factors as the rhythmic banding of segregated seams of ice (ice lenses) that commonly form in heaved ground, nor could it account for excessive heaves of up to two feet which would require frozen front depths of some twenty feet in order to be explained using this theory. With the advent of the electric refrigerator, Taber (1930) was able to experiment extensively with open systems[2]. He found that he could not explain many of his observations using the above theory; most strikingly he found that if water is replaced with a liquid that solidifies with a *decrease* in volume, frost heave will still occur.

Taber's experiments revealed many other characteristics of the frost heave process. He found that in relatively incompressible soils ice lenses usually form and that their total thickness was equal to the amount of surface heave. Their formation seemed to depend on several factors, the most important being the size and shape of the soil particles, the rate of cooling and the surface load.

Taber put forward a tentative hypothesis to explain how an ice lens was able to grow in a freezing soil. He supposed the existence of a thin adsorbed film of water surrounding each soil particle separating it from the ice lens. He reasoned that because of the pore geometry, the water in the pores below the ice lens would not freeze readily but would remain in a supercooled state until the temperature had dropped sufficiently. The water in the adsorbed film in contact with the ice lens would freeze and thus the film's thickness would be reduced. Water would then be imbibed

[1] Unlike *open systems, closed systems* are unable to draw in or expel moisture.
[2] It is found that soil usually behaves as an open system.

from the pores below the lens in order to restore the film to its original thickness. (A further discussion of the mechanics of this adsorbed force, referred to as the *disjoining pressure*, can be found in Vignes-Adler (1977), Gilpin (1979) and Fowler & Krantz (1994).) This hypothesis seemed to explain many of the mechanisms of frost heave and was supported by Beskow (1935) who also undertook an extensive investigation into frost heave. Beskow substantiated many of Taber's findings. He gave a more lucid explanation than Taber for the frost heave process and also proposed empirical relationships for heave as a function of variables such as overburden and particle size.

The complexity of the frost heave process led to no significant advances being made for the next twenty years. Gold (1957) introduced the concept of surface tension at the ice/water interface. He applied basic thermodynamical laws (including surface tension) at the ice front in order to relate freezing point depression to the curvature of the ice/water interface. From these equations he was able to conclude, as had been thought by Taber and Beskow, that because the narrow channels connecting the pores imposed constraints on the ice curvature, the water in the pores below the ice lens would not freeze until the temperature had dropped sufficiently to allow the ice to penetrate these channels.

Gold's theory predicted that the advancing ice front would first penetrate into the pores with the largest inter-connecting channels. He proposed that once ice had penetrated these pores the lens would become 'anchored' to the soil and cease to grow. If this assumption were true it would be possible from knowledge of the distribution and size of the soil particles to calculate an upper limit on the heaving pressure attainable. However, calculations of this type are found to underestimate observed heaving pressures quite considerably. Further, given the condition for a lens to cease growing, this model predicts a discontinuous heave rate. However, Taber and Beskow both observed heave rate to be a continuous function of time. Around this time further significant contributions were also made to the understanding of the frost heave process by Penner (1959) and Everett (1961).

None of the above authors, however, gives a satisfactory explanation of where and why ice lenses form within the soil. Taber suggested that once ice had penetrated pores below the ice lens, the permeability would be so greatly reduced that eventually a new ice lens would form at the freezing front. However, he gave no physical

requirement for the formation of a new lens. Models which assume that the ice lenses form at the freezing front are commonly referred to as *primary heave* models.

There is a significant amount of literature which considers the mathematical analysis of so called primary frost heave models (see review by Fasano & Primicerio (1984)) although, in general, these models do not consider ice lens formation or any heave of the soil surface. Rather these models consider the growth of the pore ice phase within a saturated soil and commonly assume that the region above the freezing front is totally frozen. With this assumption there is no water flux through the frozen region and the problem reduces to a generalisation of a classical Stefan problem. For certain classes of this type of primary heave model, Aguirre-Puente & Frémond (1975) adopt a variational formulation to show the existence and uniqueness of a solution.

It is observed (see discussion by Miller (1978)) that the formation of new ice lenses actually occurs some way *behind* the freezing front and not *at* the freezing front as all the models so far discussed have suggested. It is difficult to understand why, in general, the frozen front should not advance into the pores beneath the lowest ice lens. Consideration of surface tension at the ice/water interface and the presence of any solutes in the pore water would allow the pore water to become supercooled and may, in certain circumstances, allow primary heave to occur. However, the amount of supercooling possible, especially in lightly saline soils, is relatively small and if the temperature in the pores were to fall below this temperature the ice phase would penetrate the pores and the primary heave assumption would break down.

The region below an ice lens that contains both water and ice is termed the *frozen fringe*. Miller (1972, 1977, 1978, 1980) developed a model of frost heave that allows the formation of ice lenses to occur within the frozen fringe. This mode of heave is known as *secondary heave* and is capable of attaining much higher heaving pressures than those generated in the primary mode of heaving considered by Gold because heave is no longer constrained by the anchor theory. Contrary to Gold's belief, Miller argues that ice in the pores below the lowest lens does not act as an anchor but rather moves through the pores by the process of *thermal regelation* (see chapter 2) at the *same velocity* as the ice lens. This model is referred to as the *rigid ice* model.

Miller's rigid ice model is difficult to conceptualise in any more than one dimension and cannot be readily extended for use in the analysis of differential frost heave.

Based on the work of Gilpin (1979), Fowler & Krantz (1994) suggest that the ice in the fringe moves, by a process of thermal regelation, with a velocity proportional to the temperature gradient. However, apart from the rigid ice assumption, Miller's model of secondary frost heave is acknowledged to be the most complete and accurate available and succeeds in predicting many of the characteristics of the frost heave process, including the formation of new lenses within the frozen fringe.

The equations that describe the physics of the Miller model are presented in chapter 2 and form a complex set of coupled, non-linear partial differential equations with three moving boundaries. O'Neill & Miller (1982, 1985) solved this set of equations numerically and found that their results were in good qualitative agreement with experimental observations of frost heave. However, the algorithm they used for this simulation was extremely complicated and not at all practical.

With such a complex formulation it is difficult to elucidate the physics and controlling factors of the frost heave process. Hence, Holden *et al.* (1985), Piper *et al.* (1988), Fowler (1989) and Fowler & Krantz (1994) all simplify the model significantly by supposing that certain fringe variables, namely temperature and water pressure, are quasi-static. Fowler & Krantz (1994) simplify the model further by neglecting small terms (e.g. convective heat transport), using the fact that the hydraulic conductivity function is strongly dependent on the water fraction to find an expression for the water pressure and showing that the frozen fringe is thin relative to the frost penetration depth. It is found that the resulting equations can be solved quite easily (see Fowler & Noon (1993)) while still giving good agreement with the full numerical solution of O'Neill & Miller. More recently, Krantz & Adams (1995) have obtained good quantitative agreement with laboratory investigations of Konrad (1989).

The results on existence and uniqueness described above for the growth of the pore ice have not yet been extended to the secondary heave models. However, in certain situations, the primary heave problem described in the above mathematical analysis may, in some sense, be a limit of the secondary frost heave process. In particular, in chapter 6 we consider the formation of massive ice within permafrost. We show that lens formation occurs in a fairly rapid transient and, following this, the frozen fringe continues to grow while heave (and hence water flux) proceeds at a very slow rate. In these circumstances, the secondary heave model effectively reduces to the primary

heave model and the results of the mathematical analysis described above may be applicable.

It should be noted that the Miller model of frost heave is by no means the only one available. Other models have been formulated but these are generally simplifications of the Miller model and often rely on empirical relationships in order to produce a model which is more amenable for analytic or numerical solution. For example, many of the alternative presentations assume that the ice pressure in the pores is hydrostatic and/or the ice phase is immobile while others neglect freezing in the frozen fringe. In fact, the Miller model is the only model to allow for the movement of ice within the frozen fringe and, without the thermal regelation of the pore ice, it is difficult to visualise how frost heave may occur. The only alternative explanation would be that the ice phase is not in fact solidly connected but that microscopic connections break as necessary at the base of the lowest ice lens to allow the soil to heave. However, O'Neill & Miller (1985) argue that this hypothesis breaks down because the ice is in a state of compression at the base of the lowest ice lens. O'Neill (1983) and Williams & Smith (1989) both discuss a number of models which fall into these categories and a more complete discussion on the alternative models and how they differ from the Miller model is given in Chapter 2.

1.2 Extensions

Chapter 2 extends the Miller model to a generalised form (the 'generalised Miller model') which is fully three dimensional and includes the effects of salinity and compressibility.

The non-dimensionalisation of the generalised model is presented in chapter 3 together with the derivation of an 'averaged' version of this model. The resulting simplification, although introducing an additional moving boundary (i.e. the lens front), removes the discontinuous nature of the model associated with ice lens formation, which is the main reason why numerical simulations are complex. The boundary conditions applicable in the generalised averaged case are also derived. The methods used by Fowler & Krantz (1994) are used to reduce the generalised model to a form which is more amenable to analytic and numerical solutions. Although much of this work is based on the results of the above authors, the analysis has been extended

to the generalised model and a modified presentation is given. In particular, a more rigorous derivation is given for the boundary conditions of the 'averaged' model.

Chapter 4 considers the one dimensional situation in the absence of salinity and compressibility effects. The results are based on those of Fowler (1989), Fowler & Krantz (1994), Fowler & Noon (1993) and Fowler *et al.* (1993). Essentially, we show that the frozen fringe is thin and find an explicit expression for the water pressure. These results enable the Miller model to be reduced to two ordinary differential equations which, by an appropriate change of variables, may be transformed to a linear system.

The resulting equations are solved and a comparison presented with the solution to the unreduced Miller model for heave, frozen front penetration, lens spacing and lens thickness. The heave rate is found to depend on a dimensionless parameter which is a function of soil type, temperature conditions and the overburden applied to the soil. For each soil type (i.e. sand, clay and silt) the functional dependence of this parameter on overburden is discussed and used to explain the observed characteristics of frost heave. An original explanation of the dependence of soil type on frost heave is presented.

Chapter 5 introduces the effects of salinity and uses a similar analysis to that given in chapter 4 to reduce the model to two coupled ordinary differential equations and a parabolic partial differential equation for solute concentration. An approximate analytic solution and a full numerical solution are given and a qualitative comparison with observed results of Chamberlain (1983) is presented. This original analysis shows good qualitative agreement with observation and indicates that the Miller model can be readily extended to include salinity effects.

The results and analysis given in chapters 6 and 7 again represent original work and are discussed below.

In areas of permafrost, segregated ice seams of metres in thickness are observed to occur in the top 50 m of the permafrost. These formations are referred to as 'massive ice' and are characteristic of the frost heave mechanism but on a much larger scale. In chapter 6 we present a generalised version of the Miller model with the inclusion of gravitational affects and couple this to the groundwater flow problem beneath the frozen front. The solution to the resulting model is able to explain some of

the traits of this massive ice formation. In particular, we suggest a possible reason why the thickness of massive ice lenses does not increase with depth as is usually characteristic of frost heave and why these formations are restricted to the top region of the permafrost.

When a soil heaves, pore water is imbibed from the unfrozen region below. This removal of water may result in the unfrozen region beneath the frozen front deforming (or consolidating). As such, the effects of compressibility are included in the frost heave model given in Chapter 6 and are included in the groundwater flow problem in the unfrozen region. The usual consolidation approach of Biot (1941) assumes that the soil matrix is elastic while assuming a relationship between the porosity and the dilation. However, in general, the conservation of mass equation should be used to determine the porosity of the soil matrix. We derive a theory of consolidation for small strains which uses the conservation of mass relation to determine the porosity and, in addition, considers both elastic and elastic/plastic (critical state) rheologies.

Chapter 7 considers differential frost heave with particular consideration to the formation of patterned ground. A model is presented for the rheology of the completely frozen soil above the lowest ice lens and a linear stability analysis given for the resulting problem. It is found that, for physically relevant parameter ranges, the Miller model is always stable but a possible mechanism for the onset of patterned ground is proposed in terms of the thickness of the snow covering.

The conclusions of the present study are given in Chapter 8. In the discussion we summarise the achievements of the present thesis and also indicate directions for further research.

Chapter 2

Secondary Frost Heave Models

2.1 Introduction

In this chapter we develop a generalised set of equations which describe the secondary frost heave process. These equations are based on the model developed by Miller (1978) and O'Neill & Miller (1982, 1985) with the following differences:

1. the equations are presented in a multi-dimensional[1] form so that differential frost heave may be considered;

2. solute effects are included; and

3. compressibility effects are included.

The only remaining complications which are not considered are the effects of heave in unsaturated soils and the thawing behaviour of heaved soils.

In the second part of this chapter we consider other models for the secondary frost heave process, their shortcomings and why we have adopted the Miller model as the basis for this thesis.

Before proceeding we give a brief description of the various soil types and how they are categorised. The categorisation of soil types is not unique but a typical categorisation of soil particles by their diameter would be as follows

Gravel	2 mm - 60 mm
Sand	0.06 mm - 2 mm

[1]The model derived in this chapter does not include all the intricacies of the three dimensional problem. In particular, we do not consider in any detail the rheology of the frozen or unfrozen soil. This behaviour is considered further in chapters 6 and 7.

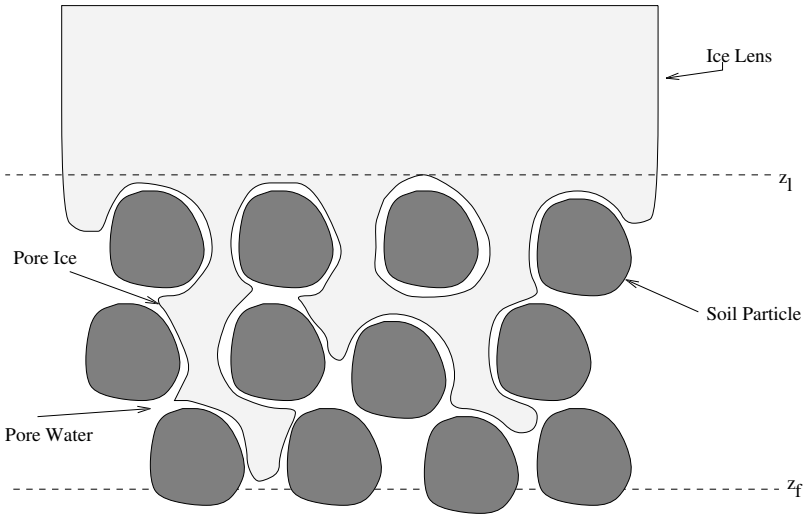


Figure 2.1: A schematic diagram of a frozen fringe.

Silt	0.002 mm - 0.06 mm
Clay	$<$ 0.002 mm.

Thus, in general, there is approximately an order of magnitude reduction in soil particle size between each soil type. Soils are generally composed of a mixture of the above soil types. Thus, for example, a soil may be categorised as a clayey silt or a silty sand.

The behaviour of mineral clay particles is dramatically different to the behaviour of the other soil types and, in particular, clay minerals are not grain like in nature but are plate like and attract water very strongly. Much of the discussion presented in this thesis does not strictly apply to soils composed only of clay particles and, as such when we refer to clay soils, we are referring, in general, to soils composed of very fine silt particles, or ones with a significant clay fraction.

2.2 The Miller Model

As discussed in the introduction, the fundamental difference between primary and secondary frost heave is the existence of a partially frozen region (the 'frozen fringe') between the base of the lowest ice lens and the frozen front. (A schematic representation of the frozen fringe is shown in figure 2.1.)

As such, a heaving soil is usually split into three sections; 1) the completely frozen soil above the base of the lowest ice lens (this region contains ice lenses separated by

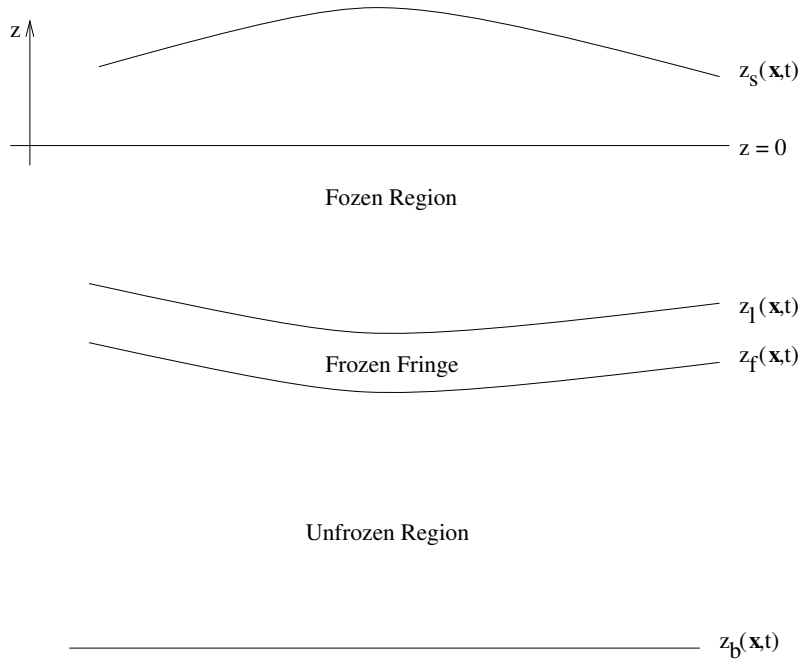


Figure 2.2: Schematic plot of a heaved soil indicating the three distinct regions; the frozen soil, the frozen fringe and the unfrozen soil.

regions of soil matrix, interstitial ice, trapped solutes and adsorbed water); 2) the frozen fringe; and 3) the unfrozen region below the frozen front. This situation is shown schematically in figure 2.2. The location of the soil surface is given by $z_s(\mathbf{x}, \mathbf{t})$, the base of the lowest ice lens is given by $z_l(\mathbf{x}, \mathbf{t})$, the base of the frozen fringe is given by $z_f(\mathbf{x}, \mathbf{t})$ and the base of the soil sample is given by $z_b(\mathbf{x}, \mathbf{t})$.

In the sections that follow we discuss the equations that are applicable in the three regions given above. These are first developed for the frozen fringe (which forms the most complex region) and then for the remaining regions. Boundary conditions are also presented and consideration is given to both the laboratory situation, in order that some form of comparison with experiment can be given, and those which occur in the field.

2.2.1 Conservation of Mass

The frozen fringe comprises three distinct phases, namely soil, pore water and ice (consideration of the solute phase is given in section 2.2.4). The ice and water phases are coupled via a source term which arises because of ice production in the fringe.

Suppose that a soil has porosity, $\phi(\mathbf{x}, t)$, with water and ice volume fractions

given by $W(\mathbf{x},t)$ and $I(\mathbf{x},t)$ respectively (so that $\phi = I + W$). Consideration of mass conservation for each phase gives

$$\begin{aligned} \frac{\partial}{\partial t}(1-\phi) + \boldsymbol{\nabla}.((1-\phi)\mathbf{u}_s) &= 0, \\ \frac{\partial W}{\partial t} + \boldsymbol{\nabla}.(W\mathbf{u}_w) &= -\frac{S_f}{\rho_w}, \\ \frac{\partial I}{\partial t} + \boldsymbol{\nabla}.(I\mathbf{u}_i) &= \frac{S_f}{\rho_i}, \end{aligned} \tag{2.1}$$

where ρ_w and ρ_i are the densities of water and ice; $\mathbf{u}_s$, $\mathbf{u}_w$ and $\mathbf{u}_i$ are the velocities of the soil matrix, pore water and ice respectively, and S_f is the rate of freezing.

2.2.2 Conservation of Energy

Due to the multi-phase nature of the frozen fringe, a strict formulation of a conservation of energy relationship would be extremely complex. For example, some account should be taken of body forces, pressure changes, stress and interaction between phases. However, common assumptions in writing down the energy balance are that the dominant terms in the conservation of energy equation are the heat conduction and heat convection terms and that the temperature in each of the three phases is equal. Thus the conservation of energy equation can be taken to be as follows

$$-LS_f + \frac{\partial}{\partial t}(\rho C_p T) + \boldsymbol{\nabla}.(\rho C_p \mathbf{U} T) = \boldsymbol{\nabla}.(k\boldsymbol{\nabla}T), \tag{2.2}$$

where L is the latent heat of fusion and

$$\begin{aligned} \rho &= W\rho_w + I\rho_i + (1-\phi)\rho_s, \\ \rho C_p &= W\rho_w c_w + I\rho_i c_i + (1-\phi)\rho_s c_s, \\ \rho C_p \mathbf{U} &= W\rho_w c_w \mathbf{u}_w + I\rho_i c_i \mathbf{u}_i + (1-\phi)\rho_s c_s \mathbf{u}_s, \\ k &= Wk_w + Ik_i + (1-\phi)k_s, \end{aligned}$$

the c_j and k_j being the specific heat capacities and thermal conductivities respectively of each of the three phases. Other ways of averaging the thermal conductivities are possible.

The conservation of mass equations may be combined to give

$$\frac{\partial}{\partial t}(\rho C_p) + \boldsymbol{\nabla}.(\rho C_p \mathbf{U}) = (c_i - c_w)S_f, \tag{2.3}$$

which allows equation 2.2 to be written as

$$-LS_f + (c_i - c_w)\, S_f T + \rho C_p \frac{dT}{dt} = \boldsymbol{\nabla}.(k\boldsymbol{\nabla}T). \tag{2.4}$$

where d/dt is the material derivative $\partial/\partial t + \mathbf{U}.\boldsymbol{\nabla}$.

Now, the difference in specific heat capacities $c_i - c_w$ is $\sim 2 \times 10^3\,\mathrm{J\,kg^{-1}\,K^{-1}}$ while the latent heat of fusion L is $\sim 3 \times 10^5\,\mathrm{J\,kg^{-1}}$. Thus, for the temperature range we consider the specific heat term $(c_i - c_w)\, S_f T$ may be neglected in comparison to the latent heat term LS_f and the resulting conservation of energy equation can be written as

$$-LS_f + \rho C_p \frac{dT}{dt} = \boldsymbol{\nabla}.(k\boldsymbol{\nabla}T). \tag{2.5}$$

2.2.3 Osmosis and the Clapeyron equation

The temperature in the frozen fringe can be related to the ice and water pressures via a generalised form of the Clapeyron equation. The standard form of the Clapeyron equation requires that the ice and water must be in both mechanical (ice and water at the same pressure) and thermal (ice and water at the same temperature) equilibrium. However, in a frozen soil the capillary-like nature of the pores allows a curvature to develop at the ice/water interface. This curvature, because of the effect of surface tension, gives rise to a pressure differential between the two phases thus violating the requirement of mechanical equilibrium. Loch (1978) derives a generalised form of the Clapeyron equation in which mechanical equilibrium at the ice/water interface is not assumed but rather the chemical potentials (see Smith (1989)) in the ice and liquid are equated. He arrives at an equilibrium equation, approximately true for small deviations in temperature from the freezing point. The freezing temperature, T, is given by

$$\frac{1}{\rho_w}(p_w - \Pi) - \frac{p_i}{\rho_i} = \frac{L}{T_0}(T - T_0), \tag{2.6}$$

where p_w and p_i are the gauge pressures (i.e. the pressure in excess of atmospheric pressure) of the water and ice respectively, T_0 is the melting point of ice, L is the latent heat of fusion and Π is the osmotic pressure (see Hillel (1980)).

The osmotic pressure term arises through the presence of solutes in the soil and the difference in solute concentrations in ice and water. Smith (1989) shows that for

relatively dilute solutions the osmotic pressure is given by

$$\Pi = RcT, \tag{2.7}$$

where T is the temperature in degrees Kelvin, c is the molar concentration of solute particles and R is the gas constant ($8.3\,\mathrm{J\,K^{-1}\,mole^{-1}}$).

Substituting this equation into the Clapeyron equation and using the fact that in our context $T_0 Rc/\rho_w L \ll 1$ we find, ignoring small quantities, that

$$T - T_0 = \frac{T_0}{L\rho_w} p_w - \frac{T_0}{L\rho_i} p_i - \frac{T_0^2 R}{L\rho_w} c. \tag{2.8}$$

This equation may more conveniently be written as

$$T - T_0 = -\frac{T_0}{L\rho_w}(\delta p_w + (1+\delta)(p_i - p_w)) - \frac{T_0^2 R}{L\rho_w} c, \tag{2.9}$$

where

$$\delta = \frac{\rho_w - \rho_i}{\rho_i}. \tag{2.10}$$

2.2.4 Solute Transport Equation

In order to determine a transport equation for solute concentration we consider conservation of mass for the solute phase. It is assumed that freezing occurs so slowly that all solutes are frozen out of the ice and remain in the liquid phase and that no sources or sinks exist in the soil[2]. With these assumptions we get

$$\frac{\partial}{\partial t}(WC^*) = -\boldsymbol{\nabla}.(W\mathbf{q}), \tag{2.11}$$

where C^* is the mass of solute per unit volume of liquid and $\mathbf{q}$ is the flux of solutes in the liquid.

The flux of solutes can effectively be split into three parts, 1) diffusion of solutes down concentration gradients, 2) convection caused by the liquid motion and 3) hydrodynamic dispersion caused by microscopic velocity fluctuations in the soil's conducting pores. The first of these is known as Fick's Law (Bear (1988)) and can be combined with the second to give

$$\mathbf{q} = C^* \mathbf{u}_w - \mathbf{D}'.\boldsymbol{\nabla} C^*, \tag{2.12}$$

[2]For example it is assumed that solutes do not become adsorbed to soil particles.

where $\mathbf{D}'$ is the diffusivity term which is found to depend strongly on water content[3].

Hillel (1980) and Bear (1988) both argue that hydrodynamic dispersion can be included in the model by simply adding a coefficient, $\mathbf{D}_d$, to the coefficient of diffusivity in Fick's Law. Bear states that this coefficient obeys a law of the form

$$\mathbf{D}_d \sim a\overline{V}^{\eta}, \tag{2.13}$$

where a is some characteristic dimension of the pore micro-structure (e.g. pore length), $\overline{V}$ is the average flow velocity and η is a constant that takes a value between 1 and 2.

Writing $\mathbf{D} = \mathbf{D}' + \mathbf{D}_d$ and noting that for relatively dilute solutions C^* is proportional to c as defined in the Clapeyron equation, the conservation of mass equation gives

$$\frac{\partial}{\partial t}(Wc) = \boldsymbol{\nabla}.(W\mathbf{D}.\boldsymbol{\nabla}c) - \boldsymbol{\nabla}.(Wc\mathbf{u}_w). \tag{2.14}$$

2.2.5 Similitude and the Capillary Relation

If an increasing suction is applied to an unfrozen soil, water will not necessarily be drawn instantaneously from it. The reason for this phenomenon depends primarily on soil type. In soils that are effectively devoid of colloidal particles (SS-soil) (i.e. granular soils, e.g. gravel, sand and silt) the curvature at an air/water interface must be large enough for water to be drawn from a soil pore. The relationship between gauge water pressure, p_w, gauge air pressure, p_a, and curvature is given by the equation

$$p_a - p_w = \sigma_{aw}\left(\frac{1}{r_1} + \frac{1}{r_2}\right), \tag{2.15}$$

where σ_{aw} is the surface tension and r_1 and r_2 are principal radii of curvatures of the air/water interface.

Increasing the suction, $p_a - p_w$, allows larger curvatures to develop and thus more and more pores are able to empty. Hence it is clear that in SS-soil, water content is a function of suction alone.

In soils entirely composed of colloidal particles (SLS-soil) (i.e non-granular soils, e.g. clay), water is adsorbed to the surface of the soil particles. With increasing suction, an increasing amount of water is able to overcome the adsorbed forces and

[3]Hillel (1980) notes that $\mathbf{D}'$ should also depend on tortuosity but argues that tortuosity is strongly dependent upon water content.

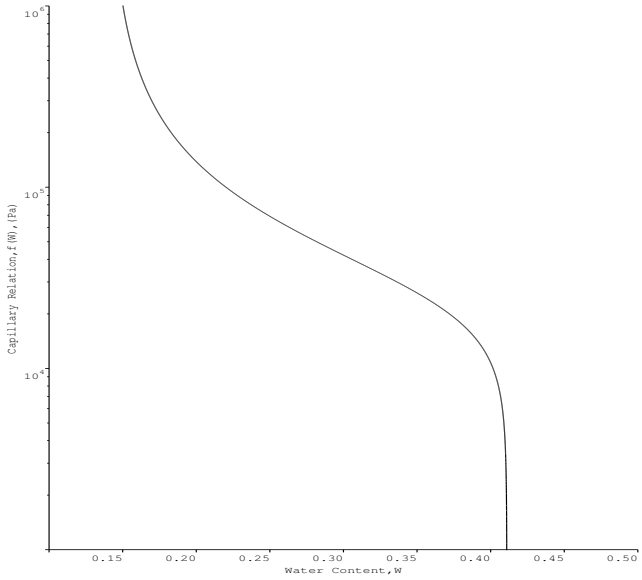


Figure 2.3: Plot of a typical capillary suction curve for a silty soil. Taken from O'Neill and Miller (1985) and used in the numerical results presented in chapter 4.

thus the water content decreases. Again we can conclude that water content is a function of $p_a - p_w$.

The relationship between suction and water content is referred to as the Soil Water Characteristic curve (SWC). Koopmans & Miller (1966) found that similar curves are obtained if the difference in ice and water pressure is plotted against water content in a freezing saturated soil. These curves are referred to as Soil Freezing Characteristic curves (SFC). For the purposes of our work we ignore the effects of hysteresis which arise on freezing and subsequent thawing and use the resulting capillary relation

$$p_i - p_w = f(S), \tag{2.16}$$

where S is the relative water saturation W/ϕ. (A typical capillary relation is given in figure 2.3.)

Miller (1966), and Koopmans & Miller (1966), argue that analogies can be drawn between the drying and wetting of ice-free soil and the freezing and thawing of air-free soil. Koopmans & Miller (1966) show empirically that for SLS-soils the SWC curve and the SFC curve coincide, while in SS-soils these curves coincide if $p_i - p_w$ is scaled by σ_{aw}/σ_{iw}, where σ_{iw} is the surface tension at the ice/water interface. Miller refers to this analogy as similitude and, since more studies have been conducted on unfrozen

unsaturated soil, he uses it frequently throughout his work.

2.2.6 The Liquid and Ice Fluxes

The conservation of momentum relation takes the form of Darcy's Law which, in its three dimensional form, is as follows

$$W\mathbf{u}_w = -\frac{k_h}{\rho_w g}\boldsymbol{\nabla}(p_w + \rho_w g z), \tag{2.17}$$

where g is the acceleration due to gravity and k_h is known as the hydraulic conductivity.

Fundamentally, Darcy's Law is an expression of conservation of linear momentum and as such could be replaced by a macroscopic momentum equation. However, it is found that if inertia terms are small, the resulting equation reduces to Darcy's Law.

The expression given above assumes that the soil is isotropic and that the soil matrix is rigid. Scheidegger (1957) suggested that water flux in an anisotropic soil with a moving soil skeleton should obey the law

$$W(\mathbf{u}_w - \mathbf{u}_s) = -\frac{1}{\rho_w g}(\mathbf{k}_h.\boldsymbol{\nabla})(p_w + \rho_w g z). \tag{2.18}$$

where $\mathbf{k}_h$ is a tensor.

Few studies have been conducted into the applicability of Darcy's Law in a freezing soil. However, Richards (1931) considered flows through unsaturated soils and suggested that the water flux through the pores should still be governed by a Darcy type law, but that the hydraulic conductivity should be a function of water content. Miller (1980) invokes the idea of similitude to suggest that water flux in a saturated frozen soil should obey this same rule. O'Neill & Miller (1982, 1985) suggest a possible form for the dependence of hydraulic conductivity, k_h, on the water content, W, in an isotropic soil as follows

$$k_h(W) = k_0\left(\frac{W}{\phi}\right)^{\gamma} = k_0 S^{\gamma}, \tag{2.19}$$

where O'Neill & Miller (1982) use $\gamma = 7$ but later argue (1985) that this value is too small and use $\gamma = 9$. The form of this hydraulic conductivity function plays a crucial role in the analysis presented in the following chapter. Essentially, the strong dependence of the hydraulic conductivity function on the water content, through the large parameter γ, allows the form of the water pressure p_w to be determined.

As discussed previously, Miller's theory of secondary frost heave allows the ice phase to grow into the pores below the lowest ice lens[4]. Ice being a solid, it seems difficult to visualise how an ice lens is capable of continued growth while connected to ice in the frozen fringe. This apparent paradox is explained by Miller (1978, 1980) using the concept of regelation.

Regelation occurs when particles move through ice under an applied pressure or temperature gradient. In either of these cases a particle is able to move by continual thawing and re-freezing of the ice around the particle. Regelation under an applied pressure is readily seen using the classic experiment of placing a thin wire with weights at each end over a block of ice. The wire is seen to pass through the ice while leaving it as a solid block. Investigations into thermally induced regelation have been conducted by Hoekstra & Miller (1967), Römkens & Miller (1973) and Gilpin (1979). Gilpin (1979) derives a theoretical relationship for the ice velocity in terms of the temperature gradient and applied pressure.

Miller suggests that if soil particles are held stationary then thermal regelation will cause ice in the frozen fringe to move towards the ice lens (i.e. towards lower temperatures). Miller assumes that the ice in the fringe moves with a velocity dependent only on time (i.e as a rigid body) equal to the rate of heave. However, for differential frost heave, the non-spatial dependence of the ice velocity clearly breaks down and, as such, this model for ice velocity can only be considered in the one dimensional case. Thus, in this situation, the ice velocity is given by

$$u_i = u_i(t). \tag{2.20}$$

Fowler & Krantz (1994) suggest that, in general, the ice velocity in the fringe is given by a form of the relationship established by Gilpin (1979) as follows

$$\mathbf{u}_i - \mathbf{u}_s = -\lambda \boldsymbol{\nabla} T, \tag{2.21}$$

where we take λ to be a constant, the value of which is inferred from the works cited above. The value of λ should strictly be a temperature dependent function (see Römkens & Miller (1973) and Gilpin (1979)). Here, we assume that λ is independent of temperature; its value is discussed further in appendix B.

[4]The ability of soil moisture to supercool by several degrees allows the ice in a saturated soil to grow as a continuous phase.

We briefly consider the mechanics of equation 2.21. As previously discussed, thin adsorbed water films separate the soil particles and the ice phase. Under an applied temperature gradient, these films will be thinner where the temperature is colder and hence we expect the film thickness to be proportional to the temperature gradient. Now, the forces which exist in these thin films are dominated by the 'disjoining pressure' force which is thought to take the following form (see Gilpin (1979), Fowler (1996))

$$p_i^m - p_w^m = \frac{c}{h^\alpha}, \tag{2.22}$$

where p_i^m and p_w^m are the microscopic ice and water pressures, c and α are constants and h is the film thickness. If we assume that the microscopic ice pressure is approximately a constant, then the above equation implies that a gradient in the film thickness induces a negative gradient in the water pressure. Thus, this negative gradient in water pressure will induce a microscopic upward water flux to try and restore a uniform film thickness. This increase in film thickness will cause the soil particles and ice phase to move away from each other, the ice moving upwards and the soil particles moving down.

There have been few experiments which consider thermal regelation and the appropriate value of λ. Romkens & Miller (1973) consider the velocity of 25 μm glass beads through ice under a fairly large temperature gradient. The value of λ applicable to this situation can be inferred from their results as

$$\lambda \sim 10^{-10}\,\mathrm{m^2\,s^{-1}\,K^{-1}}, \tag{2.23}$$

at a temperature of -0.1° C. Further discussion of this important issue is given in appendix B, where a resumé of Gilpin's theory is given. While a range of values of λ up to $10^{-8}\,\mathrm{m^2\,s^{-1}\,K^{-1}}$ is possible, we will focus on the value given by 2.23 in this thesis.

2.2.7 Mechanics of the Soil Matrix

If we assume that individual soil particles are incompressible, then, when stresses are applied to a soil, the only means by which the soil may change volume is through the expulsion or intake of pore fluid. The behaviour of the soil matrix under a particular range of applied stresses can be either elastic or plastic depending on whether the

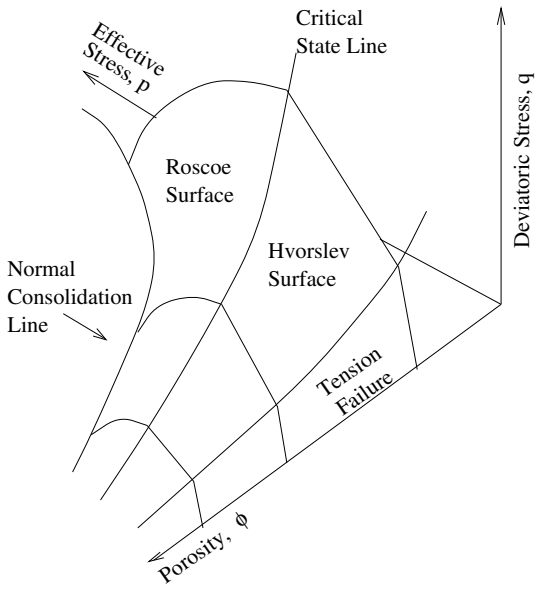


Figure 2.4: A schematic plot of the State Boundary Surface.

stresses which are applied fall under or on the State Boundary Surface (see figure 2.4). For stress paths under this surface the soil matrix deformations are elastic and recoverable while movement across this surface is plastic and irrecoverable.

The State Boundary Surface comprises three distinct regions, the Roscoe Surface, the Hvorslev Surface and the Tension Failure Surface. Failure of the soil matrix occurs at the Critical State Line which joins the Roscoe Surface and the Hvorslev Surface.

The mechanical behaviour of a soil is governed by the range of stresses applied to the soil matrix and the stress path followed beneath and on the State Boundary Surface. A further discussion and analysis of the mechanical behaviour of soil is given in chapter 6 and for the remaining part of this chapter we consider the situation wherein the deviatoric stress is zero and the soil moves along the 'Normal Consolidation Line'. This process is referred to as consolidation and is one of the fundamental processes of soil mechanics.

The change in volume of a soil element is governed by the 'effective pressure' (see section 2.2.8) in the soil matrix (see Skempton (1960), Biot (1941, 1955) and Gibson *et al.* (1967)) and a typical relationship for a consolidating soil under a sufficiently large effective stress is as follows:

$$\frac{\phi(p_e)}{1-\phi(p_e)} = \frac{\phi_0}{1-\phi_0} + C\log\left(\frac{p_e}{p_0}\right), \tag{2.24}$$

where p_0 and ϕ_0 are the soil's initial effective pressure and porosity respectively and C is a constant called the index of compression.

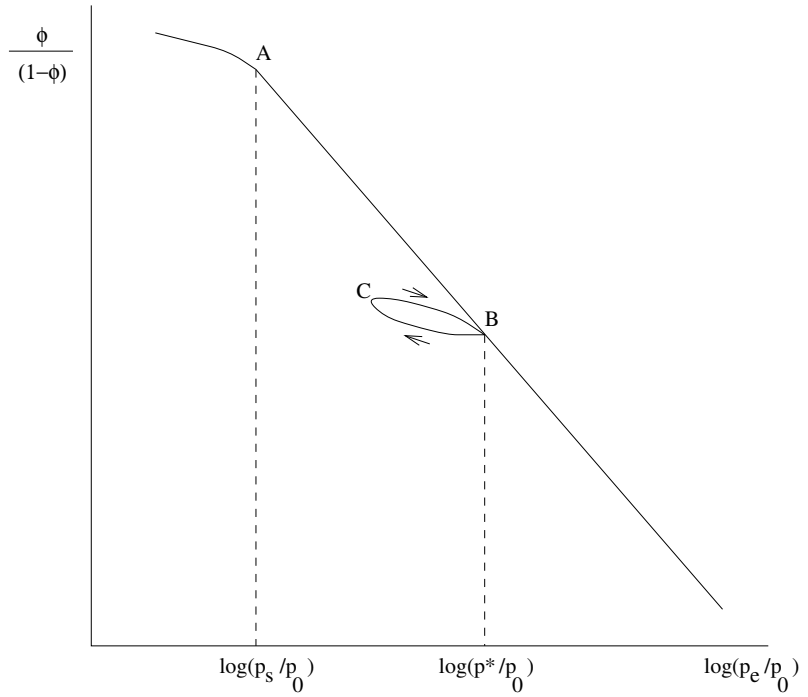


Figure 2.5: A schematic diagram of the typical behaviour of a soil on the normal consolidation line.

It is found that soils have a memory property whereby they remember the previous maximum effective pressure, p_s, to which they have been subjected and for effective pressures above this maximum value soils behave according to the relationship given above. However, below this level, the change in volume witnessed is much less than that predicted via the above formula and a typical relationship is shown in figure 2.5.

For example, suppose a soil is at a point A on the normal consolidation line under an effective stress equal to the maximum value it has experienced, p_s. If the effective stress is increased to p^*, the soil's porosity moves along the normal consolidation line to B. On subsequent unloading to a point C and reloading back to B the soil's porosity would typically follow a path as illustrated. While the porosity follows a path away from the normal consolidation line, the soil is referred to as being over consolidated. In our analysis we ignore the hysteresis that is observed when unloading and reloading an over-consolidated soil.

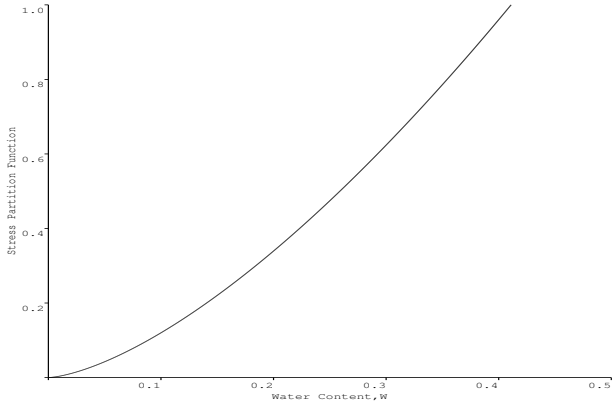


Figure 2.6: A plot of a typical capillary suction curve as used in the numerical results given in chapter 4

2.2.8 Initiation of an Ice Lens

Terzaghi (1936) showed empirically that the compression and strength of a saturated soil is determined by the effective stress, p_e, given by the relation

$$p_e = P - p_w, \tag{2.25}$$

where P is the confining pressure and p_w is the pressure in the permeating liquid.

Bishop & Blight (1963) suggest that Terzaghi's result can be extended to the case of two permeating continua (in our case ice and water) by defining effective stress as

$$p_e = P - (1 - \chi)p_i - \chi p_w, \tag{2.26}$$

where χ is a stress partition function. This relationship may be more conveniently written as

$$p_e = P - (1 - \chi)(p_i - p_w) - p_w. \tag{2.27}$$

If the two permeating fluids are air and water, it is found that χ is strongly dependent on relative water saturation, S, (although it is also influenced by other factors such as soil structure and the process of wetting and drying). (A typical form for the stress partition function is given in figure 2.6.)

In an SS-soil, the effective stress is approximately the stress between the soil grains, the difference being related to the area of contact between the soil grains (see

Skempton (1960)). For most purposes the corrective factor is small and we will ignore it in our analysis. Miller uses this in his model to determine the location of a new lens. He argues that if the effective pressure becomes zero within the soil, the soil particles there will readily separate and this location will be the most favourable position for the formation of a new lens. Thus, in the Miller model, the condition for new lens formation is

$$p_e = 0. \tag{2.28}$$

It is worth pointing out that this criterion is a mechanical condition rather than a thermal one and, as such, gives rise to the existence of an additional distinct region which could also be included in the generalised Miller model (see Fowler & Krantz (1994)). This region contains ice lenses which are separated by regions of 'partially' frozen soil which freeze on the conductive time scale. This additional region makes little difference to the resulting analysis but acts to make the model even more complex and we therefore exclude this region from the generalised model.

2.2.9 Frozen and Unfrozen Regions

The equations applicable in these regions are mostly a subset of those which arise in the frozen fringe, simply with fewer phases and no latent heat term. Thus, in the frozen region $z_s(\mathbf{x}, t) > z > z_l(\mathbf{x}, t)$, the governing equation is

$$\rho C_p \frac{dT}{dt} = \boldsymbol{\nabla}.(k_f \boldsymbol{\nabla} T). \tag{2.29}$$

where k_f is the thermal conductivity of the frozen soil. In addition, information about the rheology of this region is required in order to relate the flux at the base of the lowest ice lens to the displacement of the surface $z_s(\mathbf{x}, t)$. A full discussion of the rheology of ice segregated soil is presented in chapter 7 where we consider differential frost heave. However, in the chapters preceding chapter 7 we only consider the one dimensional situation and, in this case, the surface heave is simply given by the net flux at the base of the lowest ice lens and the rheology of the frozen soil is not required for the solution.

In the unfrozen region $z_f(\mathbf{x}, t) > z > z_b(\mathbf{x}, t)$, the governing equations are

$$\frac{\partial}{\partial t}(1 - \phi) + \boldsymbol{\nabla}.((1 - \phi)\mathbf{u}_s) = 0$$

$$
\begin{aligned}
&\frac{\partial W}{\partial t} + \boldsymbol{\nabla}.(W\mathbf{u}_w) = 0 \\
&\rho C_p \frac{dT}{dt} = \boldsymbol{\nabla}.(k_u \boldsymbol{\nabla} T) \\
&\phi(\mathbf{u}_w - \mathbf{u}_s) = -\frac{k_0}{\rho_w g}\boldsymbol{\nabla}(p_w + \rho_w g z) \\
&P = p_e + p_w \\
&\frac{\partial}{\partial t}(Wc) - \boldsymbol{\nabla}.(W\mathbf{D}.\boldsymbol{\nabla} c) + \boldsymbol{\nabla}.(Wc\mathbf{u}_w) = 0, \qquad (2.30)
\end{aligned}
$$

where k_u is the thermal conductivity of the unfrozen soil. In addition, a total stress balance and the constitutive stress/strain relations are required for the rheology of this region. A brief discussion of soil rheology was given in section 2.2.7 and a more complete discussion and a derivation of the governing equations are given in chapter 6.

2.2.10 Boundary Conditions

In general, the prescription of the boundary conditions depends on whether we consider laboratory conditions or conditions which are applicable in the field. In particular, laboratory tests are usually conducted on small samples of soil under high temperature gradients and are run for relatively short time periods (e.g. days). In the field situation, the frozen front can be hundreds of metres below the surface, shallow temperature gradients usually apply and the time scale can be extremely long. We present the boundary conditions applicable in both situations.

The boundary conditions at the surface of the soil, $z_s(\mathbf{x}, t)$, are taken as prescribed temperature and pressure (overburden) relations

$$
\begin{aligned}
T &= T_s(\mathbf{x}, t), \\
P &= P(\mathbf{x}, t). \qquad (2.31)
\end{aligned}
$$

Similarly, the boundary conditions at the base of the soil, $z_b(\mathbf{x}, t)$, are prescribed. However, the prescription of these boundary conditions depends on whether we consider laboratory or field conditions. In laboratory tests, the boundary conditions at $z_b(\mathbf{x}, t)$ would typically be

$$
\begin{aligned}
&T = T_b(\mathbf{x}, t) \\
&u_{sn} = 0,
\end{aligned}
$$

$$p_w = p_\infty(\mathbf{x}, t)$$
$$c = c_\infty(\mathbf{x}, t), \tag{2.32}$$

where the suffix n denotes the upward normal component and $p_\infty(\mathbf{x}, t)$, $c_\infty(\mathbf{x}, t)$ and $T_b(\mathbf{x}, t)$ represent the prescribed basal water pressure, salinity and temperature profiles.

The field boundary conditions are discussed in more detail in chapter 6 where the groundwater flow problem in the unfrozen region is solved. However, we give here a brief discussion of the differences between the field and laboratory problems. In the field, the water table will usually be restricted at the base by some impermeable material which would usually be some way below the frozen front. This condition can be idealised by letting $z_b(\mathbf{x}, t) \to -\infty$. The water pressure would continue to have some prescribed far field value due to the presence of external supplies of water (e.g. oceans, seas or lakes) and similarly the far field salinity would be prescribed. The far field temperature condition would not be a prescribed temperature but rather a prescribed heat flux. This arises because the earth's mantle radiates a heat flux G equal to approximately $0.05\,\mathrm{W\,m^{-2}}$. Thus the temperature condition at the far field would be

$$-k_u \frac{\partial T}{\partial n} = G. \tag{2.33}$$

This heat flux is equivalent to a temperature gradient of approximately 1 K per 50 m and, in field conditions, acts to define an appropriate length scale (see chapter 3). Finally, we would have $u_{sn} = 0$ on the impermeable base and no water flux through this boundary.

Boundary conditions at the frozen front $z_f(\mathbf{x}, t)$ are continuity conditions for fluxes and internal variables across this boundary. Thus we have

$$[T]^+_- = 0,$$
$$[p_w]^+_- = 0,$$
$$[u_w]^+_- = 0,$$
$$[u_i]^+_- = 0,$$
$$[u_s]^+_- = 0,$$
$$[c]^+_- = 0,$$

$$\left[\frac{\partial c}{\partial n}\right]_-^+ = 0, \tag{2.34}$$

where $[\ ]_-^+$ denotes the difference of the quantity on each side of the boundary. The general Stefan condition at this boundary can be written as

$$[I]_-^+ V_f = [I]_-^+ u_{in} + \left[\frac{k}{L\rho_i}\frac{\partial T}{\partial n}\right]_-^+,$$

where V_f is the rate of growth of the ice phase at the frozen front and can be related to the frozen front position $z_f(\mathbf{x}, t)$ through a kinematic condition at the frozen front. For simplicity we have assumed that the thermal conductivities of the unfrozen soil and frozen fringe (i.e. k_u and k respectively) are equal. The final boundary condition needs to be an expression for the change in ice fraction (or equivalently the water fraction) across the frozen front.

Miller (1978) indicates schematically that the ice pressure (and hence the ice fraction) is non-zero at the frozen front. However O'Neill & Miller (1985) present a numerical solution to the Miller model that indicates a zero ice pressure at the frozen front (see their figure 3).

Holden *et al.* (1985) and Piper *et al.* (1988) present an analysis of the Miller model of secondary frost heave that considers a non-zero ice fraction at the frozen front. However, the ice fraction at this boundary is found by specifying the temperature at the frozen front. Specification of this temperature does not correspond to any physical condition and is essentially equivalent to specifying the ice fraction.

Fowler (1989) and Fowler & Krantz (1994) assume a zero ice fraction at the frozen front.

There would appear to be no experimental or theoretical basis for a non-zero jump in ice fraction at the frozen front. In particular, the existence of a frozen fringe arises because, if the ice phase were not to grow into the pores beneath the lowest ice lens, the pore fluid in this region would be below its Clapeyron freezing temperature (i.e. supercooled). This would suggest that a reasonable condition to apply at the freezing front would be one of no supercooling (i.e. $[I]_-^+ = 0$).

In addition, the frozen fringe can be thought of as being analogous to the existence of 'mushy zones' that arise in alloy solidification problems (see Fowler (1985)), in which an analogous assumption is often made.

Therefore, although there is no formal basis for supposing that the ice fraction at the frozen front is zero, it would seem reasonable to make this assumption and it has been adopted for the purposes of this thesis. Thus the boudary conditions we use at $z = z_f(\mathbf{x}, \mathbf{t})$ are as follows

$$\begin{aligned}
&[S]_-^+ = 0, \\
&[T]_-^+ = 0, \\
&\left[\frac{\partial T}{\partial n}\right]_-^+ = 0, \\
&[p_w]_-^+ = 0, \\
&[u_w]_-^+ = 0, \\
&[u_i]_-^+ = 0, \\
&[u_s]_-^+ = 0, \\
&[c]_-^+ = 0, \\
&\left[\frac{\partial c}{\partial n}\right]_-^+ = 0,
\end{aligned} \tag{2.35}$$

Finally, we consider the necessary conditions at the base of the lowest ice lens $z_l(\mathbf{x}, t)$. The temperature and stress conditions are again continuity conditions while the remaining boundary conditions are simple mass and energy balances (the latter a Stefan condition). Thus we have

$$\begin{aligned}
&[T]_-^+ = 0, \\
&p_i = P, \\
&cWu_{wn} - DW\frac{\partial c}{\partial n} = Wcu_{sn}, \\
&Wu_{sn} - Wu_{wn} = \frac{1}{L\rho_w}\left[k\frac{\partial T}{\partial n}\right]_-^+, \\
&u_i^+ = (1+\delta)Wu_{wn} + (\phi - W)u_{in} + (1 - \phi - \delta W)u_{sn},
\end{aligned} \tag{2.36}$$

where u_i^+ is the ice flux at the base of the ice lens, W refers to the water volume fraction just below the lens, and again $\delta = (\rho_w - \rho_i)/\rho_i$. The ice flux at the base of the ice lens is related to the surface displacement via the rheology of the frozen soil. However, in the one dimensional case the rheology is not required and we have

$$\dot{z}_s = u_i^+. \tag{2.37}$$

In addition, we have a kinematic condition which equates the soil matrix velocity and the lens velocity at $z_l(\mathbf{x}, t)$. In one dimension this condition is expressed as

$$\dot{z}_l = u_s, \tag{2.38}$$

at $z_l(\mathbf{x}, t)$.

2.3 Other Models

It appears to be generally accepted that the Miller model of secondary frost heave formulates the most complete description of the frost heave process (see Gilpin (1980)). However, it can be argued that the resulting model is far too complex for use in prediction or understanding how particular physical conditions affect the frost heave process. As a result, a number of other, less complex models have been developed, which attempt a simpler formulation of secondary frost heave. In general, these models tend to be less complete than the Miller model and in some cases rely on empirical relationships.

Although a number of authors have put forward alternative formulations to that proposed by Miller, they tend to fall into two distinct categories which we call hydrodynamic models and other models and each of these approaches is discussed below.

2.3.1 The Hydrodynamic Model

Harlan (1973) set out the equations describing the transport of heat and moisture in a freezing soil. These equations have subsequently been used by a number of authors to form the basis of what we have termed hydrodynamic models.

The hydrodynamic model is based on the physical processes described in the preceding section with the following simplifying assumptions:

1. the soil is one dimensional, solute free and incompressible (i.e. ϕ is a constant and, as such, $u_s = 0$);

2. the ice pressure is either not considered or is assumed to be atmospheric;

3. the interstitial ice is assumed to be immobile;

4. the effects of gravity are negligible; and

5. the convective heat flux is negligible.

These assumptions allow us to reduce the Miller model equations for the frozen fringe described above to

$$\begin{aligned}
&\phi = W + I, \\
&-\frac{\partial}{\partial z}(W u_w) = \frac{\partial W}{\partial t} + \frac{\rho_i}{\rho_w}\frac{\partial I}{\partial t} \\
&W u_w = -\frac{k_h}{\rho_w g}\frac{\partial p_w}{\partial z} \\
&\rho C_p \frac{\partial T}{\partial t} = \frac{\partial}{\partial z}\left(k\frac{\partial T}{\partial z}\right) + \rho_i L \frac{\partial I}{\partial t}.
\end{aligned} \tag{2.39}$$

These four equations are for the five unknown variables W, I, p_w, u_w and T and, as such, a fifth relation is required to complete the system. This final equation is often some form of empirical relation between water content, W, and temperature, T, or water pressure, p_w (e.g. Taylor & Luthin (1978), Berg *et al.* (1980), Guymon *et al* (1980)). However, some authors (e.g. Konrad & Morgenstern (1980) and Konrad & Duquennoi (1993)) use the Clapeyron equation i.e.

$$T - T_0 = -\frac{T_0}{L} p_w \left(\frac{1}{\rho_i} - \frac{1}{\rho_w}\right).$$

Hopke (1980) also uses this relation and further includes the concept of capillary suction and, at least initially, is more concerned about the ice pressure term. However, ultimately he sets the ice pressure as atmospheric and thus the model falls into the hydrodynamic category.

The lens initiation criterion used with these models is not consistent. The most common assumption is that lens initiation occurs when the permeability becomes low and this is usually measured by the ice saturation (e.g. Taylor & Luthin (1978), Berg *et al.* (1980), Konrad & Morgenstern (1980)). Typical values of the ice saturation used are 85%-90%. Konrad & Duquennoi (1993) derive a condition for lens initiation using thermodynamic principles based on a similar permeability condition. Hopke (1980), in apparent contradiction to his assumption that ice pressure is atmospheric, assumes that lens initiation occurs when the ice pressure equals the overburden.

Besides the lens initiation criterion, the fundamental differences between the hydrodynamic model approach and the Miller model are the restrictions imposed on the ice phase and, in some cases, the use of empirical relationships. Consequently, models

based on this approach are likely to produce results which are in general qualitative agreement with observation. However, in neglecting ice pressure and movement, these models may be neglecting significant terms which should be included in any complete model. In particular, the solution to the Miller model (see O'Neill & Miller (1985)) show these terms to be significant. Further, in order to gain a more complete understanding of frost heave, it is clearly more appropriate to produce a model which uses the most fundamental physical relationships rather than empirical relations or oversimplification.

The dependence of the lens formation criterion on ice saturation is clearly not a physical condition. However, this condition may serve as some form of proxy for the criterion proposed by Miller (i.e. the effective stress becoming zero) because, as the ice saturation increases, more of the overburden is taken by the ice phase and consequently we would expect the effective pressure to decrease and become zero at some value of the ice saturation.

2.3.2 Other Models

Gilpin (1980) and Nixon (1991) introduce the effects of ice pressure into the Clapeyron equation, due to the surface tension effects between the water and ice phases. However, the remaining assumptions used in the hydrodynamic model are retained and, in particular, the ice phase is assumed to be immobile. Consequently, an additional relation is required to find the additional unknown variable, the ice pressure. Nixon (1991) introduces an empirical relationship between the water content and temperature which can be thought of as being equivalent to Miller's capillary suction relation whereas Gilpin (1980) introduces further simplifications (i.e. freezing only occurs at the base of the lowest ice lens and at the freezing front and that the temperature profile in the frozen fringe is linear).

Both these authors assume that ice lenses are initiated when the ice pressure becomes equal to the overburden plus an additional separation pressure. This relationship is a mechanical condition and, in some ways, is comparable to the requirement of zero effective stress in the Miller model. Thus, overall, these models, especially that of Nixon (1991), are beginning to approach the Miller model but still retain some simplifying assumptions (e.g. an immobile ice phase).

Nakano (1993) offers an alternative approach to modelling the secondary frost heave process in which the water flux is represented by a generalisation of Darcy's law. Nakano assumes that the water flux depends on both the water pressure gradient and the temperature gradient.

Chapter 3

Continuous Approximation

3.1 Introduction

The Miller model, a generalisation of which was presented in the previous chapter, appears to have many of the observable characteristics of the frost heave process. Numerical simulations have also been encouraging with those performed by O'Neill & Miller (1982, 1985) giving good qualitative agreement with experiment.

The model developed by Miller makes no allowance for factors such as salinity, compressibility or differential frost heave. The effects of these factors are themselves the subject of much on-going research work (see references in subsequent chapters) and, as such, in order to understand further these effects, we consider the generalised Miller model described in the previous chapter.

The major drawback in analysing frost heave using the Miller model, or any model which predicts lens initiation, is the discrete nature of the process. The fringe equations, which are already extremely complex and in particular non-linear, need to be solved up to the formation of each new lens (i.e. when $p_e = 0$). Since typically hundreds of ice lenses form during the frost heave process, the computation required by a numerical algorithm is immense.

In this chapter we derive a continuous version of the generalised Miller model. We show that to a good approximation we may treat lens formation as a continuous process and hence treat the lens front as a continuous moving boundary. The resulting equations need then only be solved once, although some extra work is required in locating the lens front. We follow an approach similar to that used by Fowler & Krantz (1994) in using the form for the hydraulic conductivity function, $k_h(W)$, to

establish an asymptotic representation of the water pressure, p_w, and then show that the transient following lens initiation is more rapid than any macroscopic time scale we consider. This allows us to treat the fringe variables as quasi-static and enables us to justify the continuum approach.

The work done by Holden (1983), Holden *et al.* (1985) and Piper *et al.* (1988) adopts a similar approach by implicitly assuming that the fringe variables are quasi-static and adopting a similar form for the water pressure, p_w, as derived in section 3.3 below. However, the continuum approach was not used and, as such, the resulting simplified equations were solved for each lens formation.

For simplicity, the mathematical analysis presented here considers the one dimensional situation. The theory and techniques used readily extend to higher dimensions and, indeed, an analysis of differential frost heave is presented in chapter 7. Further, the solute diffusivity term, D, is assumed to be independent of the water saturation, S. Again, this assumption is adopted for simplicity and all of the results presented in this chapter readily extend to the situation where D is a function of water saturation.

For completeness, and to aid our comparison with the simulations produced by O'Neill & Miller (1985), we consider both Miller's 'rigid ice' model (i.e. the ice phase moves at a constant velocity by a process of thermal regelation) and the approach suggested by Fowler & Krantz (1994) that the ice phase in the frozen fringe moves down temperature gradients, again by a process of thermal regelation (see Gilpin (1979)).

3.2 Non-dimensionalisation

3.2.1 Model Summary

Before proceeding to non-dimensionalise, we collect together the generalised Miller model equations and boundary conditions derived in the previous chapter for the one dimensional situation. After some simplification, writing Wu_w as U_w and assuming that the solute diffusivity term, D_0, is independent of the relative water saturation, S, the governing equations become

$z_s > z > z_l$:

$$\rho C_p \frac{dT}{dt} = k_f \frac{\partial^2 T}{\partial z^2} \tag{3.1}$$

$z_l > z > z_f$:

$$
\begin{aligned}
&-\frac{\partial \phi}{\partial t} + \frac{\partial}{\partial z}((1-\phi)u_s) = 0, \\
&\frac{\partial \phi}{\partial t} + \delta\frac{\partial W}{\partial t} + \frac{\partial}{\partial z}((1+\delta)U_w + (\phi - W)u_i) = 0, \\
&\frac{\partial W}{\partial t} + \frac{\partial U_w}{\partial z} + \frac{\rho C_p}{L\rho_w}\frac{dT}{dt} = \frac{k}{L\rho_w}\frac{\partial^2 T}{\partial z^2}, \\
&U_w - W u_s = -\frac{k_0}{\rho_w g}S^\gamma\left(\frac{\partial p_w}{\partial z} + \rho_w g\right), \\
&p_i - p_w = f(S), \\
&P = p_e + (1-\chi(S))f(S) + p_w, \\
&P = P_0 + \rho_f g(z_s - z_l), \\
&u_i - u_s = -\lambda\frac{\partial T}{\partial z} \quad \text{(Gilpin)}, \\
\text{or} \qquad &u_i = \dot{z}_s \qquad\qquad\quad \text{(Rigid Ice)}, \\
&T - T_0 = -\frac{T_0}{L\rho_w}(\delta p_w + (1+\delta)f(S)) - \frac{T_0^2 R}{L\rho_w}c, \\
&\frac{\partial}{\partial t}(Wc) - D_0\frac{\partial}{\partial z}\left(W\frac{\partial c}{\partial z}\right) + \frac{\partial}{\partial z}(cU_w) = 0.
\end{aligned}
\tag{3.2}
$$

$z_f > z > z_b$ (or equivalently $-\infty$ in the field):

$$
\begin{aligned}
&-\frac{\partial \phi}{\partial t} + \frac{\partial}{\partial z}((1-\phi)u_s) = 0, \\
&\frac{\partial \phi}{\partial t} + \frac{\partial U_w}{\partial z} = 0, \\
&\rho C_p\frac{dT}{dt} = k\frac{\partial^2 T}{\partial z^2}, \\
&U_w - \phi u_s = -\frac{k_0}{\rho_w g}\left(\frac{\partial p_w}{\partial z} + \rho_w g\right), \\
&P = p_e + p_w, \\
&P = P_0 + \rho_f g(z_s - z_l), \\
&\frac{\partial}{\partial t}(\phi c) - D_0\frac{\partial}{\partial z}\left(\phi\frac{\partial c}{\partial z}\right) + \frac{\partial}{\partial z}(cU_w) = 0,
\end{aligned}
\tag{3.3}
$$

where we have included the weight of the overlying soil in the overburden P, with the density of this region equal to ρ_f and the surface load equal to P_0. In addition, we require equations for the rheology of each of the three regions. However, these equations do not affect the analysis given in this chapter and hence, necessary relations are derived in chapters 6 and 7 when they are required.

The boundary conditions for this problem are then given at the boundaries z_s, z_l, z_f and z_b and are as follows:
at $z = z_s$

$$T = T_s(t). \tag{3.4}$$

at $z = z_l$

$$\begin{aligned}
&[T]_-^+ = 0,\\
&p_i = P,\\
&cU_w - D_0 W \frac{\partial c}{\partial z} = W c u_s,\\
&W u_s - U_w = \frac{k_f}{L\rho_w} \left.\frac{\partial T}{\partial z}\right|_+ - \frac{k}{L\rho_w} \left.\frac{\partial T}{\partial z}\right|_-,\\
&\dot{z}_s = (1+\delta)U_w + (\phi - W)u_i + (1 - \phi - \delta W)u_s,\\
&\dot{z}_l = u_s.
\end{aligned} \tag{3.5}$$

at $z = z_f$

$$\begin{aligned}
&S = 1,\\
&[T]_-^+ = 0,\\
&\left[\frac{\partial T}{\partial z}\right]_-^+ = 0,\\
&[p_w]_-^+ = 0,\\
&[U_w]_-^+ = 0,\\
&[u_s]_-^+ = 0,\\
&[c]_-^+ = 0,\\
&\left[\frac{\partial c}{\partial z}\right]_-^+ = 0.
\end{aligned} \tag{3.6}$$

at $z = z_b$ for the laboratory situation or equivalently $z \to -\infty$ in the field case

$$\begin{aligned}
&T = T_b(t), \qquad \text{(Laboratory)}\\
&-k\frac{\partial T}{\partial z} = G, \qquad \text{(Field)}\\
&u_s = 0,\\
&p_w = p_\infty,\\
&c = c_\infty.
\end{aligned} \tag{3.7}$$

It is useful at this stage to check that the problem is correctly specified in terms of the type and number of equations in each region and the number of associated boundary conditions. In doing this, because we have not considered the rheology of the partially and unfrozen soil regions, we suppose that the soil is incompressible (i.e. ϕ is a constant and $u_s = 0$).

In the completely frozen zone we have a parabolic equation in temperature for which we require 2 temperature boundary conditions. In the unfrozen region we require 1 boundary condition for each of U_w and p_w and 2 for each of the parabolic equations in T and c.

Consideration of the equations in the frozen fringe is more complex because of the various constitutive relations. However, we require 1 boundary condition for each of U_w and p_w and 2 for each of W (or equivalently T) and c.

Thus we require 14 conditions plus 1 for each of the moving boundaries z_s, z_l and z_f making a 17 in total. This agrees with the number of conditions we have that do not involve u_s and hence the problem appears to be hopefully well-posed.

3.2.2 Non-dimensionalisation

The equations and boundary conditions given above are non-dimensionalised with the following scalings:

$$\begin{aligned} c &= c_\infty c^*, \\ T - T_0 &= \Delta T\, T^*, \\ p_j &= \sigma p_j^* \quad (j = i, w, e), \\ f &= \sigma f^*, \\ U_w &= U U_w^*, \\ u_j &= U u_j^* \quad (j = i, s), \\ z &= d\, z^*, \\ t &= \frac{d}{U} t^*, \end{aligned} \tag{3.8}$$

where σ is the intrinsic pressure scale within the soil which is found from the capillary function $f(W)$. Figure 3.1 represents a typical capillary relation function for a silty soil and for the normal range of water contents a typical scale for the capillary force would appear to be $\sim 10^5$ Pa. ΔT and d are the appropriate temperature and length

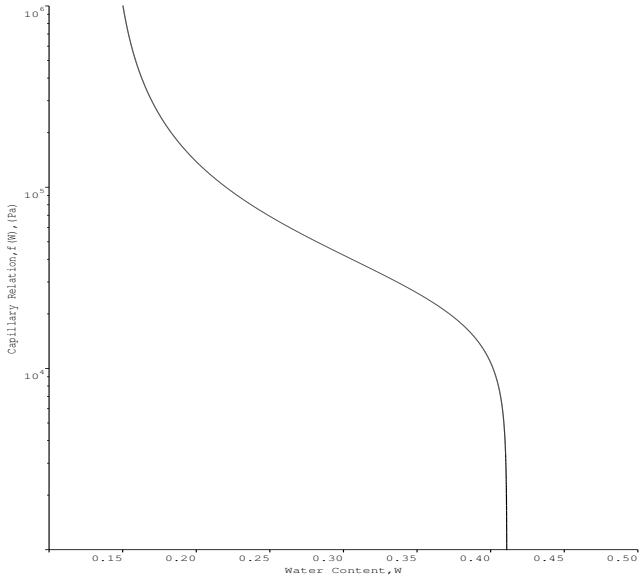


Figure 3.1: Plot of typical capillary suction curve for a silty soil. Taken from O'Neill and Miller (1985) and used in the numerical results presented in chapter 4.

scales. These depend on the physical situation we wish to consider and are discussed below.

The velocity scale, U, is chosen to be

$$U = \frac{k\Delta T}{L\rho_w d}$$

reflecting our anticipation that the velocities are controlled by the freezing processes within the fringe.

The length and temperature scales chosen are a function of the situation we wish to consider (i.e. laboratory conditions, seasonal freezing or permafrost). In the laboratory, the most appropriate length scale, d, would be the initial height of the soil column, $z_s(0) - z_b$, and the temperature scale, ΔT, would then be some mean value of $T_0 - T_s(t)$.

In regions of permafrost the length and temperature scales are governed by the geothermal heat flux discussed in chapter 2. A geothermal heat flux of $0.05\,\mathrm{W\,m^{-2}}$ corresponds to a temperature gradient of around 1 K every 50 m. Thus, taking a typical surface temperature of around 10K below freezing, a corresponding length scale would be around 500 m.

For seasonal freezing the length scale is given by equation 3.1. For a time scale

of one year (i.e. 3×10^7 s) and a thermal diffusivity (i.e. $k_f/(\rho C_p)$) of $2 \times 10^{-6}\,\mathrm{m^2\,s^{-1}}$ an appropriate length scale is approximately 8 m. An annual temperature variation would typically be around 30 K.

The solute scale chosen is simply the far field concentration, c_∞. For example, sea water would typically have a salinity of $615\,\mathrm{mole\,m^{-3}}$.

Substituting these variables into the above equations and dropping the asterisks, we get after some rearrangement

$z_s > z > z_l$:

$$\delta_1 \frac{\rho C_p}{\overline{\rho C_p}} \frac{dT}{dt} = \frac{k_f}{k} \frac{\partial^2 T}{\partial z^2}. \tag{3.9}$$

$z_l > z > z_f$:

$$\begin{aligned}
&-\frac{\partial \phi}{\partial t} + \frac{\partial}{\partial z}((1-\phi)u_s) = 0,\\
&\delta \frac{\partial W}{\partial t} + \frac{\partial}{\partial z}((1+\delta)U_w + (\phi - W)u_i + (1-\phi)u_s) = 0,\\
&\frac{\partial W}{\partial t} + \frac{\partial U_w}{\partial z} + \delta_1 \frac{\rho C_p}{\overline{\rho C_p}} \frac{dT}{dt} = \frac{\partial^2 T}{\partial z^2},\\
&U_w - W u_s = -\beta S^\gamma \left(\frac{\partial p_w}{\partial z} + \delta_2^w \right),\\
&p_i - p_w = f(S),\\
&P = p_e + (1 - \chi(S)) f(S) + p_w,\\
&P = P_0 + \delta_2^f (z_s - z_l),\\
&u_i - u_s = -\delta_3 \frac{\partial T}{\partial z} \quad \text{(Gilpin)},\\
&u_i = \dot{z}_s \qquad\qquad\quad \text{(Rigid Ice)},\\
&T = -\mu(\delta p_w + (1+\delta) f(S)) - \nu c,\\
&\frac{\partial}{\partial t}(Wc) - \alpha \frac{\partial}{\partial z}\left(W \frac{\partial c}{\partial z} \right) + \frac{\partial}{\partial z}(c U_w) = 0.
\end{aligned} \tag{3.10}$$

$z_f > z > z_b$ (or equivalently $-\infty$ in the field):

$$\begin{aligned}
&-\frac{\partial \phi}{\partial t} + \frac{\partial}{\partial z}((1-\phi)u_s) = 0,\\
&\frac{\partial \phi}{\partial t} + \frac{\partial U_w}{\partial z} = 0,\\
&\delta_1 \frac{\rho C_p}{\overline{\rho C_p}} \frac{dT}{dt} = \frac{\partial^2 T}{\partial z^2},\\
&U_w - \phi u_s = -\beta \left(\frac{\partial p_w}{\partial z} + \delta_2^w \right),
\end{aligned}$$

$$
\begin{aligned}
&P = p_e + p_w, \\
&P = P_0 + \delta_2^f (z_s - z_l), \\
&\frac{\partial}{\partial t}(\phi c) - \alpha \frac{\partial}{\partial z}\left(\phi \frac{\partial c}{\partial z}\right) + \frac{\partial}{\partial z}(cU_w) = 0.
\end{aligned} \tag{3.11}
$$

The boundary conditions become

at $z = z_s$

$$
T = T_s(t); \tag{3.12}
$$

at $z = z_l$

$$
\begin{aligned}
&[T]_-^+ = 0, \\
&p_i = P, \\
&cU_w - \alpha W \frac{\partial c}{\partial z} = W c u_s, \\
&W u_s - U_w = \frac{k_f}{k} \left.\frac{\partial T}{\partial z}\right|_+ - \left.\frac{\partial T}{\partial z}\right|_-, \\
&\dot{z}_s = (1+\delta)U_w + (\phi - W)u_i + (1 - \phi - \delta W)u_s \\
&\dot{z}_l = u_s;
\end{aligned} \tag{3.13}
$$

at $z = z_f$

$$
\begin{aligned}
&S = 1, \\
&[T]_-^+ = 0, \\
&\left[\frac{\partial T}{\partial z}\right]_-^+ = 0, \\
&[p_w]_-^+ = 0, \\
&[U_w]_-^+ = 0, \\
&[u_s]_-^+ = 0, \\
&[c]_-^+ = 0, \\
&\left[\frac{\partial c}{\partial z}\right]_-^+ = 0;
\end{aligned} \tag{3.14}
$$

at $z = z_b$ for the laboratory situation or equivalently $z \to -\infty$ in the field case

$$
\begin{aligned}
&T = T_b(t), \quad \text{(Laboratory)} \\
&\frac{\partial T}{\partial z} = -1, \quad \text{(Permafrost)}
\end{aligned}
$$

$$\frac{\partial T}{\partial z} = -\delta_4, \quad \text{(Seasonal)}$$
$$u_s = 0,$$
$$p_w = p_\infty,$$
$$c = 1. \tag{3.15}$$

In scaling these equations we have chosen the temperature and length scales for the appropriate physical situation we are considering (i.e. laboratory conditions, seasonal freezing or permafrost).

The parameters given in these equations are as follows

$$\delta = \frac{\rho_w - \rho_i}{\rho_i}, \qquad \delta_1 = \frac{\overline{\rho C_p}\Delta T}{L\rho_w},$$
$$\delta_2^w = \frac{\rho_w g d}{\sigma}, \qquad \delta_2^f = \frac{\rho_f g d}{\sigma},$$
$$\delta_3 = \frac{\lambda L \rho_w}{k}, \qquad \beta = \frac{k_0 \sigma L}{g k \Delta T},$$
$$\alpha = \frac{D_0 L \rho_w}{k\Delta T}, \qquad \mu = \frac{T_0 \sigma}{L\rho_w \Delta T},$$
$$\nu = \frac{T_0^2 R c_\infty}{L\rho_w \Delta T} \qquad \delta_4 = \frac{G\, d}{k\Delta T},$$

where $\overline{\rho C_p}$ is some mean value of ρC_p. Through the size of these parameters we are able to determine the relative importance of each of the physical factors which contribute to the frost heave process. We briefly discuss the relevance of each parameter.

1. δ is a measure of the change in volume when water changes phase to ice.

2. δ_1 is a measure of the relative importance of heat advection to heat conduction.

3. δ_2^w and δ_2^f are measures of the importance of hydrostatic pressure to the capillary suction.

4. δ_3 is a measure of the regelative ice flux contribution to the heave rate.

5. β compares the flow which results from the water pressure gradient with the heave rate

6. α compares the diffusion and convection of the solute phase.

7. μ and ν are measures of the temperature variation due to pore water pressure and salinity, respectively, across the frozen fringe.

8. δ_4 compares the seasonal temperature gradient with the temperature gradient which arises because of the geothermal heat flux.

3.2.3 Parameter Values

Typical values of the constants occurring in the parameters listed above depend on the physical situation and soil type considered. For all the cases, typical values are as follows

$$
\begin{aligned}
\rho_f &\sim 2 \times 10^3 \,\mathrm{kg\,m^{-3}} \\
\rho_i &\sim 917 \,\mathrm{kg\,m^{-3}} \\
\rho_w &\sim 1000 \,\mathrm{kg\,m^{-3}} \\
L &\sim 3.35 \times 10^5 \,\mathrm{J\,kg^{-1}} \\
k &\sim 1 \,\mathrm{W\,m^{-1}\,K^{-1}} \\
k_f &\sim 2 \,\mathrm{W\,m^{-1}\,K^{-1}} \\
g &\sim 10 \,\mathrm{m\,s^{-2}} \\
\overline{\rho C_p} &\sim 10^6 \,\mathrm{J\,K^{-1}\,m^{-3}} \\
\sigma &\sim 10^5 \,\mathrm{Pa} \\
\Delta T &\sim 1 \,\mathrm{K} \quad \text{(Laboratory)} \\
&\sim 10\mathrm{K} \quad \text{(Permafrost)} \\
&\sim 30\mathrm{K} \quad \text{(Seasonal)} \\
d &\sim 0.1 \,\mathrm{m} \quad \text{(Laboratory)} \\
&\sim 500 \,\mathrm{m} \quad \text{(Permafrost)} \\
&\sim 8 \,\mathrm{m} \quad \text{(Seasonal)} \\
\gamma &\sim 9 \\
T_0 &\sim 273 \,\mathrm{K} \\
D_0 &\sim 7 \times 10^{-9} \,\mathrm{m^2\,s^{-1}} \\
R &\sim 8.3 \,\mathrm{J\,K^{-1}\,mole^{-1}} \\
k_0 &\sim 10^{-4} - 10^{-2} \,\mathrm{m\,s^{-1}} \quad \text{(Sand)} \\
&\sim 10^{-9} - 10^{-7} \,\mathrm{m\,s^{-1}} \quad \text{(Silt)} \\
&\sim 10^{-12} - 10^{-10} \,\mathrm{m\,s^{-1}} \quad \text{(Clay)}
\end{aligned}
$$

$$\begin{aligned} \lambda &\sim 10^{-10}\,\mathrm{m^2\,s^{-1}\,K^{-1}} \\ G &\sim 0.05\,\mathrm{W\,m^{-2}} \end{aligned}$$

The value of the regelation constant, λ, used is the value which can be inferred from Gilpin (1979) for a temperature of $-0.1°$C and the value used by Fowler & Krantz (1994). In reality, the whole concept of regelation in the frost heave process and the dependence of λ on temperature, pressure gradients and soil type warrants further study which is beyond the scope of this thesis. A brief discussion of the approach adopted by Gilpin (1979) and how this may be extended to include pressure regelation effects is given in appendix B. However, the point to note about the analysis presented in this and subsequent chapters is that the value of the ice velocity, u_i, is only required at the lens front, z_l, and a more complex prescription of u_i is relatively straightforward to incorporate.

Substitution of the above values into the parameters gives the following values

1. Laboratory

$$\delta \sim 0.09 \qquad \delta_1 \sim 3 \times 10^{-3} \quad \delta_2^w,\, \delta_2^f \sim 0.01 \qquad \alpha \sim 2 \qquad \mu \sim 0.08.$$

$$\begin{aligned} \beta &\sim 10^5 - 10^7 \quad \text{(Sand)} \\ &\sim 1 - 10^2 \quad \text{(Silt)} \\ &\sim 10^{-3} - 10^{-1} \quad \text{(Clay)} \\ \delta_3 &\sim 3 \times 10^{-2}. \end{aligned}$$

2. Permafrost

$$\delta \sim 0.09 \qquad \delta_1 \sim 3 \times 10^{-2} \quad \delta_2^w,\, \delta_2^f \sim 50 \qquad \alpha \sim 0.2 \qquad \mu \sim 8 \times 10^{-3}.$$

$$\begin{aligned} \beta &\sim 10^4 - 10^6 \quad \text{(Sand)} \\ &\sim 10^{-1} - 10 \quad \text{(Silt)} \\ &\sim 10^{-4} - 10^{-2} \quad \text{(Clay)} \\ \delta_3 &\sim 3 \times 10^{-2} \end{aligned}$$

3. Seasonal

$$\delta \sim 0.09 \quad \delta_1 \sim 0.1 \qquad \delta_2^w,\, \delta_2^f \sim 0.8 \qquad \alpha \sim 0.07 \qquad \mu \sim 3 \times 10^{-3}.$$

$$\begin{aligned} \beta &\sim 10^4 - 10^6 \qquad \text{(Sand)} \\ &\sim 10^{-1} - 10 \qquad \text{(Silt)} \\ &\sim 10^{-4} - 10^{-2} \qquad \text{(Clay)} \\ \delta_3 &\sim 3 \times 10^{-2} \\ \delta_4 &\sim 10^{-2} \end{aligned}$$

The parameter ν depends on the far field concentration c_∞ which itself depends on the particular physical situation we wish to consider. There are effectively three relevant régimes which arise from consideration of the Clapeyron equation as follows:

$$\begin{aligned} \nu &\ll \mu, \\ \nu &\sim \mu, \\ \nu &\gg \mu. \end{aligned} \tag{3.16}$$

In the first case, the effects of salinity uncouple and, in the absence of compressibility and gravity, the one dimensional model reduces to that considered by Fowler & Krantz (1994). An analysis of this situation is presented in Chapter 4.

In order to consider the far field concentrations applicable in the second and third cases it is useful to look at the following ratio

$$\frac{\mu}{\nu} = \frac{\sigma}{T_0 R c_\infty},$$

which is a measure of the ratio of the capillary suction to the osmotic pressure.

Using this ratio with the typical values of the constants listed above, we find that the case $\nu \sim \mu$ corresponds to salinities of around $c_\infty \sim 44\,\mathrm{mole\,m^{-3}}$. For the case where $\nu \gg \mu$ we restrict our attention to salinities of $c_\infty \sim 615\,\mathrm{mole\,m^{-3}}$, the typical value given for sea water, corresponding to 35ppt. This then gives that $\mu/\nu \sim 0.1$.

At this point it is also worth considering the velocity scales which arise for each of the laboratory, permafrost and seasonal problems. These are

$$\begin{aligned} U &\sim 3 \times 10^{-8}\,\mathrm{m\,s^{-1}} \quad \text{Laboratory}, \\ U &\sim 6 \times 10^{-11}\,\mathrm{m\,s^{-1}} \quad \text{Permafrost}, \\ U &\sim 1 \times 10^{-8}\,\mathrm{m\,s^{-1}} \quad \text{Seasonal}. \end{aligned} \tag{3.17}$$

Having non-dimensionalised the problem and considered typical values of the various parameters, we are now in a position to neglect some of the physical processes in our subsequent analysis. In particular, the parameters δ (volume change on freezing) and δ_1 (heat advection) are small for any of the scalings considered above. Thus, we may neglect the corresponding terms. The parameters μ and ν are, in general, small. However, these parameters control the temperature, and hence the thickness, of the frozen fringe and, as such, become significant when we rescale in this region. The remaining parameters fluctuate widely depending on the soil type and the particular physical situation considered and are therefore retained in the subsequent analysis.

3.3 Continuous Approximation

Having now established that heat advection and the volume change on freezing may be neglected, we proceed to simplify the model further by showing that, because the inter-lens spacing is small and the transient following the formation of a new lens is rapid, we may treat lens formation as a continuous process and are therefore able to develop an 'averaged' continuum model. This removal of the discrete nature of ice lensing, introduces a new moving boundary (i.e. the 'lens front') for which an additional boundary condition is derived.

3.3.1 Lens Spacing

The first stage in establishing the continuum version of the generalised Miller model is to obtain an expression for the water pressure, p_w, from Darcy's equation $(3.10)_4$. A uniformly valid expression for p_w can be obtained because of the large exponent, $\gamma\,(=9)$ appearing in the hydraulic conductivity function, $k_h(W)$. From this we are able to show that the inter-lens spacing is small.

Now, Darcy's equation may be rearranged to give

$$\frac{\partial}{\partial z}(p_w + \delta_2^w z) = -\frac{(U_w - W u_s)}{\beta} S^{-\gamma}, \tag{3.18}$$

where $S = W/\phi$. Integrating this expression gives

$$\begin{aligned} p_w + \delta_2^w z + C(t) &= -\frac{1}{\beta}\int_{z_l}^{z} (U_w - W u_s) S^{-\gamma} d\xi \\ &= -\frac{1}{\beta}\int_{z_l}^{z} (U_w - W u_s) \exp\left(-\gamma \log S\right) d\xi. \end{aligned} \tag{3.19}$$

Recasting Darcy's equation in this form allows us to apply Laplace's method to obtain an asymptotic representation for the integral. Since a negative temperature gradient exists, we expect $h(S) = -\log S$ to have a maximum at $z = z_l$. Further, because $\gamma \gg 1$, the asymptotic representation of p_w is given by the above integral with $z_l - z \ll 1$ (since all other contributions to the integral will be exponentially small). If we now suppose that $h(S)$ and $(U_w - Wu_s)$ have Taylor expansions in z about $z = z_l$ we may write:-

$$\begin{aligned} h(S) &= -(\log S_l + \frac{1}{S_l}\left.\frac{\partial S}{\partial z}\right|_l (z - z_l) + O((z - z_l)^2), \\ U_w - Wu_s &= (U_{wl} - W_l u_{sl}) + O(z - z_l), \end{aligned}$$

where the suffix l refers to a quantity evaluated at $z = z_l$.

Substituting these expressions into 3.19 gives that the leading order behaviour of the water pressure, p_w, is given by

$$p_w + \delta_2^w z + C(t) = -\frac{(U_{wl} - W_l u_{sl})}{\beta} S_l^{-\gamma} \int_{z_l}^{z} \exp\left(-\frac{\gamma S_l'}{S_l}(\xi - z_l)\right) d\xi,$$

where $|z - z_l| \ll 1$ and S_l' is simply $\partial S/\partial z$ evaluated at $z = z_l$.

Integrating this expression and assuming that the water pressure, p_f, is known at $z = z_f$, we arrive at the following uniformly valid expression for water pressure, p_w, in the frozen fringe

$$p_w = p_f + \delta_2^w (z_f - z) + \frac{(U_{wl} - W_l u_{sl})}{\gamma \beta S_l'} S_l^{-\gamma+1} \exp\left(-\frac{\gamma S_l'(z - z_l)}{S_l}\right). \tag{3.20}$$

The water pressure at the frozen front is used because in general this water pressure will be found from the solution to the groundwater flow problem in the unfrozen region beneath the frozen fringe. In the laboratory situation the water pressure at the frozen front will simply be the prescribed water pressure at the base of the sample, p_∞.

As expected, equation 3.20 shows that the water pressure, p_w, exhibits boundary layer behaviour in the region close to the base of the lowest ice lens. The thickness of this boundary layer is $O(\delta_w/\gamma)$, where δ_w is the dimensionless length scale over which the water saturation S varies (which must be at most the fringe thickness). This boundary layer behaviour in p_w forces lens initiation to occur within this boundary layer and, as such, we are able to show that the inter-lens spacing is small relative to

the fringe thickness. This observation turns out to be crucial to the development of the continuous model. However, before proceeding to show this we recast boundary condition $(3.13)_2$ ($p_i = P$ at $z = z_l$), using the above expression for p_w together with the capillary relation $(3.10)_5$, into a form which gives a less complex expression for p_w and makes the subsequent analysis slightly neater. Thus, the boundary condition $(3.13)_2$ together with equation $(3.10)_5$ gives

$$P = p_i = p_{wl} + f(S_l).$$

Hence, substituting the above expression for p_w, we get, after some rearrangement, the following expression for S_l':

$$\left.\frac{\partial S}{\partial z}\right|_l = -\tilde{\beta}(U_{wl} - W_l u_{sl}) \tag{3.21}$$

where

$$\tilde{\beta} = \frac{S_l^{-\gamma+1}}{\gamma\beta(p_f + \delta_2^w(z_f - z_l) - P + f(S_l))}.$$

Thus, we may more conveniently express p_w in the form

$$p_w = p_f + \delta_2^w(z_f - z) - [p_f + \delta_2^w(z_f - z_l) - P + f(S_l)] \exp\left(-\frac{\gamma S_l'}{S_l}(z - z_l)\right). \tag{3.22}$$

Lens initiation occurs when the effective stress, p_e, becomes zero; substituting this into the stress relation $(3.10)_6$ shows that lens initiation occurs when

$$p_w - P = -(1 - \chi)f. \tag{3.23}$$

The functions on each side of this equation are monotonic increasing with respect to $-z$ and hence lens initiation will occur when these curves on each side of 3.23 have a tangency. Now $p_w - P$ varies over a length scale $O(1/\gamma)$ times the length scale over which $(1 - \chi)f$ varies (providing f and χ are order one functions of S). Therefore, from figure 3.2, we see that intersection of these functions will occur within the water pressure boundary layer and thus inter-lens spacing is small. Further, it is possible to see that this intersection will in fact occur when S_l increases to a value which approximately solves

$$p_f + \delta_2^w(z_f - z_l) - P = -(1 - \chi(S_l))f(S_l). \tag{3.24}$$

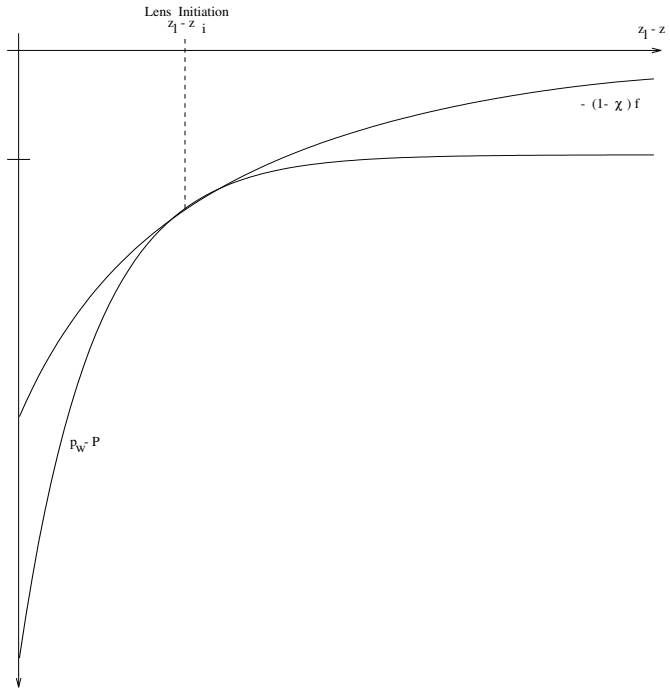


Figure 3.2: Graphs of $p_w - P$ and $-(1-\chi)f$ against distance below the lowest ice lens, indicating the boundary layer nature of p_w. Taken from the numerical result presented in chapter 4

The comment '*providing f and χ are order one functions of S*' needs to be discussed in more detail. Typical $\chi(S)$ profiles always satisfy this criterion. However, typical $f(S)$ profiles (e.g. see figure 3.1) reveal rapid growth in the region close to a soil's minimum water content. This effect will not alter the above analysis providing the overburden, P, is not too large, but will have an effect for moderate to large loads. In particular, equation 3.24 will provide a solution for most forms of capillary relation whatever the size of the overburden, P, implying that frost heave will always occur however small. However, Fowler & Noon (1993) suggest that a soil's capillary relation places an upper limit on the overburden at which lens initiation can occur and that this limit only manifests itself if consideration is given to rapid growth in the capillary relation, $f(S)$, close to the soil's minimum water content. We present a further analysis of this upper limit on the overburden in chapter 4 where it is referred to as the 'critical heaving pressure'

In order to reveal the exact effect of $f(S)$ we provide an analytic argument to determine the inter-lens spacing.

If the curves on each side of equation 3.23 are tangential then we have

$$\begin{aligned} p_{wi} - P &= -g(S_i), \\ \left.\frac{\partial p_w}{\partial z}\right|_i &= -g'(S_i)\left.\frac{\partial S}{\partial z}\right|_i, \end{aligned} \tag{3.25}$$

where the suffix i indicates a quantity evaluated at the point of tangency and we define g to be $(1-\chi)f$. Substituting the expression for water pressure, p_w, some simple rearrangement gives the following relations

$$\begin{aligned} p_f + \delta_2^w(z_f - z_i) - P + g(S_i) &= -\frac{(g'(S_i)S_i' - \delta_2^w)S_l}{\gamma S_l'}, \\ z_i - z_l &= -\frac{S_l}{\gamma S_l'}\log\left(\frac{p_f + \delta_2^w(z_f - z_i) - P + g(S_i)}{p_f + \delta_2^w(z_f - z_l) - P + f(S_l)}\right). \end{aligned} \tag{3.26}$$

where $S_i' = \partial S/\partial z|_i$. We see from the second of these equations that if

$$\log\left(\frac{p_f + \delta_2^w(z_f - z_l) - P + f(S_l)}{p_f + \delta_2^w(z_f - z_i) - P + g(S_i)}\right) \sim \gamma\frac{S_l'}{S_l}\delta_w$$

then $z_i - z_l \sim O(\delta_w)$ (i.e. varies over the same length scale as the frozen fringe) and inter-lens spacing is no longer small relative to the fringe thickness. However, because $S_l'\delta_w$ is $\sim O(1)$, in this situation we would have an $O(1)$ change in S producing an $O(e^\gamma)$ change in $f(S)$ which is not the type of behaviour a capillary suction curve would exhibit. Therefore, if a solution to equations 3.26 exists (i.e. lens initiation occurs) then the fringe is thin and we may write

$$S_i \approx S_l + S_l'(z_i - z_l).$$

Substituting this into $(3.26)_2$ to eliminate $z_i - z_l$ and using $S_i' \approx S_l'$ we arrive at two equations for the unknowns S_i and S_l which may be written as

$$\begin{aligned} p_f + \delta_2^w(z_f - z_i) - P + g(S_i) &= -\frac{(g'(S_i)S_l' - \delta_2^w)S_l}{\gamma S_l'}, \\ S_i - S_l &= -\frac{S_l}{\gamma}\log\left(\frac{p_f + \delta_2^w(z_f - z_i) - P + g(S_i)}{p_f + \delta_2^w(z_f - z_l) - P + f(S_l)}\right), \end{aligned} \tag{3.27}$$

where S_l' is given by equation 3.21.

Now if $f'(S)$ is less than $O(\gamma)$ then, since $S_i \approx S_l$, the first relation simply reduces to equation 3.24. However, if this condition is not satisfied, then equations 3.27 must be solved to determine S_l. We show in chapter 4 that, when $f'(S)$ becomes large (i.e.

these soil's minimum water content is approached), equations 3.27 impose a restriction on the maximum overburden, P, above which a solution to these equations does not exist. From this result we are able to explain the observed dependence of frost heave on soil type. We also show that the approximate solution 3.24 to 3.27 is invalid when $P - p_f$ (and hence S_i and S_l) tend to zero (at least if $\delta_2^w \ll \gamma$) [1].

Solving the above equations produces the water saturations S_i and S_l which, together with equation 3.21, allow the location of the initiation of the next ice lens to be determined. However, in section 3.3.2 we show that lens initiation may be treated as a continuous process and, as such, the determination of S_l becomes a boundary condition which determines the position of the lens front.

We should note at this point that we have assumed that $S_l^{'}$ is bigger than $O(1/\gamma)$. If equation 3.21 implies that this is not the case then we need to go to the second order in the Taylor expansion of S given at the beginning of this section. We then find that the thickness of the pressure boundary layer is in fact $O((\gamma S_l^{''})^{-\frac{1}{2}})$ and a similar analysis to that given above follows through. We get

$$p_w = p_f + \delta_2^w(z_f - z) - [p_f + \delta_2^w(z_f - z_l) - P + f(S_l)]\frac{2}{\sqrt{\pi}}\int_{h(z)}^{\infty}\exp(-\xi^2)d\xi,$$

where $S_l^{''}$ is the second derivative of S evaluated at $z = z_l$ and $h(z)$ is given by

$$h(z) = \sqrt{\frac{\gamma S_l^{''}}{2S_l}}(z_l - z).$$

Substituting this expression into equations 3.25 we find after some rearrangement that lens initiation occurs when:-

$$\left(\frac{p_f + \delta_2^w(z_f - z_i) - P + g(S_i)}{p_f + \delta_2^w(z_f - z_l) - P + f(S_l)}\right) = \frac{2}{\sqrt{\pi}}\int_{h(z_i)}^{\infty}\exp(-\xi^2)d\xi,$$

$$p_f + \delta_2^w(z_f - z_i) - P + g(S_i) = -\frac{(g'(S_i)S_i^{'} - \delta_2^w)}{\sqrt{\frac{\gamma S_l^{''}}{2S_l}}}\exp[h(z_i)^2]\int_{h(z_i)}^{\infty}\exp(-\xi^2)d\xi.$$

If we suppose that $h(z_i) \gg 1$ (i.e. $z_l - z_i \gg \gamma^{-\frac{1}{2}}$) then using simple asymptotics to expand the above integrals, the first of the above equations gives to leading order that

$$\left(\frac{p_f + \delta_2^w(z_f - z_i) - P + g(S_i)}{p_f + \delta_2^w(z_f - z_l) - P + f(S_l)}\right) = \frac{\exp(-h(z_i)^2)}{\sqrt{\pi}h(z_i)},$$

[1] In section 3.2.3 we found that $\delta_2^w \gg \gamma$ when we considered the permafrost problem. However, in chapter 6 we show that the depth scale over which lens formation occurs is much smaller than the frost penetration depth scale and, hence, the parameter $\delta_2^w \ll \gamma$.

which again gives unrealistic behaviour for the capillary relation, $f(S)$, and thus the lens spacing must again be thin. Also, if we find that $f^{'}(S)$ is less than $O(\gamma^{-\frac{1}{2}})$ then since $S_i \approx S_l$ the second relation simply reduces to equation 3.24. Otherwise we need to solve the equations simultaneously to determine S_l.

In this section we have established an explicit expression for the water pressure, p_w, in the frozen fringe (i.e. equation 3.22) and used this to establish that lens spacing is small compared to the frozen fringe thickness. We have also derived equations 3.27, which apply at the point of lens initiation, for the water saturations at the base of the lowest ice lens and at the point where the new ice lens is initiated.

3.3.2 Continuous Approximation

To transform the discrete model given in the previous chapter into an 'averaged' continuous model we need to consider what happens during the transient following the formation of an ice lens. If we can show that this transient is rapid compared to the time between successive initiations then we may argue that the system can be treated as quasi-static, the first step in justifying the continuous model.

We have shown that (dimensionless) inter-lens spacing, δ_l, is very much smaller than the fringe thickness. The time between successive lens initiations is therefore simply of order δ_l (providing that $\dot{z}_f$ is $O(1)$). We now proceed to show that, on lens formation, the fringe variables relax to their equilibrium values on a time scale much faster than δ_l.

Lens initiation perturbs the equilibrium values of S and c in a region of thickness $O(\delta_l)$ below the lowest ice lens. By eliminating T and p_w from equations 3.10 it is quite straightforward to show that S and c satisfy advection-diffusion type equations[2]. Thus, following a lens initiation, the time scale for relaxation to equilibrium of S and c will be of order δ_l^2.

Now, the temperature in the frozen fringe is controlled by the Clapeyron equation $(3.10)_{10}$. Because we do not anticipate any boundary layer behaviour in temperature the (dimensionless) fringe thickness, δ_w, must vary over the same scale as the temperature variation. We show in subsequent chapters that in all cases, even for large salinities (i.e. $\nu \gg 1$), the fringe thickness is of $O(\mu)$.

[2]It is assumed that temperature relaxes to the equilibrium equation $(3.10)_{10}$ on a time scale much faster than any we consider.

Thus, because we have that $\delta_l^2 \ll \delta_l \ll \delta_w \ll 1$ and further that $\delta_l^2 \ll \delta_1$, the transient following the formation of a new ice lens is more rapid than any other microscopic time scale we consider. As such, we may take S, c and hence all fringe variables to be quasi-static and hence as functions which vary over an $O(1)$ time scale.

We may now use these results (i.e. that the fringe is thin and that the transient following lens initiation is very rapid) to justify treating the lens front as a continuous moving boundary. This is achieved by considering a time scale that is much larger than the time between successive lens formations, δ_l ($\ll 1$). By doing this we see that lens initiation is effectively continuous and thus equations 3.27 are continually satisfied giving an extra boundary condition for the water saturation, S_l, which determines the position of the lens front.

We need to take care at this point to distinguish between the local ice velocity, given by the kinematic condition (i.e. equation $(3.13)_7$) at the base of the lowest ice lens, with the velocity of the position of the lens front in the 'averaged' sense derived above. From this point on, z_l will refer to the location of the lens front and allowance for the kinematic condition is made in the derivation of the boundary conditions for the 'averaged' situation given in the following section.

3.3.3 Continuous Model

In making the continuous approximation a question arises as to whether the boundary conditions applicable in the discrete case follow through to the continuous situation. It seems clear that we need to consider the boundary conditions at the boundary $z = z_l$ and construct simple 'pill-box' type arguments to determine the boundary conditions in the averaged model. When doing this we also take into consideration the fact that z_l now refers to the position of the lens front and care is taken to distinguish its rate of change from the soil matrix velocity. Each of the boundary conditions at the boundary z_l is considered below.

1.

$$[T]_-^+ = 0.$$

This condition clearly remains unchanged since the temperature has to remain continuous.

2.

$$p_i = P.$$

Again this boundary condition will remain unchanged since the bottom ice lens is still supporting the overburden. It is convenient to change this boundary condition into one for the relative water fraction S as shown in section 3.3.1. Thus we have

$$\frac{\partial S}{\partial z} = -\tilde{\beta}(U_w - W u_s).$$

3.

$$cU_w - \alpha W \frac{\partial c}{\partial z} = W c u_s.$$

This boundary condition expresses the fact in the discrete case that solutes cannot pass through the lowest lens (i.e. flux up equals flux down). In the continuous case, lens initiation 'traps' solute above z_l at a rate $-W_l c_l(\dot{z}_l - u_s)$. Hence, since the soil is heaving at a rate $\dot{z}_s$, the 'average' solute concentration, c^+, just above $z_l(t)$ is simply given by

$$W^+ c^+ = -\frac{W c(\dot{z}_l - u_s)}{\dot{z}_s - \dot{z}_l}.$$

From equation $(3.10)_{11}$ we see that the appropriate boundary condition is of the form

$$[Wc]^+_- \dot{z}_l = \left[-\alpha W \frac{\partial c}{\partial z} + cU_w\right]^+_-.$$

Therefore since the diffusive flux of the solute is zero above z_l we have

$$W^+ c^+ \dot{z}_l - c^+ U_w^+ - W c \dot{z}_l = \alpha W \frac{\partial c}{\partial z} - cU_w.$$

Now the convective flux U_w^+ is simply $W^+ \dot{z}_s$ and thus the L.H.S. of the above expression is simply $-W c u_s$. The required boundary condition is then just

$$cU_w - \alpha W \frac{\partial c}{\partial z} = W c u_s,$$

exactly as it was in the discrete case.

4.

$$W u_s - U_w = \frac{k_f}{k} \left.\frac{\partial T}{\partial z}\right|_+ - \left.\frac{\partial T}{\partial z}\right|_-.$$

In the discrete case, this boundary condition represents energy conservation (i.e. the difference in heat fluxes at z_l is the amount of freezing at z_l).

By using a similar argument to that given for the previous boundary condition, the required boundary condition is of the form

$$[W]^+_- \dot{z}_l = [U_w]^+_- - \left(\frac{k_f}{k} \left. \frac{\partial T}{\partial z} \right|_+ - \left. \frac{\partial T}{\partial z} \right|_- \right)$$

which may be expanded to give

$$-W^+(\dot{z}_l - \dot{z}_s) - U_w + W\dot{z}_l = \frac{k_f}{k} \left. \frac{\partial T}{\partial z} \right|_+ - \left. \frac{\partial T}{\partial z} \right|_-$$

where W^+ is the 'average' water content above $z_l(t)$. We now need to determine W^+. If no freezing occurs above $z_l(t)$ then

$$W^+ = -\frac{W_l(\dot{z}_l - u_s)}{\dot{z}_s - \dot{z}_l}.$$

and we again have the same boundary condition as in the discrete case. However, it is more realistic to suppose that the water above $z_l(t)$ freezes and that we have

$$W^+ = -\frac{W_m(\dot{z}_l - u_s)}{\dot{z}_s - \dot{z}_l},$$

where W_m is the soil's minimum obtainable water content. Substituting this into the above boundary condition gives

$$(W - W_m)\dot{z}_l + W_m u_s - U_w = \frac{k_f}{k} \left. \frac{\partial T}{\partial z} \right|_+ - \left. \frac{\partial T}{\partial z} \right|_- .$$

This boundary condition is different to that given in the discrete case. It expresses the fact that the lens front is growing by thermal processes and thus justifies our choice for the velocity scale given in section 3.2.

5.

$$\dot{z}_s = (1 + \delta)U_w + (\phi - W)u_i + (1 - \phi - \delta W)u_s.$$

This boundary condition is a statement of conservation of mass at z_l. Applying the techniques used above we find that this boundary condition remains the same as it was in the discrete case.

3.3.4 Field Boundary Conditions

When deriving the asymptotic expression for the water pressure we assumed that the water pressure p_f at the freezing front was specified. As previously mentioned, in the laboratory this value will simply be the value at the base of the sample. However, in field conditions, we would not know the water pressure at the freezing front and this would, in general, be determined from the solution to the ground water flow problem in the unfrozen region. This problem is considered in chapter 6 where it is found that a diffusion equation for the effective stress at the frozen front can be established. Once the effective stress has been determined at the frozen front the water pressure at the frozen front can be calculated from equation $(3.11)_5$. The soil matrix velocity at the frozen front is also determined in solving the groundwater flow problem given in chapter 6 and, for now, we also assume that this velocity is specified.

3.4 Temperature Solution

In the laboratory the temperature at the base of the sample is prescribed and the leading order behaviour of the temperature equations 3.9 and $(3.11)_3$ (i.e. neglecting terms of $O(\delta_1)$) is

$$\frac{\partial^2 T}{\partial z^2} = 0. \tag{3.28}$$

Thus, in the laboratory case the temperature profiles are linear and the temperature in each of these regions is simply

$z_s > z > z_l$

$$T = T_s + \frac{(T_s - T_l)}{z_s - z_l}(z - z_s), \tag{3.29}$$

$z_f > z > z_b$

$$T = T_f + \frac{(T_f - T_b)}{z_f - z_b}(z - z_f), \tag{3.30}$$

where T_f and T_l are the temperatures at the frozen front and lens front respectively and are determined from the solution to the fringe equations.

Clearly, in the field we can not prescribe the temperature in the far field but rather we specify the far field (geothermal) heat flux. The temperature profile in the frozen region above the lowest ice lens is again a linear profile and the solution is as given above for the laboratory situation. However, we need to consider the solution to the temperature problem in the region below the freezing front when $z_b \to -\infty$ and we

have a prescribed far field flux. For convenience, we consider the one dimensional case, which gives the following equations and boundary conditions

$$\delta_1 \frac{dT}{dt} = \frac{\partial^2 T}{\partial z^2}, \tag{3.31}$$

with $T = T_f$ on $z = z_f$ and $\partial T/\partial z \to -1$ (Permafrost) or $-\delta_4$ ($\ll 1$) (Seasonal) as $z_b \to -\infty$. Because, with the field scaling, the parameter δ_1 is again $\ll 1$, the leading order solution to this problem is simply

$$\begin{aligned} T &= T_f - (z - z_f) \quad \text{(Permafrost)} \\ T &= T_f \qquad\qquad\quad \text{(Seasonal).} \end{aligned} \tag{3.32}$$

3.5 Reduced Equations

We are now in a position to write down the generalised 'averaged' model in a non-dimensional form. We have shown that heat advection and the volume expansion on freezing are both small and, to leading order, may be neglected. The smallness of heat advection allowed us to solve the temperature profile in the frozen and unfrozen regions and these can be used to give the temperature boundary conditions on each side of the frozen fringe.

Finally, we suppose the water pressure and the soil matrix velocity are specified at the freezing front. In the laboratory, because of the boundary layer in water pressure at the base of the lowest lens, the water pressure at the frozen front will simply be the water pressure at the base of the sample. The equivalent pressure in the field comes from the solution to the groundwater flow problem in the unfrozen region which is considered in chapter 6. In the incompressible problem, the soil matrix velocity will be zero at the frozen front and throughout the fringe.

Thus, the averaged continuous version of the generalised Miller model may be written as follows

$z_l > z > z_f$:

$$\begin{aligned} &-\frac{\partial \phi}{\partial t} + \frac{\partial}{\partial z}((1-\phi)u_s) = 0, \\ &\frac{\partial}{\partial z}\left(U_w + (\phi - W)u_i + (1-\phi)u_s\right) = 0, \\ &\frac{\partial W}{\partial t} + \frac{\partial U_w}{\partial z} = \frac{\partial^2 T}{\partial z^2}, \end{aligned}$$

$$
\begin{aligned}
&p_w = p_f + \delta_2^w(z_f - z) - [p_f + \delta_2^w(z_f - z_l) - P + f(S_l)] \exp\left(-\frac{\gamma S_l^{'}}{S_l}(z - z_l)\right),\\
&T = -\mu(\delta p_w + f(S)) - \nu c,\\
&u_i - u_s = -\delta_3 \frac{\partial T}{\partial z} \quad \text{(Gilpin)},\\
&u_i = \dot{z}_s \qquad\qquad\quad \text{(Rigid Ice)},\\
&p_e = P - (1-\chi)f - p_w,\\
&P = P_0 + \delta_2^f(z_s - z_l),\\
&\frac{\partial}{\partial t}(Wc) - \alpha \frac{\partial}{\partial z}\left(W \frac{\partial c}{\partial z}\right) + \frac{\partial}{\partial z}(cU_w) = 0.\\
&S = \frac{W}{\phi}
\end{aligned} \tag{3.33}
$$

$z_f > z > z_b$

$$
\frac{\partial}{\partial t}(\phi c) - \alpha \frac{\partial}{\partial z}\left(\phi \frac{\partial c}{\partial z}\right) + \frac{\partial}{\partial z}(cU_w) = 0. \tag{3.34}
$$

The boundary conditions are

at $z = z_l$

$$
\begin{aligned}
&S = S_l,\\
&\frac{\partial S}{\partial z} = -\tilde{\beta}(U_w - W u_s),\\
&cU_w - \alpha W \frac{\partial c}{\partial z} = W c u_s,\\
&(W - W_m)\dot{z}_l + W_m u_s - U_w = \frac{k_f}{k}\frac{(T_l - T_s)}{(z_l - z_s)} - \frac{\partial T}{\partial z},\\
&\dot{z}_s = U_w + (\phi - W)u_i + (1-\phi)u_s,
\end{aligned} \tag{3.35}
$$

at $z = z_f$

$$
\begin{aligned}
&S = 1,\\
&p_w = p_f,\\
&u_s = u_{sf},\\
&[c]_-^+ = 0,\\
&\left[\frac{\partial c}{\partial z}\right]_-^+ = 0,\\
&\frac{\partial T}{\partial z} = \frac{(T_f - T_b)}{(z_f - z_b)} \quad \text{(Laboratory)},\\
&\frac{\partial T}{\partial z} = -1 \qquad\quad \text{(Permafrost)},
\end{aligned}
$$

$$\frac{\partial T}{\partial z} = 0 \qquad \text{(Seasonal)}, \tag{3.36}$$

at $z = z_b$ or as $z \to -\infty$

$$c = 1, \tag{3.37}$$

where we have substituted the linear temperature profiles in the regions above and below the fringe into the relevant boundary conditions and the water saturation at the base of the lowest ice lens, S_l, is calculated from equations 3.27.

In addition to the equations given above we also require a rheology for the unfrozen region and, when considering the three dimensional problem, a rheology for the frozen soil to replace boundary condition $(3.35)_5$. To avoid over complicating the problem at this stage the additional relationships are considered as they are required in chapters 6 and 7.

Having changed the model so dramatically, it is worth checking that the system still appears to be hopefully well-posed. In doing this we again suppose the porosity ϕ is a constant and that $u_s = 0$.

In the fringe we require 1 boundary condition for each of U_w and p_w and two for each of c and T (or equivalently W). In the unfrozen region we require 2 boundary conditions for c. Thus, in total we require 8 boundary conditions plus 3 for the moving boundaries making a total of 11. Assuming that we have enough boundary conditions to solve the groundwater flow problem, this agrees with the number we have (excluding the condition on u_s) and hence the problem is hopefully well-posed.

Chapter 4

Incompressible, Solute Free Soils in One Dimension

4.1 Introduction

Much of the experimental and theoretical work on frost heave has been done assuming a one dimensional, solute free and incompressible system. In this chapter we consider this problem and show how, for this situation, the 'averaged' version of the Miller model derived in chapter 2 may be reduced to a pair of non-linear ordinary differential equations for the ground surface position, z_s, and the lens front, z_l. This reduction is possible because the frozen fringe can be shown to occupy a thin region relative to the frost penetration depth. This observation allows the fringe equations to be integrated and the resulting system can then be solved to give the equations for z_s and z_l.

By a simple change of variables, the two non-linear ordinary differential equations may be converted to a linear system and the exact solution written down. However, in order to elucidate some of the features of the system, an asymptotic solution for small and long times is produced which gives rise to a condition on the heave parameter, α_{fk}, which must apply if a frozen fringe is to form and heave is to occur.

The heave rate, $\dot{z_s}$, is found to be proportional to a heave parameter, α_{fk}, which depends on the particular soil type through the capillary relation $f(W)$, and the hydraulic conductivity characteristics through k_0 and the exponent γ. The heave parameter is also found to depend on the applied load, P, through the effective stress at the frozen front (i.e. $N = P - p_f$). From the heave parameter's dependence on effective stress, we are able to show the sensitivity of the magnitude of heave produced

to the applied overburden.

As mentioned in chapter 1, different soil types exhibit different heaving characteristics. In particular, gravels and sands are not generally susceptible to heave whereas silts can produce spectacular heave providing the overburden is not too great and clays heave small amounts but can overcome substantial loads. These observations can be explained through the heave parameter, α_{fk}, and the limitations imposed on the size of the effective stress at which lens initiation can occur from the solution to equations 3.27 for the water saturation at the lens front. An analysis of equations 3.27 for large overburdens reveals that there is a critical value of the overburden at which the lens front cannot advance (i.e. lens initiation cannot occur) and hence frost heave cannot occur. This critical value of overburden is found to depend on soil type through the form of the capillary suction characteristic, $f(W)$, and is found to increase as the soil type moves from gravel to clays. Thus, this mechanism offers a possible explanation for the observed dependence of frost heave on soil type.

As an additional comparison of the reduced system with observation, and with numerical solutions to the full system, it is useful to derive approximate expressions for the lens spacing and lens thickness. Although we have derived an averaged model in which the lens front moves continuously, it is nevertheless possible to derive approximate expressions for these quantities and to consider how lens spacing and thickness vary over time and according to soil type.

Finally, a comparison is given between the results of the reduced system of ordinary differential equations for the ground surface position, z_s, and the lens front, z_l, and the full numerical simulation of O'Neill & Miller (1985). In the absence of the complete description of the soil, freezing and load conditions applied by O'Neill & Miller, the comparison given is qualitative. We describe the general form of the dependences of heave, frozen front penetration, inter-lens spacing and lens thickness as functions of time. These results are in good qualitative agreement with the numerical results of O'Neill & Miller.

4.2 Thin Fringe Approximation

Before proceeding to show that the frozen fringe is thin it is worth restating the continuum version of the Miller model for the situation we wish to consider. Thus,

the equations presented at the end of chapter 3 may be written as

$z_l > z > z_f$:

$$
\begin{aligned}
&\frac{\partial}{\partial z}\left(U_w + (\phi - W)u_i\right) = 0,\\
&\frac{\partial W}{\partial t} + \frac{\partial U_w}{\partial z} = \frac{\partial^2 T}{\partial z^2},\\
&p_w = p_f^h(z) - [p_f^h(z_l) - P + f(W_l)]\exp\left(-\frac{\gamma W_l'}{W_l}(z - z_l)\right),\\
&T = -\mu(\delta p_w + f(W)),\\
&u_i = -\delta_3\frac{\partial T}{\partial z} \quad \text{(Gilpin)},\\
\text{or} \qquad &u_i = \dot{z}_s \qquad\quad \text{(Rigid Ice)},\\
&P = P_0 + \delta_2^f(z_s - z_l),\\
&p_f^h = p_f + \delta_2^w(z_f - z).
\end{aligned} \tag{4.1}
$$

The boundary conditions are

at $z = z_l$

$$
\begin{aligned}
&W = W_l,\\
&\frac{\partial W}{\partial z} = -\phi\tilde{\beta}U_w,\\
&(W - W_m)\dot{z}_l - U_w = \frac{k_f}{k}\frac{(T_l - T_s)}{(z_l - z_s)} - \frac{\partial T}{\partial z},\\
&\dot{z}_s = U_w + (\phi - W)u_i.
\end{aligned} \tag{4.2}
$$

at $z = z_f$

$$
\begin{aligned}
&W = \phi,\\
&\frac{\partial T}{\partial z} = \frac{(T_f - T_b)}{(z_f - z_b)} \qquad \text{(Laboratory)},\\
&\frac{\partial T}{\partial z} = -1 \qquad\quad \text{(Permafrost)},\\
&\frac{\partial T}{\partial z} = 0 \qquad\quad \text{(Seasonal)},
\end{aligned} \tag{4.3}
$$

where W_l, the water content at the base of the lowest lens, is found from equations 3.27 and we suppose that p_f is prescribed.

The temperature in the frozen fringe is controlled by the Clapeyron equation $(4.1)_4$. In each of the laboratory, permafrost and seasonal scalings given in section 3.2.3, the parameter μ is $\ll 1$ and this suggests that the temperature variation across

the fringe is small. Therefore, because we anticipate that the temperature gradient in the fringe will be $O(1)$, the fringe thickness must also be of $O(\mu)$ (i.e. the same order of magnitude as the temperature variation in the fringe). Thus, the frozen fringe is thin and we use this fact to simplify, even further, the 'averaged' model given above.

We rescale in the frozen fringe with the following change of variables

$$z = z_l - \mu\xi, \qquad\qquad T = \mu\theta.$$

This change of variables gives the following relationships

$$\begin{aligned} \frac{\partial}{\partial t} &= \frac{\dot{z}_l}{\mu}\frac{\partial}{\partial \xi} + \frac{\partial}{\partial t}, \\ \frac{\partial}{\partial z} &= -\frac{1}{\mu}\frac{\partial}{\partial \xi}. \end{aligned} \tag{4.4}$$

Substituting this change of variables into the averaged fringe equations and boundary conditions we find that the leading order behaviour of this system is as follows:
$0 < \xi < \xi_f$:

$$\begin{aligned} &\frac{\partial}{\partial \xi}(U_w + (\phi - W)u_i) = 0, \\ &\dot{z}_l \frac{\partial W}{\partial \xi} - \frac{\partial U_w}{\partial \xi} = \frac{\partial^2 \theta}{\partial \xi^2}, \\ &p_w = p_f^h(\xi) - [p_f^h(0) - P + f(W_l)] \exp\left(-\frac{\gamma}{W_l} \left.\frac{\partial W}{\partial \xi}\right|_l \xi \right), \\ &\theta = -(\delta p_w + f(W)), \\ &u_i = \delta_3 \frac{\partial \theta}{\partial \xi} \qquad \text{(Gilpin)}, \\ \text{or} \qquad &u_i = \dot{z}_s \qquad \text{(Rigid Ice)}, \\ &P = P_0 + \delta_2^f (z_s - z_l), \\ &p_f^h = p_f + \delta_2^w \mu(\xi - \xi_f). \end{aligned} \tag{4.5}$$

The boundary conditions become
at $\xi = 0$

$$\begin{aligned} &W = W_l, \\ &\frac{\partial W}{\partial \xi} = \mu\phi\tilde{\beta}U_w, \\ &(W - W_m)\dot{z}_l - U_w = -\frac{k_f}{k}\frac{T_s}{(z_l - z_s)} + \frac{\partial \theta}{\partial \xi}, \\ &\dot{z}_s = U_w + (\phi - W)u_i, \end{aligned} \tag{4.6}$$

at $\xi = \xi_f$

$$\begin{aligned} & W = \phi, \\ & \frac{\partial \theta}{\partial \xi} = \frac{T_b}{(z_l - z_b)}, \quad \text{(Laboratory)}, \\ & \frac{\partial \theta}{\partial \xi} = 1, \quad \text{(Permafrost)}, \\ & \frac{\partial \theta}{\partial \xi} = 0, \quad \text{(Seasonal)}. \end{aligned} \tag{4.7}$$

where $\xi_f = (z_l - z_f)/\mu\,(\sim 1)$. The hydrostatic component of the water pressure in the fringe is $\sim \delta_2^w \mu$. From the analysis in section 3.2.3, we find that with the laboratory and seasonal scales, $\delta_2^w \mu \ll 1$. However, in the permafrost problem $\delta_2^w \mu \sim 0.4$, which is approaching an $O(1)$ quantity. Nevertheless, in order to simplify the subsequent expressions we suppose that $\delta_2^w \mu \ll 1$ in all cases, and thus ignore the hydrostatic component of the water pressure in the fringe.

Therefore, integrating the above equations and applying the appropriate boundary conditions we get
$0 < \xi < \xi_f$:

$$\begin{aligned} & \dot{z}_s = U_w + (\phi - W)u_i, \\ & \dot{z}_l(W - W_m) - U_w - \frac{\partial \theta}{\partial \xi} = -\frac{k_f}{k}\frac{T_s}{(z_l - z_s)}, \\ & p_w = p_f - [p_f - P + f(W_l)] \exp\left(-\frac{\gamma}{W_l}\left.\frac{\partial W}{\partial \xi}\right|_l \xi\right), \\ & \theta = -(\delta p_w + f(W)), \\ & u_i = \delta_3 \frac{\partial \theta}{\partial \xi} \quad \text{(Gilpin)}, \\ \text{or} \quad & u_i = \dot{z}_s \quad \text{(Rigid Ice)}, \\ & P = P_0 + \delta_2^f (z_s - z_l), \end{aligned} \tag{4.8}$$

where the remaining boundary conditions are
at $\xi = 0$

$$\begin{aligned} & W = W_l, \\ & \frac{\partial W}{\partial \xi} = \mu \phi \tilde{\beta} U_w, \end{aligned} \tag{4.9}$$

at $\xi = \xi_f$

$$W = \phi,$$

$$\frac{\partial\theta}{\partial\xi} = \frac{T_b}{(z_l - z_b)}, \qquad \text{(Laboratory)},$$
$$\frac{\partial\theta}{\partial\xi} = 1, \qquad \text{(Permafrost)},$$
$$\frac{\partial\theta}{\partial\xi} = 0, \qquad \text{(Seasonal)}. \tag{4.10}$$

Thus, we have a first order partial differential equation and three unknown boundaries z_s, z_l and z_f for which we have four boundary conditions. Hence, providing we can find the water pressure p_f the problem appears to be hopefully well-posed.

However, because we know that the moving boundaries z_l and z_f are $O(\mu)$ apart and hence, in terms of our $O(1)$ length scale, are effectively at the same location and, furthermore, because we are not particularly interested in the profiles of the fringe variables, we can find z_s and z_l without solving the above system explicitly.

Evaluating equation $(4.8)_2$ at $\xi = \xi_f$ gives

$$\dot{z}_l(\phi - W_m) - U_{wf} - \left.\frac{\partial\theta}{\partial\xi}\right|_f = \frac{k_f}{k}\frac{T_s}{(z_s - z_l)}, \tag{4.11}$$

where the additional suffix f refers to a variable evaluated at $\xi = \xi_f$. Further, evaluating $(4.8)_1$ at $\xi = \xi_f$ gives $U_{wf} = \dot{z}_s$ which, when substituted into equation 4.11, means that this equation becomes

$$\dot{z}_l(\phi - W_m) - \dot{z}_s = \left.\frac{\partial\theta}{\partial\xi}\right|_f + \frac{k_f}{k}\frac{T_s}{(z_s - z_l)}. \tag{4.12}$$

The value of $\left.\frac{\partial\theta}{\partial\xi}\right|_f$ is taken from boundary condition $(4.10)_{2,3}$ depending on whether the field or laboratory conditions are being considered.

Equation 4.12 then becomes the first of our differential equations for z_s and z_l. The remaining differential equation is a little more difficult to write down but is found by evaluating $(4.8)_1$ at $z = z_l$. Expressions for U_{wl} and $\partial\theta/\partial\xi|_l$ are then found by manipulation of the equations and boundary conditions.

Evaluation of $(4.8)_1$ at $z = z_l$ gives

$$\dot{z}_s = U_{wl} + (\phi - W_l)\dot{z}_s, \qquad \text{(Rigid Ice)}$$
$$\dot{z}_s = U_{wl} + \delta_3(\phi - W_l)\frac{\partial\theta}{\partial\xi}. \qquad \text{(Gilpin)} \tag{4.13}$$

Differentiating $(4.8)_4$, evaluating the resulting expression at $\xi = 0$ and using $(4.8)_3$ to eliminate the gradient in water pressure we arrive at

$$\left.\frac{\partial\theta}{\partial\xi}\right|_l = -\frac{(\delta\gamma(p_f - P + f(W_l)) + W_l f'(W_l))}{W_l}\left.\frac{\partial W}{\partial\xi}\right|_l.$$

Now using boundary condition $(4.9)_2$ we may write the above expression as

$$\left.\frac{\partial\theta}{\partial\xi}\right|_l = \frac{U_{wl}}{\beta_{fk}}, \tag{4.14}$$

where β_{fk} is given by

$$\beta_{fk} = -\left(\frac{\phi\mu\tilde{\beta}}{W_l}(\delta\gamma(p_f - P + f(W_l)) + W_l f^{'}(W_l))\right)^{-1}. \tag{4.15}$$

If we expand β_{fk} using the definitions of μ and ϕ derived in chapter 3 we get

$$\begin{aligned}\beta_{fk} &= -\frac{\gamma L^2\rho_w k_0}{T_0 g k}\left(\frac{W_l}{\phi}\right)^{\gamma}\left(\frac{(p_f - P + f(W_l))}{\delta\gamma(p_f - P + f(W_l)) + W_l f'(W_l)}\right)\\ &= -\frac{\gamma L^2\rho_w k_0}{T_0 g k}\left(\frac{W_l}{\phi}\right)^{\gamma}\left(\frac{(f(W_l) - N)}{\delta\gamma(f(W_l) - N) + W_l f'(W_l)}\right),\end{aligned} \tag{4.16}$$

where N is the effective stress at the frozen front (i.e. $P - p_f$). To leading order the parameter β_{fk} is the as same the parameter $\tilde{\beta}$ defined in Fowler & Krantz (1994) (equation (66)). Evaluating $(4.8)_2$ at $z = z_l$ we obtain the following expression for U_{wl}

$$U_{wl} = (W_l - W_m)\dot{z}_l - \frac{k_f}{k}\frac{T_s}{(z_s - z_l)} - \left.\frac{\partial\theta}{\partial\xi}\right|_l. \tag{4.17}$$

Therefore solving equations 4.14 and 4.17 for U_{wl} and $\left.\frac{\partial\theta}{\partial\xi}\right|_l$ we get

$$\begin{aligned}\left.\frac{\partial\theta}{\partial\xi}\right|_l &= \frac{1}{(1+\beta_{fk})}\left((W_l - W_m)\dot{z}_l - \frac{k_f}{k}\frac{T_s}{(z_s - z_l)}\right)\\ U_{wl} &= \frac{\beta_{fk}}{(1+\beta_{fk})}\left((W_l - W_m)\dot{z}_l - \frac{k_f}{k}\frac{T_s}{(z_s - z_l)}\right).\end{aligned} \tag{4.18}$$

Substituting these relations into equations 4.13 we get the second differential equation for z_s and z_l as follows

$$\begin{aligned}\dot{z}_s &= \frac{\beta_{fk}}{(1+\beta_{fk})(1-\phi+W_l))}\left((W_l - W_m)\dot{z}_l - \frac{k_f}{k}\frac{T_s}{(z_s - z_l)}\right), \quad \text{(Rigid Ice)}\\ \dot{z}_s &= \frac{(\beta_{fk} + \delta_3(\phi - W_l))}{(1+\beta_{fk})}\left((W_l - W_m)\dot{z}_l - \frac{k_f}{k}\frac{T_s}{(z_s - z_l)}\right). \qquad \text{(Gilpin)}\end{aligned} \tag{4.19}$$

Collecting together the resulting heave equations we have

$$\begin{aligned}\dot{z}_l(\phi - W_m) &= \dot{z}_s + \left.\frac{\partial\theta}{\partial\xi}\right|_f + \frac{k_f}{k}\frac{T_s}{(z_s - z_l)},\\ \dot{z}_s &= \alpha_{fk}\left((W_l - W_m)\dot{z}_l - \frac{k_f}{k}\frac{T_s}{(z_s - z_l)}\right),\end{aligned} \tag{4.20}$$

where $\frac{\partial\theta}{\partial\xi}\Big|_f$ is given by

$$\begin{aligned}
\frac{\partial\theta}{\partial\xi} &= \frac{T_b}{(z_l - z_b)}, \quad \text{(Laboratory)}, \\
\frac{\partial\theta}{\partial\xi} &= 1, \quad \text{(Permafrost)}, \\
\frac{\partial\theta}{\partial\xi} &= 0, \quad \text{(Seasonal)}.
\end{aligned} \tag{4.21}$$

and α_{fk} corresponds, to leading order, to the heave parameter α defined by Fowler & Krantz (1994) (i.e. equations (70) and (72)) and is given by

$$\begin{aligned}
\alpha_{fk} &= \frac{\beta_{fk}}{(1+\beta_{fk})(1-\phi+W_l)}, \quad \text{(Rigid Ice)} \\
\alpha_{fk} &= \frac{(\beta_{fk} + \delta_3(\phi - W_l))}{(1+\beta_{fk})}. \quad \text{(Gilpin)}.
\end{aligned} \tag{4.22}$$

Thus we have reduced the Miller model to a pair of non-linear ordinary differential equations which essentially express conservation of mass across the frozen fringe through equation $(4.20)_2$, and conservation of energy across the frozen fringe (i.e. a Stefan condition) through equation $(4.20)_1$.

Throughout this section we have implicitly assumed that in the case of a semi-infinite soil the pore water pressure at the frozen front is specified. As discussed in chapter 3 this value of the pore water pressure is found by considering the groundwater flow problem in the unfrozen region beneath the frozen fringe. The resulting equations for this pore pressure (which are derived in chapter 6) are then coupled with the heave equations given by 4.20. In the laboratory, the water pressure at the frozen front is simply the water pressure at the base of the sample p_∞.

Equations 4.20 form a non-linear autonomous system and a phase plane analysis could be considered. However, by an appropriate change of variables, equations 4.20 may be converted to a linear system and an exact solution written down. Therefore, a phase analysis is not considered here.

4.3 Variation in Heave Rate

In this section we consider the limitations which apply to the frost heave process as a result of the various conditions which apply to the simplified non-linear system given above by equations 4.20. These constraints on the heaving process arise in the following way:

1. equations 3.27 only provide a solution for the water content at the lens front for values of effective stress less than some critical value N_c. For values of effective stress higher than N_c, lens initiation will not occur and hence a soil will not heave. The value of the critical overburden, N_c, depends on the soil type through the capillary suction function, $f(W)$; and

2. the amount of heave is controlled by the size of the heaving parameter, α_{fk}, appearing in equations 4.20. The size α_{fk} depends on the soil type, and the effective stress at the frozen front.

Through the analysis of these constraints, we are able to explain some of the characteristics of frost heave discussed in chapter 1. In particular, we are able to show that:

1. gravels and sands are not susceptible to heave because in general heave is suppressed by very low values of effective stress, N;

2. silts can produce spectacular heave providing the overburden is small; and

3. clays only heave small amounts but can overcome substantial loads.

4.3.1 Lens Initiation Constraint

The water saturations, S_l $(= W_l/\phi)$ at the base of the lowest ice lens and S_i at the next lens initiation point, are given by the solution to equations 3.27 which can be expressed as

$$\begin{aligned} g(S_i) - N &= -\frac{(g^{'}(S_i)S_l^{'} - \delta_2^w)S_l}{\gamma S_l^{'}}, \\ S_i - S_l &= -\frac{S_l}{\gamma}\log\left(\frac{g(S_i) - N}{f(S_l) - N}\right), \end{aligned} \tag{4.23}$$

where $g = (1-\chi(S))f(S)$ and, because we are ignoring the hydrostatic pressure term in the frozen fringe, the effective stress $N = P - p_f$. In addition, as discussed in chapter 3, we suppose that $\delta_2^w \ll \gamma$. The gradient in water saturation, $S_l^{'}$, at the lens front is given by equation $(4.2)_2$ as

$$\left.\frac{\partial S}{\partial z}\right|_l = -\tilde{\beta}U_{wl}, \tag{4.24}$$

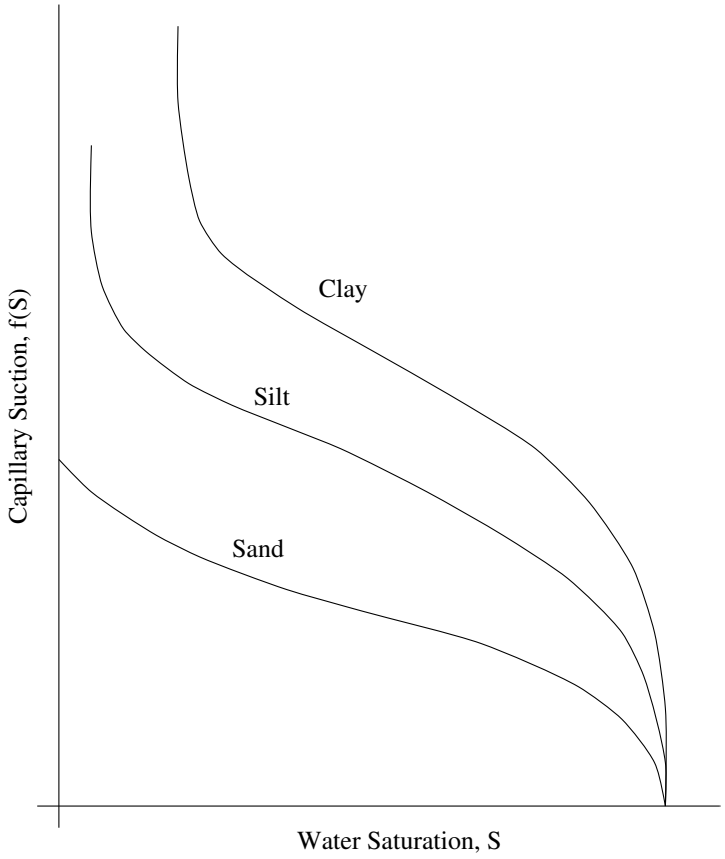


Figure 4.1: Schematic Plot of Typical Capillary Suction Curves.

and U_{wl} is given by $(4.18)_2$.

For certain soil types (i.e. clays and silts), equations 4.23 may not have a solution for a large but finite overburden. For these soils, the capillary relation function will typically have an asymptote at some finite value of the water saturation (see Black (1990)). Thus, as the overburden increases, and hence the water saturation at the lowest ice lens decreases, the term $g^{'}(S)/\gamma$ becomes significant and this imposes a restriction on how large the overburden may become. Typical forms of the soil characteristic function for various soil types are shown in figure 4.1. In the region close to a soil's minimum water content, the form of the capillary suction characteristic is typically as follows:

$$f(S) \sim \frac{c}{(S - S_0)^{\alpha}}, \tag{4.25}$$

where S_0 is the soil's minimum water saturation and the constants c and α characterise the soil type. Typically, larger values of the constants α, c and S_0 correspond to finer

grained soil types. From the form of $f(S)$ we have

$$f'(S) \sim -\frac{\alpha f(S)}{(S - S_0)}. \tag{4.26}$$

Thus, to determine the constraint on the overburden imposed by the solutions to equations 4.23, we consider relative water saturations close to the minimum value, S_0, by writing

$$S = S_0 + \frac{\sigma}{\gamma} \tag{4.27}$$

Substituting this relationship into the equations 4.23 we get, after some rearrangement, that the leading order behaviour of the system is as follows:

$$\begin{aligned} 1 - \nu\sigma_i^{\alpha} &= \frac{\alpha S_0}{\sigma_i}, \\ \sigma_i - \sigma_l &= S_0 \log\left(1 + \frac{\sigma_i}{\alpha S_0}\left(\frac{1}{(1-\chi(S_0))}\left(\frac{\sigma_i}{\sigma_l}\right)^{\alpha} - 1\right)\right), \end{aligned} \tag{4.28}$$

where we have defined the load parameter $\nu = N/((1-\chi(S_0))\gamma^{\alpha}c)$, and $\sigma_{i,l}$ correspond to $S_{i,l}$.

Plotting equation $(4.28)_1$ in (ν, σ_i) space gives the curve shown in figure 4.2. This plot reveals that for each load parameter ν (less than ν_c), there are two possible values of σ_i. However, physically, we would expect the larger value of σ_i to occur first as this would require less freezing. Furthermore, as $\sigma_i \to \infty$ we would expect to recover the the normal solution when $f^{'}(S) \sim 1$. Thus, we anticipate that the right hand side of figure 4.2 provides the physically correct value of σ_i. This result would imply that, as the load parameter ν increases, the water content σ_i decreases along the portion of the curve marked with an arrow until the critical point (σ_i^c, ν_c) is reached. For values of ν greater than ν_c, no solution exists to equations 4.23 and lens initiation is suppressed. Consequently, if lenses cannot form, then secondary frost heave cannot be initiated and no heave occurs.

Consideration of the maximum value of ν_c from equation $(4.28)_1$ shows that the critical point is given by

$$\begin{aligned} \sigma_i^c &= (\alpha + 1)S_0, \\ \nu_c &= \frac{1}{(\alpha+1)^{\alpha+1}S_0^{\alpha}}. \end{aligned} \tag{4.29}$$

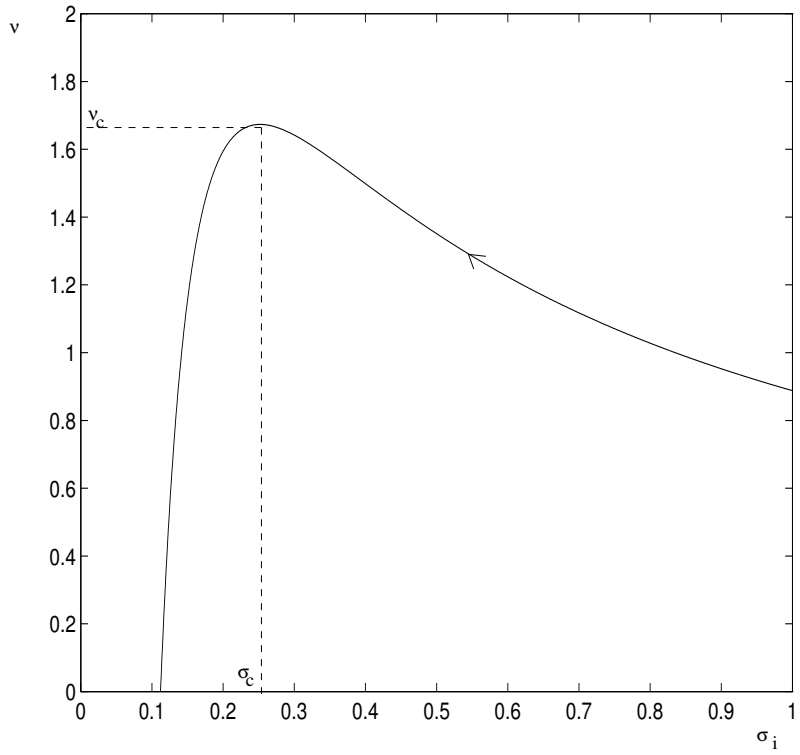


Figure 4.2: A typical plot of ν against σ_i showing critical values ν_c and σ_i^c at which the lens front stops advancing.

(It is also worth noting that the point at which $\nu = 0$ occurs is at $\sigma_i = \alpha S_0$.) The critical load, N_c, at which heave is suppressed is then given by

$$N_c = \frac{(1 - \chi(S_0))\gamma^\alpha c}{(\alpha + 1)^{\alpha+1} S_0^\alpha}. \tag{4.30}$$

For typical soil types we might have the following parameter values and corresponding critical overburdens

Parameter	**Sand**	**Silt**	**Clay**
α	0.00	0.35	0.80
c	0.15	0.50	0.70
S_0	0.00	0.33	0.33
$\chi(S_0)$	0.00	0.20	0.20
N_c	0.15	0.85	2.74

The critical value of N_c in the above table requires some comment. Some thought indicates that the correct way to let α and S_0 tend to zero is to let α tend to zero first. In that way, we find that the critical value N_c for soils with finite $N(0) = c$ is simply c, and in fact this can be ascertained directly from examination of $(4.23)_1$.

Thus, clay is capable of overcoming much greater loads than silt or sand but, as will be discussed in the next section, the amount of heave is much less for clays at a given overburden. The low value of N_c for sands suggests that a minimal value of effective stress will prevent them heaving. Thus, in field situations, sands may not heave at all if, for example, there is some resistance from the frozen soil above the frozen front to deformation or (for an unsaturated soil) if the water table is some way below the ground surface.

We have so far assumed that the physical solution to equation $(4.28)_1$ corresponds to the right hand side of figure 4.2 (i.e. $\sigma_i > \sigma_i^c = (\alpha+1)S_0$) so that the water content decreases as the effective stress increases. Although this physically seems reasonable, we should check that equation $(4.28)_2$ is consistent with this solution.

We define new variables as follows

$$y = \frac{\sigma_i}{\sigma_l}, \qquad\qquad x = \frac{\sigma_i}{S_0}. \tag{4.31}$$

Substituting these into equation $(4.28)_2$ we get

$$x\left(1 - \frac{1}{y}\right) = \ln\left(1 + \frac{x}{\alpha}\left(\frac{y^\alpha}{1 - \chi(S_0)} - 1\right)\right). \tag{4.32}$$

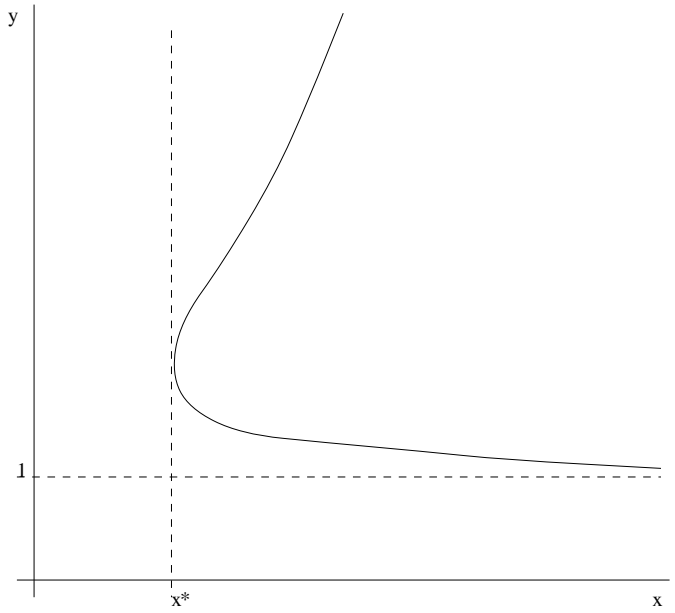


Figure 4.3: Schematic plot of x and y.

We first consider the limit as $x \to \infty$. In this case there are two solutions for y, one is ~ 1 and the other is $\sim e^{\frac{x}{\alpha}}$. Specifically we find that as $x \to \infty$ the behaviour of y is as one of the following:

$$\begin{aligned} y &\sim 1 + \frac{1}{x} \ln\left(\frac{x\chi(S_0)}{\alpha(1-\chi(S_0))}\right), \\ y &\sim \left(\frac{\alpha(1-\chi(S_0))}{x}\right)^{\frac{1}{\alpha}} e^{\frac{x}{\alpha}}. \end{aligned} \tag{4.33}$$

By considering the intersections of the right hand and left hand sides of 4.32 as functions of y for various x, it is easy to see that (for $y > 1$, i.e. $\sigma_i > \sigma_l$, which is physically required) 4.32 determines a curve indicated schematically in figure 4.3, with a nose at some value $x = x^*$. We can now combine the (x, y) plot and the (ν, σ_i) plot to obtain the dependence of y on ν. The shape of these plots depends on the location of the turning point x^* in the (x, y) plot and each of the possible outcomes is shown in figure 4.4. The various possibilities occur for values $x^* > \alpha + 1$, $\alpha < x^* < \alpha + 1$ and $x^* < \alpha$ (left to right in figure 4.4).

Thus from figures 4.2 and 4.4 it can be seen that for each load ν we have multiple roots for x and y, and hence for the water saturations σ_i and σ_l, which are all physically reasonable (i.e. $y > 1$). In discussing figure 4.2, we indicated that although all the solutions may be feasible, in practice we select the first to occur, and that,

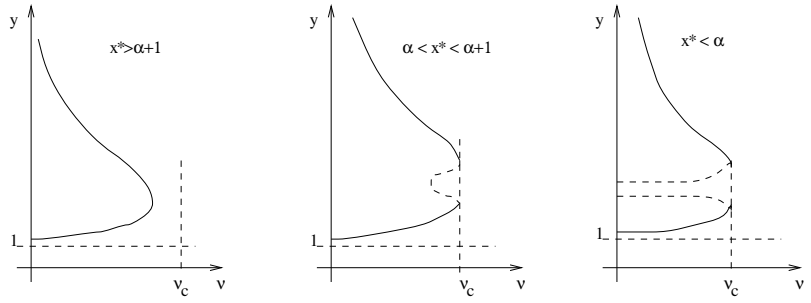


Figure 4.4: Plots of y versus ν for the possible values of x^*.

plausibly, this is the one which involves the least amount of freezing, and hence the highest values of S_i and S_l. In terms of x and y, this means selecting the higher value of x (or σ_i) in figure 4.2, and the solutions on this branch are represented in figure 4.4 by the unbroken lines. For these diagrams, we then select the smaller value of y, corresponding to the larger value of σ_l. In this way, we see that the lower branch of the curves in figure 4.4 is always selected, and that as ν tends to zero, y tends to 1, i.e. $S_i \approx S_l$, which corresponds to the large γ solution of 4.23.

4.3.2 The Heave Parameter, α_{fk}

The magnitude of heave depends on the parameter α_{fk} appearing in equation $(4.20)_2$. The parameter α_{fk} is expressed in terms of β_{fk} which, for a given soil, is essentially a function of the effective stress N at the frozen front. The soil type enters the parameter β_{fk} through the hydraulic conductivity function (i.e. specification of k_0 and γ) and the capillary suction function curve $f(S)$. In this section, we discuss the dependence of the parameter β_{fk} (and hence the heave parameter) on the soil type and the effective stress.

The parameter β_{fk} may be written as

$$\beta_{fk} = -\beta_0 S^\gamma \left(\frac{(f(S_l) - N)}{\delta\gamma(f(S_l) - N) + S_l f'(S_l)} \right) \tag{4.34}$$

and β_0 and δ_3 are given by

$$\begin{aligned} \beta_0 &= \frac{\gamma L^2 \rho_w k_0}{T_0 g k}, \\ \delta_3 &= \frac{\lambda L \rho_w}{k}. \end{aligned} \tag{4.35}$$

In chapter 3, section 3.2.3, we give values of the various constants appearing in these parameters. For each of the soil types clay, silt and sand, these parameters take the following values

$$\begin{aligned} &\beta_0 \sim 10^{-1} - 10 \quad \text{Clay} \\ &\beta_0 \sim 10^{2} - 10^{4} \quad \text{Silt} \\ &\beta_0 \sim 10^{7} - 10^{9} \quad \text{Sand} \end{aligned} \tag{4.36}$$

and we assume $\delta_3 \sim 3 \times 10^{-2}$ (cf. appendix B).

If we take a typical value of the saturation W_l/ϕ to be 0.5 then a typical value of the parameter β_{fk} for each soil type is as follows

$$\begin{aligned} &\beta_{fk} \sim 10^{-3} \quad \text{Clay} \\ &\beta_{fk} \sim 1 \quad \text{Silt} \\ &\beta_{fk} \sim 10^{5} \quad \text{Sand.} \end{aligned} \tag{4.37}$$

Thus, from the definition of α_{fk}, we would expect that, for a given overburden, silts and sands would produce (dimensionless) heave of ~ 1 whereas clays would produce (dimensionless) heave of $\sim 10^{-2}$ or $\sim 10^{-3}$ depending on whether the Gilpin or rigid ice approach is adopted.

Increasing the effective stress will act to decrease the water content at the base of the lowest lens and thus dramatically reduce β_{fk} because of the large exponent γ which is applied to the water saturation. Hence, in general, the amount of heave decreases exponentially (and rapidly) with increasing effective stress.

Fowler & Krantz (1994) also consider the variation in heave with the term

$$\beta_m = -\left(\frac{(f(S_l) - N)}{\delta\gamma(f(S_l) - N) + S_l f'(S_l)}\right), \tag{4.38}$$

appearing in the definition of β_{fk}. By using the leading order behaviour of equation $(4.23)_1$ to write $f - N = \chi f$, this may be written more simply as

$$\beta_m = \frac{1}{(S_l/\chi(S_l))[\ln(1/f(S))]'_l - \delta\gamma}. \tag{4.39}$$

Fowler & Krantz (1994) then consider the following functional forms of the capillary suction characteristic curve, $f(S)$, and the stress partition function, $\chi(S)$,

$$\begin{aligned} f(S) &= \frac{(1-S)^p}{S^q}, \\ \chi(S) &= S^r, \end{aligned} \tag{4.40}$$

for $0 < p < 1$, $q \geq 0$ and $r > 0$. Substitution of these relations into equation 4.39 then gives

$$\beta_m = \frac{1}{qS_l^{-r} + pS_l^{-(r-1)}/(1 - S_l) - \delta\gamma}. \tag{4.41}$$

where the saturation S_l is given by

$$\frac{(1 - S^r)(1 - S)^p}{S^q} = N. \tag{4.42}$$

Fowler & Krantz show that two behaviours are possible, depending on the values of q, p, r and $\delta\gamma$. When $r = 1$, the second of these, in which $\beta_m \to \infty$ as $N \to N_c$, only occurs if $p < \delta\gamma + q$ and $q < (\sqrt{p} - \sqrt{\delta\gamma})^2$ (this condition is given incorrectly by Fowler & Krantz), which for reasonable choices of the parameters unlikely to occur. For example, if $p = 0.5$ and $\delta\gamma = 0.9$ then $q < 0.06$.

Otherwise, β_m is a unimodal (humped) function of N, with β_m tending to zero as $N \to 0$ and $N \to \infty$. When multiplied by $\beta_0 S^\gamma$ in 4.34, this suggests that β_{fk} will be a strongly decreasing function of N for $N = O(1)$. The region near $N = 0$ where β_{fk} is apparently increasing is an artifact, due to the fact that the approximation involved in writing 3.24 for 3.27 also breaks down as $N \to 0$ (i.e. $S \to 1$), as can be seen from 4.23.

4.4 Linear System

Equations 4.20 are two first order differential equations which can be solved numerically using any standard solver, such as a Runge Kutta method, providing some care is taken at $t = 0$ where there is a singularity in the heave rate, $\dot{z}_s$, and lens front speed, $\dot{z}_l$. However, where the hydrostatic pressure effects can be ignored (i.e. $\delta_2^f \ll 1$) so that the heave parameter is independent of z_s and z_l, equations 4.20 for the laboratory problem may be converted to a linear system by the following change of variables

$$\begin{aligned} h_1 &= z_s - z_l, \\ h_2 &= z_l - z_b, \\ \frac{dt}{d\tau} &= h_1 h_2. \end{aligned} \tag{4.43}$$

With this change of variables, equations 4.20 may be written as

$$\dot{h}_2 \;=\; \frac{k_f}{k} T_s A_{fk} h_2 + B_{fk} h_1,$$

$$\begin{aligned}\dot{h}_1 &= -\frac{k_f}{k}T_s(A_{fk}+\alpha_{fk}(1-A_{fk}(W_l-W_m)))h_2 \\ &\quad -B_{fk}(1-\alpha_{fk}(W_l-W_m))h_1, \end{aligned} \tag{4.44}$$

where the overdots now refer to differentiation with respect to τ and the constants A_{fk} and B_{fk} are given by

$$\begin{aligned}A_{fk} &= \frac{1-\alpha_{fk}}{(\phi-W_m)-\alpha_{fk}(W_l-W_m)}, \\ B_{fk} &= \frac{T_b}{(\phi-W_m)-\alpha_{fk}(W_l-W_m)}. \end{aligned} \tag{4.45}$$

These parameters can be shown to be the same as those defined by Fowler & Krantz (1994) (see their equations (86) and (87)).

Equations 4.44 are a simple linear system to which the exact solution may be written down in terms of exponentials in the non-linear time variable τ. The numerical procedure used in section 4.7 uses the solution to the linear system 4.44 to find the solution to the nonlinear system 4.20.

4.5 Approximate Analytic Solution

In this section we present asymptotic solutions to the non-linear system 4.20 for small and long times. The small time solution takes the form of a similarity solution whereas the long time solution takes advantage of the fact that the frost penetration depth is controlled by thermal processes. As such, at least in the case where heave rate is small, the frozen front will tend to a constant depth.

4.5.1 Small Time Analysis

For small times the gravitational effects are small and hence we can find a similarity solution, valid in all instances, of the form

$$z_s = a\sqrt{t} \qquad\qquad z_l = -b\sqrt{t}.$$

Substituting these forms into equations 4.20 and ignoring terms of $O(\sqrt{t})$ we get the following algebraic relationship for a and b

$$\begin{aligned}-\frac{b(\phi-W_m)}{2} &= \frac{a}{2}+\frac{k_fT_s}{k(a+b)} \\ \frac{a}{2} &= \alpha_{fk}\left(-(W_l-W_m)\frac{b}{2}-\frac{k_fT_s}{k(a+b)}\right). \end{aligned} \tag{4.46}$$

Solving these relationships for a and b we get

$$\begin{aligned} a &= \alpha_{fk}(\phi - W_l)\sqrt{\frac{-2T_s\frac{k_f}{k}}{(\phi - W_m - \alpha_{fk}(W_l - W_m))(1 - \alpha_{fk}(1 - \phi + W_l))}} \\ b &= \frac{(1-\alpha_{fk})}{\alpha_{fk}(\phi - W_l)}a. \end{aligned} \tag{4.47}$$

These relations show that a fringe will only form (i.e. $b \geq 0$) if the heave parameter $\alpha_{fk} \leq 1$. From equations 4.22 we have that the heave parameter α_{fk} is given by

$$\begin{aligned} \alpha_{fk} &= \frac{\beta_{fk}}{(1+\beta_{fk})(1-\phi+W_l)}, \quad \text{(Rigid Ice)} \\ \alpha_{fk} &= \frac{(\beta_{fk} + \delta_3(\phi - W_l))}{(1+\beta_{fk})}. \qquad \text{(Gilpin).} \end{aligned} \tag{4.48}$$

The discussion in section 4.3.2 showed that the heave parameter α_{fk} is ~ 1 for sand and silt type soils when β_{fk} is $\sim 10^5$ and ~ 1 respectively. For these soil types, the regelative flux parameter $\delta_3 \ll \beta_{fk}$ and hence it is interesting to note from equations 4.48 that the Gilpin version of the heave parameter will always satisfy the condition that it is less than 1 whereas the rigid ice version will not.

4.5.2 Long Time Analysis

We consider a long time analysis in the case of a small heaving parameter, α_{fk}. As $t \to \infty$ we expect the lens front speed, $\dot{z}_l$, to tend to 0 (i.e. $z_l \to$ constant). Substituting this into equations 4.20 and solving the resulting system for the laboratory situation we find

$$\begin{aligned} z_l &= -\frac{\frac{k_f}{k}T_s z_b}{T_b - \frac{k_f}{k}T_s}, \\ z_s &= \frac{\alpha_{fk}k_f T_s}{k z_l}t + C, \end{aligned} \tag{4.49}$$

where C is an arbitrary constant. The freezing front reaches an equilibrium position while the heave rate becomes constant. For the permafrost problem, the equilibrium position of the frozen front is given by $z_l = (k_f/k)T_s$ and the long term heave rate takes the same form as that given above.

4.6 Lens Spacing and Lens Thickness

In chapter 3 we derived an 'averaged' continuum version of the discrete generalised Miller model. However, when comparing this averaged model with the full numerical

solution and observation it is useful to also compare lens spacing and lens thickness. In particular, we are able to show that lens thickness and lens spacing increase with depth as is the case for the numerical results of O'Neill & Miller (1985).

After some rearrangement of equations 3.26 we can show that lens spacing, $d_l = (z_l - z_i)$, is approximately equal to

$$d_l = \frac{\mu W_l}{\gamma \left.\frac{\partial W}{\partial \xi}\right|_l} \log\left(\frac{g(W_i) - N}{f(W_l) - N}\right). \tag{4.50}$$

Using equations 4.15, $(4.18)_2$ and $(4.20)_2$ it is relatively straightforward to show that boundary condition $(4.6)_2$ may be written as

$$\left.\frac{\partial W}{\partial \xi}\right|_l = -\frac{W_l}{(\delta\gamma(f(W_l) - N) + W_l f'(W_l))} \frac{1}{(1 + \beta_{fk})} \frac{\dot{z}_s}{\alpha_{fk}} \tag{4.51}$$

which, together with equation 4.50, gives the following equation for the lens spacing, d_l, in terms of the heave rate, $\dot{z}_s$

$$d_l = \frac{\mu}{\gamma} D_l \frac{\alpha_{fk}}{\dot{z}_s} \tag{4.52}$$

where D_l is given by

$$D_l = -(\delta\gamma(f(W_l) - N) + W_l f^{'}(W_l))(1 + \beta_{fk}) \log\left(\frac{g(W_i) - N}{f(W_l) - N}\right). \tag{4.53}$$

The heave rate $\dot{z}_s$ is a decreasing function of time and, if α_{fk} is small, it tends to a constant on intermediate time scales. As such, lens spacing will increase with time and will level off if the heave parameter is small. This is in agreement with the numerical results of O'Neill & Miller (1985). Furthermore, the parameter D_l is essentially a linear function of the parameter β_{fk} discussed in section 4.3.2. From this analysis we can conclude that lens spacing increases as the soil type moves from clay through to sands.

Let t_l^{n-1} be the time of the formation of the $(n-1)$th lens. Then t_l^n is given approximately by

$$z_l(t_l^{n-1}) - z_l(t_l^n) = d_l(t_l^n) \tag{4.54}$$

and hence lens thickness, h_l, is simply

$$h_l = z_s(t_l^n) - z_l(t_l^{n-1}). \tag{4.55}$$

Since typically hundreds of ice lenses will form, the time between successive lens formation will be small and these relationships can be written approximately as

$$\begin{aligned} t_l^n - t_l^{n-1} &= -\frac{d_l}{\dot{z}_l} \\ h_l &= -d_l \frac{\dot{z}_s}{\dot{z}_l}. \end{aligned} \tag{4.56}$$

The second of these relationships says the the instantaneous lens thickness divided by the instantaneous lens spacing is equal to the heave rate divided by the absolute value of the frost penetration rate.

Full numerical solutions to the recurrence relations for the approximate lens spacing and lens thickness are presented in section 4.7.

4.7 Numerical Solution

In this section we compare the solution to the system given by equations 4.20 with the numerical solution to the full system given by O'Neill & Miller (1985). This comparison is only a qualitative one as the information on the soil sample and freezing conditions provided in this paper is not sufficient to fully describe the situation. However, as many as possible of the conditions which actually applied are replicated for the purpose of this comparison. In particular, the capillary suction function, $f(W)$, has been obtained from the O'Neill & Miller paper by an approximate least squares fit. The full specification of the freezing soil sample used to produce our results is as follows:

Density of water, ρ_w	$1000\,\mathrm{kg\,m^{-3}}$
Density of ice, ρ_i	$917\,\mathrm{kg\,m^{-3}}$
Acceleration due to gravity, g	$9.8\,\mathrm{m\,s^{-2}}$
Latent heat of fusion for water, L	$3.35 \times 10^5\,\mathrm{J\,kg^{-1}}$
Thermal conductivity, k, for all phases	$4\,\mathrm{W\,m^{-1}\,K^{-1}}$
Hydraulic conductivity, k_0	$1.0 \times 10^{-9}\,\mathrm{m\,s^{-1}}$
Overburden, P	10, 20, 30, 40, 45 kPa
Far field water pressure, p_∞	0 kPa
Soil surface temperature, T_s	272.5 K
Base temperature, T_b	274 K

Freezing point of water, T_0	$273\,\mathrm{K}$
Height of soil sample, d	$0.153\,\mathrm{m}$
Capillary relation, $\log f(W)$	$0.34394\log(0.411-W)$
	$-8.5\times10^{-3}(\log(0.411-W))^2$
	$-0.78334\log(W-0.14)$
	$+3.91\times10^{-2}(\log(W-0.14))^2$
	$+4.29$
Stress partition function, $\chi(W)$	$\left(\frac{W}{\phi}\right)^{1.5}$
Hydraulic conductivity, $k(W)$	$k_0\left(\frac{W}{\phi}\right)^9$

Throughout this section we consider a step freezing experiment whereby a temperature below freezing is suddenly applied to the surface of the soil sample. Thus, initial conditions to the nonlinear system 4.20 are $z_s = z_l = 0$ at $t = 0$.

The results given below are taken from Fowler & Noon (1993) and use the 'rigid ice' form of the heave parameter α_{fk}.

4.7.1 Heave and Frozen Front Depth

The simplified system produced in this chapter was solved by first considering the solution to the linear system derived in section 4.4 and then integrating the quadrature equation for time. These equations are only solved up to the point where the frozen front stops advancing (i.e. $\dot{z}_l = 0$) because after this point the 'averaged' approach used in deriving the reduced equations breaks down.

It was found that for this particular capillary relation the critical heave pressure (see section 3.3.1) was around 46kPa and, in fact, as expected, the numerical algorithm used to find the water content at the base of the lowest ice lens, W_l, breaks down at around this point. Thus, lens initiation is suppressed after the load exceeds this critical pressure and, as a result, we only consider overburdens up to 45kPa.

For the range of overburdens considered, the heaving parameters were as follows

$\alpha_{fk}(\times10^{-2})$	P (kPa)
24	10
7	20
3	30
0.9	40
0.4	45

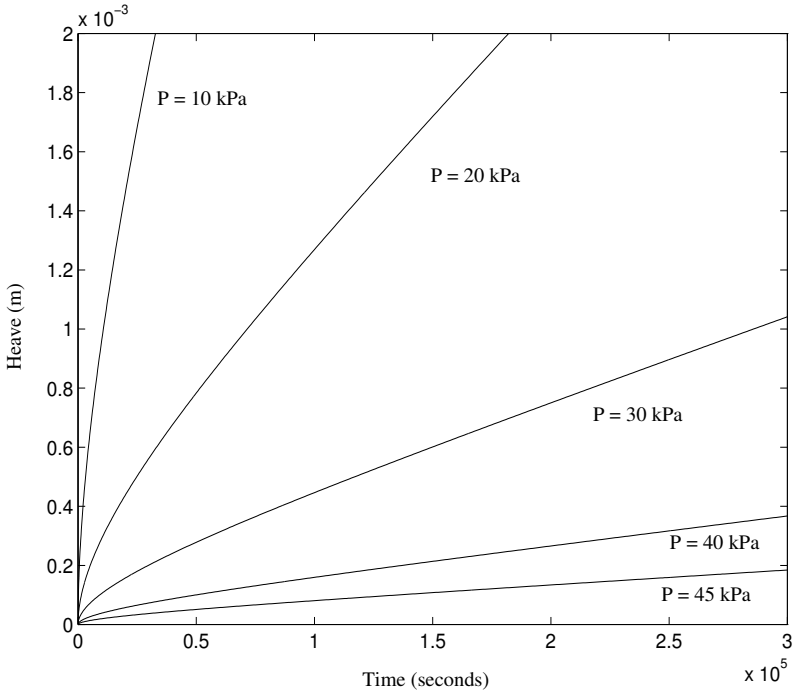


Figure 4.5: Plots of heave against time for various overburdens.

Plots of heave and frozen front depth against time are shown in figures 4.5 and 4.6 and can be directly compared with figures 5 and 7 shown in the paper of O'Neill & Miller.

In each case, the solutions to the reduced equations are in good qualitative agreement with the solution obtained by O'Neill & Miller. In particular, heave initially behaves like the square root of time before becoming linear while the frozen front also initially behaves like the square root of time before becoming constant (compare this with the asymptotic solutions given in section 4.5).

4.7.2 Lens Spacing and Thickness

Another qualitative comparison of the numerical results produced by O'Neill & Miller and our reduced system, is consideration of the lens spacing and lens thickness. The recurrence relations established in section 4.6 were solved using the z_s and z_l profiles established above up to the formation of the final lens (i.e. $\dot{z}_l = 0$). In order to initiate lens formation, a small perturbation needed to be applied to the initial conditions given above; otherwise, due to the singularity in z_s and z_l at $t = 0$, only one lens

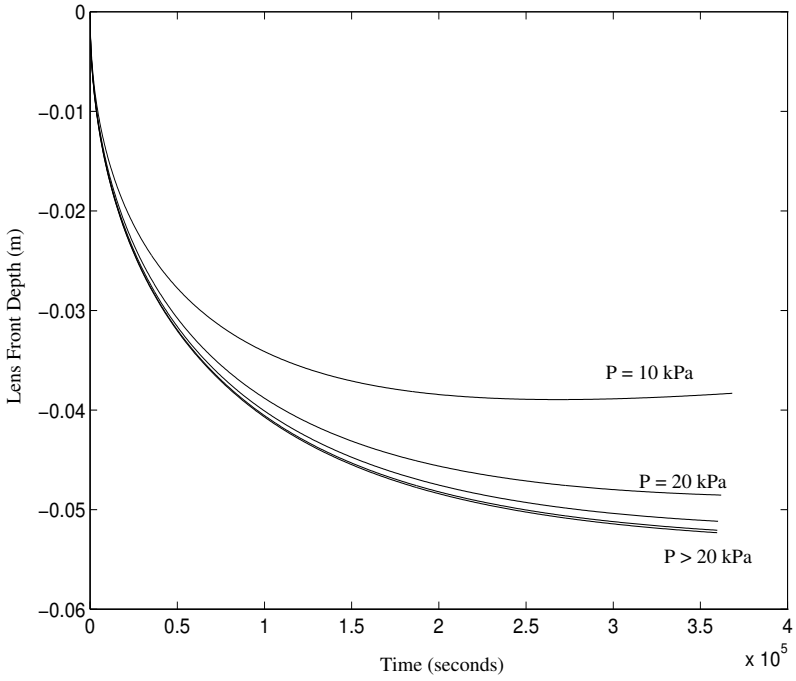


Figure 4.6: Plots of the lens front depth against time for various overburdens

would form on the surface of the soil.

The solutions to these recurrence relations are given in figures 4.7 and 4.8. These again show good qualitative agreement with the results of O'Neill & Miller (see their figure 4). In particular, lens spacing increases with time and levels off towards the production of the final lens. Similarly, lens thickness increases with time.

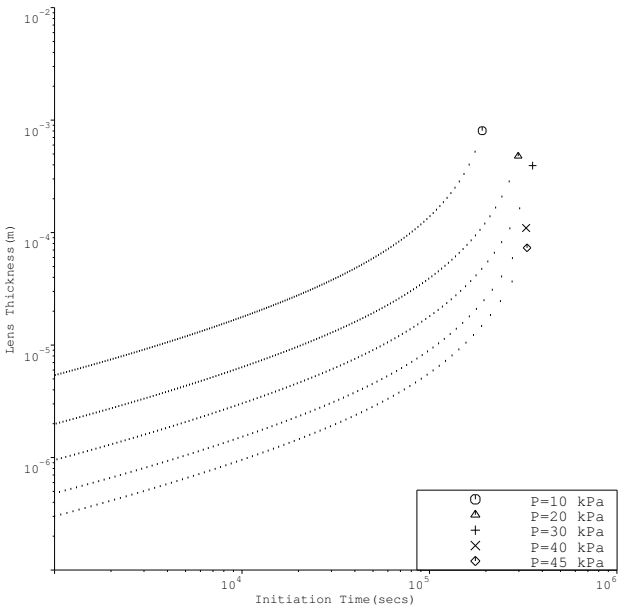


Figure 4.7: Plots of lens thickness against time for various overburdens.

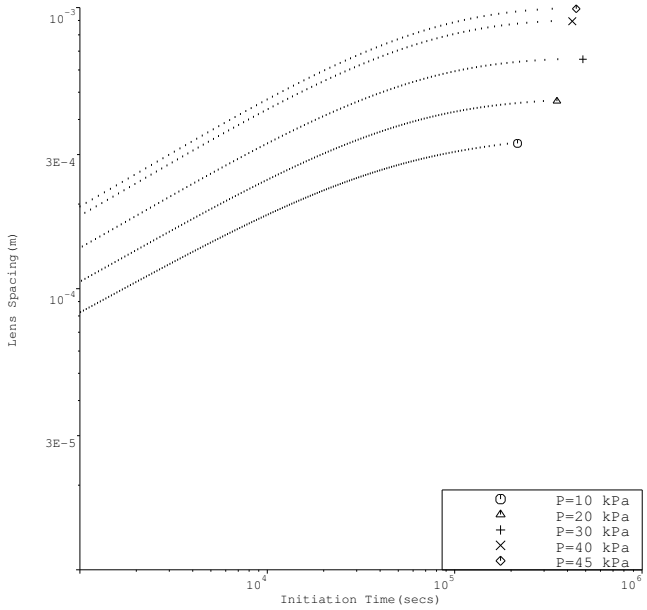


Figure 4.8: Plots of lens spacing against time for various overburdens.

Chapter 5

Saline Soils

5.1 Introduction

Despite a significant amount of engineering interest (e.g. the construction of artificial islands within arctic waters and the use of salines to control frost heave), there have been very few empirical or theoretical studies that have considered the effects of salinity on the frost heave process.

Beskow (1935) was among the first to perform such experiments and found that the presence of solutes significantly decreased the amount of heave. More recently, Chamberlain (1983) quantified the reduction in heave attributable to the presence of solutes by directly comparing the heave produced by soil samples containing distilled water and sea water. For both the sand and clay samples considered, the reduction for the particular range of applied temperatures was in excess of 50%.

However, there have been a number of investigations on the redistribution of solutes within a freezing soil in which the frozen front is propagating downwards, and where the soils are not usually susceptible to frost heave. Hallet (1978) discusses the concept of solute rejection at the freezing front (i.e. solutes are rejected from the ice phase into the unfrozen pore water) and this appears to be a well documented phenomenon. This, together with other solute redistribution characteristics, has also been considered empirically by Kay & Groenevelt (1983) and Baker & Osterkamp (1989). These empirical studies confirm the 'freezing out' phenomenon and suggest that the convective-diffusion equation and the associated boundary conditions for the solute redistribution derived in chapter 2 is the correct approach. Panday & Corapcioglu (1991) numerically solve this type of convective-diffusion equation for a

non-heaving soil and obtain solute profiles that agree with a number of experimental observations.

Frost heave models with the inclusion of solutes have been derived by Cary (1987), Noon (1990), Panday & Corapcioglu (1991) and Padilla & Villeneuve (1992). With the exception of the model given by Cary, these models are essentially generalisations of the Miller model and the inclusion of solutes is incorporated via the Clapeyron relation. The Clapeyron equation controls the temperature required to freeze the pore water and, consequently, the inclusion of solutes may act to depress this temperature further (i.e. allowing the pore water to supercool further). Thus, the presence of solutes acts to decrease the freezing rate within the fringe (and thus reduce the heave rate) and also reduces the depth to which the frozen front may advance. This effect is compounded by freezing out the solutes at the lens front which, because the diffusive and convective time scales are similar, causes the solute concentration at the frozen front to increase. In this chapter we apply a similar procedure to that used in chapter 4 in the absence of solutes to reduce the generalised Miller model to a pair of ordinary differential equations for the frost penetration depth and heave, coupled to a convective-diffusion equation for solute concentration in the unfrozen zone. A heave parameter, α_{cl}, is established which depends on the solute concentration in the frozen fringe. A brief comparison is given between the reduced system with the inclusion of solutes and the reduced system 4.20 derived in chapter 4, through the form of the respective heave parameters and the reduction in the jump in heat flux across the frozen fringe.

Asymptotic solutions are given for small times in the form of a similarity solution and for long times a steady state solution is found when the heaving parameter is small. A full numerical solution is also given for a step freezing problem and the results are compared with the asymptotic solutions.

Finally, a qualitative comparison is given between the numerical solution of the reduced system and the empirical results of Chamberlain (1983).

5.2 Solution to the Fringe Equations

In this section we show how the fringe equations may be reduced to a pair of ordinary differential equations which depend on the solute concentration within the frozen

fringe. As in chapter 4, this simplification is a result of the frozen fringe thickness being small, which allows us to integrate the fringe equations and solve the resulting system.

The temperature in the frozen fringe is controlled by the Clapeyron relation $(3.33)_5$ which is a function of the capillary suction through the parameter μ and the osmotic potential through the parameter ν. In some instances (e.g. pore water is sea water) the osmotic potential may be high relative to capillary suction (i.e. $\nu \gg \mu$). However, we will anticipate that the variation in osmotic pressure over the fringe will be $\sim \mu$ and, as such, we expect the fringe rescaling to be as follows

$$z = z_l - \mu\xi, \qquad T = -\nu c_l(t) + \mu\theta, \qquad c = c_l(t) - \mu\kappa.$$

where $c_l(t)$ is the solute concentration at the lens front, z_l. Substituting these rescalings into the averaged fringe equations and boundary conditions given at the end of chapter 3 we find that, for an incompressible soil, the leading order behaviour of these equations is as follows:

$0 < \xi < \xi_f$:

$$\begin{aligned}
&\frac{\partial}{\partial\xi}\left(U_w + (\phi - W)u_i\right) = 0,\\
&\dot{z}_l\frac{\partial W}{\partial\xi} - \frac{\partial U_w}{\partial\xi} = \frac{\partial^2\theta}{\partial\xi^2},\\
&p_w = p_f - [p_f - P + f(W_l)]\exp\left(-\frac{\gamma}{W_l}\left.\frac{\partial W}{\partial\xi}\right|_l \xi\right),\\
&\theta = -(\delta p_w + f(W)) + \nu\kappa,\\
&u_i = \delta_3\frac{\partial\theta}{\partial\xi} \qquad \text{(Gilpin)},\\
\text{or} \qquad &u_i = \dot{z}_s \qquad\quad \text{(Rigid Ice)},\\
&P = P_0 + \delta_2^f(z_s - z_l),\\
&\dot{z}_l c_l\frac{\partial W}{\partial\xi} + \alpha\frac{\partial}{\partial\xi}\left(W\frac{\partial\kappa}{\partial\xi}\right) - c_l\frac{\partial U_w}{\partial\xi} = 0,
\end{aligned} \tag{5.1}$$

where we have again neglected the hydrostatic pressure in the frozen fringe and assumed that the water pressure p_f is prescribed at the frozen front z_f. The boundary conditions become

at $\xi = 0$

$$W = W_l,$$

$$
\begin{aligned}
&\frac{\partial W}{\partial \xi} = \phi\mu\tilde{\beta}U_w, \\
&c_l U_w = \alpha W \frac{\partial \kappa}{\partial \xi}, \\
&(W - W_m)\dot{z}_l - U_w = -\frac{k_f}{k}\,\frac{(T_s + \nu c_l)}{(z_l - z_s)} + \frac{\partial \theta}{\partial \xi}, \\
&\dot{z}_s = U_w + (\phi - W)u_i,
\end{aligned} \tag{5.2}
$$

at $\xi = \xi_f$

$$
\begin{aligned}
&W = \phi, \\
&[\kappa]^+_- = 0, \\
&\left[\frac{\partial \kappa}{\partial \xi}\right]^+_- = 0, \\
&\frac{\partial \theta}{\partial \xi} = \frac{T_b + \nu c_l}{(z_l - z_b)}, \quad \text{(Laboratory)} \\
&\frac{\partial \theta}{\partial \xi} = 1, \quad \text{(Permafrost)} \\
&\frac{\partial \theta}{\partial \xi} = 0, \quad \text{(Seasonal)}
\end{aligned} \tag{5.3}
$$

where $\xi_f = (z_l - z_f)/\mu$ and the water content at the lens front, W_l, is given by equations 3.27.

Equations 5.1 may now be integrated and a similar analysis to that given in chapter 4 may be used to find explicit relations for the frozen front depth, z_l, and the soil surface, z_s. We do not present the full analysis here but rather give the key steps required.

The equations for the heave rate, $\dot{z}_s$, and frost penetration rate, $\dot{z}_l$, are unchanged from those given by equations 4.13 and 4.12 derived in chapter 4 apart from the fact that the (dimensionless) temperature in the fringe is now $-\nu c_l(t)$ rather than 0. Thus, we have

$$
\begin{aligned}
&\dot{z}_l(\phi - W_m) - \dot{z}_s = \left.\frac{\partial \theta}{\partial \xi}\right|_f + \frac{k_f}{k}\,\frac{T_s + \nu c_l}{z_s - z_l}, \\
&\dot{z}_s = U_{wl} + (\phi - W_l)\dot{z}_s, \quad \text{(Rigid Ice)} \\
&\dot{z}_s = U_{wl} + \delta_3(\phi - W_l)\left.\frac{\partial \theta}{\partial \xi}\right|_l, \quad \text{(Gilpin)}
\end{aligned} \tag{5.4}
$$

where the suffices l and f refer to quantities evaluated at the base of the lowest ice lens and at the frozen front respectively.

The temperature gradient at the freezing front is found from boundary conditions $(5.3)_{4,5}$ and hence we need to calculate the temperature gradient and water flux at the lens front from the manipulation of the integrated fringe equations and boundary conditions. We find that the equivalent relations to equations 4.14 and 4.17 for the temperature gradient and water flux at the lens front are as follows:

$$\left.\frac{\partial\theta}{\partial\xi}\right|_l = \left(\frac{1}{\beta_{fk}} + \frac{\nu c_l}{\alpha W_l}\right) U_{wl},$$
$$U_{wl} = (W_l - W_m)\dot{z}_l - \frac{k_f}{k}\frac{(T_s + \nu c_l)}{(z_s - z_l)} - \left.\frac{\partial\theta}{\partial\xi}\right|_l, \tag{5.5}$$

where β_{fk}, defined in chapter 4, is as follows

$$\beta_{fk} = -\frac{\gamma L^2 \rho_w k_0}{T_0 g k}\left(\frac{W_l}{\phi}\right)^{\gamma}\left(\frac{(f(W_l) - N)}{\delta\gamma(f(W_l) - N) + W_l f'(W_l)}\right), \tag{5.6}$$

and N is the effective stress at the frozen front (i.e. $P - p_f$).

These relations can be solved to give the water flux and temperature gradient at the base of the lowest ice lens which may then be substituted into equations 5.4 to give the expressions for the heave rate and frost penetration rate as follows

$$\begin{aligned}\dot{z}_l(\phi - W_m) &= \dot{z}_s + \left.\frac{\partial\theta}{\partial\xi}\right|_f + \frac{k_f}{k}\frac{T_s + \nu c_l}{z_s - z_l},\\ \dot{z}_s &= \alpha_{cl}\left((W_l - W_m)\dot{z}_l - \frac{k_f}{k}\frac{T_s + \nu c_l}{z_s - z_l}\right),\end{aligned} \tag{5.7}$$

where $\left.\frac{\partial\theta}{\partial\xi}\right|_f$ is given by

$$\begin{aligned}\left.\frac{\partial\theta}{\partial\xi}\right|_f &= \frac{T_b + \nu c_l}{(z_l - z_b)} \quad \text{(Laboratory)},\\ \left.\frac{\partial\theta}{\partial\xi}\right|_f &= 1 \quad \text{(Permafrost)},\\ \left.\frac{\partial\theta}{\partial\xi}\right|_f &= 0 \quad \text{(Seasonal)}.\end{aligned} \tag{5.8}$$

The heaving parameter, α_{cl}, written in terms of the heaving parameters 4.22 derived in chapter 4 (i.e. α^R_{fk} is the rigid ice parameter and α^G_{fk} is the Gilpin parameter), are as follows:

$$\begin{aligned}\alpha_{cl} &= \frac{\alpha^R_{fk}}{(1 + \tau_l\alpha^R_{fk})}, \quad \text{(Rigid Ice)}\\ \alpha_{cl} &= \frac{(\alpha^G_{fk} + \delta_3(\phi - W_l)\tau_l\alpha^R_{fk})}{(1 + \tau_l\alpha^R_{fk})}, \quad \text{(Gilpin)}\end{aligned} \tag{5.9}$$

where

$$\tau_l = \frac{\nu(1-\phi+W_l)c_l}{\alpha W_l}. \tag{5.10}$$

The salinity at the lens front, c_l, is found from the solution to equation 3.34 in the unfrozen region where the boundary condition for this equation at the freezing front is found by integrating equation $(5.1)_8$ across the frozen fringe and applying boundary condition $(5.2)_3$. This gives

$$\alpha\phi\frac{\partial c}{\partial z} = c(\dot{z}_s - \dot{z}_l(\phi - W_l)) \tag{5.11}$$

where we have removed the fringe rescaling.

Thus, the equation and boundary conditions which need to solved to determine the solute concentration at the lens front are as follows

$$\frac{\partial c}{\partial t} - \alpha\frac{\partial^2 c}{\partial z^2} + \frac{\dot{z}_s}{\phi}\frac{\partial c}{\partial z} = 0, \tag{5.12}$$

with $c = 1$ on $z = z_b$ (or equivalently $z_b = -\infty$ in the field) and

$$\alpha\phi\frac{\partial c}{\partial z} = c(\dot{z}_s - \dot{z}_l(\phi - W_l)) \tag{5.13}$$

on $z = z_l$.

Equations 5.7 and 5.12 now form the reduced description of frost heave with the inclusion of solutes. For clarity in the subsequent analysis we consider the laboratory situation only.

This reduced system has been derived without any recourse to the salinity of a particular soil. From the discussion in chapter 3 on the size of the various parameters we identified the following three limits

$$\begin{aligned} \nu &\ll \mu, \\ \nu &\sim \mu, \\ \nu &\gg \mu. \end{aligned} \tag{5.14}$$

However, because $\mu \ll 1$, the first two of these limits fall into the category $\nu \ll 1$ (lightly saline soils). Thus, in these cases, because $\nu \ll 1$ implies that $\tau_l \ll 1$, we can see that, to leading order, the effects of salinity uncouple from equations 5.7 and we are left with the equations 4.20 as given in chapter 4. In the third limit, the most common occurrence will be $\nu \sim 1$, which corresponds to the salinity of sea water.

Analytic and numerical solutions of these equations are presented in the following sections.

5.3 Physical Implications

The introduction of solutes into a freezing soil depresses the temperature at which pore water will freeze and this affects the frost heave process in a number of ways.

Most obviously, lower freezing temperatures are required for the initial nucleation of pore ice and, as such, in a period of decreasing temperature, the onset of frost heave in salt enriched soil will be later than that for a similar soil with a lower salt content.

The lower required freezing temperatures will mean that less pore water freezes within the frozen fringe of a saline soil than in the equivalent lower salinity soil and, as a result, the overall heave will be less. Further, the lower required freezing temperatures will restrict the advancement of the frozen front.

These results can be seen directly from the reduced systems of equations 5.7 and 4.20 (in the absence of solutes) and the heaving parameters which occur in these systems. In the case of a saline soil, we have expressed the heaving parameter, α_{cl}, in terms of the heaving parameters which occur in the absence of solutes (i.e. α^G_{fk} and α^R_{fk}) and this allows us to give a direct comparison between the various heaving parameters.

In general, the regelative flux parameter, δ_3, is small for most heaving soils (see chapter 3). Thus, from equations 5.9, we see that the introduction of solutes into a freezing soil scales the heaving parameter by a factor of $(1 + \tau_l \alpha^R_{fk})^{-1}$ where

$$\tau_l = \frac{\nu(1 - \phi + W_l)c_l}{\alpha W_l}. \tag{5.15}$$

Consequently, the introduction of solutes will reduce that heave parameter and hence the amount of heave. The heaving parameter α^R_{fk} increases as the soil type moves from clay to sand (see the discussion in section 4.3.2) and, as such, this analysis suggests that the reduction in the heaving parameter will be proportionately greater as the soil type moves from clay to sand.

The second mechanism by which the reduction in heave and frozen front propagation can be seen is through the reduction in the jump in heat fluxes across the frozen fringe due to the lower pore water freezing temperature, $-\nu c_l$. Thus, at a given frost penetration depth below the surface, the heave rate, $\dot{z}_s$, and frozen front penetration rate will be lower than the equivalent lower salinity soil.

Finally, it is worth pointing out that the introduction of solutes will not affect the level of the maximum overburden a soil can heave as this is determined by the capillary suction curve, $f(W)$.

5.4 Approximate Analytic Solution

In this section we present asymptotic solutions to the system derived above for small and long times. The small time solution takes the form of a similarity solution whereas the long time solution describes the steady state.

For this analysis we consider a step freezing problem with an initial uniform solute profile. Thus, the appropriate initial conditions are

$$\begin{aligned} c(z,0) &= 1, \\ z_s(0) &= 0, \\ z_l(0) &= 0. \end{aligned} \tag{5.16}$$

5.4.1 Small Time Analysis

A small time similarity solution to equations 5.7 and 5.12 exists in the form

$$\begin{aligned} z_s &= a\sqrt{t} & z_l &= -b\sqrt{t} \\ c &= c(\eta) & \eta &= \frac{z}{\sqrt{t}} \end{aligned}$$

Substituting these variables into equations 5.7 and 5.12 and the associated boundary conditions, the leading order behaviour of equations 5.7 is given by

$$\begin{aligned} a &= 2\alpha_{cl}\left(-\frac{(W_l - W_m)}{2}b - \frac{k_f}{k}\frac{(T_s + \nu c_l)}{(a+b)}\right). \\ b &= -\frac{2(1-\alpha_{cl})\frac{k_f}{k}}{(\phi - W_m - \alpha_{cl}(W_l - W_m))}\frac{(T_s + \nu c_l)}{(a+b)}. \end{aligned} \tag{5.17}$$

The solute transport equation in the unfrozen region becomes

$$\frac{d^2c}{d\eta^2} = -\frac{1}{2\alpha}\left(\eta - \frac{a}{\phi}\right)\frac{dc}{d\eta}, \tag{5.18}$$

with boundary conditions $c \to 1$ as $\eta \to -\infty$ and

$$\alpha\phi\frac{dc}{d\eta} = \frac{c}{2}(a + b(\phi - W_l)$$

on $\eta = -b$.

Integrating the solute equation gives the following expression for the solute profile in the unfrozen region

$$c(z,t) = 1 + A(a,b)\,\mathrm{erfc}\left(\frac{1}{2\sqrt{\alpha}}\left(-\frac{z}{\sqrt{t}} + \frac{a}{\phi}\right)\right), \tag{5.19}$$

where $\mathrm{erfc}(x)$ is the complementary error function and $A(a,b)$ is given by

$$\frac{(a + b(\phi - W_l)\sqrt{\alpha\pi}}{2\alpha\phi \exp\left[-\left(\frac{1}{2\sqrt{\alpha}}\left(b + \frac{a}{\phi}\right)\right)^2\right] - (a + b(\phi - W_l))\sqrt{\alpha\pi}\,\mathrm{erfc}\left(\frac{1}{2\sqrt{\alpha}}\left(b + \frac{a}{\phi}\right)\right)}.$$

Thus, evaluating this expression at $z = z_l$ will give us the small time value of $c_l(t)$ required for equations 5.17 as follows:

$$c_l = \left(1 - \frac{(a + b(\phi - W_l))\sqrt{\pi}\,\mathrm{erfc}\left(\frac{1}{2\sqrt{\alpha}}\left(b + \frac{a}{\phi}\right)\right)}{2\sqrt{\alpha}\phi \exp\left[-\left(\frac{1}{2\sqrt{\alpha}}\left(b + \frac{a}{\phi}\right)\right)^2\right]}\right)^{-1}. \tag{5.20}$$

Equations 5.17 and 5.20 form a non-linear set of equations for a, b and c_l which determine the small time solution for the heave and frost penetration depth.

5.4.2 Long Time Solution

For long times and for a small heaving parameter, α_{cl}, we anticipate a steady state solution given by

$$\begin{aligned} \dot{z}_s &= \text{ Constant}, \\ z_l &= \text{ Constant}. \end{aligned} \tag{5.21}$$

Substituting these relations for $\dot{z}_s$ and z_l into 5.7 and solving the resulting system using the fact that $\alpha_{cl} \ll 1$ we get

$$\begin{aligned} \dot{z}_s &= -\frac{\alpha_{cl}}{z_b}\left((T_b + \nu c_l) - \frac{k_f}{k}(T_s + \nu c_l)\right) \\ z_l &= -z_b \frac{(T_s + \nu c_l)\frac{k_f}{k}}{\left((T_b + \nu c_l) - \frac{k_f}{k}(T_s + \nu c_l)\right)}. \end{aligned} \tag{5.22}$$

The steady state solute profile given by

$$\phi\alpha\frac{\partial^2 c}{\partial z^2} = \dot{z}_s\frac{\partial c}{\partial z}, \tag{5.23}$$

with $c = 1$ on $z = z_b$ and

$$\alpha\phi\frac{\partial c}{\partial z} = c\dot{z}_s \tag{5.24}$$

on $z = z_l$.

Integrating this system and evaluating the resulting expression at $z = z_l$ we get

$$c_l = \exp\left(\frac{\dot{z}_s}{\alpha\phi}(z_l - z_b)\right). \tag{5.25}$$

Thus, 5.22 and 5.25 form the long time steady state solution when $\alpha_{cl} \ll 1$.

5.5 Numerical Solution

We consider a numerical solution to equations 5.7 and 5.12 and the associated boundary conditions for the step freezing initial conditions given at the beginning of the previous section.

5.5.1 The Numerical Procedure

The method adopted for the solution is to first consider a change in variable which fixes the domain in which we wish to solve equation 5.12. Thus, we write

$$\xi = \frac{z - z_b}{z_l - z_b},$$

whence equation 5.12 becomes

$$\frac{\partial c}{\partial t} = \frac{\alpha}{(z_l - z_b)^2}\frac{\partial^2 c}{\partial \xi^2} - \frac{1}{(z_l - z_b)}\left(\frac{\dot{z}_s}{\phi} - \xi\dot{z}_l\right)\frac{\partial c}{\partial \xi}, \tag{5.26}$$

with boundary conditions $c = 1$ on $\xi = 0$ and

$$\frac{\alpha\phi}{(z_l - z_b)}\frac{\partial c}{\partial \xi} = c(\dot{z}_s - \dot{z}_l(\phi - W_l))$$

on $\xi = 1$.

The method by which we solve 5.26 is one suggested in Crank (1984). The spatial domain is split into $N + 1$ equally spaced points given by

$$\xi_j = \frac{j}{N} = j\,\Delta\xi$$

for $j = 0, ..., N$. The first and second spatial derivatives of c are then approximated by

$$\begin{aligned} \frac{\partial c}{\partial \xi} &\approx \frac{c_{j+1} - c_{j-1}}{2\Delta\xi}, \\ \frac{\partial^2 c}{\partial \xi^2} &\approx \frac{c_{j+1} - 2c_j + c_{j-1}}{\Delta\xi^2}. \end{aligned} \tag{5.27}$$

Thus, we may write 5.26 as a system of N ordinary differential equations as follows

$$\frac{dc_j}{dt} = \frac{\alpha}{(z_l - z_b)^2}\left(\frac{c_{j+1} - 2c_j + c_{j-1}}{\Delta\xi^2}\right) - \frac{1}{(z_l - z_b)}\left(\frac{\dot{z}_s}{\phi} - \xi_j \dot{z}_l\right)\left(\frac{c_{j+1} - c_{j-1}}{2\Delta\xi}\right), \tag{5.28}$$

for $j = 1, ..., N$. The terms $c_0(t)$ and $c_{N+1}(t)$ come from the boundary conditions at $\xi = 0$ and $\xi = 1$ and may be written as $c_0(t) = 1$ and

$$c_{N+1} = c_{N-1} + c_N \frac{2\Delta\xi}{\alpha\phi}(z_l - z_b)(\dot{z}_s - \dot{z}_l(\phi - W_l)).$$

We have then approximated the reduced frost heave equations 5.7 and 5.12 as a system of $N + 2$ ordinary differential equations for z_s, z_l and c_j $(j = 1, ..., N)$ where $c_l(t) = c_N(t)$. This system is then amenable to solution using the NAG routine D02BBF which uses a Runge-Kutta-Merson method to integrate a system of ordinary differential equations and returns the solution at intermediate time intervals.

The form of the small time similarity solution derived in section 5.4.1 indicates that the initial heave and frost penetration rates are infinite. This introduces a singularity at $t = 0$ in the numerical scheme derived above and, to overcome this, the small time similarity solution is used to obtain the initial conditions for the numerical procedure.

5.5.2 The Numerical Solution

The soil sample used in this numerical simulation is as described in section 4.7 for the situation without solutes. The thermal and stress conditions used together with the additional information required are as follows

Effective Stress, $N = P - p_f$	30 kPa
Soil surface temperature, T_s	270 K
Base temperature, T_b	274 K
Freezing point of water, T_0	273 K

Solute Diffusivity, D_0	$7 \times 10^{-9}\,\mathrm{m^2\,s^{-1}}$
Far Field Solute Concentration, c_∞	$615\,\mathrm{mole\,m^{-3}}$

For comparison, numerical simulations were done both with and without the presence of solutes.

In order to start the numerical algorithm described in the previous section, the equations for the small time similarity solution were solved to find the initial behaviour of the surface heave, lens front and the salinity profile. The solutions to this system for the soil, temperature and stress conditions described above were found to be as follows

	Sea Water	Distilled Water
a	5.92×10^{-3}	15.50×10^{-3}
b	1.43	2.67
c_l	1.90	–

This similarity solution was used for (dimensionless) times less than 10^{-3} and from this point the numerical scheme was used until the frost penetration rate, $\dot{z}_l$, became zero. The results of these calculations for the heave and frozen front depth are shown in figures 5.1 and 5.2 respectively. These plots show the results obtained for both the sea water and distilled water situations and reveal, as expected, that the overall heave and frost penetration depth are much reduced in the case of the sea water saturated soil (these plots are discussed further in the next section).

Figures 5.3 and 5.4 show comparative plots of the asymptotic solutions and the solution to the numerical algorithm for the soil containing sea water.

5.6 Discussion

Chamberlain (1983) directly compared the heave produced by soils containing sea water with that produced by soils containing distilled water. His experiments suggested that the difference in heave between soils samples containing distilled water and those containing sea water was in excess of a 50% reduction. Unfortunately, the exact conditions which applied during his experiments and the particular characteristics of the Dartmouth sand and Morin clay he used are difficult to infer from the

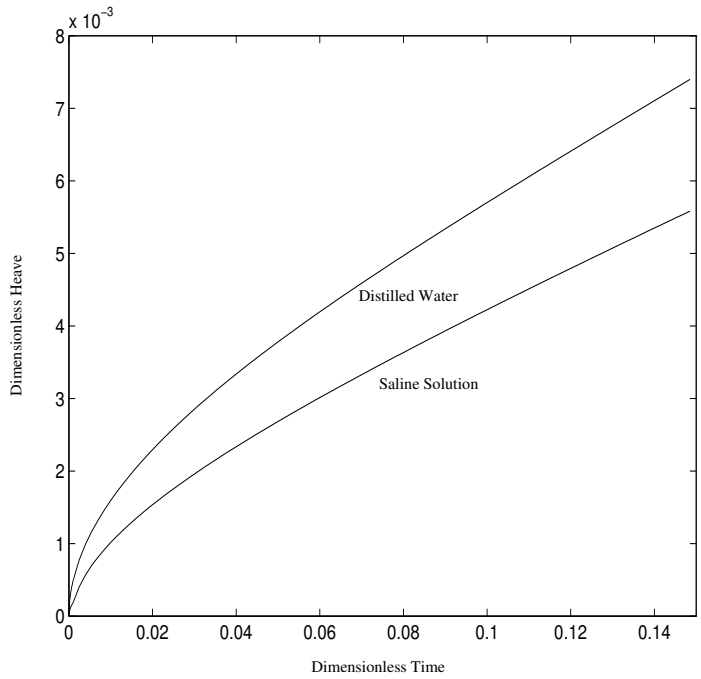


Figure 5.1: Plots of (dimensionless) heave against (dimensionless) time for a soil containing sea water and a soil containing distilled water.

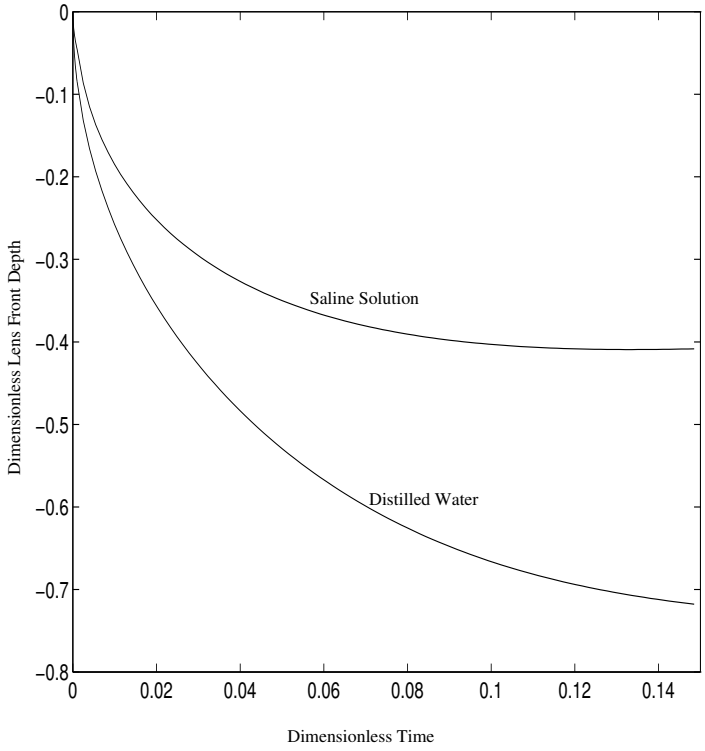


Figure 5.2: Plots of (dimensionless) lens front depth against (dimensionless) time for a soil containing sea water and a soil containing distilled water.

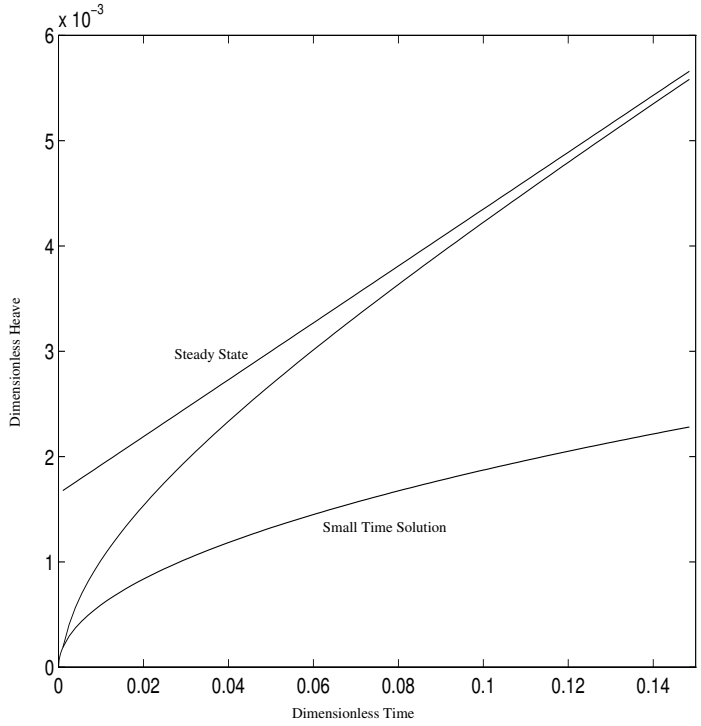


Figure 5.3: Comparative plots of the small and long time asymptotic solutions against the numerical solution for the (dimensionless) heave.

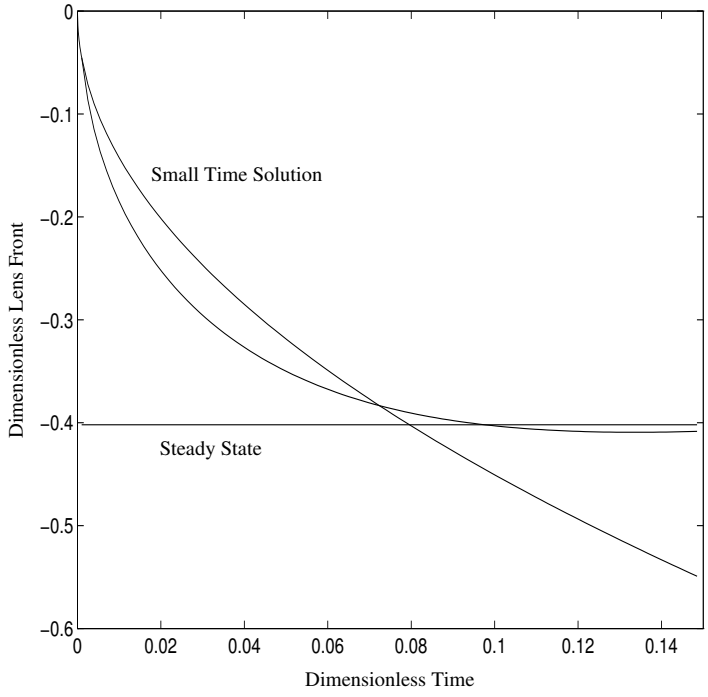


Figure 5.4: Comparative plots of the small and long time asymptotic solutions against the numerical solution for the (dimensionless) lens front depth.

published paper. As such, we are only able to give a qualitative comparison of his results with the theory produced in this chapter.

Chamberlain's experiments considered Morin Clay and Dartmouth Sand soil types and appear to be split into three distinct stages in which different thermal conditions apply. The first stage (Stage I) applied a constantly decreasing temperature at the soil surface until the frozen front reached a prescribed depth range. Following this (Stage II) the constant temperatures reached were applied for at least 100 hours and finally (Stage III) the soil sample was frozen rapidly to the bottom.

The comparative heave rates during Stage I of Chamberlain's experiments were between 60% and 70% lower in the presence of sea water for both soil types. This order of magnitude reduction agrees with the initial asymptotic solutions shown in the table given in section 5.5.2 (i.e. $(15.50 - 5.92)/15.50 = 62\%$ reduction in heave rate).

Stage I of the experiments appear to be $2 - 3$ times longer for the sea water saturated soil samples indicating a lower frost penetration rate in the saline soil and a lower ultimate frozen front depth. This agrees with the short and long term asymptotic solutions given in section 5.4 and in the table given in section 5.5.2.

Stage II of Chamberlain's experiments indicate that the reduction in heave rate attributable to the effects of salinity was greater for the Dartmouth Sand than for the Morin Clay. This agrees with the analysis given in section 5.3 of the dependence of the heave parameter, α_{cl}, on soil type.

Thus overall, the results of this chapter are apparently consistent with the results of Chamberlain's experiments and consequently the Miller model appears to readily generalise to the inclusion of solutes.

Chapter 6

Massive Ice Formation

6.1 Introduction

The work presented so far has essentially focused on laboratory simulations of frost heave. In the following two chapters we consider in more detail the field situation through the introduction of the rheology of the frozen and unfrozen regions.

In permafrost regions, large ice formations, often several metres thick, are observed to have formed within the permafrost. These ice formations are termed *massive ice* and at least some of it is thought to have been formed as a result of frost heave when ice sheets retreated and permafrost aggradation occurred (see Burn & Smith (1993)). Bore holes which have been drilled in permafrost also reveal rhythmic banding of segregated seams of massive ice which is a classic trait of frost heave and gives additional support to this theory. Detailed information on the distribution of segregated massive ice is scarce. However, Williams & Smith (1989) suggest that these ice layers form in the top 50 or 60 metres of the ground surface and, contrary to the usual view of ice lenses in frost heave, lens thickness decreases with depth.

Mackay (1971) attempted to explain the formation of massive ice in terms of a frost heave mechanism based on a simple primary heave type approach. In this chapter we show how secondary frost heave could be a possible mechanism for the formation of segregated massive ice in permafrost and, in particular, how the secondary frost heave approach gives good qualitative agreement with observation.

The analysis presented in chapter 3 assumed the existence of a prescribed water pressure, p_f, (or equivalently an effective stress, N) at the frozen front. Laboratory conditions allow this quantity to be prescribed as simply the water pressure at the base

of the sample. However, in the field situation, it will not be possible to prescribe the water pressure at the freezing front and, consequently, the groundwater flow problem for the unfrozen region will need to be solved. In chapter 2 the governing equations for the unfrozen region were derived and an example of soil rheology was given (i.e. movement on the 'Normal Consolidation Line', $\phi = \phi(p_e)$). In general, the rheology of unfrozen soil is more complex than this and the types of behaviour that soils can exhibit are discussed below.

As previously described, a heaving soil induces a water pressure gradient at the lens front which causes pore water to be imbibed from the unfrozen region and may result in this region deforming (i.e consolidating). Laboratory experiments performed by Konrad & Seto (1994) and Konrad & Nixon (1994) have suggested that this process may be an important factor in the analysis of frost heave.

In this chapter we first present an extension of the thin fringe analysis given in chapter 4 with the inclusion of gravity and a deformable unfrozen region. The analysis is given in one dimension and we again find that the fringe equations reduce to a pair of ordinary differential equations for the heave z_s, and the lens front z_l, in terms of the porosity ϕ_f, the effective pressure N, and soil matrix velocity u_{sf} at the freezing front.

The terms ϕ_f, N and u_{sf} must be found from the solution to the groundwater flow problem. In order to solve this problem the usual conservation of mass and momentum equations for the unfrozen soil are written down before discussing soil rheology. Typical analyses of consolidation type problems (see Biot (1941) and Audet & Fowler (1992)) suppose the soil matrix behaves elastically while assuming also a relationship between the porosity and the effective stress (e.g. the normal consolidation line). However, the porosity relation should, in general, come from the consideration of conservation of mass. The analysis presented here follows that given by Fowler & Noon (1996) in making no explicit assumption regarding the porosity but rather establishing this from conservation of mass considerations. Further, critical state soil mechanics suggests that the mechanical behaviour of soil can be either elastic (i.e. recoverable) or elastic/plastic (i.e. irrecoverable). As such, we give a generalised formulation of the problem which allows the soil to exhibit elastic or elastic/plastic behaviour.

Once the groundwater flow problem has been derived it is non-dimensionalised

with the consolidation scales and this gives rise to a small dimensionless parameter, ϵ, which is the ratio of the stress applied to the soil and the shear modulus of the soil skeleton. In general we would expect this parameter to be $\ll 1$ and, as such, allowing this parameter to tend to zero produces a simplified formulation of the groundwater flow problem for both the elastic and elastic/plastic régimes for the fully three dimensional problem.

The small aspect ratio (i.e. the ratio of the depth scale to the lateral length scale) which is typically appropriate allows the use of the Dupuit-Forchheimer approximation (see Fowler (1996)). The groundwater flow problem is rescaled using the small aspect ratio parameter, δ_l, and, by solving the resulting problem to the second order terms in the asymptotic expansion of the variables, we obtain a non-linear diffusion equation for the effective pressure, N, at the frozen front and an expression for the soil matrix velocity, u_{sf}. A simplified example is given in which the heave and frozen front depth are considered to be functions of time only, the base of the aquifer is taken as a constant and the porosity is a function of depth. These simplifications allow us to write the non-linear diffusion equation for the effective pressure in a simpler form.

There are essentially three time scales for the field frost heave problem; the vertical consolidation time scale, t_v; the lateral consolidation time scale, t_l; and the frost heave time scale, t_f. We find that, in general, the relationship between these time scales is $t_v \ll t_f \ll t_l$ and, as such, the diffusion equation established from the groundwater problem will not allow lateral diffusion on the frost heave time scale. Thus, on the frost heave time scale, the evolution equation for the effective stress, N, does not involve any horizontal spatial derivatives, except in a boundary layer on the bounding domain.

We then find that the field frost heave problem reduces to three coupled ordinary differential equations for the cumulative lens thickness, the frost penetration depth and the effective stress. A numerical solution of the resulting equations is given in which permafrost aggradation is simulated by a step freezing experiment for the one dimensional problem. The results of this analysis exhibit the type of behaviour associated with segregated seams of massive ice except that the lens thickness is less than would be expected. A number of explanations are given for this and in particular consideration is given to the growth of the final ice lens. A model for the formation

of the final ice lens is derived based on the Miller model of secondary frost heave and this shows that the growth of this ice lens could account for massive ice formation.

6.2 The Fringe Equations

In this section we establish equations analogous to equations 4.20 derived in chapter 4 for the frost penetration depth, z_f, and the heave, z_s. This reduction is again achieved by using the thin fringe approximation and the analysis is similar to that given in chapters 4 and 5. As in chapter 5 we only give the key steps in the reduction.

The fringe rescaling takes the form

$$z = z_l - \mu\xi, \qquad T = \mu\theta \qquad \phi = \phi_f(t) + \mu\phi^*.$$

The scaling reflects our anticipation that the variation in porosity across the fringe will be $\sim \mu$. Substituting this rescaling into the averaged heave equations given at the end of chapter 3, the leading order behaviour is as follows: $0 < \xi < \xi_f$:

$$\begin{aligned}
&\frac{\partial}{\partial\xi}((1-\phi_f)u_s) = 0,\\
&\frac{\partial}{\partial\xi}(U_w + (\phi_f - W)u_i + (1-\phi_f)u_s) = 0,\\
&\dot{z}_l\frac{\partial W}{\partial\xi} - \frac{\partial U_w}{\partial\xi} = \frac{\partial^2\theta}{\partial\xi^2},\\
&p_w = p_f - (p_f - P + f(W_l))\exp\left(-\frac{\gamma}{W_l}\left.\frac{\partial W}{\partial\xi}\right|_l \xi\right),\\
&\theta = -(\delta p_w + f(W)),\\
&u_i - u_s = \delta_3\frac{\partial\theta}{\partial\xi} \qquad \text{(Gilpin)},\\
\text{or}\quad &u_i = \dot{z}_s \qquad\qquad \text{(Rigid Ice)},\\
&P = \delta_2^f(z_s - z_l),\\
&P = p_e + (1-\chi(W))f(W) + p_w,
\end{aligned} \tag{6.1}$$

where we have again neglected the hydrostatic component of water pressure in the fringe. The boundary conditions become
at $\xi = 0$

$$\begin{aligned}
&W = W_l,\\
&\frac{\partial W}{\partial\xi} = \mu\phi_f\tilde{\beta}(U_w - Wu_s),
\end{aligned}$$

$$
\begin{aligned}
&(W - W_m)\dot{z}_l + W_m u_s - U_w = -\frac{k_f}{k}\,\frac{T_s}{(z_l - z_s)} + \frac{\partial \theta}{\partial \xi},\\
&\dot{z}_s = U_w + (\phi_f - W)u_i + (1 - \phi_f)u_s,
\end{aligned}
\tag{6.2}
$$

at $\xi = \xi_f$

$$
\begin{aligned}
&W = \phi_f,\\
&\frac{\partial \theta}{\partial \xi} = 1,\\
&u_s = u_{sf},\\
&p_e = N,
\end{aligned}
\tag{6.3}
$$

where, for the time being, we have assumed that the soil matrix velocity, u_{sf}, the effective stress, N, and the porosity, ϕ_f, are all prescribed at the freezing front. In reality expressions for these variables come from the solution to the groundwater flow problem considered in subsequent sections.

At this point it is again worth checking that we have the correct number of boundary conditions for the problem described by equations 6.1. Taking into account the constitutive laws included in equations 6.1, we require 1 boundary condition for u_s, 1 for U_w, 2 for θ (or equivalently W), 1 for p_w and 3 for the unknown moving boundaries. Thus, we require 8 boundary conditions in total which agrees with the number we have and, hence, the problem appears to be correctly specified.

Integrating $(6.1)_1$ and applying boundary condition $(6.3)_3$ gives that $u_s = u_{sf}$ throughout the fringe. Now, following a similar approach to that given in chapters 4 and 5, we get, by integrating equations 6.1 and applying the appropriate boundary conditions, the following relationships

$$
\begin{aligned}
&\dot{z}_l(\phi - W_m) + W_m u_{sf} - \dot{z}_s = \left.\frac{\partial \theta}{\partial \xi}\right|_f + \frac{k_f}{k}\,\frac{T_s}{(z_s - z_l)} - (1 - \phi_f)u_{sf},\\
&\dot{z}_s = U_{wl} + (\phi_f - W_l)\dot{z}_s + (1 - \phi_f)u_{sf}, \qquad \text{(Rigid Ice)}\\
&\dot{z}_s = U_{wl} + \delta_3(\phi_f - W_l)\left.\frac{\partial \theta}{\partial \xi}\right|_l + (1 - W_l)u_{sf}, \qquad \text{(Gilpin)}\\
&\left.\frac{\partial \theta}{\partial \xi}\right|_l = \frac{1}{(1 + \beta_{fk})}\left((W_l - W_m)(\dot{z}_l - u_{sf}) - \frac{k_f}{k}\,\frac{T_s}{(z_s - z_l)}\right),\\
&U_{wl} - W_l u_{sf} = \frac{\beta_{fk}}{(1 + \beta_{fk})}\left((W_l - W_m)(\dot{z}_l - u_{sf}) - \frac{k_f}{k}\,\frac{T_s}{(z_s - z_l)}\right),\\
&U_{wf} = \dot{z}_s - (1 - \phi_f)u_{sf},
\end{aligned}
\tag{6.4}
$$

where the parameter, β_{fk}, is given by

$$\beta_{fk} = -\frac{\gamma L^2 \rho_w k_0}{T_0 g k} \left(\frac{W_l}{\phi_f}\right)^{\gamma} \left(\frac{(f(W_l) - N)}{\delta\gamma(f(W_l) - N) + W_l f'(W_l)}\right), \tag{6.5}$$

and N is the effective stress at the frozen front, given by $P - p_f$.

Therefore, substituting equations $(6.4)_{4,5}$ into $(6.4)_{2,3}$ and boundary condition $(6.3)_2$ into $(6.4)_1$, we get the heave equations with the inclusion of compressibility:

$$\begin{aligned}(\phi_f - W_m)(\dot{z}_l - u_{sf}) &= (\dot{z}_s - u_{sf}) + 1 + \frac{k_f}{k}\frac{T_s}{(z_s - z_l)}, \\ \dot{z}_s - u_{sf} &= \alpha_{fk}\left((W_l - W_m)(\dot{z}_l - u_{sf}) - \frac{k_f}{k}\frac{T_s}{(z_s - z_l)}\right),\end{aligned} \tag{6.6}$$

where the parameter α_{fk} is

$$\alpha_{fk} = \frac{\beta_{fk}}{(1 + \beta_{fk})(1 - \phi + W_l)}, \tag{6.7}$$

if the 'rigid ice' approach is adopted or

$$\alpha_{fk} = \frac{(\beta_{fk} + \delta_3(\phi - W_l))}{(1 + \beta_{fk})} \tag{6.8}$$

with the Gilpin thermal regelation approach. Equations 6.6 are equivalent to equations 4.20 derived in chapter 4, the only difference being that the ground surface position and frost penetration depth are expressed relative to the movement of the soil matrix.

The reduced heave equations 6.6 depend on the effective stress, N, the soil matrix velocity, u_{sf}, and the porosity, ϕ_f, which are found from the solution to the groundwater flow problem given in the subsequent sections.

6.3 The Rheology of the Unfrozen Region

As discussed in the introduction, frost heave induces a water pressure gradient (i.e a suction) in the unfrozen pore water beneath the lens front which causes the pore water to flow towards the lens front. This extraction of pore water may cause some form of deformation in the region below the lens front and the purpose of this section is to analyse the processes which occur in this region.

6.3.1 The Governing Equations

The equations applicable in the unfrozen region are similar to those presented in chapter 2. For completeness these equations are briefly derived again in their dimensional form.

Conservation of mass for the soil and water phases gives

$$\begin{aligned} \frac{\partial}{\partial t}(1-\phi) + \boldsymbol{\nabla}.((1-\phi)\mathbf{u}_s) &= 0, \\ \frac{\partial \phi}{\partial t} + \boldsymbol{\nabla}.(\phi \mathbf{u}_w) &= 0, \end{aligned} \tag{6.9}$$

where ϕ is the porosity of the soil matrix and $\mathbf{u}_s$ and $\mathbf{u}_w$ are the velocities of the soil matrix and water phase respectively.

Conservation of momentum for each phase takes the form of Darcy's equation for the fluid flux and a total stress balance for the soil matrix as follows

$$\begin{aligned} \phi(\mathbf{u}_w - \mathbf{u}_s) &= -\frac{k_0}{\rho_w g}\boldsymbol{\nabla}(p_w + \rho_w g z), \\ \boldsymbol{\nabla}.\boldsymbol{\sigma} &= (\phi\rho_w + (1-\phi)\rho_s)g\mathbf{k}, \\ \boldsymbol{\sigma} &= \boldsymbol{\sigma}^e - p_w\boldsymbol{\delta}, \end{aligned} \tag{6.10}$$

where k_0 is the permeability of the soil[1], ρ_s and ρ_w are the densities of the soil matrix and pore fluid respectively, p_w is the pore water pressure, g is the acceleration due to gravity, $\mathbf{k}$ is the unit vector in the upwards direction, $\boldsymbol{\sigma}$ is the total stress tensor, $\boldsymbol{\sigma}^e$ is the effective stress tensor and $\boldsymbol{\delta}$ is the unit stress tensor.

6.3.2 The Constitutive Relations

The behaviour of a soil matrix under applied stress falls into the domain of 'Critical State Soil Mechanics' (see Atkinson & Bransby (1978)). The response of the soil under a particular range of applied stresses is most usually considered to be either elastic (and recoverable), if the applied stresses fall beneath the State Boundary Surface (see figure 6.1), or plastic (and irrecoverable) if the range of stresses falls on the State Boundary Surface. Stress states above this surface are not possible by virtue of the fact that the soil matrix would have failed (i.e. suffered a complete loss of strength).

[1]In general, the permeability, k_0, will depend on the porosity, ϕ. However, for simplicity, we suppose that k_0 is a constant.

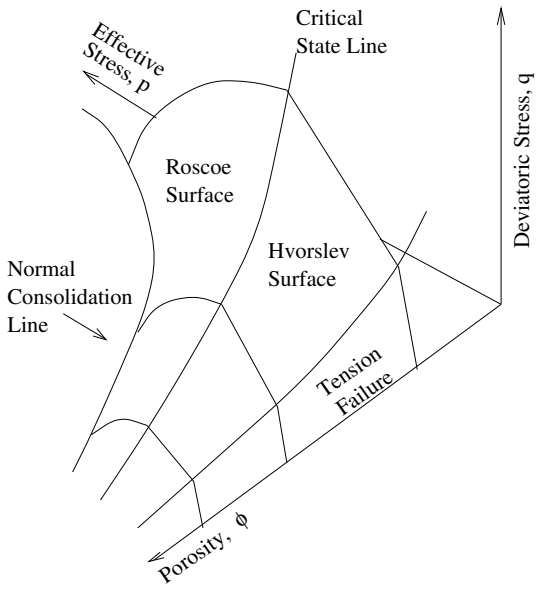


Figure 6.1: A schematic plot of the State Boundary Surface.

The State Boundary Surface comprises three distinct regions, the Roscoe Surface, the Hvorslev Surface and the Tension Failure Surface. Plastic flow occurs along these surfaces with complete failure (if applicable) occurring at the intersection of the Roscoe and the Hvorslev Surfaces (the Critical State Line).

The 'Normal Consolidation Line', which was discussed in chapter 2, is given by the intersection of the State Boundary Surface with the plane in which the deviatoric stress is zero. Typical presentations of the mechanical behaviour of consolidating soils assume that the soil matrix is elastic (see Biot (1941, 1955)), and hence (implicitly) that it follows stress paths beneath the State Boundary Surface, while further assuming a relationship for the porosity in terms of the effective stress or, in Biot's case, the dilation. This second assumption will, in general, be in contradiction with the conservation of mass equations 6.9 from which the porosity should be determined. Further, the assumption of an elastic rheology will not hold when the stress paths move along the State Boundary Surface (e.g. the Normal Consolidation Line) and some form of elastic/plastic rheology will be necessary. We adopt the approach given by Fowler & Noon (1996) in giving a more general formulation of the consolidation/compaction problem.

Incremental strains in an elastic/plastic rheology for the soil matrix are given by

$$d\boldsymbol{\varepsilon} = d\boldsymbol{\varepsilon}^e + d\boldsymbol{\varepsilon}^p \tag{6.11}$$

(see Coussy (1995)) where $\boldsymbol{\varepsilon}^e$ and $\boldsymbol{\varepsilon}^p$ represent the elastic and plastic strain tensors

respectively. The elastic component of strain can be found in terms of the stresses by inverting the usual stress strain relation (see Biot (1941))

$$\boldsymbol{\sigma}^e = 2G\boldsymbol{\varepsilon}^e + \frac{2G\nu}{1-2\nu}\varepsilon^e_{kk}\boldsymbol{\delta}, \tag{6.12}$$

where G is the shear modulus and ν is the Poisson ratio of the soil matrix. Inversion of this relation then gives the incremental elastic strain as

$$d\boldsymbol{\varepsilon}^e = \frac{1}{2G}d\boldsymbol{\sigma}^e - \frac{\nu}{2G(1+\nu)}d\sigma^e_{kk}\boldsymbol{\delta}. \tag{6.13}$$

A common assumption (the normality rule) made in the theory of plasticity is that the component of plastic strain is orthogonal to the yield surface, which, in our case, is the State Boundary Surface. Further, writing the State Boundary Surface in the form $\phi = h(\sigma_{ij})$, it can be shown that, with an assumption of minimum work, the plastic strain component can be written as

$$d\boldsymbol{\varepsilon}^p = \mathbf{H}d\lambda \tag{6.14}$$

where the tensor $\mathbf{H}$ has components $\frac{\partial h}{\partial \sigma}_{ij}$ and λ is a scalar quantity, referred to as the plastic multiplier, which is a function of the components of stress and the strain history. λ is determined from the condition that the stress path followed remains on the yield surface.

Thus, for flow on the State Boundary Surface, the total increment of strain is given by

$$d\boldsymbol{\varepsilon} = \frac{1}{2G}d\boldsymbol{\sigma}^e - \frac{\nu}{2G(1+\nu)}d\sigma^e_{kk}\boldsymbol{\delta} + \mathbf{H}d\lambda, \tag{6.15}$$

where the increments refer to increments in time. For stress paths beneath the State Boundary Surface, the plastic component of strain, $\mathbf{H}d\lambda$, is zero and the resulting constitutive relation can be integrated to give the usual elastic relation. A complication arises for relation 6.15 when considering the increment in time because the time derivative of the stress tensor should be taken following the soil matrix which, in the case of tensors, does not lead to an objective (i.e. frame indifferent) formulation of the problem (see Fowler & Noon (1996)) and some objective definition of the tensor derivative needs to be chosen. For example Fowler & Noon (1996) use the Jaumann derivative which has the property that it preserves tensor invariants.

Now, the velocity of the soil matrix $\mathbf{u}_s$ is the material derivative of the displacement vector, $\mathbf{U}$, and thus may be written as

$$\mathbf{u}_s = \frac{\partial \mathbf{U}}{\partial t} + (\mathbf{u}_s.\boldsymbol{\nabla})\mathbf{U}. \tag{6.16}$$

The incremental strain tensor, $d\boldsymbol{\varepsilon}$, may also be written in terms of the incremental displacement vector, $\mathbf{U}$, as follows

$$\begin{aligned} d\varepsilon_{ij} &= \frac{1}{2}\left(\frac{\partial}{\partial x_j}dU_i + \frac{\partial}{\partial x_i}dU_j\right) \\ &= \frac{1}{2}\left(\boldsymbol{\nabla} d\mathbf{U} + (\boldsymbol{\nabla} d\mathbf{U})^T\right)_{ij}. \end{aligned} \tag{6.17}$$

6.3.3 Model for Groundwater Flow

We may now collect together the equations controlling the flow of the groundwater in the unfrozen region for the field situation. These are as follows

$$\begin{aligned} &\frac{\partial}{\partial t}(1-\phi) + \boldsymbol{\nabla}.((1-\phi)\mathbf{u}_s) = 0, \\ &\frac{\partial \phi}{\partial t} + \boldsymbol{\nabla}.(\phi \mathbf{u}_w) = 0, \\ &\phi(\mathbf{u}_w - \mathbf{u}_s) = -\frac{k_0}{\rho_w g}\boldsymbol{\nabla}(p_w + \rho_w g z), \\ &\mathbf{u}_s = \frac{\partial \mathbf{U}}{\partial t} + (\mathbf{u}_s.\boldsymbol{\nabla})\mathbf{U}, \\ &\boldsymbol{\nabla}.\boldsymbol{\sigma} = (\phi\rho_w + (1-\phi)\rho_s)g\mathbf{k}, \\ &\boldsymbol{\sigma} = \boldsymbol{\sigma}^e - p_w\boldsymbol{\delta}, \\ &d\boldsymbol{\varepsilon} = \frac{1}{2G}d\boldsymbol{\sigma}^e - \frac{\nu}{2G(1+\nu)}d\sigma^e_{kk}\boldsymbol{\delta} + \mathbf{H}d\lambda, \\ &d\boldsymbol{\varepsilon} = \frac{1}{2}\left(\boldsymbol{\nabla} d\mathbf{U} + (\boldsymbol{\nabla} d\mathbf{U})^T\right). \end{aligned} \tag{6.18}$$

This system describes the elastic/plastic problem and one final constraint is required to determine the plastic multiplier, λ. This additional constraint is that the stresses applied to the soil matrix must lie on the yield surface. Hence we require $\phi = h(\sigma^e_{ij})$.

In the elastic case, the incremental plastic component of strain, $\mathbf{H}d\lambda$, is absent from the stress strain relationship, $(6.18)_7$, and the incremental relationships may be integrated to give the usual elastic constitutive laws. Technically, in the elastic case, we will also require that the applied stresses fall beneath the State Boundary Surface.

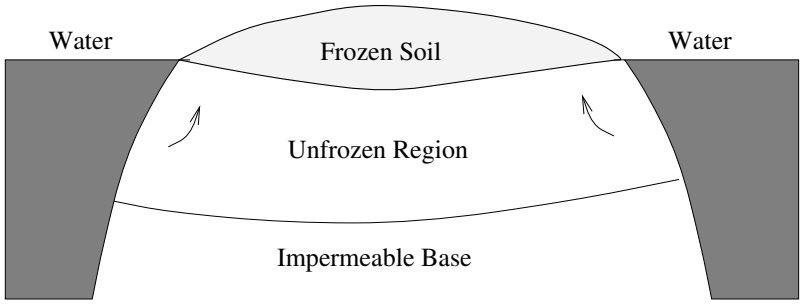


Figure 6.2: Schematic diagram of the domain in which the far field pressure problem needs to be solved.

We now need to prescribe appropriate boundary conditions in the unfrozen region in which we wish to solve the groundwater flow problem. Figure 6.2 is a schematic representation of the regional field freezing problem showing that, in general, we would expect the unfrozen region to be connected to an external supply of water (e.g. a lake). To prescribe the boundary conditions we need to divide the domain surrounding the unfrozen region into three distinct surfaces; the freezing front $z = z_f(\mathbf{x}, t)$; the impermeable base (i.e. bed rock) of the unfrozen region $z = z_b(\mathbf{x}, t)$; and the region of the domain which is connected to the external supply of water $z = z_d(\mathbf{x}, t)$.

We assume that the normal components of effective stress and total stress are prescribed at the frozen front together with the condition of zero tangential strain and a prescription of the relative water flux. At the impermeable bed rock base we have zero displacement and no normal component of water flux. At the external sources of water we prescribe zero normal and tangential stress and a hydrostatic water pressure. These boundary conditions are written in their dimensionless form in the following section.

From the solution to the frozen fringe equations we have an expression for the water flux at the freezing front in terms of the porosity, the soil matrix velocity and effective stress on this surface. Thus, by prescribing the effective stress at the freezing front we are expecting that the solution to the groundwater flow problem will produce a relation for this effective stress, N, and for the porosity and soil matrix velocity in terms of N. The field frost heave problem will then be fully specified.

6.4 Non-dimensionalisation and Simplification

We now non-dimensionalise the groundwater flow equations 6.18 using the following scalings

$$\mathbf{x} = d\mathbf{x}^* \qquad \mathbf{u}_{s,w} = k_0\mathbf{u}^*_{s,w} \qquad \boldsymbol{\varepsilon},\ \lambda = \frac{\rho_w g d}{G}\,\boldsymbol{\varepsilon}^*,\ \lambda^*$$

$$\mathbf{U} = \frac{\rho_w g d^2}{G}\mathbf{U}^* \qquad t = \frac{d^2\rho_w g}{k_0 G}t^* \qquad \boldsymbol{\sigma}^e,\ p_w = \rho_w g d\,\boldsymbol{\sigma}^{e*},\ p^*_w$$

where d is the depth of the aquifer. At the present time do not consider the frost heave scalings which are likely to be different to those given above. Once we have solved the groundwater flow problem, we will reconsider the significance of the frost heave scales.

Substituting these scalings into equations 6.18 we find, after some simplification and dropping the asterisks, that

$$\begin{aligned}
&-\frac{\partial\phi}{\partial t} + \epsilon\boldsymbol{\nabla}.((1-\phi)\mathbf{u}_s) = 0,\\
&\boldsymbol{\nabla}.(\phi\mathbf{u}_w + (1-\phi)\mathbf{u}_s) = 0,\\
&\phi(\mathbf{u}_w - \mathbf{u}_s) = -\boldsymbol{\nabla}(p_w + z),\\
&\mathbf{u}_s = \frac{\partial\mathbf{U}}{\partial t} + \epsilon(\mathbf{u}_s.\boldsymbol{\nabla})\mathbf{U},\\
&\boldsymbol{\nabla}.\boldsymbol{\sigma}^e - \boldsymbol{\nabla}p_w = (1 + (1-\phi)r)\mathbf{k},\\
&d\boldsymbol{\varepsilon} = \frac{1}{2}d\boldsymbol{\sigma}^e - \frac{\nu}{2(1+\nu)}d\sigma^e_{kk}\boldsymbol{\delta} + \mathbf{H}d\lambda,\\
&d\boldsymbol{\varepsilon} = \frac{1}{2}\left(\boldsymbol{\nabla}d\mathbf{U} + (\boldsymbol{\nabla}d\mathbf{U})^T\right).
\end{aligned} \tag{6.19}$$

where $r = (\rho_s/\rho_w - 1)$ and the dimensionless parameter ϵ is given by

$$\epsilon = \frac{\rho_w g d}{G}.$$

The parameter ϵ is a ratio of the applied stress scale to the shear modulus of the unfrozen soil. In general, we would expect the shear modulus, G, to increase as the soil matrix becomes more compact and hence be an increasing function of depth. The shear modulus for soil near to the ground surface is $\sim 10^6$ Pa and for rock is $\sim 10^{10}$ Pa and, as such, we would expect the shear modulus to vary with depth between these two extremes. For example, on a length scale, d, of 1,000 m, an appropriate value

for the shear modulus may be 10^8 Pa and thus $\epsilon \sim 0.1$. The value of the parameter ϵ and how it varies with depth can also be considered from a theoretical viewpoint. From Audet & Fowler (1992) it can be inferred that for small elastic strains the shear modulus, G, satisfies the following relation

$$G \sim \frac{p_e}{C_s(1-\phi)^2}, \tag{6.20}$$

where C_s is the compression index. For a soil in the field the effective stress scale will be at least equal to the overlying weight of the the soil matrix and therefore the parameter ϵ is less than or equal to $\sim C_s(1-\phi)^2$. Bell (1992, page 25) gives ranges of compression indices for various soil types which, in general, show that $C_s \sim 0.1$ for most soil types. Thus, it would seem reasonable to suppose that the parameter $\epsilon \sim 0.1$.

The boundary conditions for the problem, discussed at the end of section 6.3, become

at $z = z_f(\mathbf{x}, t)$

$$\begin{aligned} \mathbf{U} \times \mathbf{n} &= \mathbf{0}, \\ \boldsymbol{\sigma}.\mathbf{n} &= -P_f \mathbf{k}, \\ -\boldsymbol{\sigma}^e.\mathbf{n} &= N, \\ \phi(\mathbf{u^w} - \mathbf{u^s}).\mathbf{n} &= V_f, \end{aligned} \tag{6.21}$$

at $z = z_b(\mathbf{x}, t)$

$$\begin{aligned} \mathbf{U} &= \mathbf{0}, \\ \mathbf{n}.\boldsymbol{\nabla}(p_w + z) &= 0, \end{aligned} \tag{6.22}$$

at $z = z_d(\mathbf{x}, t)$

$$\begin{aligned} \boldsymbol{\sigma}^e.\mathbf{n} &= \mathbf{0}, \\ p_w + z &= 0, \end{aligned} \tag{6.23}$$

where the (dimensionless) normal load P_f is given by

$$P_f = \frac{\rho_f}{\rho_w}(z_s - z_f),$$

and V_f is the dimensionless vertical relative water flux at z_f.

We now proceed to solve this system, first for the case of elastic strains, and then for the case of plastic strains.

6.5 Purely Elastic Strains

For purely elastic deformations, the plastic component of strain $\mathbf{H}d\lambda$, is absent from equation $(6.19)_6$ and the resulting relationship may be integrated and inverted to give the usual elastic stress/strain relationship 6.12. Now, if we let $\epsilon \to 0$, then equations 6.19 give after some simplification

$$\begin{aligned}
&\phi = \phi(\mathbf{x}),\\
&\boldsymbol{\nabla}.\mathbf{u}_s = \boldsymbol{\nabla}.\left(\boldsymbol{\nabla}(p_w + z)\right),\\
&\boldsymbol{\nabla}(p_w + z) = \boldsymbol{\nabla}.\boldsymbol{\sigma}^e - r(1-\phi)\mathbf{k},\\
&\mathbf{u}_s = \frac{\partial \mathbf{U}}{\partial t},\\
&\boldsymbol{\sigma}^e = 2\boldsymbol{\varepsilon} + \frac{2\nu}{1-2\nu}\varepsilon_{kk}\boldsymbol{\delta},\\
&\boldsymbol{\varepsilon} = \frac{1}{2}\left(\boldsymbol{\nabla}\mathbf{U} + (\boldsymbol{\nabla}\mathbf{U})^T\right).
\end{aligned} \tag{6.24}$$

Substitution of $(6.24)_3$ and $(6.24)_4$ into $(6.24)_2$ gives, after some further simplification, that

$$\begin{aligned}
&\phi = \phi(\mathbf{x}),\\
&\Delta = \boldsymbol{\nabla}.\mathbf{U},\\
&\frac{\partial \Delta}{\partial t} = \boldsymbol{\nabla}.\left(\boldsymbol{\nabla}.\boldsymbol{\sigma}^e\right) + r\frac{\partial \phi}{\partial z},\\
&\boldsymbol{\nabla}.\boldsymbol{\sigma}^e = 2\boldsymbol{\nabla}.\boldsymbol{\varepsilon} + \frac{2\nu}{1-2\nu}\boldsymbol{\nabla}\Delta,\\
&2\boldsymbol{\nabla}.\boldsymbol{\varepsilon} = 2\boldsymbol{\nabla}\Delta - \boldsymbol{\nabla}\times\boldsymbol{\nabla}\times\mathbf{U}.
\end{aligned} \tag{6.25}$$

Substituting $(6.25)_{4,5}$ into $(6.25)_3$, we can write the above system as a diffusion equation for the dilation, Δ, as follows

$$\frac{\partial \Delta}{\partial t} = \frac{2(1-\nu)}{(1-2\nu)}\nabla^2\Delta + r\frac{\partial \phi}{\partial z}, \tag{6.26}$$

where the porosity profile is the soil's initial porosity profile which, in general, would be found empirically.

The order of solution for this system would be to first solve the diffusion equation, 6.26. Equations $(6.24)_3$ and $(6.25)_{2,4,5}$ then form a pair of Navier Stokes type equations for the water pressure, p_w, and the displacement, $\mathbf{U}$, which, given suitable boundary conditions, may be solved for these variables. Finally, having determined p_w and $\mathbf{U}$, all other variables follow from the remaining equations.

6.6 Elastic/Plastic Strains

When the soil matrix deformation is elastic/plastic a similar analysis to that given in the elastic case can be achieved providing the strains are small. In this situation, the time increments of strain are, to leading order, the usual time derivatives and we do not need to consider the objectivity of the material derivative of the stress tensor[2].

Inverting the stress/strain relation given by $(6.19)_6$ and integrating $(6.19)_7$, the rheology of the unfrozen region is given by

$$\begin{aligned}\dot{\boldsymbol{\sigma}}^e &= 2\dot{\boldsymbol{\varepsilon}} + \frac{2\nu}{(1-2\nu)}\dot{\varepsilon}_{kk}\boldsymbol{\delta} - 2\boldsymbol{\Gamma}\dot{\lambda}, \\ \dot{\boldsymbol{\varepsilon}} &= \frac{1}{2}\left(\boldsymbol{\nabla}\mathbf{u}_s + (\boldsymbol{\nabla}\mathbf{u}_s)^T\right),\end{aligned} \tag{6.27}$$

where the overdots signify time derivatives and the tensor $\boldsymbol{\Gamma}$ is given by

$$\boldsymbol{\Gamma} = \mathbf{H} + \frac{\nu}{1-2\nu}H_{kk}\boldsymbol{\delta}.$$

Taking the divergence of equations 6.27 gives

$$\begin{aligned}\boldsymbol{\nabla}.\dot{\boldsymbol{\sigma}}^e &= 2\boldsymbol{\nabla}.\dot{\boldsymbol{\varepsilon}} + \frac{2\nu}{1-2\nu}\boldsymbol{\nabla}\theta - 2\boldsymbol{\nabla}.(\boldsymbol{\Gamma}\ \dot{\lambda}), \\ 2\boldsymbol{\nabla}.\dot{\boldsymbol{\varepsilon}} &= 2\boldsymbol{\nabla}\theta - \boldsymbol{\nabla}\times\boldsymbol{\nabla}\times\mathbf{u_s}, \\ \theta &= \boldsymbol{\nabla}.\mathbf{u_s}.\end{aligned} \tag{6.28}$$

Taking the time derivative of $(6.25)_3$ and substituting the above constitutive relations we get the following diffusion equation for θ

$$\frac{\partial\theta}{\partial t} = \frac{2(1-\nu)}{(1-2\nu)}\nabla^2\theta - 2\frac{\partial^2}{\partial x_i\partial x_j}(\Gamma_{ij}\dot{\lambda}). \tag{6.29}$$

Thus we have a similar situation to the elastic case except that we have an additional unknown parameter λ, for which we require an additional constraint. This comes form the requirement that the applied stress must lie on the yield surface $h(\sigma^e_{ij}) = \phi$.

6.7 Thin Region Approximation

In general, the region in which we wish to solve the groundwater flow problem will have a relatively small aspect ratio. That is, the depth scale will be very much smaller

[2]Fowler & Noon (1996) also consider the large strain problem

than the length scale. Typically we would expect a depth scale to be $\sim 1\,\mathrm{km}$ whereas the horizontal length would be $\sim 10-1000\,\mathrm{km}$ giving an aspect ratio $\delta_l \sim 10^{-3}-10^{-1}$. Thus, the problems derived in the previous two sections may be rescaled to produce some simplification via the use of a Dupuit-Forchheimer type approach. For simplicity the purely elastic strain problem only is considered.

For the elastic problem the governing equations and boundary conditions may be written as

$$\begin{aligned}
&\boldsymbol{\nabla}(p_w + z) = \boldsymbol{\nabla}.\boldsymbol{\sigma}^e - r(1-\phi)\mathbf{k},\\
&\Delta = \boldsymbol{\nabla}.\mathbf{U},\\
&\boldsymbol{\sigma}^e = 2\boldsymbol{\varepsilon} + \frac{2\nu}{1-2\nu}\Delta\boldsymbol{\delta},\\
&\frac{\partial\Delta}{\partial t} = \frac{2(1-\nu)}{(1-2\nu)}\nabla^2\Delta + r\frac{\partial\phi}{\partial z},\\
&\boldsymbol{\varepsilon} = \frac{1}{2}\left(\boldsymbol{\nabla}\mathbf{U} + (\boldsymbol{\nabla}\mathbf{U})^T\right),
\end{aligned} \tag{6.30}$$

where the porosity, ϕ, is a prescribed function of $\mathbf{x}$.

The boundary conditions are then

at $z = z_f(\mathbf{x}, t)$

$$\begin{aligned}
\mathbf{U}\times\mathbf{n} &= \mathbf{0},\\
\boldsymbol{\sigma}.\mathbf{n} &= -P_f\mathbf{k},\\
-\boldsymbol{\sigma}^e.\mathbf{n} &= N,\\
\phi(\mathbf{u^w} - \mathbf{u^s}).\mathbf{n} &= V_f,
\end{aligned} \tag{6.31}$$

at $z = z_b(\mathbf{x}, t)$

$$\begin{aligned}
\mathbf{U} &= \mathbf{0},\\
\mathbf{n}.\boldsymbol{\nabla}(p_w + z) &= 0,
\end{aligned} \tag{6.32}$$

at $z = z_d(\mathbf{x}, t)$

$$\begin{aligned}
\boldsymbol{\sigma}^e.\mathbf{n} &= \mathbf{0},\\
p_w + z &= 0.
\end{aligned} \tag{6.33}$$

We rescale the above system to allow for the small aspect ratio by writing

$$
\begin{array}{lll}
x = \dfrac{x^*}{\delta_l}, & y = \dfrac{y^*}{\delta_l} & U_1 = \delta_l U_1^* \\
U_2 = \delta_l U_2^* & \sigma^e_{13} = \delta_l \sigma^*_{13} & \sigma^e_{23} = \delta_l \sigma^*_{23} \\
\sigma^e_{12} = \delta_l^2 \sigma^*_{12} & t = \dfrac{t^*}{\delta_l^2} & V_f = \delta_l^2 V_f^*.
\end{array}
$$

where δ_l ($\ll 1$) is the aspect ratio (i.e. the vertical aquifer length scale divided by the horizontal length scale). The choice of time scale reflects the fact that we expect the vertical variation to rapidly relax to a quasi-steady state and functions which are dependent on the horizontal length scale only (e.g. the effective stress at the frozen front, N), will be controlled by the horizontal diffusive time scale.

Substituting these rescalings into the above equations and boundary conditions allows us, after some simplification and dropping the asterisks, to write the system as

$$
\begin{aligned}
&\sigma^e_{33} = \frac{2(1-\nu)}{(1-2\nu)}\Delta - 2\delta_l^2 \boldsymbol{\nabla}_H.\mathbf{U}_H, \\
&\frac{\partial p_w}{\partial z} + 1 = \frac{\partial \sigma^e_{33}}{\partial z} - r(1-\phi) + \delta_l^2 \boldsymbol{\nabla}_H.\boldsymbol{\tau}_H, \\
&\boldsymbol{\nabla}_H p_w = \frac{2\nu}{(1-2\nu)}\boldsymbol{\nabla}_H \Delta + \frac{\partial \boldsymbol{\tau}_H}{\partial z} + \delta_l^2 \left(\nabla_H^2 \mathbf{U}_H + \boldsymbol{\nabla}_H (\boldsymbol{\nabla}_H.\mathbf{U}_H) \right), \\
&\boldsymbol{\tau}_H = \frac{\partial \mathbf{U}_H}{\partial z} + \boldsymbol{\nabla}_H U_3, \\
&\Delta = \frac{\partial U_3}{\partial z} + \delta_l^2 \boldsymbol{\nabla}_H.\mathbf{U}_H, \\
&\frac{2(1-\nu)}{(1-2\nu)}\frac{\partial^2 \Delta}{\partial z^2} + r\frac{\partial \phi}{\partial z} = \delta_l^2 \left(\frac{\partial \Delta}{\partial t} - \frac{2(1-\nu)}{(1-2\nu)} \nabla_H^2 \Delta \right),
\end{aligned}
\tag{6.34}
$$

where we have written

$$
\begin{aligned}
\boldsymbol{\nabla}_H &= \left(\frac{\partial}{\partial x}, \frac{\partial}{\partial y} \right), \\
\mathbf{U}_H &= (U_1, U_2), \\
\boldsymbol{\tau}_H &= (\sigma_{13}, \sigma_{23}).
\end{aligned}
\tag{6.35}
$$

The boundary conditions become

at $z = z_f(\mathbf{x}, t)$

$$
\begin{aligned}
\mathbf{U}_H &= \mathbf{0}, \\
-\sigma^e_{33} + p_w &= P_f - \delta_l^2 \boldsymbol{\tau}_H.\boldsymbol{\nabla}_H z_f, \\
-\sigma^e_{33} &= N + \delta_l^2 \left((\boldsymbol{\sigma}_H.\boldsymbol{\nabla}_H z_f).\boldsymbol{\nabla}_H z_f - 2\boldsymbol{\tau}_H.\boldsymbol{\nabla}_H z_f + N \left| \boldsymbol{\nabla}_H z_f \right|^2 \right), \\
\frac{\partial p_w}{\partial z} + 1 &= -\delta_l^2 V_f^* + \delta_l^2 \boldsymbol{\nabla}_H z_f.\boldsymbol{\nabla}_H p_w.
\end{aligned}
\tag{6.36}
$$

at $z = z_b(\mathbf{x}, t)$

$$\begin{aligned} \mathbf{U}_H &= \mathbf{0}, \\ U_3 &= 0, \\ \frac{\partial p_w}{\partial z} + 1 &= \delta_l^2 \boldsymbol{\nabla}_H z_b . \boldsymbol{\nabla}_H p_w \end{aligned} \tag{6.37}$$

at $z = z_d(\mathbf{x}, t)$

$$\begin{aligned} \sigma_{33}^e &= \delta_l^2 \boldsymbol{\tau}_H . \boldsymbol{\nabla}_H z_d, \\ \boldsymbol{\tau}_H &= \boldsymbol{\sigma}_H . \boldsymbol{\nabla}_H z_d + \delta_l^2 \tau_{12} \left(\frac{\partial z_d}{\partial y}, \frac{\partial z_d}{\partial x} \right), \\ p_w + z &= 0, \end{aligned} \tag{6.38}$$

where we have used the dimensionless version of Darcy's law to re-express the water flux boundary condition at the freezing front and $\boldsymbol{\sigma}_H = \mathrm{diag}(\sigma_{11}^e, \sigma_{22}^e)$.

Integrating $(6.34)_2$ and applying boundary condition $(6.36)_2$, gives, to leading order

$$p_w - (z_f - z) = \sigma_{33}^e + r \int_z^{z_f} (1 - \phi)\, dz + P_f. \tag{6.39}$$

Integrating $(6.34)_6$, substituting equation $(6.34)_1$, and applying equation $(6.34)_2$ with boundary condition $(6.36)_4$, gives the following relation

$$\frac{\partial \sigma_3^e}{\partial z} - r(1 - \phi) = 0. \tag{6.40}$$

Thus, the leading order solution to this system can then be written as

$$\begin{aligned} p_w &= P_f - N + z_f - z, \\ \sigma_{33}^e &= -\left(N + r \int_z^{z_f} (1 - \phi) dz \right), \\ \Delta &= -\frac{(1 - 2\nu)}{2(1 - \nu)} \left(N + r \int_z^{z_f} (1 - \phi)\, dz \right), \\ U_3 &= -\frac{(1 - 2\nu)}{2(1 - \nu)} \left(N(z - z_b) + r \int_{z_b}^{z} \int_s^{z_f} (1 - \phi)\, du\, ds \right), \\ \frac{\partial^2}{\partial z^2} (\boldsymbol{\nabla}_H . \mathbf{U}_H) &= \nabla_H^2 \left(p_w - \frac{\Delta}{(1 - 2\nu)} \right). \end{aligned} \tag{6.41}$$

(The leading order behaviour is expressed in this form because it facilitates our later analysis.)

The most direct method by which the evolution equation for the effective stress, N, can be found is by integrating with respect to z equation $(6.34)_6$ across the unfrozen

region. In doing this it is found that the $O(\delta_l^2)$ terms become significant and for this reason they are retained in our subsequent analysis. Integrating equation $(6.34)_6$ gives

$$\left[\frac{2(1-\nu)}{(1-2\nu)}\frac{\partial\Delta}{\partial z} - r(1-\phi)\right]_{z_b}^{z_f} = \delta_l^2 \int_{z_b}^{z_f} \left(\frac{\partial\Delta}{\partial t} - \frac{2(1-\nu)}{(1-2\nu)}\nabla_H^2\Delta\right) dz. \tag{6.42}$$

Substituting equations $(6.34)_{1,2}$ into 6.42 allows us to write the left hand side of this equation as

$$\left[\frac{\partial p_w}{\partial z} + 1 + 2\delta_l^2\frac{\partial}{\partial z}(\boldsymbol{\nabla}_H.\mathbf{U}_H) - \delta_l^2\boldsymbol{\nabla}_H.\boldsymbol{\tau}_H\right]_{z_b}^{z_f}. \tag{6.43}$$

Applying boundary conditions $(6.36)_4$ and $(6.37)_3$ then allows us to write this expression as

$$\delta_l^2\left(-V_f^* + \boldsymbol{\nabla}_H z_f.\,\boldsymbol{\nabla}_H p_w|_f - \boldsymbol{\nabla}_H z_b.\,\boldsymbol{\nabla}_H p_w|_b + \left[2\frac{\partial}{\partial z}(\boldsymbol{\nabla}_H.\mathbf{U}_H) - \boldsymbol{\nabla}_H.\boldsymbol{\tau}_H\right]_{z_b}^{z_f}\right), \tag{6.44}$$

where the subscripts f and b denote quantities evaluated at $z = z_f$ and $z = z_b$ respectively. Now, using equation $(6.34)_4$ and boundary condition $(6.37)_2$, we may write

$$\begin{aligned}\left[2\frac{\partial}{\partial z}(\boldsymbol{\nabla}_H.\mathbf{U}_H) - \boldsymbol{\nabla}_H.\boldsymbol{\tau}_H\right]_{z_b}^{z_f} &= \left[\frac{\partial}{\partial z}(\boldsymbol{\nabla}_H.\mathbf{U}_H) - \nabla_H^2 U_3\right]_{z_b}^{z_f} \\ &= \int_{z_b}^{z_f}\frac{\partial^2}{\partial z^2}(\boldsymbol{\nabla}_H.\mathbf{U}_H)dz - \nabla_H^2 U_3\Big|_f\end{aligned} \tag{6.45}$$

Collecting together the above decomposition of the right hand side of equation 6.42, we may write this equation as

$$\begin{aligned}-V_f^* - \nabla_H^2 U_3\Big|_f - \boldsymbol{\nabla}_H z_b.\,\boldsymbol{\nabla}_H p_w|_b + \boldsymbol{\nabla}_H z_f.\,\boldsymbol{\nabla}_H p_w|_f = \\ \int_{z_b}^{z_f}\left(\frac{\partial\Delta}{\partial t} - \frac{2(1-\nu)}{(1-2\nu)}\nabla_H^2\Delta - \frac{\partial^2}{\partial z^2}(\boldsymbol{\nabla}_H.\mathbf{U}_H)\right)dz.\end{aligned} \tag{6.46}$$

Now, using $(6.41)_5$ to eliminate the term in $\mathbf{U}_H$ and collecting together the required leading order variables, the diffusion equation for the effective stress, N, and the equation for the soil matrix velocity, u_{sf}, are given by

$$\begin{aligned}-V_f^* - \nabla_H^2 U_3\Big|_f - \boldsymbol{\nabla}_H z_b.\,\boldsymbol{\nabla}_H p_w|_b + \boldsymbol{\nabla}_H z_f.\,\boldsymbol{\nabla}_H p_w|_f &= \int_{z_b}^{z_f}\frac{\partial\Delta}{\partial t} - \nabla_H^2(\Delta + p_w)\,dz, \\ u_{sf} = \frac{\partial U_3}{\partial t}\Big|_f,\end{aligned} \tag{6.47}$$

where from equations 6.41 we have

$$\begin{aligned} p_w &= P_f - N + z_f - z, \\ \Delta &= -\frac{(1-2\nu)}{2(1-\nu)}\left(N + r\int_z^{z_f}(1-\phi)\,dz\right), \\ U_3 &= -\frac{(1-2\nu)}{2(1-\nu)}\left(N(z-z_b) + r\int_{z_b}^{z}\int_s^{z_f}(1-\phi)\,du\,ds\right). \end{aligned} \tag{6.48}$$

Thus equations 6.47 together with 6.48 form the additional relationships required to complete the field frost heave problem derived in section 6.2. To complete the problem, we require boundary conditions for the non-linear diffusion equation $(6.47)_1$. These can be specified on the bounding domain of the surface $z = z_f$, where the frozen front intersects the surface of the ground (i.e. the plane $z = 0$). In this bounding region the effective stress will be some prescribed function that can be measured. Similarly, the initial condition might be a prescribed effective stress over the whole bounding domain which could again be measured.

The form of the diffusion equation $(6.47)_1$ can be simplified further by making the following approximations

$$z_b = \text{Constant}, \qquad\qquad \phi = \phi(z).$$

Making these approximations allows us to write

$$\begin{aligned} \left.\frac{\partial U_3}{\partial t}\right|_f &= -\frac{(1-2\nu)}{2(1-\nu)}(z_f - z_b)\left(\frac{\partial N}{\partial t} + r(1-\phi_f)\frac{\partial z_f}{\partial t}\right), \\ \left.\nabla_H^2 U_3\right|_f &= -\frac{(1-2\nu)}{2(1-\nu)}(z_f - z_b)\left(\nabla_H^2 N + r(1-\phi_f)\nabla_H^2 z_f\right), \\ \frac{\partial \Delta}{\partial t} &= -\frac{(1-2\nu)}{2(1-\nu)}\left(\frac{\partial N}{\partial t} + r(1-\phi_f)\frac{\partial z_f}{\partial t}\right), \\ \nabla_H^2 \Delta &= -\frac{(1-2\nu)}{2(1-\nu)}\left(\nabla_H^2 N + r(1-\phi_f)\nabla_H^2 z_f\right), \\ \nabla_H^2 p_w &= (s+1)\nabla_H^2 z_s - s\nabla_H^2 z_f - \nabla_H^2 N, \end{aligned} \tag{6.49}$$

where $s = \rho_f/\rho_w - 1$. Substituting these relations into equations 6.47 we get

$$\begin{aligned} &\frac{(1-2\nu)}{2(1-\nu)}\frac{\partial N}{\partial t} = \nabla_H^2 N + \frac{\boldsymbol{\nabla}_H z_f . \boldsymbol{\nabla}_H N}{(z_f - z_b)} + \frac{V_f^*}{(z_f - z_b)} + f(z_s, z_f), \\ &u_{sf} = -\frac{(1-2\nu)}{2(1-\nu)}(z_f - z_b)\left(\frac{\partial N}{\partial t} + r(1-\phi_f)\frac{\partial z_f}{\partial t}\right), \end{aligned} \tag{6.50}$$

where

$$\begin{aligned} f(z_s, z_f) &= -r(1-\phi_f)\frac{(1-2\nu)}{2(1-\nu)}\frac{\partial z_f}{\partial t} - (s+1)\nabla_H^2 z_s + s\nabla_H^2 z_f \\ &\quad -(s+1)\frac{\boldsymbol{\nabla}_H z_s . \boldsymbol{\nabla}_H z_f}{(z_f - z_b)} + s\frac{|\nabla_H z_f|^2}{(z_f - z_b)}. \end{aligned} \tag{6.51}$$

Thus, equations 6.50 form the model for the groundwater flow problem where the aspect ratio is small. In general, these equations, together with the soil's initial porosity profile, will be coupled to the solution to the fringe equations to give a complete description of the field frost heave problem.

6.8 Analysis of Time Scales

The frost heave fringe equations derived in section 6.2 and the groundwater flow equations derived in the previous section have been non-dimensionalised with different scalings and, as a result, this may give rise to different time scales for each problem. Because of the small aspect ratio, the groundwater flow problem gives rise to two natural time scales; 1) a lateral time scale, t_l, which controls the relaxation of the diffusion equation, 6.47, and hence the lateral relaxation of the variables in the unfrozen region; and 2) a vertical time scale, t_v, which controls the vertical relaxation (the usual consolidation time scale). If we denote the frost heave time scale by t_f then we have

$$\begin{aligned} t_l &= \frac{1}{\delta_l^2}\frac{d^2\rho_w g}{k_0 G}, \\ t_v &= \frac{d^2\rho_w g}{k_0 G}, \\ t_f &= \frac{d^2 L\rho_w}{k\Delta T}. \end{aligned} \tag{6.52}$$

The ratios of these time scales are independent of the depth scale of the aquifer and are at most only dependent on the aspect ratio, δ_l. Typical values of the constants in these parameters are

$$\begin{aligned} g &\sim 10\,\mathrm{m\,s^{-2}} \\ \rho_w &\sim 1000\,\mathrm{kg\,m^{-3}} \\ L &\sim 3.35 \times 10^5\,\mathrm{J\,kg^{-1}} \end{aligned}$$

$$
\begin{aligned}
k &\sim 1\,\mathrm{W\,m^{-1}\,K^{-1}} \\
\Delta T &\sim 10\,\mathrm{K} \\
G &\sim 1 \times 10^{8}\,\mathrm{Pa} \\
d &\sim 500\,\mathrm{m} \\
k_0 &\sim 10^{-3} - 10^{-11}\,\mathrm{m\,s^{-1}} \quad \text{(Sand)} - \text{(Clay)}.
\end{aligned}
$$

Thus, for an aspect ratio $\delta_l \sim 10^{-3}$, we find that the time scales for this problem are

$$
\begin{aligned}
t_v &\sim 10^{-3} - 10^{5}\,\text{years} \\
t_f &\sim 10^{5}\,\text{years} \\
t_l &\sim 10^{3} - 10^{11}\,\text{years}
\end{aligned}
$$

and, in general, these time scales satisfy $t_v \ll t_f \ll t_l$. Consequently, on the frost heave time scale, the vertical groundwater flow problem rapidly relaxes to equilibrium while the lateral problem does not get time to diffuse and hence does not relax to an equilibrium. In our later analysis we find that another time scale exists for lens front penetration. This time scale turns out to be very much more rapid than the frost heave time scale and depending on the soil type may be faster (sands), slower (clays) or comparable (silts) to the vertical consolidation time scale. However, we go on to show that the heave and frost penetration which occur in this transient are small compared to the ultimate values and therefore this transient is not important in affecting the consolidation.

This time scale analysis shows that the diffusion equation for the effective stress will not have time to diffuse on the frost heave time scale and thus the horizontal diffusive term may be neglected apart from in the regions close to where the boundary conditions are applied. Thus, the (outer) solution to the lateral groundwater flow problem is given by the solution to

$$
\begin{aligned}
\frac{(1-2\nu)}{2(1-\nu)}\frac{\partial N}{\partial t} &= \frac{(\dot{z}_s - u_{sf})}{(z_f - z_b)} - r(1-\phi_f)\frac{(1-2\nu)}{2(1-\nu)}\frac{\partial z_f}{\partial t}, \\
u_{sf} &= -\frac{(1-2\nu)}{2(1-\nu)}(z_f - z_b)\left(\frac{\partial N}{\partial t} + r(1-\phi_f)\frac{\partial z_f}{\partial t}\right) \qquad (6.53)
\end{aligned}
$$

where we have substituted relation $(6.4)_6$ from the fringe equations for the relative water flux. In making this substitution we have rescaled equation $(6.4)_6$ onto the lateral groundwater flow scaling.

The solution to 6.53 is reconciled with the boundary condition for N on the bounding domain via a boundary layer of thickness $(t_f/t_l)^{\frac{1}{2}}$. Rescaling equation $(6.50)_1$ using this length scale retains the diffusion term which allows the boundary condition to be satisfied while matching with the outer solution given by equation 6.53. However, we are not concerned here with the solution to the boundary layer problem and do not consider it any further.

It is immediate from equations 6.53 that they combine to give $\dot{z}_s = 0$ and hence for a step freezing type experiment we get that, to leading order, the ground surface, z_s, is undisturbed. This result is essentially a result of the time scale analysis given above. The induced suction resulting from the frost heave causes the soil to rapidly consolidate on the vertical scale, which accommodates the ice lens which grows as a result of the imbibed fluid. Any surface movement is thus a second order process from the change in phase of the water to ice and the lateral water flux.

At this point we rescale equations 6.53 using the frost heave scales by writing

$$t = \frac{[t_f]}{[t_l]}t^* \qquad N = \frac{[\sigma_f]}{[\sigma_g]}N^* \qquad z = \frac{[d_f]}{[d_g]}z^* \qquad u_{sf} = \frac{[u_f]}{[u_g]}u^*_{sf}$$

where the terms in square brackets represent the time, stress, length and velocity scales respectively and the suffices f and g refer to the frost heave and groundwater flow scales respectively. Making these substitutions and dropping the asterisks, equations 6.53 become

$$\begin{aligned} \dot{z}_s &= 0, \\ \frac{u_{sf}}{\epsilon} &= -\frac{(1-2\nu)}{2(1-\nu)}(z_f - z_b)\left(\psi\frac{\partial N}{\partial t} + r(1-\phi_f)\frac{\partial z_f}{\partial t}\right) \end{aligned} \tag{6.54}$$

where ψ and ϵ are given by

$$\psi = \frac{\sigma_f}{\rho_w g d_g}, \qquad \epsilon = \frac{\rho_w g d_g}{G}.$$

$[\sigma_f]$ is the suction characteristic scale which would typically take values of 10^5 Pa, G is the shear modulus of the soil sample for which a typical value may be 10^8 Pa and $\rho_w g d_g$ is the hydrostatic stress which, on a length scale of 500 m is $\sim 5 \times 10^6$ Pa. Thus, the parameters ϵ and ψ take values which are $\ll 1$ and the effect of this is discussed in the next section.

6.9 Discussion and Numerical Solution.

In this section we consider the resulting frost heave equations given by equations 6.6 and 6.54 and ascertain whether the observations discussed at the beginning of this chapter can be explained from our analysis. In particular, we would like to show that

1. very thick ice lenses can form;
2. lens formation is restricted to a region close to the ground surface; and
3. lens thickness may not generally increase with depth.

The small parameter ψ in equation $(6.54)_2$ suggests that the effective stress, N, will equilibrate at a value which is $O(\psi^{-1})$. From our analysis in chapter 4, this implies that the critical effective stress will be reached in the early stages of permafrost growth. Thus the lens front will stop in the early stages of permafrost growth and hence we expect the ice lens formation to be restricted to a region 'close' to the ground surface. Furthermore , because the size of the heave parameter, α_{fk}, is sensitive to the effective stress (see chapter 4), the increasing effective stress with frost penetration depth may be a mechanism for lens thickness to decrease with depth.

6.9.1 Numerical Solution

If we suppose that the freezing front is a function of time only, the porosity is a constant and the thermal conductivities k_f and k are equal then the complete field frost heave model given by equations 6.6 and 6.54 may be written as

$$\begin{aligned}(\phi - W_m)(\dot{z}_f - u_{sf}) &= -u_{sf} + 1 - \frac{T_s}{z_f},\\ -u_{sf} &= \alpha_{fk}\left((W_l - W_m)(\dot{z}_f - u_{sf}) + \frac{T_s}{z_f}\right),\\ \frac{u_{sf}}{\epsilon} &= -\frac{(1-2\nu)}{2(1-\nu)}(z_f - z_b)\left(\psi\dot{N} + r(1-\phi)\dot{z_f}\right), \qquad (6.55)\end{aligned}$$

where α_{fk} is a function of the effective stress, N, and ψ and ϵ are dimensionless parameters. We consider step freezing boundary conditions, which may approximate the situation following deglaciation by a retreating ice sheet. Thus we have $z_s = z_f = u_{sf} = 0$ and for convenience choose $N = 0$ at $t = 0$.

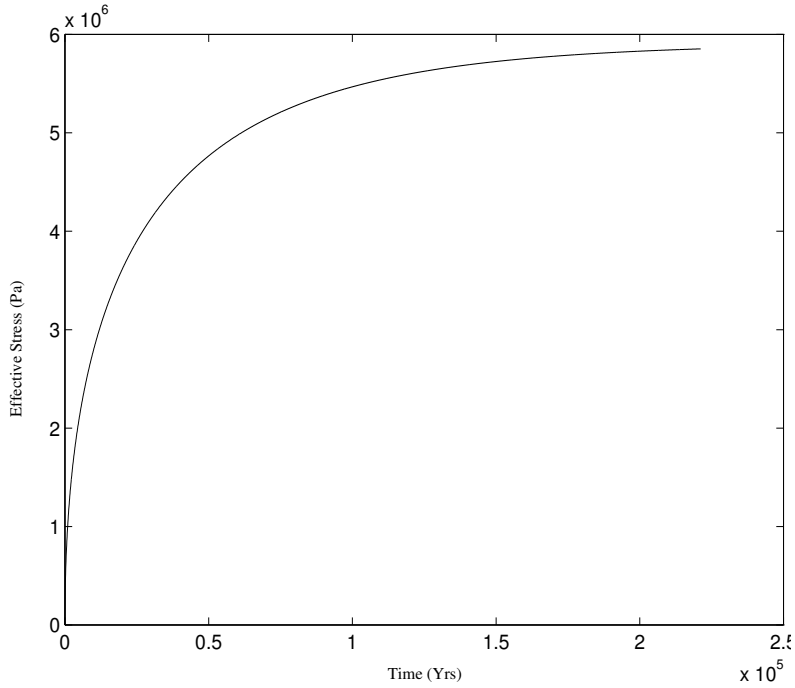


Figure 6.3: Plot of effective stress against time.

We solve this system for the soil/freezing characteristics described in chapter 4 with the following changes

Soil surface temperature, T_s	$261\,\mathrm{K}$
Depth of aquifer, d	$1,000\,\mathrm{m}$
Density of soil matrix, ρ_s	$2 \times 10^3\,\mathrm{kg\,m^3}$,
Shear modulus of soil matrix, G	$10^8\,\mathrm{Pa}$,
Poisson's ratio, ν	0.25.

Equations 6.55 are solved using NAG routine D02BBF and the plots of effective stress at the frozen front and frozen front penetration are shown in figures 6.3 and 6.4.

It is interesting to consider the plots of cumulative lens thickness (i.e. $\int u_{sf}\,dt$), lens thickness and lens spacing. By similar arguments to those given in section 4.6 the time of the formation of the nth lens, t_l^n, for a compressible soil can be shown to be given by the following recurrence relation

$$z_f^R(t_l^{n-1}) - z_f^R(t_l^n) = d_l(t_l^n) \tag{6.56}$$

where z_f^R is the relative frost penetration depth (i.e. $z_f - \int u_{sf}\,dt$). The lens spacing,

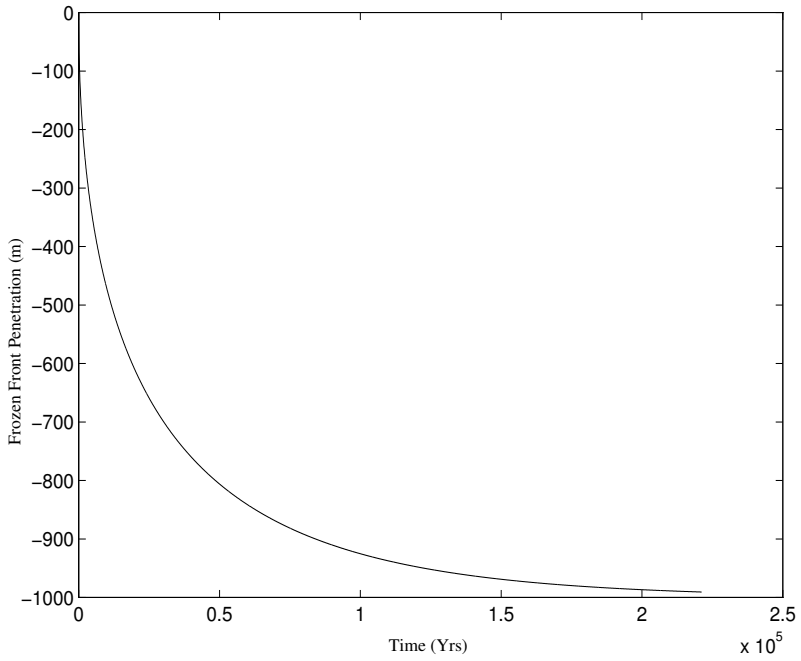


Figure 6.4: Plot of frost penetration depth against time.

d_l is given by

$$d_l = \frac{\mu}{\gamma}\frac{D_l \alpha_{fk}}{\dot{z}_s^R} = \frac{\mu}{\gamma}\frac{D_l \alpha_{fk}}{\dot{z}_s - u_{sf}} \tag{6.57}$$

and the term D_l is given by equation 4.53. From the lens initiation times, t_l^n, the lens spacing and lens thickness are easily found by subtraction of the relative frost penetration depth and cumulative lens thickness respectively. Figures 6.5, 6.6 and 6.7 are plots of the cumulative lens thickness, the lens thickness against lens initiation time and lens spacing against lens initiation time.

The plots of lens thickness can be seen generally to decrease with time to lens formation and hence depth. Also, the time scale for lens formation and hence heave appears to occur in the early stages of permafrost formation and hence 'close' to the ground surface. These results are in general agreement with massive formations except that the cumulative amount of heave and the thickness of ice lenses appear small compared to massive ice formations that are observed. There are a number of possible explanations for this as follows:

1. As discussed in chapter 4, the extent of heave is controlled by the capillary suction and the hydraulic conductivity functions. These functions have been inferred from the analysis of O'Neill & Miller (1985) and, as such, may not accurately reflect the relevant soil conditions in the field;

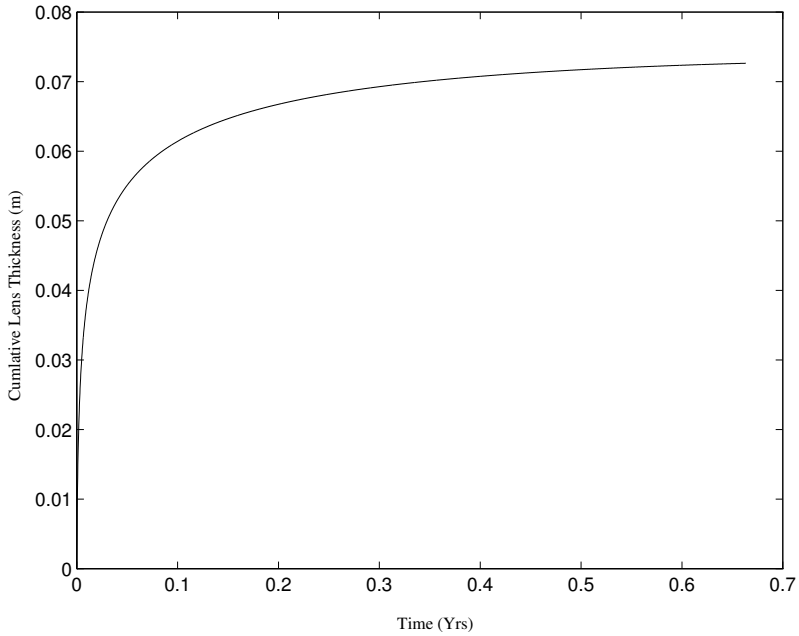


Figure 6.5: Plot of cumulative lens thickness against time.

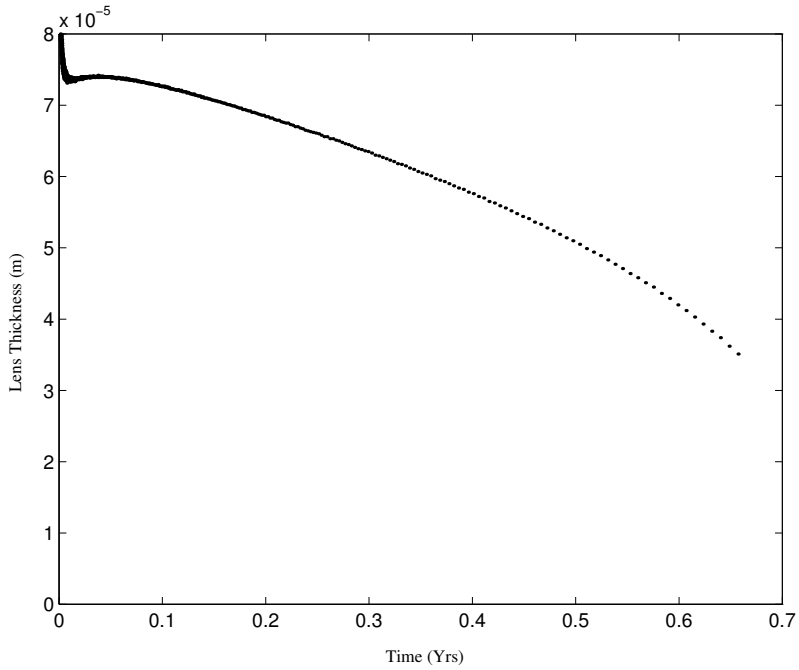


Figure 6.6: Plot of lens thickness against time of lens initiation.

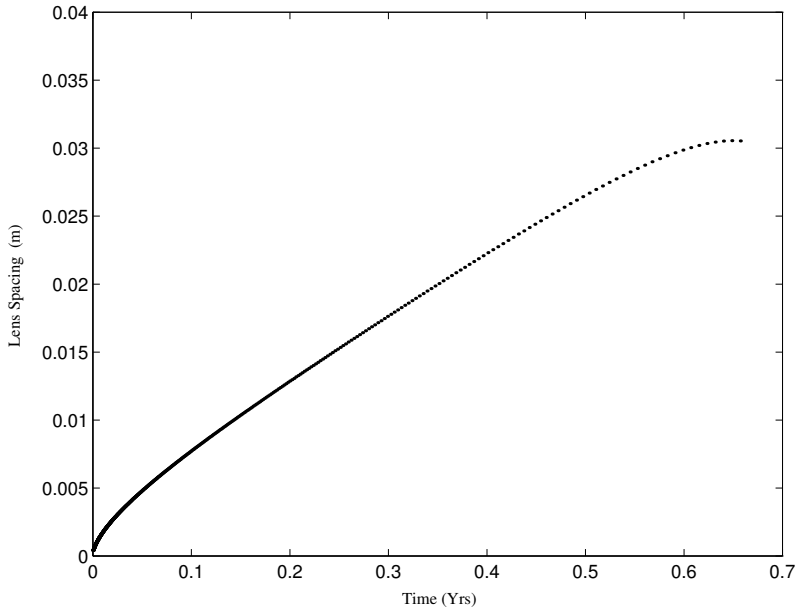


Figure 6.7: *Plot of lens spacing against time of lens initiation.*

2. Mackay & Dallimore (1992) observe that (segregated) massive ice often forms where a fine grained frost susceptible soil is above a coarse grained soil which is conducive to the upward flow of groundwater. This situation may encourage the growth of a large single ice lens at the boundary of these soils rather than many small ice lenses (see Williams & Smith (1989));

3. Freeze/thaw effects close to the ground surface as a result of the seasonal variation in climate may affect the distribution of massive ice within the active layer;

4. Finally, the increase in effective stress implies that new ice lenses are not able to form because the critical overburden described in chapter 4 has been reached. However, the final ice lens is still able to grow because water can reach the final lens through the growing frozen fringe from the unfrozen region region below. For example, in the simulation given above the (dimensionless) heave rate at the point where the critical overburden is reached is approximately 4×10^{-3}. If we suppose that this rate were to continue indefinitely then a relatively thick ice lens could eventually form. In particular, if this heave rate were to continue, albeit at a very slow rate, for the period of frozen front penetration, then this would result in a final lens thickness of $\sim 4\,\mathrm{m}$. Thus, this is a possible mechanism for massive ice formation and in the following section we consider a model for

the growth of the final ice lens.

6.9.2 The Final Ice Lens

The numerical results given in the previous section indicated that lens front advancement was very rapid compared to the frost penetration time scale and that as a result the cumulative amount of heave was not sufficient to explain massive ice formation. However, although the averaged version of the generalised Miller model breaks down, there appears to be no apparent mechanism within the discrete version of the model that would stop the continued growth of the final ice lens. As such, one possible explanation of segregated massive ice formation is that the final ice lens could continue to grow, albeit very slowly, on the frozen front penetration time scale.

In the averaged version of the model, the lens front stops advancing early in permafrost growth because the critical effective stress, N_c (see chapter 4) is reached very rapidly, because of the small parameter ψ multiplying the effective stress term N in equation $(6.55)_3$. With a static final ice lens, the frozen front will continue to grow ahead of the final lens and, consequently, we would expect that the frozen fringe will no longer be thin. If the frozen fringe becomes thick and lens penetration stops then the 'averaged' Miller model derived in chapter 3 and the reduction given at the start of this chapter become invalid and, as such, the heave and frozen front penetration equations need to be reconsidered.

At the critical value of effective stress, the water content at the lens front is very close to the minimum value, W_m, which arises in the capillary suction characteristic curve. In this situation, the temperature scale in the frozen fringe is still controlled by the Clapeyron equation and hence the temperature in the fringe is given by

$$\begin{aligned} T &= -\mu(\delta p_w + f(W)) \\ &\approx -\mu f(W). \end{aligned} \tag{6.58}$$

The parameter μ is $\ll 1$ and hence, because we expect the length scale of the fringe to be ~ 1, the capillary suction function[3] $f(W)$ will be $\sim \mu^{-1} \gg 1$. Thus, we would expect the water content in the fringe, except possibly in a boundary layer at the

[3]At water contents very close to the soil's minimum content, the measurement of capillary suction characteristic functions becomes very difficult to achieve reliably (see Black (1990)) . Around these values, a question arise as to whether the permeability of the fringe has effectively gone to zero and hence no water flow is possible through the fringe. Consideration of this is beyond the scope of this

frozen front, to be very close to the minimum water content, W_m. Thus, it would seem reasonable to assume that essentially all the freezing within the frozen fringe will occur at the base of the final ice lens and near the frozen front. However, because the effective stress is large, the heave rate will be very small and hence a relatively small amount of freezing will occur at the base of the final ice lens[4]. Thus, a reasonable assumption would be that the temperature gradient will be approximately linear between the ground surface and the frozen front (where most of the freezing will now be occurring). This temperature gradient will be approximately equal to $T_s/(z_s - z_f)$.

In order to find an equation for the heave rate when the lens front is stationary, we can apply much of the analysis used in the derivation of the averaged model given in chapter 3. In particular, the following results did not rely on the frozen fringe being thin:

1. the dimensional analysis discussed in section 3.2.2 allows us to neglect the advective transport of heat and the expansion of water on change of phase to ice;

2. the boundary layer analysis for the water pressure, p_w, given in section 3.3.1 remains valid; and

3. the solution to the temperature profiles in the frozen and unfrozen regions are linear.

Using these results, the frozen fringe equations given in section 3.2.2 for the discrete case may be written to leading order as

$$\begin{aligned}
&\frac{\partial}{\partial z}\left(U_w + (\phi - W)u_i + (1-\phi)u_s\right) = 0,\\
&\frac{\partial W}{\partial t} + \frac{\partial U_w}{\partial z} = \frac{\partial^2 T}{\partial z^2},\\
&p_w = p^h(z) - [p^h(z_l) - P(z_l) + f(W_l)]\exp\left(-\frac{\gamma W_l'}{W_l}(z - z_l)\right),\\
&T = -\mu(\delta p_w + f(W)),
\end{aligned}$$

thesis and we will assume that water flow through the fringe is always possible, albeit very slowly, and the relationships we have for the capillary suction function and the hydraulic conductivity always apply.

[4]For example, in the numerical solution given in the previous section, the heave parameter $\alpha_{fk} = 4 \times 10^{-3}$ when the critical effective stress is reached.

$$
\begin{aligned}
&u_i - u_s = -\delta_3 \frac{\partial T}{\partial z} \quad \text{(Gilpin)},\\
&u_i = \dot{z}_s \qquad\qquad\qquad \text{(Rigid Ice)},\\
&p^h = p_f + \delta_2^w (z_f - z),\\
&P = \delta_2^f (z_s - z_l),
\end{aligned} \tag{6.59}
$$

where, because the fringe is no longer thin, we have included the hydrostatic pressure terms in the expression for the water pressure (see equation 3.22).

The boundary conditions are given by

at $z = z_l$

$$
\begin{aligned}
&\frac{\partial W}{\partial z} = -\phi\tilde{\beta}(U_w - W u_s),\\
&W u_s - U_w = \frac{(T_l - T_s)}{(z_l - z_s)} - \frac{\partial T}{\partial z},\\
&\dot{z}_s = U_w + (\phi - W)u_i + (1-\phi)u_s,\\
&\dot{z}_l = u_s,
\end{aligned} \tag{6.60}
$$

at $z = z_f$

$$
\begin{aligned}
&W = \phi,\\
&p_e = N,\\
&\frac{\partial T}{\partial z} = -1,
\end{aligned} \tag{6.61}
$$

where the boundary conditions correspond to those applicable in the discrete case and, again, we suppose the thermal conductivities k_f and k are equal.

To avoid consideration of the rheology of the frozen fringe, we assume that the presence of ice in this region makes it relatively incompressible compared to the unfrozen region beneath. Thus, any deformation of the unfrozen region causes the whole frozen fringe to move downward at the same velocity as the deformation. Hence, we may write

$$
u_s = u_{sf}, \tag{6.62}
$$

where u_{sf} is the velocity of the soil matrix at the frozen front.

The analysis given in section 6.2 in deriving the evolution equation for the heave rate, $\dot{z}_s$, only uses the boundary conditions at the lens front and the first derivative

of the Clapeyron equation evaluated at the lens front. Reproducing this analysis for the discrete model we get that the heave rate is given by

$$\begin{aligned} \dot{z}_s - u_{sf} &= -\alpha_{fk} \left.\frac{\partial T}{\partial z}\right|_+, \\ \dot{z}_l &= u_{sf}, \end{aligned} \tag{6.63}$$

where $\left.\frac{\partial T}{\partial z}\right|_+$ is the temperature gradient in the frozen soil above the final ice lens and z_s and z_l are the positions of the ground surface and lens front respectively. The heave parameter, α_{fk}, takes its usual form in terms of the parameter β_{fk} (see the definitions following equation 6.6) and β_{fk} takes the form

$$\beta_{fk} = -\frac{\gamma L^2 \rho_w k_0}{T_0 g k} \left(\frac{W_l}{\phi}\right)^{\gamma} \left(\frac{(f(W_l) - N^h)}{\delta\gamma(f(W_l) - N^h) + W_l f'(W_l)}\right), \tag{6.64}$$

and N^h is the effective stress at the frozen front plus the hydrostatic water pressure term between z_l and z_f. i.e.

$$N^h = N + \delta_2^w (z_l - z_f), \tag{6.65}$$

where N is the effective stress at the frozen front.

To complete the problem we need to determine the temperature gradient in the frozen soil and an evolution equation for the frost penetration depth, z_f. As previously discussed, because the heave parameter is small, the amount of freezing at the base of the lowest ice lens will be small and hence the temperature gradient throughout the frozen zone will be approximately a constant. Thus, we may write

$$\frac{\partial T}{\partial z} \approx \frac{T_s}{z_s - z_f}, \tag{6.66}$$

and hence the heave equations 6.63 may be written approximately as

$$\begin{aligned} \dot{z}_s - u_{sf} &= -\alpha_{fk} \frac{T_s}{(z_s - z_f)}, \\ \dot{z}_l &= u_{sf}. \end{aligned} \tag{6.67}$$

Furthermore, the growth of the frozen front will essentially be a Stefan type problem from which, if we assume the thermal conductivities of the frozen and unfrozen soil are equal, the evolution equation for z_f will be given by

$$(\phi - W_m)\dot{z}_f = 1 + \frac{T_s}{z_s - z_f}. \tag{6.68}$$

Thus, equations 6.67 and 6.68 describe the growth of the final ice lens and frost penetration depth providing we are able to calculate the heave parameter α_{fk}. This requires calculation of the capillary suction function at the base of the final ice lens. At this point the water content is approximately equal to W_m and the capillary suction function and its first derivative take very large (but finite) values. Given that the temperature profile is approximately linear in the fringe, the actual water content in the fringe can be found by inverting the Clapeyron equation $(6.59)_4$. Thus we can write

$$\mu f(W_l) = -T_s \frac{(z_l - z_f)}{(z_s - z_f)}, \tag{6.69}$$

from which W_l and hence $f^{'}(W_l)$ can be determined.

Finally, coupling the frost heave equations 6.67 and 6.68 with the groundwater flow equations $(6.55)_3$ and $\dot{z}_s = 0$, we get the system for the growth of the final ice lens

$$\begin{aligned} \dot{z}_l &= -\alpha_{fk} \frac{T_s}{z_f}, \\ (\phi - W_m)\dot{z}_f &= 1 - \frac{T_s}{z_f}, \\ \dot{N} &= -\frac{r(1-\phi)}{\psi} \dot{z_f}, \end{aligned} \tag{6.70}$$

where the cumulative final lens thickness is now given by $-z_l$ and we have assumed that $\alpha_{fk} \ll \epsilon \sim 0.1$. Equation $(6.70)_3$ is unchanged as a result of the lens front stopping because the position of the lens front only comes into the groundwater flow problem through the prescription of the overburden, P_f, in the boundary conditions. On the frost penetration time scale, the prescribed load has no effect on the final groundwater flow equation.

Figure 6.8 is a plot of the solution to equations 6.70 for the cumulative heave (i.e. $-z_l$). This reveals that the final lens continues to grow at a very slow rate and this may be a possible mechanism for massive ice formation providing that this growth can continue indefinitely. In particular, providing the capillary relation is for a silt or clay soil (i.e. $f(W) \to \infty$ as $W \to W_m$) so that equation 6.69 always has a solution , the Miller model of secondary frost heave contains no mechanism which can stop the growth of the final ice lens. The total heave shown in figure 6.8 of around 0.16 m after 2×10^5 years is still relatively small compared to segregated massive ice

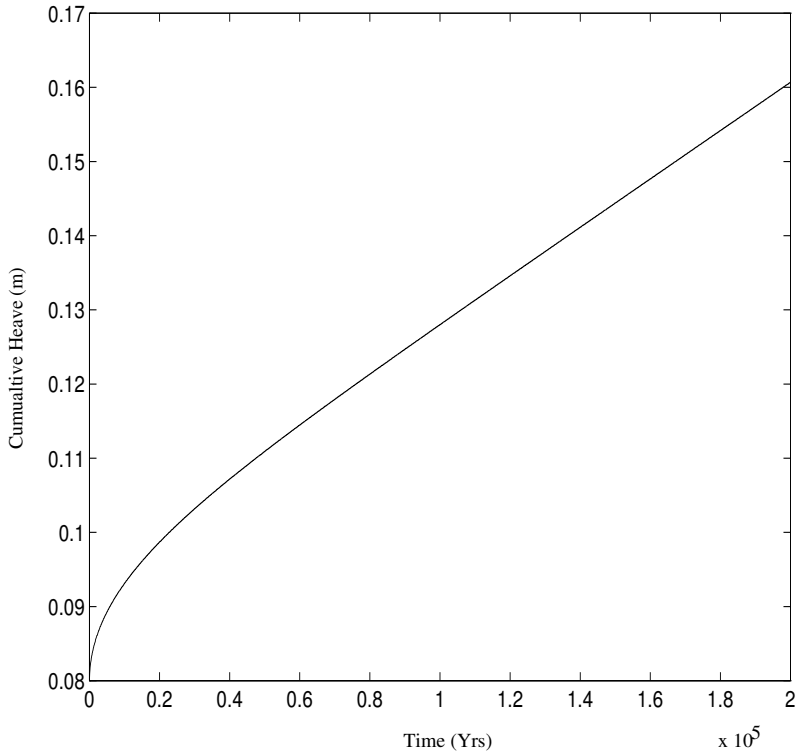


Figure 6.8: Cumulative heave as a result of the growth of the final ice lens.

formation. Possible explanations for this are given at the end of section 6.9.1 and of particular relevance is the form of the capillary suction curve used and the occurrence of stratified soil types which are often present with segregated massive ice formations. Furthermore, this numerical result uses the rigid ice form of the heave parameter and hence does not allow for the thermal regelation of the pore ice.

Thus the Miller model of secondary frost heave coupled with the solution to the groundwater flow problem provides a possible explanation for the formation of segregated massive ice which is in general agreement with observation. In particular, we have been able to show that

1. ice lens formation is restricted to the region close to the ground surface. This arises because lens front penetration depends on the effective stress at the lens front and if this becomes too large the criterion for the formation of a new lens cannot be satisfied;

2. the final ice lens can continue to grow indefinitely at a very slow rate which, on very long time scales, could give rise to segregated massive ice formation; and

3. lens thickness will, in general, decrease with depth as a result of the increase

in effective stress. However we have not shown that the secondary frost heave model can explain how multiple massive ice lenses can form and this manifestation is probably a result of the particular soil conditions that exist. For example, Mackay & Dallimore (1992) observed that segregated massive ice often forms at the boundaries of sand and silt soil types and, consequently, if relatively stratified soil conditions exist, then multiple massive ice lenses may occur.

Chapter 7

Differential Frost Heave

7.1 Introduction

Previous chapters have been concerned with a purely one dimensional approach to secondary frost heave. In general, frost heave will also result in some form of spatial variation which may arise as a result of lateral variations in load, temperature or soil type. We refer to this as differential frost heave.

In tundra areas which are also subject to a cold climate, many types of regular geometric formations are observed. These formations are referred to as *patterned ground* and differential frost heave is thought to be a possible mechanism for their formation. Some forms of isolated patterned ground (e.g. *pingos* and *palsas*) can be directly attributed to frost heave as excavation of these formations reveals the characteristic segregated ice seams. Palsas are isolated mounds of around $1 - 2\,\mathrm{m}$ in diameter and are thought to occur because of a spatial variation of temperature as a result of variations in snow cover. During the winter months, the elevated surface of a palsa will have a thinner snow cover than the troughs and consequently, because snow acts as an insulator, the peaks of the palsas will be subject to greater winter cooling and hence more heave. Pingos are usually much larger than palsas (e.g. up to $50\,\mathrm{m}$ in diameter) and arise as a result of a locally increased water supply within a permafrost region (see Williams & Smith (1989)). The origins of this increased water supply are from a drainage path (e.g. pingos often form at the bottom of slopes) or from former lakes which have either drained away leaving unfrozen saturated soil beneath or have been infilled with sediments.

Much more interesting forms of patterned ground, for which differential frost heave



Figure 7.1: Earth Hummocks - Source: W. B. Krantz

is again thought to be the mechanism, are *earth hummocks* and *stone circles* which form in regular geometric patterns over large areas. Earth hummocks (see figure 7.1) are well defined regularly spaced mounds of $1 - 2\,\mathrm{m}$ in diameter and stone circles (see figure 7.2) are piles of stones which have formed into rings several metres in diameter. The mechanisms for stone circle and earth hummock formation are thought to be similar and differ in that stone circles are simply a result of seasonal hummock formation. In particular, a consequence of frost heave and subsequent thawing is the uplifting of stones from within the ground onto the surface (see Williams and Smith (1989)). Once on the surface, hummock formation during the winter months causes the stones to roll into the troughs of the hummock. During the summer months thawing causes the hummocks to disappear leaving piles of stone circles.

Other mechanisms besides differential heave/thaw effects have been proposed for these latter forms of patterned ground (see the review by Van Vliet-Lanoë (1991)). These include (i) thermal (Rayleigh) convection type models (e.g. McKay & Straughan (1991), Krantz *et al.* (1988)) in which buoyancy driven natural convection is thought to occur in the active layer of permafrost during the summer thaw; and (ii) the 'cryostatic pressure' theory in which it is thought that unfrozen areas of soil are trapped between the permafrost table and the downward freezing soil during the



Figure 7.2: Stone Circles - Source: National Geographic, January 1987, Vol. 171(1), page 98

winter months. These unfrozen regions are subjected to increased pressures as the freezing zone encroaches and may be 'squeezed out' through weak points. Other mechanisms are discussed by Van Vliet-Lanoë (1991) who concludes that differential frost heave coupled with subsequent thawing is the most likely cause of patterned ground as the natural conditions which exist in the areas where these formations occur are not supportive of other existing theories.

Having developed a simplified model for secondary frost heave in the one dimensional case, the purpose of this chapter is to extend this reduction to the three dimensional problem and consider the linear stability of the resulting system. In doing this we hope to identify the parameter ranges, through the heave parameter α_{fk}, which result in the heave equations becoming unstable and which may thus provide a mechanism for the onset of patterned ground. One drawback of a linear stability analysis for this problem is that the basic state is time dependent and consequently we need to assume that the time scale for the instability to arise is very much faster than the time scale for heave and frost penetration.

In order to extend the Miller model of secondary frost heave to differential heaving, a rheology needs to be developed for the frozen soil above the lowest ice lens so that the ice flux at the lens front can be related to the surface displacement. The rheology of

frozen soil is complex and, in particular, extremely temperature dependent as a result of the adsorbed films of water surrounding the soil particles. However, for simplicity, we will assume that the rheology of the frozen soil is independent of temperature.

In general, the rheological behaviour of frozen soil under applied stresses is a combination of elastic and creep[1] deformations. The review by Anderson & Morgenstern (1973) states that pure ice will creep under very small applied stresses and that the inclusion of soil acts to inhibit the amount of creep deformation. Haynes (1978) considers the variation in the compressive and tensile strengths of frozen silt as a function of temperature and gives an empirical power law relationship between the strength of a frozen soil and the applied strain rate. He suggests that for low strain rates (i.e. $< 1.0\,\mathrm{s}^{-1}$) and at temperatures above $-40^{\circ}\,\mathrm{C}$ a frozen soil exhibits visco-elastic behaviour. The review by Sayles (1988) states that the initial elastic component of strain is relatively small compared to the creep component and is usually ignored.

Frost heave will give rise to very low strain rates ($\sim 10^{-8} - 10^{-9}\,\mathrm{s}^{-1}$) and the presence of ice lenses within the frozen soil will act to increase the ice content in this region. Consequently, a reasonable first approximation for the rheology of a frozen heaving soil is that of a viscous material.

In this chapter we first write down the solution to the fringe equations for the three dimensional frost heave problem for an incompressible, solute free soil. Following this the governing equations for the frozen soil are established assuming a viscous rheology and a slow flow régime. We then present a quasi-static linear stability analysis in which we consider perturbations about the time dependent one dimensional solution.

7.2 The Frost Heave Equations

The analysis in chapters 3 and 4 given for the general one dimensional problem can be directly extended to the three dimensional problem by working in terms of coordinates which are normal and tangential to the lens front surface. Following this through, it is relatively straightforward to show, by analogy with the derivation of equations 4.20 from chapter 4, that the solutions to the frozen fringe equations are simply

$$V_f(\phi - W_m) \;=\; V_i - \left.\frac{\partial T}{\partial n}\right|_f + \left.\frac{\partial T}{\partial n}\right|_l ,$$

[1] We refer to creep as an irreversible time dependent deformation

$$V_i \;=\; \alpha_{fk}\left((W_l - W_m)V_f - \left.\frac{\partial T}{\partial n}\right|_l\right), \tag{7.1}$$

where V_i is the total normal flux at the lens front, V_f is the normal velocity of the frozen fringe, $\mathbf{n}$ is the unit normal to the lens front in the upwards direction and we have assumed the thermal conductivities k_f and k are equal. The velocity of the frozen fringe is in the direction $\mathbf{n}$ and is related to the position of the frozen front by considering the rate of change of the frozen front position, $z_f(\mathbf{x}, t)$, following this surface. We have that

$$0 = \frac{d}{dt}(z - z_f) = -\frac{\partial z_f}{\partial t} + V_f \mathbf{n}.\boldsymbol{\nabla}(z - z_f), \tag{7.2}$$

where $\frac{d}{dt}$ is the derivative following z_f.

For the two dimensional problem, the upwards normal to the frozen front is simply

$$\mathbf{n} = \frac{\boldsymbol{\nabla}(z - z_f)}{(1 + {z'_f}^2)^{\frac{1}{2}}}$$

where the prime indicates differentiation with respect to x. Hence, we get that

$$V_f = \frac{1}{(1 + {z'_f}^2)^{\frac{1}{2}}}\frac{\partial z_f}{\partial t}. \tag{7.3}$$

The water content, W_l, at the lens front is obtained from the solution to equations 3.27 suitably cast in terms of normal derivatives where appropriate. Thus, the water content at the lens front is given by the solution of

$$\begin{aligned} g(W_i) - N &= -\frac{W_l}{\gamma}\frac{\partial g}{\partial n}(W_i), \\ W_i - W_l &= -\frac{W_l}{\gamma}\log\left(\frac{g(W_i) - N}{f(W_l) - N}\right), \end{aligned} \tag{7.4}$$

where $g = (1 - \chi)f$ and $\mathbf{n}$ is defined as above.

As discussed in chapter 2, Miller's 'rigid ice' theory in which the interstitial pore ice moves as a rigid body cannot be readily extended to the problem of differential frost heave. As such, the heaving parameter, α_{fk}, appearing in equations 7.1 should be interpreted as the Gilpin value.

The normal temperature gradients above and below the frozen fringe are determined from the solution to $\nabla^2 T = 0$ in the frozen and unfrozen regions. The boundary conditions for the thermal problem in the frozen region are $T = T_s$ at $z = z_s(\mathbf{x}, t)$

and $T = 0$ at $z = z_f(\mathbf{x}, t)$. In the unfrozen region the boundary conditions are $T = 0$ at $z = z_f(\mathbf{x}, t)$ and prescribed geothermal heat flux in the far field.

Patterned ground is usually associated with the seasonal freeze/thaw cycles in the active layer of permafrost. Hence, as shown in chapter 3, an appropriate length scale for the depth of the active layer is given by $\sqrt{\kappa_f t}$ where κ ($\sim 2 \times 10^{-6}\,\mathrm{m^2\,s^{-1}}$) is the soil's thermal diffusivity and t is an appropriate time scale (i.e. 1 year $\approx 3\times10^7$ s). This gives an active layer depth scale of $\sim 8\,\mathrm{m}$. The geothermal heat flux of $0.05\,\mathrm{W\,m^{-2}}$ corresponds to a temperature variation of around 1K every 50m. Thus, on the length scale we consider, the geothermal heat flux is negligible and hence the solution to the temperature problem in the region beneath the lens front can be taken to be simply $T = 0$.

7.3 The Frozen Soil Equations

As discussed in the introduction, a suitable approximation to the rheology of the frozen soil above the lens front is that of a viscous fluid undergoing slow flow. Thus, the fluid flow in this region is given by the slow flow form of the Navier-Stokes equations (see Acheson (1990)) as follows

$$\begin{aligned} -\boldsymbol{\nabla} p + \mu_f \nabla^2 \mathbf{u} - \rho_f g \mathbf{k} &= 0, \\ \boldsymbol{\nabla}.\mathbf{u} &= 0, \end{aligned} \tag{7.5}$$

where μ_f is the dynamic viscosity of the frozen soil, ρ_f is the density of the frozen soil, $\mathbf{u}$ is the velocity field, p is the pressure field, g is the acceleration due to gravity and $\mathbf{k}$ is the upwards pointing unit normal.

We non-dimensionalise equations 7.5 using the frost heave scales given in section 3.2.2 except that the pressure scale in the frozen soil is as follows

$$[p] = \frac{\mu_f [U]}{d} = \frac{\mu_f k \Delta T}{L \rho_w d^2},$$

where $[U]$ and d are frost heave velocity and length scales. Thus, the dimensionless forms of equations 7.5 are

$$\begin{aligned} -\boldsymbol{\nabla} p + \nabla^2 \mathbf{u} - \Pi \mathbf{k} &= 0, \\ \boldsymbol{\nabla}.\mathbf{u} &= 0, \end{aligned} \tag{7.6}$$

where the dimensionless parameter Π is given by

$$\Pi = \frac{\rho_f g d}{[p]} = \frac{L}{C_f \Delta T} \frac{g d^3}{\kappa_f \nu_f}, \tag{7.7}$$

where C_f is the specific heat capacity of the frozen soil, ν_f is its kinematic viscosity, μ_f/ρ_f, and κ_f is the thermal diffusivity given by

$$\kappa_f = \frac{k}{\rho_w C_f}. \tag{7.8}$$

Written in this way, the parameter Π is analogous to the Rayleigh number which occurs in convection type problems.

Typical values of the scales appearing in this dimensionless parameter are

$$\begin{aligned}
\rho_f &\sim 2 \times 10^3 \,\mathrm{kg\,m^{-3}} \\
\rho_w &\sim 1000 \,\mathrm{kg\,m^{-3}} \\
L &\sim 3.35 \times 10^5 \,\mathrm{J\,kg^{-1}} \\
k &\sim 4 \,\mathrm{W\,m^{-1}\,K^{-1}} \\
\Delta T &\sim 10 \,\mathrm{K} \\
d &\sim 10 \,\mathrm{m} \\
\mu_f &\sim 10^{14} \,\mathrm{Pa\,s} \\
g &\sim 10 \,\mathrm{m\,s^{-2}}
\end{aligned}$$

where the value of the viscosity is a representative value taken from the creep curves in Sayles (1988). In reality the viscosity of frozen soil is sensitive to temperature, stress conditions and soil type. Substituting these typical values into the parameter Π we get

$$\Pi \sim 1.$$

The parameter Π is proportional to d^3 and, as such, is sensitive to the length scale relevant to the problem. For example, if the length scale chosen was the characteristic length scale of a hummock, then $d \sim 1\,\mathrm{m}$ and $\Pi \sim 10^{-3}$.

For convenience we consider the two dimensional problem and introduce the stream function, ψ, which is defined up to an arbitrary constant by

$$\mathbf{u} = \left(\frac{\partial \psi}{\partial z}, -\frac{\partial \psi}{\partial x} \right). \tag{7.9}$$

In writing this, equation $(7.6)_2$ is automatically satisfied and, by taking the curl of equation $(7.6)_1$, we get

$$\nabla^4 \psi = 0, \tag{7.10}$$

(i.e. the biharmonic equation for the stream function, ψ). The pressure field is then given by equation $(7.6)_1$ in terms of the stream function ψ and the gravitational terms.

Boundary conditions are prescribed at each of the moving boundaries $z_s(\mathbf{x}, t)$ and $z_f(\mathbf{x}, t)$. Assuming there is no overburden, the boundary condition at $z_s(\mathbf{x}, t)$ will express the fact that there is no traction along this boundary. The components of the stress tensor in a viscous fluid, σ_{ij}, are given in a dimensionless form by

$$\sigma_{ij} = -p\delta_{ij} + \left(\frac{\partial u_i}{\partial x_j} + \frac{\partial u_j}{\partial x_i} \right). \tag{7.11}$$

The no traction condition at the surface $z_s(\mathbf{x}, t)$ may be written in terms of the stress tensor $\boldsymbol{\sigma}$ as follows

$$\begin{aligned} (\boldsymbol{\sigma}.\mathbf{n}_s).\mathbf{n}_s &= 0, \\ (\boldsymbol{\sigma}.\mathbf{n}_s).\mathbf{t}_s &= 0, \end{aligned} \tag{7.12}$$

where $\mathbf{n}_s$ and $\mathbf{t}_s$ are the normal and tangent to the surface z_s. Expressed in component terms, these conditions may be written as

$$\begin{aligned} \sigma_{11} {z_s'}^2 - 2\sigma_{21} z_s' + \sigma_{22} &= 0, \\ \sigma_{12}(1 - {z_s'}^2) + (\sigma_{22} - \sigma_{11}) z_s' &= 0, \end{aligned} \tag{7.13}$$

where again the prime denotes differentiation with respect to x. Using the constitutive viscous stress relation above, they may also be written in terms of the stream function in the following way:

$$\begin{aligned} -p(1 + {z_s'}^2) - 2\psi_{xz}(1 - {z_s'}^2) - 2(\psi_{zz} - \psi_{xx}) z_s' &= 0, \\ -4\psi_{xz} z_s' + (\psi_{zz} - \psi_{xx})(1 - {z_s'}^2) &= 0. \end{aligned} \tag{7.14}$$

At the boundary $z_f(\mathbf{x}, t)$, we have that the normal component of flux is equal to the flux, V_i, due to the heave. We suppose that the material beneath the lens front is

undeformable and consequently the final boundary condition is a 'no slip' condition. These conditions may be written as

$$\begin{aligned} \frac{w - z_f' u}{(1 + z_f'^{\,2})^{\frac{1}{2}}} &= V_i, \\ u + z_f' w &= 0, \end{aligned} \tag{7.15}$$

where $\mathbf{u} = (u, w)$. Writing these conditions in terms of the stream function we find, after some simplification, that

$$\begin{aligned} \psi_x &= -\frac{V_i}{(1 + z_f'^{\,2})^{\frac{1}{2}}}, \\ \psi_z &= -\frac{z_f'}{(1 + z_f'^{\,2})^{\frac{1}{2}}} V_i. \end{aligned} \tag{7.16}$$

Thus, the biharmonic equation 7.10 for ψ together with equation $(7.6)_1$ for the fluid pressure and boundary conditions 7.14 and 7.16 describe the situation in the frozen region. In the subsequent sections we consider this system together with the heave equations 7.1 to analyse the linear stability of the system to ascertain whether a potential instability exists which could explain the formation of patterned ground.

7.4 Linearised Problem

In the previous section we established a two dimensional model for the field frost heave problem with a viscous rheology for the frozen soil. In the one dimensional case, this system reduces to the situation described in chapter 4. In this section we perturb the two dimensional problem derived in the previous section about the solution to the one dimensional problem derived in chapter 4 to give a linearised two dimensional problem.

Collecting together the two dimensional problem we have

$$\begin{aligned} \nabla^4 \psi &= 0, \\ \nabla^2 T &= 0. \end{aligned} \tag{7.17}$$

Having solved for the stream function, ψ, the pressure term is then given by

$$\begin{aligned} p_x &= \nabla^2 \psi_z, \\ p_z &= -\nabla^2 \psi_x - \Pi. \end{aligned} \tag{7.18}$$

The boundary conditions for the problem are

at $z = z_s$

$$\begin{aligned} T &= T_s, \\ -p(1+{z'_s}^2) - 2\psi_{xz}(1-{z'_s}^2) - 2(\psi_{zz}-\psi_{xx})z'_s &= 0, \\ -4\psi_{xz}z'_s + (\psi_{zz}-\psi_{xx})(1-{z'_s}^2) &= 0, \end{aligned} \tag{7.19}$$

at $z = z_f$

$$\begin{aligned} T &= 0, \\ \psi_x &= -\frac{V_i}{(1+{z'_f}^2)^{\frac{1}{2}}}, \\ \psi_z &= -\frac{z'_f}{(1+{z'_f}^2)^{\frac{1}{2}}}V_i, \end{aligned} \tag{7.20}$$

where the ice flux at the lens front, V_i, and the frost penetration velocity are given by

$$\begin{aligned} V_f(\phi - W_m) &= V_i + \left.\frac{\partial T}{\partial n}\right|_{z_f}, \\ V_i &= \alpha_{fk}\left((W_l - W_m)V_f - \left.\frac{\partial T}{\partial n}\right|_{z_f}\right). \end{aligned} \tag{7.21}$$

Equations 7.21 can be written in the following slightly simpler form

$$\begin{aligned} V_f &= A\left.\frac{\partial T}{\partial n}\right|_{z_f}, \\ V_i &= -\alpha_{fk}BV_f, \end{aligned} \tag{7.22}$$

where the constants A and B are given by

$$\begin{aligned} A &= \frac{1-\alpha_{fk}}{\phi - W_m - \alpha_{fk}(W_l - W_m)}, \\ B &= \frac{\phi - W_l}{1-\alpha_{fk}}. \end{aligned} \tag{7.23}$$

(As discussed in chapter 4, a requirement for heave to proceed is that the heave parameter $\alpha_{fk} < 1$ and hence both A and B are greater than zero.)

Equations 7.17 and 7.22 together with the boundary conditions 7.19 and 7.20 prescribe the complete two dimensional problem. It is again worth checking that we

have the correct number of boundary conditions for the posed problem. We have a fourth order equation for the stream function, ψ, and a second order equation for the temperature, T. Thus, we require 6 boundary conditions, which agrees with the number given in 7.19 and 7.20. The flux at the lens front required by these boundary conditions is given by equation $(7.22)_2$ and the position of the moving boundary, z_f, is related to the normal velocity of the frozen front, V_f, by equation 7.3. Thus, to complete the problem, we need a kinematic condition for the displacement of the ground surface. By analogy with the derivation of equation 7.3 for the front position we have that, on $z = z_s$

$$0 = \frac{d}{dt}(z - z_s) = -\frac{\partial z_s}{\partial t} + (\mathbf{u}_s.\boldsymbol{\nabla})(z - z_s), \tag{7.24}$$

where $\mathbf{u}_s$ is the velocity of the ground surface which, since z_s is a material surface, is given by

$$\mathbf{u}_s = (\psi_z, -\psi_x), \tag{7.25}$$

evaluated at $z = z_s$, and $\frac{d}{dt}$ is the material derivative following z_s. Thus, expanding equation 7.24 gives the required additional relation

$$-\frac{\partial z_s}{\partial t} + \psi_z z_s' - \psi_x = 0. \tag{7.26}$$

We now linearise these equations around the one dimensional solution by writing

$$\begin{aligned} z_f(\mathbf{x}, t) &= \overline{z}_f(t) + \tilde{z}_f(\mathbf{x}, t) \qquad & z_s(\mathbf{x}, t) &= \overline{z}_s(t) + \tilde{z}_s(\mathbf{x}, t) \\ T &= \overline{T}(z) + \tilde{T} & \psi &= \overline{\psi}(x) + \tilde{\psi} \\ V_i &= \overline{V}_i + \tilde{V}_i & p &= \overline{p} + \tilde{p} \end{aligned}$$

where the variables with the overbars are the solution to the one dimensional problem and the variables with the tildes are the perturbations around this solution. At least initially, we ignore the effect of the perturbation on the heave rate through the change in effective stress at the lens front. Consequently we are assuming that the change in the heave parameter is small compared to the thermal and gravitational effects in the frozen soil and, in effect, we are assuming that the thermal régime will lead to an instability in the system and that this will be regulated by gravity acting on the viscous frozen soil. This gravitational regulation is similar to that which occurs in the relaxation of a viscous fluid film and, in fact, if we assume that the heave and frost penetration rates are zero, the problem reduces exactly to that situation.

The one dimensional solution satisfies the following set of equations

$$\begin{aligned}
\dot{\overline{z}}_f(\phi - W_m) &= \dot{\overline{z}}_s + \left.\frac{\partial \overline{T}}{\partial z}\right|_{\overline{z}_f}, \\
\dot{\overline{z}}_s &= \alpha_{fk}\left((W_l - W_m)\dot{\overline{z}}_f - \left.\frac{\partial \overline{T}}{\partial z}\right|_{\overline{z}_f}\right), \\
\frac{\partial \overline{T}}{\partial z} &= \frac{T_s}{\overline{z}_s - \overline{z}_f}, \\
\overline{\psi}(x) &= -\dot{\overline{z}}_s x, \\
\overline{V}_i &= \dot{\overline{z}}_s. \\
\overline{p} &= \Pi(\overline{z}_s - z).
\end{aligned} \tag{7.27}$$

The normal derivative term at the lens front can be written as

$$\frac{\partial}{\partial n} = \mathbf{n}.\boldsymbol{\nabla} = \frac{1}{(1 + {z'_f}^2)^{\frac{1}{2}}}\left(\frac{\partial}{\partial z} - z'_f \frac{\partial}{\partial x}\right), \tag{7.28}$$

and from section 7.2 the frozen front velocity can be written as

$$V_f = \frac{1}{(1 + {z'_f}^2)^{\frac{1}{2}}}\frac{\partial z_f}{\partial t}. \tag{7.29}$$

The procedure adopted in linearising equations 7.17, 7.18 and 7.22 and the boundary conditions 7.19 and 7.20 is as follows. If a function $\eta = \overline{\eta} + \tilde{\eta}$ is zero on a boundary $z = \overline{z} + \tilde{z}$ then

$$\begin{aligned}
0 = \eta(z) &= \overline{\eta}(z) + \tilde{\eta}(z), \\
&\approx \left.\frac{\partial \overline{\eta}}{\partial z}\right|_{\overline{z}} \tilde{z} + \tilde{\eta}(\overline{z}) + \cdots.
\end{aligned} \tag{7.30}$$

Using the procedure given by relation 7.30, together with the solution to the one dimensional problem given by equations 7.27 and the relationships given by equations 7.28 and 7.29, the linearised versions of equations 7.17 and the associated equations and boundary conditions become

$$\begin{aligned}
\nabla^4 \tilde{\psi} &= 0, \\
\nabla^2 \tilde{T} &= 0.
\end{aligned} \tag{7.31}$$

From the solution for the stream function, ψ, the pressure is given by

$$\begin{aligned}
\tilde{p}_x &= \nabla^2 \tilde{\psi}_z, \\
\tilde{p}_z &= -\nabla^2 \tilde{\psi}_x.
\end{aligned} \tag{7.32}$$

The boundary conditions are

at $z = \overline{z}_s$

$$\begin{aligned} \tilde{T} &= -\left.\frac{\partial \overline{T}}{\partial z}\right|_{\overline{z}_s} \tilde{z}_s, \\ \Pi \tilde{z}_s - \tilde{p} - 2\tilde{\psi}_{xz} &= 0, \\ (\tilde{\psi}_{zz} - \tilde{\psi}_{xx}) &= 0, \end{aligned} \tag{7.33}$$

at $z = \overline{z}_f$

$$\begin{aligned} \tilde{T} &= -\left.\frac{\partial \overline{T}}{\partial z}\right|_{\overline{z}_f} \tilde{z}_f, \\ \tilde{\psi}_x &= -\tilde{V}_i, \\ \tilde{\psi}_z &= -\tilde{z}'_f \dot{\overline{z}}_s, \end{aligned} \tag{7.34}$$

and the equations for the frost penetration depth and flux at the lens front may be written as

$$\begin{aligned} \frac{\partial \tilde{z}_f}{\partial t} &= A \left.\frac{\partial \tilde{T}}{\partial z}\right|_{\overline{z}_f}, \\ \tilde{V}_i &= -\alpha_{fk} B \frac{\partial \tilde{z}_f}{\partial t}. \end{aligned} \tag{7.35}$$

To complete the problem we need to relate the perturbation to the velocity of the ground surface to the perturbation of its position. We have from equation 7.26 that

$$-\frac{\partial z_s}{\partial t} + \psi_z z'_s - \psi_x = 0. \tag{7.36}$$

Using similar arguments to those used above in obtaining the linearised frost heave problem, it is relatively straightforward to show that the perturbations satisfy

$$\frac{\partial \tilde{z}_s}{\partial t} = -\left.\tilde{\psi}_x\right|_{\overline{z}_s}. \tag{7.37}$$

7.5 Linear Stability Analysis

In the preceding section the two dimensional frost heave problem was linearised about the one dimensional time dependent solution. The purpose of this linearisation is to apply some form of quasi-static linear stability analysis to the two dimensional problem to ascertain whether the secondary frost heave model derived in chapter 2 has

an instability which could explain the onset of patterned ground. The problem with the direct application of a linear stability analysis is that the basic one dimensional state is time dependent and therefore the usual separation of variables technique cannot be applied. However, if we assume that the time scale for the onset of the instability is very much smaller than the $O(1)$ frost heave time scale, then we may treat the one dimensional frost heave problem as quasi-static. This assumption may not be realistic, particularly when considering the neutral stability case.

A similar problem arises when considering the linear stability of an alloy solidification problem and a similar approach has been adopted there (see Emms (1992)). Similarly, Robinson (1976) adopts this methodology when considering the stability of a hot thermal boundary layer on the surface beneath a cold fluid. Thus, in the absence of any other suitable method for analysing the stability of a system with a time dependent basic state we adopt the quasi-static assumption.

Without loss of generality, we use the quasi-static assumption to write

$$\begin{aligned} \overline{z}_s &= 1, \\ \overline{z}_f &= 0, \\ T_s &= -1. \end{aligned} \tag{7.38}$$

The quasi-steady heave rate is then given by $\dot{\overline{z}}_s = \overline{V}_i = \alpha_{fk} AB$.

We now look for separable solutions of the form

$$\begin{aligned} \tilde{\psi} &= h(z,t)e^{ikx} & \tilde{T} &= g(z,t)e^{ikx} \\ \tilde{z}_s &= s(t)e^{ikx} & \tilde{z}_f &= f(t)e^{ikx} \\ \tilde{V}_i &= v(t)e^{ikx}, & \tilde{p} &= \Phi(z,t)e^{ikx} \end{aligned}$$

for each k, where k is the wave number.

Substituting these equations into the linearised problem given by equations 7.31 and 7.32 and boundary conditions 7.33, 7.34, 7.35 and 7.37, the linearised system becomes

$$\begin{aligned} h'''' - 2k^2 h'' + k^4 h &= 0, \\ g'' - k^2 g &= 0, \end{aligned} \tag{7.39}$$

where the prime now denotes differentiation with respect to z. By direct integration,

the solution to the pressure field is given by

$$ik\Phi = (h'' - k^2 h)'. \tag{7.40}$$

The boundary conditions may be written as:
at $z = 0$

$$\begin{aligned} v &= -\alpha_{fk} B \dot{f}, \\ g' &= \frac{\dot{f}}{A}, \\ g &= f(t), \\ h &= -\frac{v(t)}{ik}, \\ h' &= -\alpha_{fk} ABikf(t) \end{aligned} \tag{7.41}$$

at $z = 1$

$$\begin{aligned} h &= -\frac{\dot{s}}{ik}, \\ (h'' - 3k^2 h)' &= i\Pi k s(t), \\ h'' + k^2 h &= 0, \\ g &= s(t), \end{aligned} \tag{7.42}$$

where the overdots refer to the time derivatives. In obtaining this form of the boundary conditions, we have used equation 7.40 to eliminate the pressure term.

Equations 7.39 have general solutions of the form

$$\begin{aligned} h &= ae^{kz} + be^{-kz} + cze^{kz} + dze^{-kz}, \\ g &= me^{kz} + ne^{-kz}, \end{aligned} \tag{7.43}$$

where the time dependent constants a, b, c, d, m and n can be found from the six boundary conditions 7.41 and 7.42. Applying these boundary conditions gives the following algebraic relations for these constants

$$\begin{aligned} ae^k - be^{-k} + ce^k - de^{-k} &= -\frac{i\Pi s}{2k^2}, \\ ake^k + bke^{-k} + c(k+1)e^k + d(k-1)e^{-k} &= 0, \\ ak - bk + c + d &= -\alpha_{fk} ABikf(t), \\ a + b &= -\frac{v(t)}{ik}, \\ me^k + ne^{-k} &= s(t), \\ m + n &= f(t), \end{aligned} \tag{7.44}$$

from which we find that

$$
\begin{aligned}
a &= \frac{-i\left(4\alpha_{fk}ABe^{2k}fk^4 + \Pi s e^k(1+e^{2k}-k+e^{2k}k) - 2kv(1+e^{2k}+2e^{2k}k+2e^{2k}k^2)\right)}{2k^2\left(1+2e^{2k}+e^{4k}+4e^{2k}k^2\right)},\\
b &= \frac{ie^k\left(4\alpha_{fk}ABe^{k}fk^4 + \Pi s(1+e^{2k}-k+e^{2k}k) + 2e^k kv(1+e^{2k}-2k+2k^2)\right)}{2k^2\left(1+2e^{2k}+e^{4k}+4e^{2k}k^2\right)},\\
c &= \frac{-i\left(2\alpha_{fk}ABfk^2(1+e^{2k}-2e^{2k}k) - e^k\Pi s(1+e^{2k}-2k) + 2kv(1+e^{2k}+2e^{2k}k)\right)}{2k\left(1+2e^{2k}+e^{4k}+4e^{2k}k^2\right)},\\
d &= \frac{ie^k\left(-2\alpha_{fk}ABe^{k}fk^2(1+e^{2k}+2k) + \Pi s(1+e^{2k}+2e^{2k}k) + 2e^k kv(1+e^{2k}-2k\right)}{2k\left(1+2e^{2k}+e^{4k}+4e^{2k}k^2\right)},\\
m &= \frac{s-fe^{-k}}{e^k-e^{-k}},\\
n &= \frac{fe^k-s}{e^k-e^{-k}}.
\end{aligned}
\tag{7.45}
$$

Equations $(7.41)_{1,2}$ and $(7.42)_1$ for the frozen front position, the flux at the lens front and the heave can be written as

$$
\begin{aligned}
\dot{f} &= Ak(m-n),\\
v &= -\alpha_{fk}B\dot{f},\\
\dot{s} &= -ik(ae^k + be^{-k} + ce^k + de^{-k}).
\end{aligned}
\tag{7.46}
$$

Substituting the expressions for the constants given by 7.45 and eliminating the flux, v, we get, for each k, two first order equations for s and f as follows

$$
\begin{aligned}
\dot{f} &= Ak\,\frac{(s-f\cosh k)}{\sinh k},\\
\dot{s} &= -\alpha_{fk}ABf\frac{k^2\cosh k}{\cosh^2 k+k^2} - \alpha_{fk}B\dot{f}\frac{\cosh k + k\sinh k}{\cosh^2 k+k^2}\\
&\quad -\frac{\Pi}{2}\,s\,\frac{(\cosh k\sinh k - k)}{k(\cosh^2 k+k^2)}.
\end{aligned}
\tag{7.47}
$$

Equations 7.47 can be rearranged to give a second order differential equation for $f(t)$ as follows

$$
\begin{aligned}
&\ddot{f}\,\frac{\sinh k}{Ak} + \dot{f}\left(\cosh k + \alpha_{fk}B\frac{\cosh k + k\sinh k}{\cosh^2 k+k^2} + \frac{\Pi}{2}\frac{(\cosh k\sinh k - k)\sinh k}{Ak^2(\cosh^2 k+k^2)}\right)\\
&+f\left(\alpha_{fk}AB\frac{k^2\cosh k}{\cosh^2 k+k^2} + \frac{\Pi}{2}\frac{(\cosh k\sinh k - k)\cosh k}{k(\cosh^2 k+k^2)}\right) = 0.
\end{aligned}
\tag{7.48}
$$

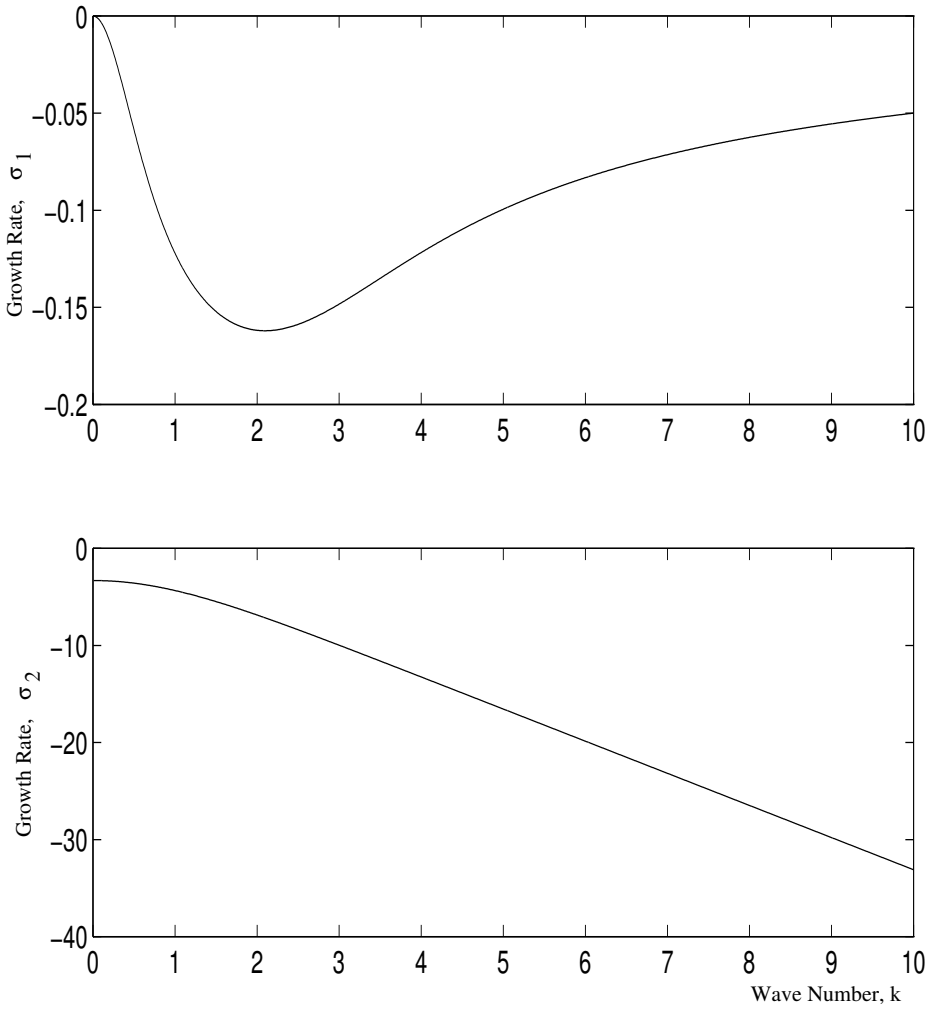


Figure 7.3: Plots of the dispersion relation with a heave parameter of $\alpha_{fk} = 10^{-2}$ and $\Pi = 1$.

Now, looking for solutions of the form $f = e^{\sigma t}$, we get the following dispersion relation for the linearised system

$$\sigma^2 \frac{\sinh k}{Ak} + \sigma \left(\cosh k + \alpha_{fk} B \frac{\cosh k + k \sinh k}{\cosh^2 k + k^2} + \frac{\Pi}{2} \frac{(\cosh k \sinh k - k) \sinh k}{Ak^2(\cosh^2 k + k^2)} \right)$$
$$+ \alpha_{fk} AB \frac{k^2 \cosh k}{\cosh^2 k + k^2} + \frac{\Pi}{2} \frac{(\cosh k \sinh k - k) \cosh k}{k(\cosh^2 k + k^2)} = 0. \tag{7.49}$$

For each wave number, k, this dispersion relation will have two roots for the growth term, σ. Plots of these growth rates as a function of the wave number k are shown in figure 7.3 for a heave parameter $\alpha_{fk} = 10^{-2}$ and $\Pi = 1$. For the remaining variables in the problem we have used $\phi = 0.4$, $W_l = 0.2$, $W_m = 0.1$ and, with these values, $A \approx 3.3$ and $B \approx 0.2$. For the range of parameter values taken here, the growth rates σ_1 and σ_2 are negative for all values of k indicating that the situation is stable.

The dispersion relation 7.49 is discussed further in the next section. However, before proceeding, it is worth considering whether this dispersion relation reduces to the case of the stability of a viscous film when the frost penetration rate and ice flux are both zero. This serves as a useful check on the above analysis and also illustrates an interesting phenomenon for large wave numbers which is also present when heave and frozen front perturbation are included in the dispersion relation. The viscous film problem can most easily be considered by putting $\alpha_{fk} = A = B = 0$ which allows us to write equation 7.49 as

$$\sigma^2 + \sigma \frac{\Pi}{2} \frac{(\cosh k \sinh k - k)}{k(\cosh^2 k + k^2)} = 0, \tag{7.50}$$

from which the solutions are given by

$$\begin{aligned} \sigma &= 0, \\ \sigma &= -\frac{\Pi}{2} \frac{(\cosh k \sinh k - k)}{k(\cosh^2 k + k^2)}. \end{aligned} \tag{7.51}$$

It can be seen from equations 7.22 and 7.47 that the first of these solutions corresponds to $\dot{f} = 0$ (with $V_f = V_i = 0$) and merely reflects the fact that z_s and z_f can take arbitrary fixed values where the neutral mode corresponding to $\sigma = 0$ consists of increasing z_f. We refer to this solution as the 'thermally neutral mode'. The second solution corresponds to the gravity driven relaxation of the ground surface perturbation and we refer to this as the 'gravity mode'. Figure 7.4 is a plot of the dispersion relation which arises from the gravity mode for $\Pi = 1$. It can be seen that the growth rate is always negative and hence the motion of the viscous layer is always stable. One interesting point to note is that as the wave number $k \to \infty$ the growth rate $\sigma \to 0$ (i.e. the system becomes neutrally stable). Essentially this observation implies that the shorter the wavelength of the perturbation, the longer it takes for the relaxation back to equilibrium.

The analysis of thin viscous film (see Acheson (1990)) assumes that the height of the viscous film is small compared to the horizontal length scale of its variation. In our theory, this is equivalent to assuming that the wavelength of the perturbation is large or, similarly, that the wave number, k, is small. Equation $(7.51)_2$ may be written as

$$\sigma = -\frac{\Pi}{4} \frac{(\sinh 2k - 2k)}{k(\cosh^2 k + k^2)}, \tag{7.52}$$

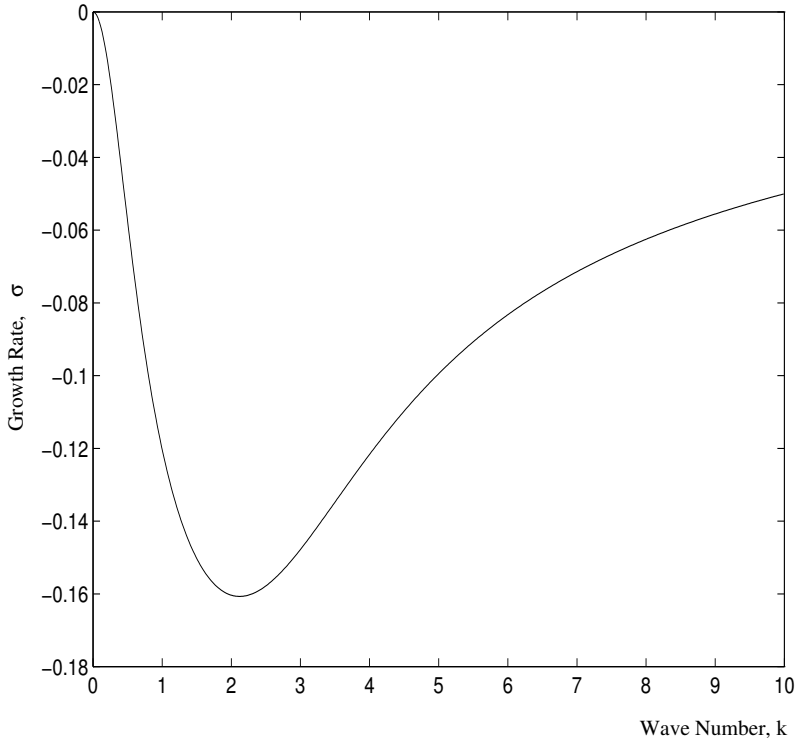


Figure 7.4: Plot of the dispersion relation for a viscous drop relaxing due to the effects of gravity.

which to leading order for small k is simply

$$\sigma = -\frac{\Pi}{4}\frac{(2k)^3}{3!k} = -\frac{\Pi k^2}{3}. \tag{7.53}$$

This relation can be shown to be equivalent to the dispersion relation for the relaxation of a thin viscous film.

Thus, our problem reduces to the more familiar problem of the relaxation of a viscous film and serves as a useful check on our analysis. This comparison has also revealed other interesting consequences about the stability of our problem. First, the two solutions to the dispersion relation correspond to a thermal mode and a gravity driven mode and secondly that the gravity mode may become neutrally stable at high wave numbers.

7.6 Analysis of the Dispersion Relation

In this section we analyse the dispersion relation 7.49 to consider whether there exists a parameter region (α_{fk}, Π) for which the the system becomes linearly unstable (i.e. $\sigma > 0$).

We write the dispersion relation 7.49 as

$$\sigma^2 + p(k)\sigma + q(k) = 0 \tag{7.54}$$

where

$$\begin{aligned} p(k) &= \frac{Ak}{\sinh k}\left(\cosh k + \alpha_{fk}B\frac{\cosh k + k\sinh k}{\cosh^2 k + k^2} + \frac{\Pi}{2}\frac{(\cosh k \sinh k - k)\sinh k}{Ak^2(\cosh^2 k + k^2)}\right), \\ q(k) &= \frac{Ak}{\sinh k}\left(\alpha_{fk}AB\frac{k^2\cosh k}{\cosh^2 k + k^2} + \frac{\Pi}{2}\frac{(\cosh k \sinh k - k)\cosh k}{k(\cosh^2 k + k^2)}\right). \end{aligned} \tag{7.55}$$

The first point to note about the coefficients $p(k)$ and $q(k)$ is that they are positive for all physically relevant parameter values (i.e. $A > 0$ and $\Pi > 0$). As such, the real part of the growth rate values must be negative for all physically relevant parameter values and hence the problem is always stable.

The solution presented in figure 7.3 suggests that neutrally stable states are possible at $k = 0$ and $k = \infty$. In order to consider the behaviour of the growth rates around these neutral states, we consider the asymptotic solutions to the dispersion relation for small and large values of the wave number, k.

At large wave numbers, the leading order behaviour of the coefficients $p(k)$ and $q(k)$ is as follows

$$\begin{aligned} p(k) &\sim Ak, \\ q(k) &\sim \frac{A\Pi}{2}. \end{aligned} \tag{7.56}$$

Thus, the leading order solutions to the quadratic dispersion relation are

$$\begin{aligned} \sigma &= -Ak, \\ \sigma &= -\frac{\Pi}{2k}. \end{aligned} \tag{7.57}$$

These growth rates correspond to those that arise from the system

$$\begin{aligned} \dot{f} &= -Akf, \\ \dot{s} &= -\frac{\Pi}{2k}s, \end{aligned} \tag{7.58}$$

which is the consistent leading order solution to equations 7.47. Thus, the first of these growth rates can be seen to correspond to the thermal mode while the second corresponds to the gravity mode. .

For small wave numbers it is again instructive to consider the leading order behaviour of the coefficients of the dispersion relation 7.54. At small wave numbers the expansion of the coefficients $p(k)$ and $q(k)$ up to terms of $O(k^2)$ are as follows

$$\begin{aligned} p(k) &\sim A(1+\alpha_{fk}B) + \left(\frac{1}{3} - \frac{2}{3}\alpha_{fk}B + \frac{\Pi}{3A}\right)k^2, \\ q(k) &\sim A\left(\frac{\Pi}{3} + \alpha_{fk}AB\right)k^2. \end{aligned} \tag{7.59}$$

Thus, the behaviour of the growth rates for small wave numbers is as follows

$$\begin{aligned} \sigma &= -A(1+\alpha_{fk}B) - \frac{\left(A - \alpha_{fk}AB\left(\frac{4}{3} + \frac{2\alpha_{fk}B}{3}\right) + \frac{\alpha_{fk}B\Pi}{3}\right)}{(1+\alpha_{fk}B)}k^2, \\ \sigma &= -\frac{\left(\frac{\Pi}{3} + \alpha_{fk}AB\right)}{(1+\alpha_{fk}B)}k^2. \end{aligned} \tag{7.60}$$

Again, the first of these growth rates corresponds to the thermal mode while the second is the gravity mode.

Finally, from the form of the coefficients of the quadratic dispersion relation, it is relatively straightforward to see that the growth rates must be continuous functions of wave number except possibly at $k = 0$ (the situation at $k = 0$ was considered above and growth rates were shown to be 'well behaved' at this point). Thus, we expect that for the parameter values considered, the of the growth rates will behave in a similar manner to the solutions given in figure 7.3 for all physically relevant parameter values. Hence, the model developed in section 7.4 does not appear to contain any mechanism for an instability and hence cannot explain the formation of patterned ground.

7.7 Change in Effective Stress

One of the assumptions made in obtaining the linearised problem was that the change in effective stress which resulted from the perturbation was small compared to the thermal and gravitational effects in the frozen soil and could be neglected. In this section we revisit this assumption and include the perturbation in effective stress to see if this can give rise to some form of instability.

A small perturbation about the one dimensional solution will result in a small change in the effective stress, N, at the frozen front and consequently a small change in the water content, W_l, at the lens front. These effects enter the linearised system

derived in section 7.4 through the perturbations in α_{fk}, A and B in equations 7.22. Thus, for this problem, equations 7.35 become

$$\begin{aligned}
\frac{\partial \tilde{z}_f}{\partial t} &= \overline{A}\left.\frac{\partial \tilde{T}}{\partial z}\right|_{\overline{z}_f} + \tilde{A}\left.\frac{\partial \overline{T}}{\partial z}\right|_{\overline{z}_f}, \\
\tilde{V}_i &= -\overline{\alpha}_{fk}\overline{B}\frac{\partial \tilde{z}_f}{\partial t} - (\tilde{\alpha}_{fk}\overline{B} + \tilde{B}\overline{\alpha}_{fk})\frac{\partial \overline{z}_f}{\partial t}.
\end{aligned} \tag{7.61}$$

where A and B are given by

$$\begin{aligned}
A &= \frac{1-\alpha_{fk}}{\phi - W_m - \alpha_{fk}(W_l - W_m)}, \\
B &= \frac{\phi - W_l}{1-\alpha_{fk}}.
\end{aligned} \tag{7.62}$$

From chapter 4, the Gilpin heaving parameter is given by

$$\alpha_{fk} = \frac{(\beta_{fk} + \delta_3(\phi - W_l))}{(1+\beta_{fk})}, \tag{7.63}$$

where

$$\beta_{fk} = -\frac{\gamma L^2 \rho_w k_0}{T_0 g k}\left(\frac{W_l}{\phi}\right)^{\gamma}\left(\frac{(f(W_l)-N)}{\delta\gamma(f(W_l)-N) + W_l f'(W_l)}\right). \tag{7.64}$$

A small perturbation in W_l will result in a much larger change in the heave parameter α_{fk} because of the large exponent γ occurring in the parameter β_{fk}. Therefore, for the purpose of the subsequent analysis, we only consider the perturbation which arises in α_{fk} (or, more accurately, the exponential term in β_{fk}). Specifically, we write

$$\tilde{\alpha}_{fk} = \frac{\overline{\beta}_{fk}(1-\overline{\alpha}_{fk})}{1+\overline{\beta}_{fk}}\ \frac{\gamma \tilde{W}_l}{\overline{W}_l}, \tag{7.65}$$

where $\tilde{W}_l$ is the perturbation in the water content at the lens front. Based on these assumptions the terms $\overline{A}$, $\tilde{A}$, $\overline{B}$ and $\tilde{B}$ in equations 7.61 are given by

$$\begin{aligned}
\overline{A} &= \frac{1-\overline{\alpha}_{fk}}{\phi - W_m - \overline{\alpha}_{fk}(\overline{W}_l - W_m)}, \\
\tilde{A} &= -\frac{\overline{A}^2(\phi - \overline{W}_l)}{(1-\overline{\alpha}_{fk})^2}\tilde{\alpha}_{fk}, \\
\overline{B} &= \frac{\phi - \overline{W}_l}{1-\overline{\alpha}_{fk}}, \\
\tilde{B} &= \frac{\overline{B}}{(1-\overline{\alpha}_{fk})}\tilde{\alpha}_{fk}.
\end{aligned} \tag{7.66}$$

From equations 7.27 the quasi-static heave rate and the temperature gradient in the frozen soil are given by

$$\begin{aligned} \dot{\overline{z}}_f &= -\overline{A}, \\ \left.\frac{\partial \overline{T}}{\partial z}\right|_{\overline{z}_f} &= -1, \end{aligned} \tag{7.67}$$

where again, without loss of generality, we have assumed that the quasi-static solution is given by 7.38.

The perturbation in the water content is related to the perturbation in the effective stress through equations 7.4. If we assume that the effective stress at the lens front is much less than the critical effective stress at which the lens front stops advancing, then the water content, W_l, is given by the leading order behaviour of equation $(7.4)_1$, i.e.

$$g(W_l) = N. \tag{7.68}$$

Thus, we get

$$g(\overline{W}_l) + g'(\overline{W}_l)\tilde{W}_l = \overline{N} + \tilde{N}, \tag{7.69}$$

and hence

$$\tilde{W}_l = \frac{\tilde{N}}{g'(\overline{W}_l)}. \tag{7.70}$$

In most usual physical situations in which stability is an issue, we would expect the heave parameter $\overline{\alpha}_{fk}$ to be small. If we adopt this assumption, then substituting the perturbations in A, B, α_{fk} and W_l into equations 7.61 we get

$$\begin{aligned} \frac{\partial \tilde{z}_f}{\partial t} &= \overline{A}\left.\frac{\partial \tilde{T}}{\partial z}\right|_{\overline{z}_f} - \mathcal{C}\tilde{N}, \\ \tilde{V}_i &= -\overline{\alpha}_{fk}\overline{B}\frac{\partial \tilde{z}_f}{\partial t} - \mathcal{B}\tilde{N}, \end{aligned} \tag{7.71}$$

where the positive parameters $\mathcal{C}$ and $\mathcal{B}$ are given by

$$\begin{aligned} \mathcal{C} &= -\frac{\overline{\beta}_{fk}\gamma\overline{A}^2(\phi - \overline{W}_l)}{g'(\overline{W}_l)\overline{W}_l}, \\ \mathcal{B} &= -\frac{\overline{\beta}_{fk}\gamma\overline{A}\,\overline{B}}{g'(\overline{W}_l)\overline{W}_l}. \end{aligned} \tag{7.72}$$

where $\overline{A} = (\phi - W_m)^{-1}$ and $\overline{B} = (\phi - W_l)$ (i.e $\overline{A}\,\overline{B} \approx 1$).

We now need to determine the perturbation in the effective stress $\tilde{N}$, which is calculated as the difference in perturbation in overburden at the lens front and the perturbation in the water pressure beneath the frozen fringe. The perturbation in the overburden actually means the perturbation in the ice pressure at the lens front because this is how the overburden enters the frost heave equations (see boundary condition $(3.13)_2$). In the three dimensional problem, it would seem reasonable that this boundary condition should equate the normal component of stress in the viscous frozen soil and the frozen fringe at their interface. Thus, writing the normal component of ice stress as P_{in}, this boundary condition becomes

$$P_{in} = -(\boldsymbol{\sigma}.\mathbf{n}).\mathbf{n}. \tag{7.73}$$

where $\mathbf{n}$ is the upwards pointing normal at z_f.

In writing equation 7.73, we are allowing the stress ice phase (including the interstitial ice) to be anisotropic . However, the model developed in chapter 2 assumed that, on length scales much larger than the pore size, the ice stress in the frozen fringe is isotropic[2]. The assumption that the interstitial ice stress is isotropic allowed a simpler formulation of the fringe equations and, in particular, allowed the use of a capillary suction function to express the difference between the ice and water pressures. The extension of this result to a three dimensional anisotropically stressed pore ice phase is beyond the scope of this thesis and for the work presented here we will assume that any macroscopic deviatoric stress within the pore ice causes the pore ice to rapidly relax, by a process of creep, to a state where the deviatoric stress is zero.

The derivation of the linearised version of boundary condition 7.73 is similar to the derivation of the linearised normal stress boundary condition$(7.33)_2$ at the stress free ground surface. The perturbed boundary condition, on $z = \overline{z}_f = 0$, is

$$-\tilde{P}_{in} = \Pi\tilde{z}_f - \tilde{p} - 2\tilde{\psi}_{xz}. \tag{7.74}$$

Writing $\tilde{P}_{in} = P^0_{in}e^{ikx}$ and substituting the expressions previously established for $\tilde{z}_f$, $\tilde{p}$ and $\tilde{\psi}$, this boundary condition may be written as

$$-P^0_{in} = \Pi f - \frac{1}{ik}(h'' - 3k^2h)'. \tag{7.75}$$

[2]On a microscopic (e.g. the pore size) length scale, the stress in the pore ice may be anisotropic as the ice regelates around the soil particles.

Substituting the expressions for h given by equation 7.43 we get

$$-P_{in}^0 = -2ik^2(a-b) + \Pi f, \tag{7.76}$$

where the constants a and b are given by equations 7.45. Substitution of these constants gives

$$-P_{in}^0 = \Pi f - \frac{(2\overline{\alpha}_{fk}\overline{A}\,\overline{B}k^4 f + \Pi s(\cosh k + k\sinh k) + kv(\sinh 2k - 2k))}{\cosh^2 k + k^2}. \tag{7.77}$$

The perturbation in the water pressure comes from the solution to the ground water flow equations. Assuming an incompressible soil matrix, the water flux is given by Darcy's law as

$$\mathbf{U}_w = -\beta\left(\boldsymbol{\nabla} p_w + \delta_2 \mathbf{k}\right), \tag{7.78}$$

where $\mathbf{U}_w$ is the water flux, $\mathbf{k}$ is the upward pointing unit normal and β and δ_2 are parameters described in section 3.2.2.

Taking the divergence of equation 7.78 and using the conservation of mass relation $\boldsymbol{\nabla}.\mathbf{U}_w = 0$, we get

$$\nabla^2 p_w = 0. \tag{7.79}$$

Linearising this equation by writing $p_w = \overline{p}_w + \tilde{p}_w$ then gives

$$\nabla^2 \tilde{p}_w = 0. \tag{7.80}$$

Again, looking for separable solutions of the form

$$\tilde{p}_w = q(z,t)e^{ikx}$$

for each wave number k, we find that $q(z,t)$ satisfies

$$q'' - k^2 q = 0 \tag{7.81}$$

which has a general solution of the form

$$q = K_1 e^{kz} + K_2 e^{-kz}. \tag{7.82}$$

Choosing the water pressure to be bounded as $z \to -\infty$ gives $K_2 = 0$ and then the constant K_1 is found from a knowledge of the water flux at the freezing front. Thus, from equation 7.78 we have that at the freezing front $\overline{z}_f = 0$

$$-\beta\frac{\partial \tilde{p}_w}{\partial z} = \tilde{U}_{wn} = \tilde{V}_i, \tag{7.83}$$

where $\tilde{U}_{wn}$ is the perturbation to the normal component of water flux at the freezing front. The perturbation to the water pressure at the freezing front can then be expressed as

$$\tilde{p}_w|_{\overline{z}_f} = -\frac{\tilde{V}_i}{\beta k} = -\frac{v(t)e^{ikx}}{\beta k} \tag{7.84}$$

where k is the wave number. The perturbation in the effective stress is given by

$$\tilde{N} = \tilde{P}_{in} - \tilde{p}_w; \tag{7.85}$$

writing $\tilde{N} = N_0 e^{ikx}$ we get that

$$N_0 = -\Pi f + \frac{(2\overline{\alpha}_{fk}\overline{A}\,\overline{B}k^4 f + \Pi s(\cosh k + k\sinh k) + kv(\sinh 2k - 2k))}{\cosh^2 k + k^2} + \frac{v}{\beta k}. \tag{7.86}$$

Substituting equation 7.86 into equation $(7.71)_2$ we get the following expression for the ice flux, v, at the lens front

$$\begin{aligned}\left(1 + \mathcal{B}\left(\frac{k(\sinh 2k - 2k)}{\cosh^2 k + k^2} + \frac{1}{\beta k}\right)\right) v = -\overline{\alpha}_{fk}\overline{B}\dot{f} \\ -\mathcal{B}\left(-\Pi f + \frac{2\overline{\alpha}_{fk}\overline{A}\,\overline{B}k^4 f}{\cosh^2 k + k^2} + \Pi s\frac{\cosh k + k\sinh k}{\cosh^2 k + k^2}\right).\end{aligned} \tag{7.87}$$

For this problem, the resulting linear system of ordinary differential equations that is analogous to equations 7.47 is as follows:

$$\begin{aligned}\dot{f} &= \overline{A}k\,\frac{(s - f\cosh k)}{\sinh k} \\ &\quad -\mathcal{C}\left(-\Pi f + \frac{2\overline{\alpha}_{fk}\overline{A}\,\overline{B}k^4 f}{\cosh^2 k + k^2} + \Pi s\frac{\cosh k + k\sinh k}{\cosh^2 k + k^2} + \left(\frac{k(\sinh 2k - 2k)}{\cosh^2 k + k^2} + \frac{1}{\beta k}\right) v\right), \\ \dot{s} &= -\overline{\alpha}_{fk}\overline{A}\,\overline{B}f\frac{k^2\cosh k}{\cosh^2 k + k^2} + v\frac{\cosh k + k\sinh k}{\cosh^2 k + k^2} - \frac{\Pi}{2}\,s\,\frac{(\cosh k\sinh k - k)}{k(\cosh^2 k + k^2)},\end{aligned} \tag{7.88}$$

where the flux v is given by equation 7.87.

We now need to consider whether the system given by equations 7.88 can be unstable for any soil types. We first consider the situation where $\mathcal{C} \ll 1$. From inspection of the prescription of this constant (see equation $(7.72)_1$), this condition corresponds to $\gamma\overline{\beta}_{fk} \ll 1$ which would be typical of fine silt or clay soil types. Thus, putting $\mathcal{C} = 0$ and again looking for solutions in terms of $e^{\sigma t}$, we can obtain a quadratic dispersion relation between the growth rate σ and the wave number k. However, we proceed to show that the coefficients of the quadratic dispersion relation are all positive and hence for these soil types the problem is always stable.

Using $(7.88)_1$ to eliminate s from equations $(7.88)_2$ and 7.87 we get

$$\ddot{f}\frac{\sinh k}{\overline{A}k}+\dot{f}\left(\cosh k+\frac{\Pi}{2}\frac{(\cosh k\sinh k-k)\sinh k}{\overline{A}k^2(\cosh^2 k+k^2)}\right)+f\left(\overline{\alpha}_{fk}\overline{A}\,\overline{B}\frac{k^2\cosh k}{\cosh^2 k+k^2}\right.$$
$$\left.+\frac{\Pi}{2}\frac{(\cosh k\sinh k-k)\cosh k}{k(\cosh^2 k+k^2)}\right)=v\frac{\cosh k+k\sinh k}{\cosh^2 k+k^2}, \tag{7.89}$$

where the water flux v is given by

$$\left(1+\mathcal{B}\left(\frac{k(\sinh 2k-2k)}{\cosh^2 k+k^2}+\frac{1}{\beta k}\right)\right)v=-\overline{\alpha}_{fk}\overline{B}\dot{f}$$
$$-\mathcal{B}\left(\Pi\dot{f}\left(\frac{\sinh k}{\overline{A}k}\right)\frac{\cosh k+k\sinh k}{\cosh^2 k+k^2}+\Pi f\frac{k}{2}\frac{(\sinh 2k-2k)}{\cosh^2 k+k^2}+\frac{2\overline{\alpha}_{fk}\overline{A}\,\overline{B}k^4 f}{\cosh^2 k+k^2}\right). \tag{7.90}$$

The coefficients multiplying the terms $\dot{f}$ and f in the expression for v are always negative for $k>0$. Thus, in equation 7.89, the coefficients multiplying the terms $\ddot{f}$, $\dot{f}$ and f will all be positive for $k>0$ and hence the coefficients of the dispersion relation will be positive. With positive coefficients, the roots of the dispersion relation will always have negative real parts and hence, for these soil types, the problem is always stable.

We now consider the problem where $\mathcal{C}$ is not small. Again looking for solutions of the form $e^{\sigma t}$, equations 7.88 give rise to a dispersion relation for the growth rate σ and the wave number k as follows

$$a(k)\sigma^2+b(k)\sigma+c(k)=0, \tag{7.91}$$

where the coefficients are given by

$$\begin{aligned}
a(k) &= \left(1-\frac{\mathcal{C}\overline{\alpha}_{fk}\overline{B}(p(k)-1)}{\mathcal{B}p(k)}\right)\left(\frac{\overline{A}k}{\sinh k}-\frac{\Pi\mathcal{C}}{p(k)}\frac{\cosh k+k\sinh k}{\cosh^2 k+k^2}\right)^{-1},\\
b(k) &= r(k)+\frac{\Pi}{4}\frac{(\sinh 2k-2k)}{k(\cosh^2 k+k^2)}a(k)+\frac{\overline{\alpha}_{fk}\overline{B}}{p(k)}\frac{\cosh k+k\sinh k}{\cosh^2 k+k^2}\\
&\quad+\left(\frac{\cosh k+k\sinh k}{\cosh^2 k+k^2}\right)^2\mathcal{B}\Pi\frac{a(k)}{p(k)},\\
c(k) &= \overline{\alpha}_{fk}\overline{A}\,\overline{B}\frac{k^2\cosh k}{\cosh^2 k+k^2}+\frac{\Pi}{4}\frac{(\sinh 2k-2k)}{k(\cosh^2 k+k^2)}r(k)\\
&\quad+\left(\frac{\cosh k+k\sinh k}{\cosh^2 k+k^2}\right)\frac{\mathcal{B}}{p(k)}\left(-\Pi+\frac{2\overline{\alpha}_{fk}\overline{A}\,\overline{B}k^4}{\cosh^2 k+k^2}+\Pi r(k)\frac{\cosh k+k\sinh k}{\cosh^2 k+k^2}\right),
\end{aligned} \tag{7.92}$$

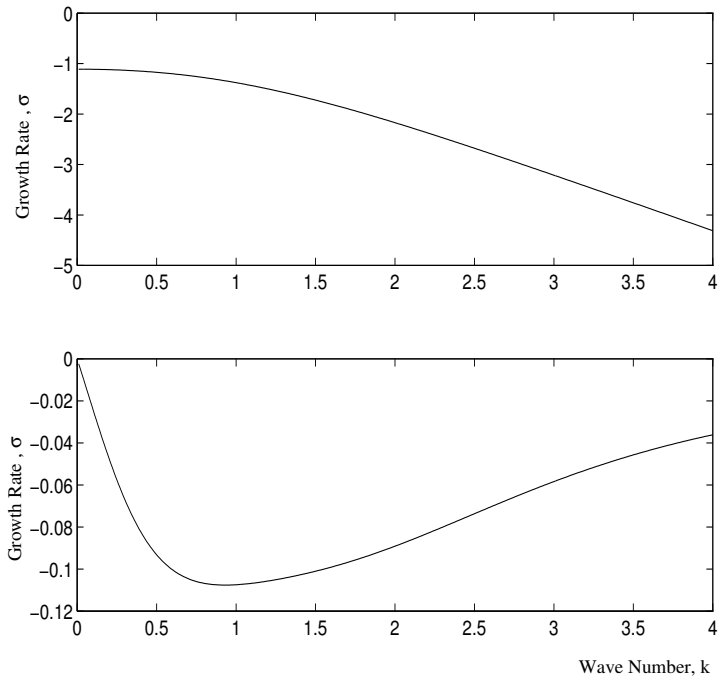


Figure 7.5: Plots of the dispersion relation with the inclusion of effective stress perturbation. $\alpha_{fk} = \beta = 10^{-1}$, $\Pi = \overline{A} = \overline{B} = 1$ and $\mathcal{C} = \mathcal{B} = 1$.

and the functions $r(k)$ and $p(k)$ are given by

$$\begin{aligned} r(k) &= \left(\frac{\overline{A}k\cosh k}{\sinh k} - \frac{\Pi\mathcal{C}}{p(k)} + \frac{2\overline{\alpha}_{fk}\overline{A}\,\overline{B}\mathcal{C}k^4}{p(k)(\cosh^2 k + k^2)}\right)\left(\frac{\overline{A}k}{\sinh k} - \frac{\Pi\mathcal{C}}{p(k)}\frac{\cosh k + k\sinh k}{\cosh^2 k + k^2}\right)^{-1}, \\ p(k) &= 1 + \mathcal{B}\left(\frac{k(\sinh 2k - 2k)}{\cosh^2 k + k^2} + \frac{1}{\beta k}\right). \end{aligned} \tag{7.93}$$

Figures 7.5 and 7.6 are illustrative plots of the growth rates σ for different values of the parameters $\mathcal{C}$ and $\mathcal{B}$. These plots reveal that with the appropriate choice of parameters, the problem can become unstable. However, it appears that the change from the unstable to the stable wavelengths is a result of a discontinuity in the solution for the growth rate which occurs because the coefficient $a(k)$ changes sign at some finite wavelength.

In reality, the parameter range required to make the problem unstable is rarely attainable. The coefficient $a(k)$ can become negative in both the numerator and the denominator while the coefficient $c(k)$ can only become negative through the function $r(k)$ becoming negative. Thus, we consider whether it is generally possible for the functions $a(k)$ and $r(k)$ to become negative and hence possibly give rise to unstable states. From inspection of $a(k)$ and $r(k)$ the size of the parameter groupings $\mathcal{C}\overline{\alpha}_{fk}\overline{B}$ and $\Pi\mathcal{C}/\overline{A}$ determine whether these functions are positive or negative. If we can show

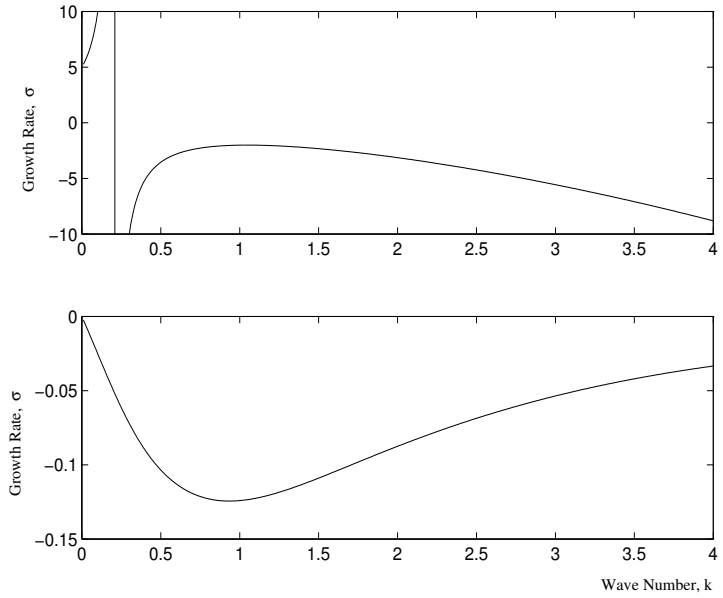


Figure 7.6: Plots of the dispersion relation with the inclusion of effective stress perturbation. $\alpha_{fk} = \beta = 10^{-1}$, $\Pi = \overline{A} = \overline{B} = 1$, $\mathcal{C} = 1.2$ and $\mathcal{B} = 0.1$.

that these parameter groupings are small then the functions $a(k)$ and $r(k)$ will, in general, be positive and hence the problem will be stable. These parameter groupings may be written as

$$\begin{aligned} \mathcal{C}\overline{\alpha}_{fk}\overline{B} &= \gamma\overline{\alpha}_{fk}\overline{\beta}_{fk}\,\frac{\overline{A}^2\overline{B}(\phi-\overline{W}_l)}{-g'(\overline{W}_l)\overline{W}_l}, \\ \frac{\Pi\mathcal{C}}{\overline{A}} &= \gamma\Pi\overline{\beta}_{fk}\,\frac{\overline{A}(\phi-\overline{W}_l)}{-g'(\overline{W}_l)\overline{W}_l}. \end{aligned} \tag{7.94}$$

In general we would expect $\gamma\overline{\alpha}_{fk}\overline{\beta}_{fk}$ to be $\ll 1$ and hence the first parameter grouping, given by $(7.94)_1$ is $\ll 1$. The size of the second parameter grouping is controlled by $\gamma\Pi\overline{\beta}_{fk}$. The parameters Π and $\overline{\beta}_{fk}$ both depend on the particular quasi-static depth of the frozen soil. At small depths Π will be small (see section 7.3) and the heave parameter will be large. As the frozen front advances Π increases while the heave rate and hence $\overline{\beta}_{fk}$ decreases dramatically. Thus, in general we would expect the product $\gamma\Pi\overline{\beta}_{fk}$ to be small and hence $(7.94)_2$ will be small. Hence, we would expect that the introduction of the perturbation in effective stress will not, in general, introduce a realistic instability mechanism into the frost heave model.

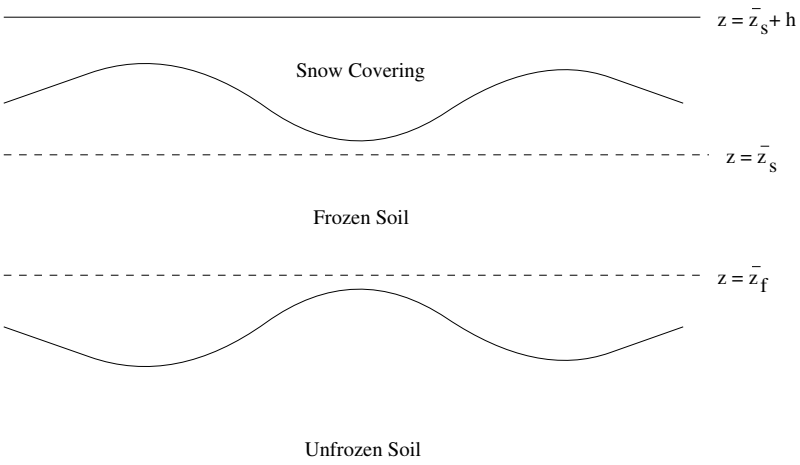


Figure 7.7: Schematic picture of snow covering over hummocks.

7.8 The Effect of Surface Snow Covering

One of the mechanisms commonly cited as a reason for the growth of hummocks is the variability in snow covering overlying the hummocks (see Williams & Smith (1989)). During the winter months troughs of hummocks fill with snow and hence the snow covering is greater in the troughs than on the crests. Because snow acts as an insulator, the crests are subject to a greater rate of cooling than the troughs and hence are subject to more heave. This is a possible mechanism for an instability in the frost heave model and in this section we consider whether the introduction of a snow phase can give rise to an instability in the secondary frost heave model. In the case of hummocks we expect the instability to arise because of the thermal conditions at the surface. For stone circles, the instability may initially be thermal instability but may become a mechanical one because of the additional weight of the piles of stones increasing the effective stress which suppresses heave beneath the rings.

Figure 7.7 is a schematic representation of a snow covering over a hummock. The snow depth is h above the unperturbed one dimensional state and we assume that the snow cover remains level even though differential frost heave may occur. The introduction of the snow phase gives rise to another region in which the temperature profile needs to be determined. For the purposes of the analysis presented here we assume that the stress free boundary conditions at the surface $z = z_s$ remain valid. The temperature in the snow phase satisfies Laplace's equation

$$\nabla^2 T = 0. \tag{7.95}$$

The boundary conditions are a prescribed temperature at the surface of the snow,

$z = 1 + h$:

$$T = T_s = -1, \tag{7.96}$$

and continuity of the temperature and heat flux at the ground surface, $z = z_s$:

$$\begin{aligned} [T]^+_- &= 0, \\ \delta \frac{\partial T}{\partial n} &= \frac{\partial T}{\partial n}, \end{aligned} \tag{7.97}$$

where $\delta = k_s/k_f$ and k_s and k_f are the thermal conductivities of the snow and the frozen viscous soil respectively. The quasi-steady one dimensional solution to the temperature at the ground surface, where $\overline{z}_s = 1$ and $\overline{z}_f = 0$, is given by

$$\overline{T} = -\frac{1}{1 + h/\delta}, \tag{7.98}$$

where we have again taken the dimensionless temperature to be -1 on the surface of the snow. This temperature reduces to that used in the previous sections in the absence of the snow covering (i.e. $\overline{T} = -1$) when considering the limits $h \to 0$ or $\delta \to \infty$.

Adopting the same perturbation procedure as that used in sections 7.4 and 7.5 we find that the perturbed temperature field, $\tilde{T}$, satisfies the following system

$$\nabla^2 \tilde{T} = 0, \tag{7.99}$$

and the perturbed boundary conditions become

$$\tilde{T} = 0, \tag{7.100}$$

on $z = 1 + h$, reflecting the fact that we are assuming that there is no perturbation in the snow surface, and

$$\begin{aligned} \left[\tilde{T}\right]^+_- + \left[\frac{\partial \overline{T}}{\partial z}\right]^+_- \tilde{z}_s &= 0, \\ \delta \left(\frac{\partial \tilde{T}}{\partial n} + \frac{\partial^2 \overline{T}}{\partial n \partial z}\tilde{z}_s\right) &= \left(\frac{\partial \tilde{T}}{\partial n} + \frac{\partial^2 \overline{T}}{\partial n \partial z}\tilde{z}_s\right), \end{aligned} \tag{7.101}$$

on $z = \overline{z}_s = 1$. Using a similar expression to equation 7.28 for the normal derivative at z_s and the fact that the quasi-steady state temperature profiles in the snow and frozen soil are linear, the boundary condition on $z = 1$ may be simplified to give

$$\begin{aligned} \left[\tilde{T}\right]^+_- &= \tilde{z}_s \frac{(1 - \delta)}{\delta + h}, \\ \delta \frac{\partial \tilde{T}}{\partial z} &= \frac{\partial \tilde{T}}{\partial z}. \end{aligned} \tag{7.102}$$

Thus, the perturbation of the temperature field is given by equation 7.99 and boundary conditions 7.100 and 7.102 and is coupled to the solution for the temperature perturbation in the frozen soil beneath. Looking for solutions of the form

$$\tilde{T} = l(z,t)e^{ikx} \tag{7.103}$$

for each wave number k, we find that l satisfies

$$l'' - k^2 l = 0. \tag{7.104}$$

which has a general solution of the form

$$l(z,t) = we^{kz} + ye^{-kz}. \tag{7.105}$$

Applying boundary conditions 7.100 and 7.102 and using the general solution to the temperature perturbation in the frozen soil given by equation 7.43, the constants w, y, m and n are given by the following system

$$\begin{aligned} we^{(1+h)k} + ye^{-(1+h)k} &= 0, \\ (w-m)e^{k} + (y-n)e^{-k} &= s(t)\frac{(1-\delta)}{\delta+h}, \\ (m-\delta w)e^{k} - (n-\delta y)e^{-k} &= 0, \\ m+n &= \frac{f(t)}{1+h/\delta}. \end{aligned} \tag{7.106}$$

Equation $(7.106)_4$ arises from the temperature boundary condition at the frozen fringe. It is slightly different to the version given in $(7.44)_6$ because the quasi-steady temperature gradient is no longer equal to -1. Equations $(7.44)_{5,6}$ derived in the absence of a snow cover can be reclaimed from the equations 7.106 by considering the limit as $\delta \to \infty$ and $h \to 0$. These simultaneous limits are required because simply letting $h \to 0$ will not recover the temperature condition $(7.44)_5$ from $(7.106)_{1,2}$. To reclaim this condition we require the temperature to be isothermal in the snow phase so that the temperature gradient there is zero and hence the limit $k_s \to \infty$ is required. The solution to the system 7.106 is relatively straightforward to obtain using a symbolic manipulation program such as *Mathematica*. However, we require an expression for the quantity $m - n$ and hence only give this quantity here (the full solution is given in appendix A). We obtain

$$m - n = -\left(\frac{\delta}{\delta+h}\right)\frac{f(\sinh k \sinh kh + \delta \cosh k \cosh kh) + s(1-\delta)\cosh kh}{\cosh k \sinh kh + \delta \sinh k \cosh kh}. \tag{7.107}$$

In considering the linear stability of this problem we neglect, for simplicity, the effects of the perturbation in effective stress which were considered in the previous section (i.e. we put $\mathcal{B} = \mathcal{C} = 0$). Thus, the differential equations for the frozen front $f(t)$ and the ground surface $s(t)$ that are analogous to equations 7.47 are

$$\begin{aligned}
\dot{f} &= -A\left(\frac{\delta}{\delta+h}\right) k \frac{f(\sinh k \sinh kh + \delta \cosh k \cosh kh) + s(1-\delta)\cosh kh}{\cosh k \sinh kh + \delta \sinh k \cosh kh}, \\
\dot{s} &= -\alpha_{fk} AB f \frac{k^2 \cosh k}{\cosh^2 k + k^2} - \alpha_{fk} B \dot{f} \frac{\cosh k + k \sinh k}{\cosh^2 k + k^2} \\
&\qquad -\frac{\Pi}{2} s \frac{(\cosh k \sinh k - k)}{k(\cosh^2 k + k^2)}.
\end{aligned} \tag{7.108}$$

If we let $\delta \to \infty$ and $h \to 0$, then equation $(7.108)_1$ becomes

$$\dot{f} = Ak \frac{(s - f\cosh k)}{\sinh k}, \tag{7.109}$$

which is exactly equation $(7.47)_1$. Using $(7.108)_1$ to eliminate s and looking for solutions of the form $e^{\sigma t}$, we get the following dispersion relation between the growth rate σ and the wave number k

$$m(k)\sigma^2 + p(k)\sigma + q(k) = 0, \tag{7.110}$$

where

$$\begin{aligned}
m(k) &= \left(\frac{\delta+h}{1-\delta}\right) \frac{\cosh k \sinh hk + \delta \sinh k \cosh kh}{A\delta k \cosh kh}, \\
p(k) &= \frac{\sinh k \sinh kh + \delta \cosh k \cosh kh}{(1-\delta)\cosh kh} - \alpha_{fk} B \frac{\cosh k + k \sinh k}{\cosh^2 k + k^2} \\
&\quad + \frac{\Pi}{4}\left(\frac{\delta+h}{1-\delta}\right) \frac{\sinh 2k - 2k}{k(\cosh^2 k + k^2)} \left(\frac{\cosh k \sinh hk + \delta \sinh k \cosh kh}{A\delta k \cosh kh}\right), \\
q(k) &= -\alpha_{fk} AB \frac{k^2 \cosh k}{\cosh^2 k + k^2} + \frac{\Pi}{4} \frac{\sinh 2k - 2k}{k(\cosh^2 k + k^2)} \left(\frac{\sinh k \sinh kh + \delta \cosh k \cosh kh}{(1-\delta)\cosh kh}\right).
\end{aligned} \tag{7.111}$$

Considering the limit as $h \to 0$ and $\delta \to \infty$, these coefficients can be shown to be equivalent to the coefficients given by equation 7.55. Plots of the growth rates against the wave number are shown in figure 7.8 for the case where $\alpha_{fk} = 10^{-1}$, $\Pi = 1$, $\delta = 0.05$ and $h = 1$. The remaining variables are the same as those used for the results given in section 7.5. It can be seen from these plots that positive values of the growth rates are possible and hence the situation can be unstable. It is

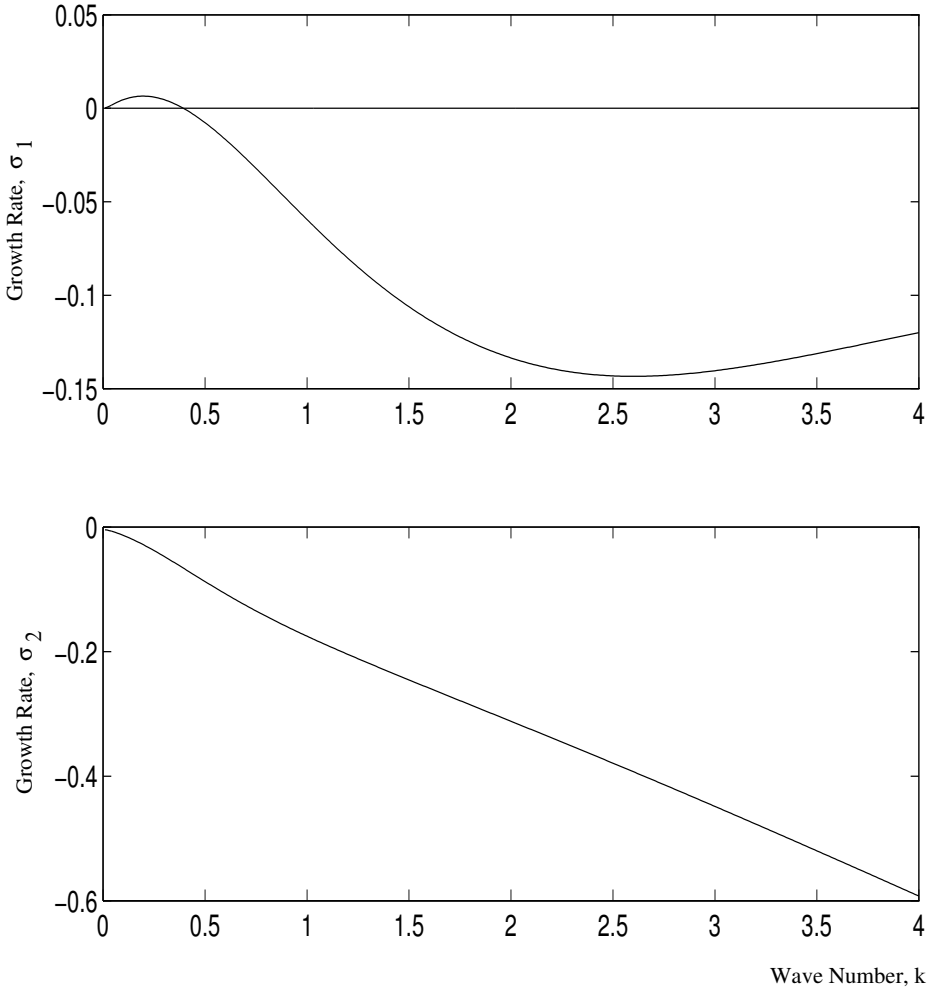


Figure 7.8: Plots of the dispersion relation with a heave parameter of $\alpha_{fk} = 10^{-1}$, $\Pi = 1$, $\delta = 0.05$ and $h = 1$.

interesting to note that the instability which arises as a result of the snow cover causes the gravitational mode to become unstable, whereas the potential instability which arose in the previous chapter was a result of the thermal mode becoming unstable.

With solutions of the form $e^{\sigma t}$, the ratio of the perturbations s/f is given by equation $(7.108)_1$ as

$$\begin{aligned}\frac{s}{f} &= -\sigma\,\frac{(\delta+h)}{\delta A k}\,\frac{(\cosh k\sinh kh+\delta\sinh k\cosh kh)}{(1-\delta)\cosh kh}\\ &\quad -\frac{(\sinh k\sinh kh+\delta\cosh k\cosh kh)}{(1-\delta)\cosh kh}.\end{aligned}\tag{7.112}$$

Thus, for positive growth rates σ (i.e. unstable modes), the left hand side of this expression is negative and hence the perturbations to the frozen front depth and heave are out of phase (i.e. as shown in figure 7.7). This result is consistent with observation (see Tarnocai & Zoltai (1978), Williams & Smith (1989) and Van Vliet-Lanoë (1991)).

We now consider in more detail the situation whereby the frost heave process is likely to become unstable and how this is related to soil type.

7.8.1 Neutral Stability

The numerical solution to the dispersion relation 7.110 shown in figure 7.8 indicates that unstable modes are possible. In order to consider when instability occurs we assume that the parameter values at which the growth rates become zero (i.e. the neutrally stable points) are associated with an exchange of stability. From the dispersion relation 7.110, we see that the neutrally stable points occur when $q(k)/m(k)=0$, which from equations 7.111 is when

$$-\alpha_{fk}ABk^3\cosh k+\frac{\Pi}{4}(\sinh 2k-2k)\left(\frac{\sinh k\sinh kh+\delta\cosh k\cosh kh}{(1-\delta)\cosh kh}\right)=0,\tag{7.113}$$

where we have cancelled the terms which are positive for all $k>0$ (these terms give a neutrally stable point at $k=\infty$). This relation can be written as

$$k^3\left(\mathcal{N}-\frac{(\sinh 2k-2k)}{4k^3(1-\delta)}\left(\tanh k\tanh kh+\delta\right)\right)=0,\tag{7.114}$$

where the parameter $\mathcal{N}$ is related to the heave parameter α_{fk} (and hence heave rate and soil type) and is given by

$$\mathcal{N}=\frac{\alpha_{fk}AB}{\Pi}=\frac{(\phi-W_l)\alpha_{fk}}{\Pi(\phi-W_m-\alpha_{fk}(W_l-W_m))}.\tag{7.115}$$

The term $\alpha_{fk}AB$ enters the problem through the quasi-static ice flux $\overline{V}_i$ and the parameter $\mathcal{N}$ may also be written as $\overline{V}_i/\Pi$. The neutral stability curve is thus given by

$$\mathcal{N} = \frac{(\sinh 2k - 2k)}{4k^3(1-\delta)} \left(\tanh k \tanh kh + \delta\right). \tag{7.116}$$

For wave numbers $k > 0$, the right hand side of equation 7.116 is a positive increasing function. Therefore, taking the limit as $k \to 0$, we see that the minimum value of the critical parameter is given by

$$\mathcal{N} = \mathcal{N}_c = \frac{\delta}{3(1-\delta)}. \tag{7.117}$$

Now, the dimensionless constant δ is the ratio of the thermal conductivities in the snow and the frozen soil. Typical values of these thermal conductivities are (see Williams & Smith (1989), page 109)

$$\begin{aligned} k_s &= 0.1\,\mathrm{W\,m^{-1}\,K^{-1}}, \\ k_f &= 2\,\mathrm{W\,m^{-1}\,K^{-1}}, \end{aligned} \tag{7.118}$$

and hence $\delta \sim 0.05$. Figure 7.9 is a plot of the neutral stability curve given by equation 7.116. From the form of the quadratic dispersion relation 7.110, a positive growth rate occurs if and only if the term $q(k)/m(k)$ is negative. After some simplification, this condition may be written in terms of $\mathcal{N}$ as

$$\mathcal{N} > \frac{(\sinh 2k - 2k)}{4k^3(1-\delta)} \left(\tanh k \tanh kh + \delta\right). \tag{7.119}$$

Therefore, the region above the neutral stability curve given in figure 7.9 represents unstable points while the region below this curve represents stable points.

From the above analysis, the neutral stability curve has a minimum positive value given by

$$\mathcal{N} = \mathcal{N}_c = \frac{\delta}{3(1-\delta)} \sim 0.02. \tag{7.120}$$

The linear stability analysis given in this chapter has considered a quasi-static approach in which it is assumed that the heave and frozen front penetration are very much slower than the onset of the instability. The critical value $\mathcal{N}_c$ defines a critical frost penetration depth at which the frost heave process becomes stable. The frost heave process is unstable if

$$\mathcal{N} > \mathcal{N}_c, \tag{7.121}$$

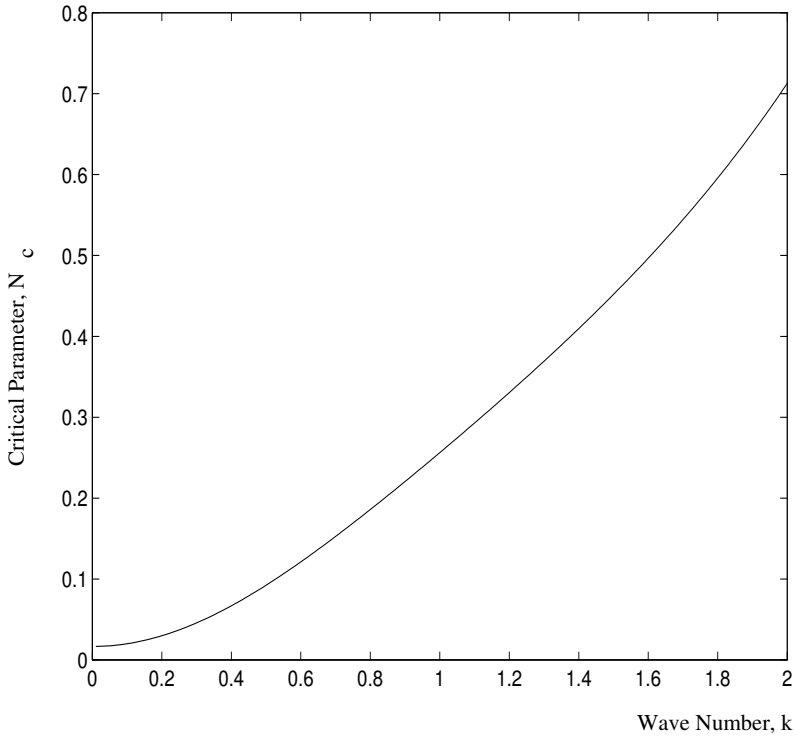


Figure 7.9: Plot of the critical parameter $\mathcal{N}_c$ against the wave number k.

which may be written as

$$\frac{\overline{V}_i}{\Pi} = \frac{\alpha_{fk} AB}{\Pi} > \mathcal{N}_c. \tag{7.122}$$

Thus, the instability condition can be related to the observed (dimensionless) heave rate V_i or to the soil type through the heave parameter α_{fk}. Writing equation 7.122 in dimensional terms and substituting the expression for Π given in section 7.3, we find that the frost heave process is unstable when

$$\frac{\nu_f}{gd^2}\overline{V}_i^* > \mathcal{N}_c, \tag{7.123}$$

where $\overline{V}_i^*$ is the dimensional heave rate. This condition may be written as

$$d < d_c = \left(\frac{\nu_f \overline{V}_i^*}{g\mathcal{N}_c}\right)^{\frac{1}{2}}, \tag{7.124}$$

where d_c is the critical frost penetration depth at which the frost heave process becomes stable. Typical dimensional heave rates for clay and silt soil types would be as follows:

$$\begin{aligned} \overline{V}_i^* &\sim 10^{-9} - 10^{-8}\,\mathrm{m\,s^{-1}}, \quad \text{(Silt)} \\ \overline{V}_i^* &< 10^{-10}\,\mathrm{m\,s^{-1}}. \qquad\qquad \text{(Clay)} \end{aligned} \tag{7.125}$$

(As discussed in chapter 4, sands and gravels are not, in general, susceptible to frost heave and are excluded from this analysis.) Thus, using the values for ν_f $(= \mu_f/\rho_f)$ and g given in section 7.3, and the value of $\mathcal{N}$ given above, we would typically expect the critical depth for silt and clay soil types to be

$$\begin{aligned} d_c &\sim 10\text{m}, \qquad \text{(Silt)} \\ d_c &\sim 1\text{m}. \qquad \text{(Clay)} \end{aligned} \tag{7.126}$$

This analysis suggests that all soil types are initially unstable. However, once the frozen front has advanced to the critical depth d_c, the one dimensional heave becomes stable. The critical depth, d_c, decreases as the soil type moves from silty soils to clay soils. Thus, soils which are very fine grained and consequently have a small critical depth, may only be unstable for a relatively short period and, hence any instability which initially occurs may disappear on the frost penetration time scale.

The observations of Tarnocai and Zoltai (1978) suggest that earth hummocks most commonly occur in soils with silt and clay content in excess of 68%. They also find that the slope of the resulting hummocks increases with increasing clay content. In order to predict the slope of the resulting hummocks a finite amplitude analysis needs to be done. However, an approximate order of magnitude expression for the slope of a hummock may be the ratio of the heave rate to the critical depth i.e.

$$\frac{\overline{V}_i}{d_c} = \left(\frac{g\mathcal{N}_c \overline{V}_i}{\nu_f} \right)^{\frac{1}{2}}. \tag{7.127}$$

At first sight this suggests that the slope decreases with heave rate, which is not consistent with the observations of Tarnocai and Zoltai (1978). However, the kinematic viscosity ν_f is likely to decrease with particle size and, therefore, this result may in fact be consistent with these observations.

In the absence of the quasi-static assumption, we would normally say that the preferred wave number of the instability occurs at the largest positive growth rate. However, the growth rates depend on the frost penetration depth and hence it is not possible from this linear stability analysis to determine any preferred wave number. To identify a preferred wave number, a finite amplitude analysis is required.

Chapter 8

Conclusion

8.1 Discussion of Results

This thesis has considered the process of secondary frost heave in freezing soils using the model developed by Miller (1972, 1978) and O'Neill & Miller (1982, 1985) (the 'Miller model'). Frost heave refers to the uplifting of the ground surface due to the growth of discrete ice lenses in the soil. Secondary heave refers to the mode of heaving in which the frozen soil is separated from the unfrozen soil by a region of partially frozen soil referred to as the 'frozen fringe'.

Chapter 2 discusses the physics of the Miller model and derives a generalised three dimensional version of the model which includes the effects of salinity and compressibility[1] (the 'generalised Miller model'). The development of the Miller model assumes that the interstitial ice moves by a process of thermal regelation as a rigid body with a velocity equal to the total flux at the base of the lowest ice lens (the 'rigid ice' assumption). The rigid ice assumption cannot be readily extended to the situation where some form of spatial variation exists. Following the work of Gilpin (1979), Fowler & Krantz (1994) suggest that the (thermal) regelative velocity of the interstitial ice phase is proportional to the temperature gradient in the frozen fringe. The discussion in appendix B suggests that it may also be appropriate to include pressure regelation effects in the prescription of the interstitial ice velocity. Furthermore, due to the lack of experimental results on the thermal regelation process, it is difficult to obtain reasonable values for the constant of proportionality that would apply in a heaving soil. These observations suggest that the process of regelation is

[1]The prescription given in chapter 2 does not give a complete account of compressibility and three dimensional effects. The additional relationships are given in chapters 6 and 7 respectively.

worthy of further study. However, it is worth pointing out that the analysis given in this thesis only relies on the ice velocity at the base of the lowest ice lens and, as such, it is relatively straightforward to incorporate more complex prescriptions for the ice flux into the model.

The discrete nature of the frost heave process makes analytical and numerical considerations of the Miller model difficult. Chapter 3 derives an 'averaged' version of the generalised Miller model in which it is shown that the location of the lowest ice lens can be treated as a continuous moving boundary. This simplification is achieved by first using the form of the hydraulic conductivity function to obtain a uniformly valid asymptotic expression for the water pressure in the frozen fringe. The form of the hydraulic conductivity function gives rise to a boundary layer in the pore water pressure which is used to show that the inter-lens spacing is small compared to the thickness of the frozen fringe. From this it is argued that the time scale for the relaxation of the fringe variables following the formation of a new lens is very rapid compared to any other time scale that arises in the problem. This then justifies the averaged model and the lens initiation condition becomes an additional boundary condition that determines the location of the lens front.

In chapter 3, the generalised Miller model is non-dimensionalised using scales which are appropriate to the laboratory, seasonal freezing and permafrost situations. In each case it is found that heat advection and the volume expansion of water on freezing can both be neglected. Neglecting the heat advection term allows the temperature profiles in the frozen and unfrozen regions to be written down for the one dimensional problem.

Chapter 4 considers frost heave in incompressible, solute free soils in one dimension. The results presented in this chapter are essentially those of Fowler (1989), Fowler & Noon (1993), Fowler & Krantz (1994) and Fowler *et al.* (1993). However, an original explanation and analysis is given for the dependence of frost heave on soil type.

In chapter 4 we show that the frozen fringe is thin compared to the frost penetration depth and this allows the frozen fringe equations to be integrated. The resulting system can then be integrated and two non-linear ordinary differential equations obtained for the heave and frost penetration depth. The amount of heave is found to

depend on a dimensionless parameter α_{fk}, which is a function of the effective stress at the frozen front and soil type through the capillary suction curve and the hydraulic conductivity function.

It is observed that sands and gravels rarely heave whereas silts can produce spectacular heave providing the load is not too great and clays only heave small amounts but can overcome substantial loads. The critical dependence of heave on the applied load (or rather the effective stress) can be explained from the lens boundary condition for the location of the lens front. If the initial effective stress is too large, the lens front will not be able to advance and hence lenses will not form and frost heave will not occur. The critical effective stress at which the lens front stops advancing is again found to be a function of soil type. Combining this result with the magnitude of heave predicted by the heaving parameter, we are able to give a possible explanation of the observed dependence of frost heave on soil type and effective stress.

Chapter 4 also gives approximate asymptotic solutions for heave and frost penetration depth for small and long times and qualitatively compares the solution to the reduced model and the full numerical solution given by O'Neill & Miller (1985). As well as comparing heave and frost penetration, approximate relationships are derived for lens thickness and lens spacing. It is found that the reduced system is in good qualitative agreement with the numerical results of O'Neill & Miller.

The effects of salinity are introduced in chapter 5. The thin fringe simplification achieved in chapter 4 is again used to reduce this problem to two ordinary differential equations for heave and frost penetration which are coupled to a parabolic partial differential equation for solute concentration in the unfrozen region beneath the frozen fringe. A small time asymptotic solution and a long time steady state solution are given together with a numerical solution. Chamberlain (1983) found experimentally that the presence of solutes reduced the observed heave by more than 50%. The form of the numerical results and the overall reduction in heave predicted is in good qualitative agreement with Chamberlain's results.

Chapter 6 considers the formation of segregated 'massive ice' in permafrost regions. The model developed in chapter 2 assumes that the pore water pressure is known at the frozen front. In the laboratory situation this value is simply the known water pressure at the base of the sample. However, in the field problem, this value is

obtained from the solution to the regional groundwater flow problem in the unfrozen region beneath the lens front.

In this chapter the physics of the unfrozen region are revisited and both elastic and elastic/plastic rheologies are discussed. Essentially, the groundwater flow problem is a consolidation type problem. The standard consolidation approach is that of Biot (1941, 1955) in which it is assumed that the soil matrix is elastic while also assuming a relationship between the porosity and the effective stress. However, this approach, in general, will not be correct as the relationship between porosity and effective stress should come from conservation of mass considerations. A corrected (small strain) version of the consolidation model is given for both the elastic and elastic/plastic rheologies.

The elastic rheology is adopted and the resulting groundwater flow equations are simplified by assuming that the aspect ratio for the regional problem is small. This allows the use of a Dupuit-Forchheimer type simplification that results in a non-linear diffusion equation for the effective stress at the frozen front. The time scale for the relaxation of the effective stress at the frozen front is shown to be much slower than the frost penetration time scale and thus the the spatial variation in the effective stress can be neglected outside a boundary layer.

Thus, three coupled ordinary differential equations are established for the frost penetration, heave and effective stress at the frozen front. The numerical results reveal that the lens front stops advancing after a short time due to the rapid increase in effective stress and further, that lens thickness reduces with depth. These two results agree with observation. However, the predicted thickness of the lenses is very much smaller than that observed. This leads to the suggestion that it is the formation of the 'final ice lens' which could lead to massive ice formation. When the lens front stops advancing, the 'averaged' model derived in chapter 3 is no longer applicable and the discrete version of the model needs to be considered. It is again found that the discrete equations can be reduced to three coupled ordinary differential equations for the frost penetration, cumulative heave and the effective stress at the frozen front. The solution to this system suggests that the the final lens growth may be a possible mechanism for the formation of segregated massive ice. Multiple massive ice lens formation is not predicted using this theory. However we suggest that multiple

massive ice formation could be a result of stratification of different soil types.

Chapter 7 is concerned with the formation of 'patterned ground' in tundra regions (e.g. earth hummocks, stone circles). A viscous rheology is assumed for the frozen soil above the lens front and the three dimensional generalisation of the frost heave equations, analogous to those given in chapter 4, are written down. A quasi-static linear stability analysis is applied to the generalised Miller model in the absence of solute and compressibility effects. The quasi-static approach assumes that the onset of an instability is more rapid than the frost heave time scale. This assumption is not entirely satisfactory, especially when considering the neutral stability points, but has been used in other time dependent basic state problems (e.g. Robinson (1976) and Emms (1992)).

The linear stability analysis gives rise to two growth rates which correspond to two instability modes, the 'gravity mode' and the 'thermal mode'. When the perturbation in the effective stress is ignored, each of these modes is stable. Introducing the perturbation in effective stress at the frozen front gives rise to the possibility that the thermal mode can become unstable. However, the soil parameter range at which this instability occurs is not particularly realistic and we conclude that the perturbation in effective stress does not introduce a realistic instability mechanism into the frost heave model.

In the absence of any realistic instability mechanism in the model, the snow covering overlying the hummocks is introduced. This additional phase gives rise to the possibility that the gravity mode can become unstable. By considering the neutral stability points, a parameter $\mathcal{N}$ is identified, depending on the heave rate and gravity effects, which determines the wave numbers at which the gravity mode is unstable. The neutral stability curve is found to have a minimum positive value, above which a soil has unstable modes and below which it is always stable. Because we have made a quasi-static assumption, this critical minimum value of the parameter $\mathcal{N}$ identifies a critical depth for the frozen front penetration. Above this depth the problem is unstable and below this depth the frost heave process becomes stable.

Because of the quasi-static assumption and the variation of the growth rates with frost penetration depth, it is not possible to identify the preferred wavelength of the hummock formation. This will require a finite amplitude analysis.

8.2 Further Work

In general, the results given in this thesis are consistent with observation. This would suggest that the generalised Miller model derived in chapter 2 is a feasible description of the frost heave process. This thesis has extended the Miller model to include solute effects, compressibility and differential frost heave. However, further work is necessary in the following areas:-

1. We have assumed throughout this thesis that the soil is saturated. In the field problem, the water table is, in general, some way below the ground surface and the region above the water table is only partially saturated. Consideration should be given to the differences which arise as a result of frost heave in an unsaturated soil.

2. The interstitial ice has been assumed to move through the frozen fringe by a process of thermal regelation with a velocity proportional to the temperature gradient. As briefly discussed in Appendix B, it is possible that pressure regelation should also be included in this model. Furthermore, both theoretical and experimental work have only considered the motion of individual particles in applied thermal gradients. These results need to be extended to a soil matrix and reliable values of the constant of proportionality obtained.

3. A finite amplitude analysis is required for the differential frost heave problem given in chapter 7. This would confirm the linear stability analysis and identify the preferred wavelength of any instability.

Appendix A

The following linear system arises in section 7.8 when solving for the perturbed temperature profiles in the snow and the frozen soil (see equation 7.106)

$$\begin{aligned} we^{(1+h)k} + ye^{-(1+h)k} &= 0, \\ (w-m)e^{k} + (y-n)e^{-k} &= s(t)\frac{(1-\delta)}{\delta+h}, \\ (m-\delta w)e^{k} - (n-\delta y)e^{-k} &= 0, \\ m+n &= \frac{f(t)}{1+h/\delta}, \end{aligned} \tag{A.1}$$

where m, n, w and y are the variables we wish to find. The solution to this system is given by

$$\begin{aligned} m &= \frac{\delta f}{\delta+h}\left(1 - \frac{e^{k}(\sinh kh + \delta\cosh kh)}{2(\cosh k\sinh kh + \delta\sinh k\cosh kh)}\right) \\ &\quad -\frac{\delta s}{\delta+h}\left(\frac{(1-\delta)\cosh kh}{2(\cosh k\sinh kh + \delta\sinh k\cosh kh)}\right), \\ n &= \frac{\delta f}{\delta+h}\left(\frac{e^{k}(\sinh kh + \delta\cosh kh)}{2(\cosh k\sinh hk + \delta\sinh k\cosh kh)}\right) \\ &\quad +\frac{\delta s}{\delta+h}\left(\frac{(1-\delta)\cosh kh}{2(\cosh k\sinh kh + \delta\sinh k\cosh kh)}\right), \\ w &= -\frac{e^{-k(1+h)}}{2(\delta+h)}\left(\frac{\delta f + (1-\delta)\cosh kh}{\cosh k\sinh kh + \delta\sinh k\cosh kh}\right), \\ y &= \frac{e^{k(1+h)}}{2(\delta+h)}\left(\frac{\delta f + (1-\delta)\cosh kh}{\cosh k\sinh kh + \delta\sinh k\cosh kh}\right). \end{aligned} \tag{A.2}$$

Appendix B

Gilpin (1979) analyses the regelative motion of a particle through ice at sub-freezing temperatures. The motion is effected through the existence of a thin film between the particle and the ice, in which the motion of the particle is compensated by an opposing lubrication flow in the film. Gilpin assumes that the film exists because of a 'disjoining' pressure between the particle and the ice, and is led to a lubrication equation for the thickness of the film as a function of polar angle θ (where $\theta = 0$ corresponds to the direction of flow). From Gilpin's equation [33], the dimensionless film thickness can be written as

$$-\alpha h^{2-\alpha}\frac{\partial h}{\partial \theta} = (v - (R_v v - g^*)h^3)\sin\theta, \tag{B.1}$$

where the disjoining pressure is proportional to $h^{-\alpha}$ and h, v and g^* are dimensionless film thickness, particle velocity and thermal gradient (both in the direction $\theta = 0$). This equation assumes a spherical particle and steady, slow flow, and is obtained by solving the Reynolds equation in the film together with the temperature fields in ice and particle. The film thickness H, particle velocity V and temperature gradient G are defined by

$$H = h_c\, h, \quad V = V_{c\eta}\, v, \quad G = G_c\, g^*, \tag{B.2}$$

where

$$\begin{aligned} V_{c\eta} &= \frac{v_s^2 h_c^3 L(-T_c)}{6\eta v_l^2 \Delta v R^2 T_a}, \\ G_c &= \frac{\overline{k} v_s(-T_c)}{3k_s v_l R}, \\ a h_c^{-\alpha} &= \frac{L(-T_c)}{T_a,} \end{aligned} \tag{B.3}$$

and the disjoining pressure is effectively $aH^{-\alpha}$. The other constants appearing in these relations are the specific volume of ice v_s, the specific volume of water v_l,

$\Delta v = (v_s - v_l)$, the latent heat of fusion L, the water viscosity η, the particle radius R, the ambient absolute temperature T_a, the ice thermal conductivity k_s and $\overline{k} = k_f + 2k_s$, where k_f is the particle thermal conductivity. The temperature T_c is the ambient sub-cooling below freezing. (The definition of $V_{c\eta}$ in $(B.3)_1$ differs from that incorrectly given by Gilpin (1979, equation [30]) by a factor h_c^2.) The dimensionless parameter R_v in B.1 is then defined by

$$R_v = \frac{\rho_s L V_{c\eta}}{3k_s G_c}, \tag{B.4}$$

where $\rho_s = 1/v_s$ and we define

$$\psi = \delta R_v = \frac{\rho_l^2 L^2 h_c^3}{6\eta T_a \overline{k} R}, \tag{B.5}$$

and $\delta = \Delta v / v_l$.

The equation B.1 is to be solved subject to the condition

$$\int_0^\pi \frac{d\theta}{h^\alpha} = \pi, \tag{B.6}$$

which expresses the assumption that the far field stress in the ice is unperturbed by the particle motion. Our object is then to relate the particle velocity V to the applied temperature gradient G. In the notation of chapter 2, (see equation 2.21), we seek the parameter λ in the form

$$V = \lambda G. \tag{B.7}$$

Note that the particle moves up temperature gradients (ice moves down them), and that the extension of the present single particle analysis to the regelation within the fringe is at best quantitatively crude.

We define

$$\lambda = \lambda_0 \Lambda, \quad \lambda_0 = \frac{3k_s}{\rho_s L}, \tag{B.8}$$

noting that with $k_s \sim 2\,\mathrm{W\,m^{-1}\,K^{-1}}$, $\rho_s \sim 0.9 \times 10^3\,\mathrm{kg\,m^{-3}}$, $L \sim 3.35 \times 10^5\,\mathrm{J\,kg^{-1}}$, then $\lambda_0 \sim 2 \times 10^{-8}\,\mathrm{m^2\,s^{-1}\,K^{-1}}$. Λ is then determined by the definition of v, as

$$v = \frac{\Lambda}{R_v} g^* \tag{B.9}$$

together with the force balance equation ([38b] of Gilpin (1979)), which can be written as

$$p^* = -2 \int_0^\pi \frac{\sin\theta \cos\theta}{h^\alpha}\, d\theta + \frac{4}{3}(1+\delta)(R_v v - g^*), \tag{B.10}$$

where p^* is the dimensionless applied pressure which has been scaled with

$$L(-T_c)/(\Delta v T_a), \tag{B.11}$$

and pure thermal regelation occurs if $p^* = 0$.

From equation $(B.3)_2$ we have $G_c \sim (-T_c)/R$. Hence, we would expect g^* to be of order R/d_f, where d_f is the frozen fringe thickness, (i.e. $G_c g^* \sim (-T_c)/d_f$) and thus g^* will, in general, be very small (hence from B.9, we anticipate that v will also be small). In this case, it is straightforward to find the solution, h, to equation B.1, satisfying B.6, as a power series in g^* as follows:

$$h \approx 1 + \frac{g^*}{\alpha}\left(\frac{\Lambda}{R_v} - (\Lambda - 1)\right)\cos\theta + \cdots. \tag{B.12}$$

B.10 then determines Λ as

$$\Lambda = \frac{\psi}{1+\psi}\left(1 + \frac{3p^*}{4\delta g^*}\right). \tag{B.13}$$

At least if p^* is small, say $p^* = O(\delta g^*)$, then this confirms that $\Lambda \leq O(1)$ and hence that $R_v v$ $(= \Lambda g^*)$ is small in B.1. Also $\Lambda/R_v = \delta\Lambda/\psi \leq O(1)$, so that $v = O(g^*)$. Hence the approximation is consistent, whatever the size of ψ. In fact, taking $\rho_l = 10^3\,\mathrm{kg\,m^{-3}}$, $\eta = 10^{-3}\,\mathrm{Pa\,s}$, $\overline{k} = 2\,\mathrm{W\,m^{-1}\,K^{-1}}$, $T_a = 273\,\mathrm{K}$, $L \sim 3.35 \times 10^5\,\mathrm{J\,kg^{-1}}$, $R = 2 \times 10^{-5}\,\mathrm{m}$ (i.e. 20 microns), $h_c = 10\,\mathrm{nm}$, we find $\psi \sim 0.5 \times 10^{-3}$. Thus, typically, we may have $\psi \ll 1$ and therefore, to leading order,

$$\Lambda = \psi\left(1 + \frac{3p^*}{4\delta g^*}\right). \tag{B.14}$$

If we ignore the loading by putting $p^* = 0$, then with $\psi = 0.5 \times 10^{-3}$ and $\lambda_0 = 2 \times 10^{-8}\,\mathrm{m^2\,s^{-1}\,K^{-1}}$ we get $\lambda \sim 10^{-11}\,\mathrm{m^2\,s^{-1}\,K^{-1}}$.

Variation of λ occurs with soil type and temperature through particle radius R and film thickness h_c. From B.3 we have $h_c \propto (-T_c)^{-\frac{1}{\alpha}}$ and hence from B.5, B.8 and B.14 we have that

$$\lambda \propto h_c^3 \propto \frac{1}{R(-T_c)^{\frac{3}{\alpha}}} \tag{B.15}$$

where Gilpin uses $\alpha = 2$. In the frozen fringe, however, where the ice is at 'the' melting point, the value of h_c may be much thicker than Gilpin's preferred range of $2.5 - 14$ nm. From B.13 the upper limit of $\Lambda \sim O(1)$ may thus be attainable and hence $\lambda \sim 10^{-8}\,\mathrm{m^2\,s^{-1}\,K^{-1}}$. In this thesis, we have chosen an intermediate value of

$\lambda \sim 10^{-10}\,\mathrm{m^2\,s^{-1}\,K^{-1}}$ which is the value used by Fowler & Krantz (1994). However, it is clear that the issue of regelation within the frozen fringe is worthy of further study.

The other question of interest is whether loading should be included in the fringe. A particle will move from low to high pressures by pressure-melting. This suggests that, in the frozen fringe, the appropriate choice of dimensional load pressure should be $2R\frac{\partial p_i}{\partial z}$ (for a velocity in the z direction). Now, in the fringe we have, from the generalised Clapeyron equation 2.9 in the absence of solutes, that

$$\frac{L}{v_l T_a} G = -\delta \frac{\partial p_w}{\partial z} - (1+\delta)\frac{\partial f}{\partial z}, \tag{B.16}$$

where $p_i - p_w = f(W)$. We can write

$$\frac{\partial p_i}{\partial z} = \frac{\partial p_w}{\partial z} + \frac{\partial f}{\partial z}. \tag{B.17}$$

Therefore, putting $\Omega = 3p^*/4\delta g^*$, we find that Ω in the fringe is given by

$$\begin{aligned} \Omega &= \frac{3}{4\delta}\frac{\left[2R\frac{\partial p_i}{\partial z}\right]}{\left[\frac{L(-T_c)}{T_a \Delta v}\right]}\frac{1}{G}\left(\frac{\overline{k}v_s}{3k_s v_l}\right)\frac{(-T_c)}{R} \\ &= \left(\frac{\overline{k}v_s}{2k_s v_l}\right)\frac{\left[\frac{\partial p_w}{\partial z} + \frac{\partial f}{\partial z}\right]}{\left[-\delta\frac{\partial p_w}{\partial z} - (1+\delta)\frac{\partial f}{\partial z}\right]}. \end{aligned} \tag{B.18}$$

where we have used the pressure scale given by B.11. The term $(\overline{k}v_s)/(2k_s v_l) \sim 1$ and hence, outside the water pressure boundary layer, we have that $\Omega = O(1)$. In the water pressure boundary layer, the term $\frac{\partial p_w}{\partial z} \sim \gamma$ and hence we have $\Omega = O(\gamma)$. Using B.17 and B.18 we find that in this boundary layer the leading order behaviour of Ω is given by

$$\Omega = \left(\frac{\overline{k}v_s}{2k_s v_l}\right)\frac{v_l T_a}{LG}\frac{\partial p_w}{\partial z}. \tag{B.19}$$

The size of the term Ω suggests that it may be appropriate to include a pressure regelation term in the frozen fringe. Based on equation B.7, a possible generalisation of the ice velocity in the fringe is given by

$$V = -\lambda(G + \omega\Pi) \tag{B.20}$$

where we have reversed the sign in equation B.7, Π is the pore ice pressure gradient and

$$\omega = \frac{k' v_l T_a}{L}, \tag{B.21}$$

with $k' = (\overline{k}v_s)/(2k_s v_l) \sim 1$. Non-dimensionalising equation B.21 using the frost heave scales introduced in chapter 3 we get

$$v_i = -\delta_3 \frac{\partial T}{\partial z} - \delta_4 \frac{\partial p_i}{\partial z}, \tag{B.22}$$

where

$$\delta_3 = \frac{L\rho_w \lambda}{k}, \qquad \delta_4 = \frac{k' T_a \sigma \lambda}{k \Delta T}, \tag{B.23}$$

and $\sigma \sim 10^5$ is the stress scale in the frozen fringe. Now,

$$\frac{\delta_4}{\delta_3} \sim \frac{k' T_a \sigma}{\Delta T L \rho_w} \sim 0.1, \tag{B.24}$$

where we have used the values of the constants given previously with $\sigma = 10^5\,\mathrm{Pa}$ and $\Delta T = 1\,\mathrm{K}$. Thus, outside the water pressure boundary layer, the pressure regelation effects are small.

The analysis given in chapter 4 in deriving the differential equations for the heave and frost penetration depth only required the ice velocity at the lens front. In the region close to the lens front the ice pressure gradient is given by

$$\frac{\partial p_i}{\partial z} = \frac{\partial p_w}{\partial z} + \frac{\partial f}{\partial z} \approx \frac{\partial p_w}{\partial z}. \tag{B.25}$$

Thus, using equation 3.22 to calculate the water pressure gradient at the lens front, the dimensionless ice velocity at the freezing is given by

$$v_i = -\delta_3 \left.\frac{\partial T}{\partial z}\right|_l - \delta_4 \gamma (f_l - N). \tag{B.26}$$

Thus there is an additional dependence in the frost heave process on the effective stress at the freezing front.

Bibliography

[1] Acheson, D.J., 1990. *Elementary Fluid Dynamics.* Clarendon Press, Oxford.

[2] Aguirre-Puente, J., Frémond, M., 1975. Frost propagation in wet porous media. In *Applications of methods of functional analysis to problems in mechanics (Joint Symposium, Marseille)*, pages 137–147. Springer, Berlin.

[3] Anderson, D.M., Morgenstern, N.R., 1973. Physics, Chemistry and Mechanics of Frozen Ground: A review. In *Permafrost; Second Int. Conf.; Physics, Physical Chemistry, and Mechanics of Frozen Ground and Ice.*, pages 257–288.

[4] Atkinson, J.H., Bransby, P.L., 1978. *The Mechanics of Soils; an Introduction to Critical State Soil Mechanics.* McGraw Hill.

[5] Audet, D.M., Fowler, A.C., 1992. A mathematical model for compaction in sedimentary basins. *Geophys. J. Int.*, 110(3):577–590.

[6] Baker, G.C., and Osterkamp, T.E., 1989. Salt redistribution during freezing of saline sand columns at constant rates. *Water Resour. Res.*, 25(8):1825–1831.

[7] Bear, J. 1988. *Dynamics of Fluids in Porous Media.* Dover Publications.

[8] Bell, F.G., 1992. *Engineering Properties of Soils and Rocks.* Butterworth-Heinemann.

[9] Berg, R.L., Guymon, G.L., and Johnson, T.C., 1980. Mathematical model to correlate frost heave of pavements with laboratory predictions. Technical report, CRREL Rep. 80-10.

[10] Beskow, G. 1935. Soil freezing and frost heaving with special application to roads and railroads. Swed. Geol. Soc., Ser. C, No. 375, 26th year book No. 3 (translated

by J.O. Osterberg, Northwestern Univ., 1947). Reprinted in: Technical Report, CRREL Rep. 91-23, 26.

[11] Biot, M.A., 1941. General theory of three-dimensional consolidation. *J. Appl. Phys.*, 12:155–164.

[12] Biot, M.A., 1955. Theory of elasticity and consolidation for a porous anisotropic solid. *J. Appl. Phys.*, 26(2):182–185.

[13] Bishop, A.W., Blight, G.E. 1963. Some aspects of effective stress in saturated and partly saturated soils. *Geotechnique*, 13:177–197.

[14] Black, P.B. 1990. Three functions that model empirically measured unfrozen water content data and predict relative hydraulic conductivity. Technical report, CRREL Rep. 90-5.

[15] Burn, C.R., Smith, M.W. 1993. Issues in Canadian permafrost research. *Prog. Phys. Geog.*, 17(2):156–172.

[16] Cary, J.W., 1987. A new method for calculating frost heave including solute effects. *Water Resour. Res.*, 23(8):1620–1624.

[17] Chamberlain, E.J. 1983. Frost heave of saline soils. In *Proc. Fourth Int. Conf. Permafrost*, pages 121–126.

[18] Coussy, O., 1995. *Mechanics of Porous Continua.* John Wiley.

[19] Crank, J., 1984. *Free and Moving Boundary Problems.* Clarendon Press, Oxford.

[20] Emms, P., 1992. *Compositional convection and freckle formation in solidification of binary alloys.* PhD thesis, University of Oxford.

[21] Everett, D.H. 1961. The thermodynamics of frost damage to porous solids. *Trans. Faraday. Soc.*, 57(2):1541–1551.

[22] Fasano, A., Primicerio, M., 1984. Freezing in porous media; a review of mathematical models. In *Applications of mathematics in technology.*, pages 288–311. Teubner.

[23] Fowler, A.C., 1985. The formation of freckles in binary alloys. *IMA J. Appl. Math.*, 35:159–174.

[24] Fowler, A.C. 1989. Secondary frost heave in freezing soils. *SIAM J. Appl. Math.*, 49(4):991–1008.

[25] Fowler, A.C., 1996. *Mathematical Modelling in the Applied Sciences.* Cambridge University Press. In press.

[26] Fowler, A.C., Krantz, W.B., 1994. A generalized secondary frost heave model. *SIAM J. Appl. Math.*, 54(6):1650–1675.

[27] Fowler, A.C., Noon, C.G., 1993. A simplified numerical solution of the Miller model of secondary frost heave. *Cold Reg. Sci. Tech.*, 21(4):327–336.

[28] Fowler, A.C., Noon, C.G. 1996. Compaction, consolidation and regional groundwater flow modelling. *Geophys. J. Int., Submitted.*

[29] Fowler, A.C., Noon, C.G., Krantz, W.B. 1993. A computationally feasible reduction of the O'Neill-Miller model of secondary frost heave. In *Proc. Sixth Int. Conf. Permafrost.*, pages 1100–1104.

[30] Gibson, R.E., England, G.L., Hussey, M.J.L., 1967. The theory of one-dimensional consolidation of saturated clays. *Geotechnique.*, 17:261–273.

[31] Gilpin, R.R. 1979. A model of the 'liquid like' layer between ice and a substrate with applications to wire regelation and particle migration. *J. Colloid Interface Sci.*, 68:235–251.

[32] Gilpin, R.R. 1980. A model for the prediction of ice lensing and frost heave in soils. *Water Resour. Res.*, 16(5):918–930.

[33] Gold, L.W. 1957. A possible force mechanism associated with the freezing of water in porous materials. *Highw. Res. Board Bull.*, 168:65–72.

[34] Guymon, G.L., Hromadka, T.V., Berg, R.L., 1980. A one-dimensional frost heave model based upon simultaneous heat and water flux. *Cold Reg. Sci. Tech.*, 3:252–262.

[35] Hallet, B., 1978. Solute redistribution in freezing ground. In *Proc. Third Int. Conf. Permafrost.*, pages 86–91.

[36] Harlan, R.L., 1973. Analysis of coupled heat-fluid transport in partially frozen soil. *Water Resour. Res.*, 9(5):1314–1323.

[37] Haynes, F.D., 1978. Strength and deformation of frozen silt. In *Proc. Int. Conf. Permafrost.*, pages 655–661.

[38] Hillel, D. 1980. *Fundamentals of Soil Physics.* Academic Press.

[39] Hoekstra, P., Miller, R.D. 1967. On the mobility of water molecules in the transition layer between ice and a solid surface. *J. Colloid Interface Sci.*, 25:166–173.

[40] Holden, J.T. 1983. Approximate solutions for Miller's theory of secondary heave. In *Proc. Fourth Int. Conf. Permafrost*, pages 498–503.

[41] Holden, J.T., Piper, D., Jones, R.H. 1985. Some developments of a rigid-ice model of frost heave. In *Fourth Int. Symp. Ground Freezing.*, pages 93–99.

[42] Hopke, S.W., 1980. A model for frost heave including overburden. *Cold Reg. Sci. Tech.*, 3:111–127.

[43] Kay, B.D., Groenevelt P.H., 1983. The redistribution of solutes in freezing soil: Exclusion of solutes. In *Proc. Fourth Int. Conf. Permafrost*, pages 584–588.

[44] Konrad, J.M., 1989. Influence of overconsolidation on the freezing characteristics of clayey silt. *Can. Geotech. J.*, 26:9–21.

[45] Konrad, J.M., Duquennoi, C., 1993. A model for water transport and ice lensing in freezing soils. *Water Resour. Res.*, 29(9):3109–3124.

[46] Konrad, J.M., Morgenstern, N.R., 1980. A mechanistic theory of ice lens formation in fine-grained soils. *Can. Geotech. J.*, 17(4):473–486.

[47] Konrad, J.M., Nixon, J.F., 1994. Frost heave characteristics of a clayey silt subjected to small temperature gradients. *Cold Reg. Sci. Tech.*, 22(3):299–310.

[48] Konrad, J.M., Seto, J.T.C., 1994. Frost heave characteristics of undisturbed sensitive Champlain sea clay. *Can. Geotech. J.*, 31:285–298.

[49] Koopmans, R.W.R., Miller, R.D. 1966. Soil freezing and soil water characteristic curves. *Soil Sci. Soc. Amer. Proc.*, 30:680–685.

[50] Krantz, W.B., Adams, K.E., 1995. Validation of a Fully Predictive Model for Secondary Frost Heave. *Arctic and Alpine Research.* In Press.

[51] Krantz, W.B., Gleason, K.J., and Caine, N., 1988. Patterned ground. *Scientific American.*, pages 44–50.

[52] Loch, J.P.G. 1978. Thermodynamic equilibrium between ice and water in porous media. *Soil Sci.*, 126(2):77–80.

[53] Mackay, J.R. 1971. The origin of massive icy beds in permafrost, western Arctic coast, Canada. *Can. J. Earth Sci.*, 8(4):397–422.

[54] Mackay, J.R., Dallimore, S.R., 1992. Massive ice of the Tuktoyaktuk area, western Arctic coast, Canada. *Can. J. Earth Sci.*, 29:1235–1249.

[55] McKay, G., Straughan, B., 1991. The influence of a cubic density law on patterned ground formation. *Mathematical Models and Methods in Applied Sciences.*, 1(1):27–39.

[56] Miller, R.D. 1966. Phase equilibria and soil freezing. In *Proc. Int. Conf. Permafrost.*, pages 193–197.

[57] Miller, R.D. 1972. Freezing and heaving of saturated and unsaturated soils. *Highw. Res. Rec.*, 393:1–11.

[58] Miller, R.D. 1977. Lens initiation in secondary heaving. In *Proc. Int. Symp. Frost Action in Soils*, pages 68–74.

[59] Miller, R.D. 1978. Frost heaving in non-colloidal soils. In *Proc. Third. Int. Conf. Permafrost*, pages 708–713.

[60] Miller, R.D. 1980. Freezing phenomena in soils. In D Hillel, editor, *Applications of Soil Physics*, chapter 11, pages 254–299. Academic Press.

[61] Nakano, Y., 1993. Application of existing hypotheses used in the mathematical description of ice segregation in freezing soils. In Chadam, J.M., Rasmussen, H.R., eds., *Free boundary problems in fluid flow with applications.,* pages 225–242. Longman.

[62] Nixon, J.F., 1991. Discrete ice lens theory for frost heave in soils. *Can. Geotech. J.*, 28:843–859.

[63] Noon, C.G., 1990. Secondary frost heave in saline soils. Transfer Dissertation.

[64] O'Neill, K. 1983. The physics of mathematical frost heave models: A review. *Cold Reg. Sci. Tech.*, 6:275–291.

[65] O'Neill, K., Miller, R.D. 1982. Numerical solutions for a rigid ice model of secondary frost heave. Technical report, CRREL Rep. 82-13.

[66] O'Neill, K., Miller, R.D. 1985. Exploration of a rigid ice model of frost heave. *Water Resour. Res.*, 21(3):281–296.

[67] Padilla, F., Villeneuve, J.P., 1992. Modeling and experimental studies of frost heave including solute effects. *Cold Reg. Sci. Tech.*, 20:183–194.

[68] Panday, S., Corapcioglu, M.Y., 1991. Solute rejection in freezing soils. *Water Resour. Res.*, 27(1):99–108.

[69] Penner, E. 1959. The mechanism of frost heaving in soils. *Highw. Res. Board Bull.*, 225:1–13.

[70] Piper, D., Holden, J.T. and Jones, R.H. 1988. A mathematical model of frost heave in granular materials. In *Proc. Fifth Int. Conf. Permafrost.*, pages 370–376.

[71] Richards, L.A. 1931. Capillary conduction of liquids in porous mediums. *Physics*, 1:318–333.

[72] Robinson, J.L., 1976. Theoretical analysis of convective instability of a growing horizontal thermal boundary layer. *The Physics of Fluids.*, 19(6):778–791.

[73] Romkens, M.J.M., Miller, R.D. 1973. Migration of mineral particles in ice with a temperature gradient. *J. Colloid Interface Sci.*, 42:103–111.

[74] Sayles, F.H., 1988. State of the art: Mechanical properties of frozen soil. In *Fifth Int. Symp. Ground Freezing*, pages 143–159.

[75] Scheidegger, A.E. 1957. *The Physics of Flow through Porous Media*. Macmillan, New York.

[76] Skempton, A.W., 1960. Effective stress in soils, concrete and rocks. In *Proc. Conf. Pore Pressure and Suction in Soils*, pages 4–16.

[77] Smith, E.B. 1989. *Basic Chemical Thermodynamics*. Clarendon Press.

[78] Taber, S. 1930. The mechanics of frost heaving. *J. Geol.*, 38:303–317.

[79] Tarnocai, C., Zoltai, S.C., 1978. Earth hummocks of the Canadian Arctic and Subarctic. *Arctic and Alpine Research.*, 10(3):581–594.

[80] Taylor, S.G., Luthin, J.N., 1978. A model for coupled heat and moisture transfer during soil freezing. *Can. Geotech. J.*, 15:548–555.

[81] Terzaghi, K., 1936. The shearing resistance of saturated soil and the angle between the planes of shear. In *Proc. First Int. Conf. Soil Mechanics and Foundation Engineering*, pages 54–56.

[82] Van Vliet-Lanoë, B., 1991. Differential frost heave, load casting and convection: Converging mechanisms; a discussion of the origin of cryoturbations. *Permafrost and Periglacial Processes.*, 2:123–139.

[83] Vignes-Adler, M., 1977. On the origin of the water aspiration in a freezing dispersed medium. *J. Colloid Interface Sci.*, 60(1):162–171.

[84] Williams, P.J., Smith, M.W., 1989. *The Frozen Earth. Fundamentals of Geocryology.* Cambridge University Press.